Aberrant TGFβ/BMP signalling in connective tissue disease associated pulmonary hypertension

Adrian Gilbane

Thesis submitted for the degree of

Doctor of Philosophy

2015

University College London

Division of Medicine
Centre for Rheumatology & Connective Tissue Diseases
Rowland Hill Street
London
NW3 2PF

Statement of contribution

I, Adrian Gilbane, confirm that the work presented in this thesis is my own. Where information has been derived from other sources, I confirm that this has been indicated in the thesis.

Adrian Gilbane

Abstract

Up to 10 percent of systemic sclerosis (SSc) patients develop pulmonary arterial hypertension (PAH). This risk persists throughout the disease and is time dependent, suggesting that SSc operates as a susceptibility factor. Outcomes for SSc-PAH patients remain poor compared with heritable (HPAH) or idiopathic (HPAH) forms, despite clinical and pathological similarities. Whereas susceptibility in HPAH and HPAH is strongly associated with gene mutations that lead to reduced expression of functional bone morphogenetic protein type II receptor (BMPRII), these mutations have not been observed in SSc-PAH.

My initial aim was to investigate BMPRII expression and downstream signalling pathways in whole lung tissue and explant cultured fibroblasts derived from a murine model of SSc (TβRIIΔk-fib) that is susceptible to developing PAH Complementary studies examined SSc or control lung tissue and fibroblasts. My results suggest reduced BMPRII levels, impaired signalling and altered receptor turnover could be due to increased TGFβ activity in a model of SSc-PAH. Similarly a significant reduction in BMPRII expression is observed in SSc lung tissue and fibroblasts. Increased proteasomal degradation of BMPRII appears to underlie this and may result from heightened TGFβ activity. Proteasomal inhibition restored BMPRII expression and cellular responses. Collectively suggesting that impaired TGFβ/BMP signalling leading to increased receptor degradation, may promote PAH susceptibility in SSc and provide a unifying mechanism across different forms of PAH.

Since more than one cell type contribute to the development of PAH and the pathophysiology of the disease BMPRII expression and TGFβ responses in pulmonary arterial smooth muscle cells (PASMCs) were also investigated. Initial studies generated a synthetic “disease” like PASMC that also displayed a reduction in BMPRII expression and increased response to TGFβ, which was similar to IPAH cells

Finally, the role of epigenetic inhibition in the TβRIIΔk-fib model was investigated. The epigenetic inhibitor JQ1 was able to attenuate the spontaneous development of PAH in the TβRIIΔk-fib model of PAH. Taken together, work described in this thesis strongly suggests that a reduction in BMPRII is a susceptibility factor to the development of PAH in a pre-clinical model of SSc and in SSc patients.

Acknowledgements

My deepest thanks go to my supervisors and mentors Professor Christopher Denton Dr Alan Holmes and Dr Emma Derrett Smith for their continuous support, input, ideas and guidance throughout this thesis. I would also like to thank them both for the opportunity to participate in national and international conferences where I was exposed to world leading researchers in my field.

I would like to acknowledge the essential facility and financial support provided by the Centre of Rheumatology and Connective tissues Diseases, UCL. I would also like to thank the individuals who all contributed to this thesis; I would especially like to thank Dr Sarah Trinder who performed the *in-vivo* measurement of mean arterial blood pressure and right ventricular systolic pressures. I would also like to thank Dr Xu-Shi-Wen and Mr Robert Good for their experimental help and Dr Alan Holmes and Dr Emma Derrett Smith for having all the patience to teach me so many practical skills. In addition this work could not have been completed without the help of Rebekah Yu, Mark Portou, David Abraham, Markella Ponticos, Richard Stratton, Johanna Donavan and all the past and present staff in the Centre of Rheumatology for their continued help, support and friendship throughout my studies.

I would also like to express sincere gratitude to Dr Andrew Pearce of Novartis Pharmaceuticals for his guidance and support and to Novartis for providing an educational grant for completion of this thesis.

Finally I would like to thank my family and friends and in particular my mum and dad for their constant financial support and encouragement throughout my education. I dedicate this thesis to them because without them it would not have been possible.

Publications arising from this thesis

Peer reviewed journals

Derrett-Smith EC, DooleyA, **Gilbane AJ**, Trinder SL, Khan K, Baliga R, Holmes AM, Hobbs AJ, Abraham D, Denton CP.

Endothelial injury in a transforming growth factor β-dependent mouse model of scleroderma induces pulmonary arterial hypertension. *Arthritis Rheum* 2013, 11:2928-39.

Gilbane AJ, Denton CP, Holmes AM.

Scleroderma pathogenesis: a pivotal role for effector cells. *Arthritis Res Ther* 2013, **3**:215.

Gilbane AJ, Derrett-Smith EC, Good R, Trinder SL, Pearce A, Denton CP, Holmes AM.

Impaired BMPRII signalling in a TGFβ dependent mouse model of pulmonary hypertension and in systemic sclerosis *AJRCCM*

Good R, **Gilbane AJ**, Trinder SL, Denton CP, Coghlan G, Abraham DA, Holmes AM.

Endothelial to mesenchymal transition contributes to endothelial dysfunction in pulmonary arterial hypertension. *Am J Path*.

Selected presentations at national and international conferences

Gilbane AJ, Derrett-Smith EC, Trinder SL, Ahmed-Abdi B, Pearce A, Denton CP, Holmes AM.

Imbalance in TGFβ and BMP axis may contribute to the development of PAH in a novel murine model of SSc. Scleroderma Workshop Boston 2013, Poster presentation.

Gilbane AJ, Ahmed-Abdi B, Derrett-Smith EC, Pearce A, Denton CP, Holmes AM.

Altered cellular responses by a differentiated PASMC may contribute to the development of SSc-PAH. Scleroderma Workshop Boston 2013, Poster presentation.

Gilbane AJ, Derrett-Smith EC, Trinder SL, Pearce A, Denton CP, Holmes AM.

Altered BMP signalling may contribute to the development of PAH in a novel murine model of SSc. American College of Rheumatology 2013, Poster presentation.

Gilbane AJ, Derrett-Smith EC, Trinder SL, Pearce A, Denton CP, Holmes AM.

Altered BMP signalling may contribute to the development of PAH in a novel murine model of SSc. London Matrix Meeting 2013, Poster prize winner.

Gilbane AJ, Derrett-Smith EC, Good RW, Trinder SL, Pearce A, Denton CP, Holmes AM.

The role of TGFβ in the development of associated forms of pulmonary hypertension. Royal Free Hospital Graduate Day 2013, Oral Presentation.

Gilbane AJ, Derrett-Smith EC, Pearce A, Denton CP, Holmes AM.

Aberrant BMP signalling may contribute to the development of PAH in a novel murine model of SSc. World Scleroderma Congress, Rome 2013. Poster presentation.

Gilbane AJ, Derrett-Smith EC, Good RW, Pearce A, Denton CP, Holmes AM.

Altered cellular responses by a differentiated PASMC may contribute to the development of SSc-PAH. The International Society for Applied Cardiovascular Biology 2014, Poster presentation.

Gilbane AJ, Derrett-Smith EC, Good R, Trinder SL, Pearce A, Denton CP, Holmes AM.

Increased degradation of BMPRII in a TGFβ dependent transgenic model of scleroderma may underlie susceptibility to pulmonary hypertension. American Thoratic Society 2014, Poster presentation.

Gilbane AJ, Good RW, Derrett-Smith EC, Pearce A, Denton CP, Holmes AM.

Differentiated PASMCs share many cardinal features to those of PAH patients and contribute to endothelial dysfunction in the vasculature. European Society of Vascular Surgery 2014, Poster presentation.

Gilbane AJ, Derrett-Smith EC, Good R, Trinder SL, Pearce A, Denton CP, Holmes AM.

Increased degradation of BMPRII in a TGFβ dependent transgenic model of scleroderma may underlie susceptibility to pulmonary hypertension. American College of Rheumatology 2014, Poster presentation.

Table of Contents

List of Figures

List of Tables

List of Abbreviations

Alpha smooth muscle actin – α-SMA

Anti-centromere antibody - ACA

Anti-RNA polymerase antibody - ARA

Anti-topoisomerase I antibody – ATA

Beta-tubulin – β-tubulin

Bone marrow derived cells – BMDC

Bone morphogenetic protein – BMP

Bone morphogenetic protein one B – BMPRIB

Bone morphogenetic protein receptor one A – BMPRIA

Bone morphogenetic protein receptor two – BMPRII

Bromodomain – BRD

Caveolin-1 deficient mice - Caveolin-1

Chronic obstructive pulmonary disease – COPD

Chronic thromboembolic pulmonary hypertension – CTEPH

Collagen type-1, alpha-2, connective tissue growth factor mice - COL1α2-CTGF

Connective tissue growth factor – CTGF

Constitutively active transforming growth factor-β receptor 1 mice - TβR1CA Cre-ER

Diaminobenzidine – DAB

Diffusing lung capacity for carbon monoxide – DLCO

Distilled H20 - dH20

Dubecco's Modified Eagle Medium - DMEM

ECM – Extracellular matrix

Endothelial to Mesenchymal Transition – EndoMT

Enzyme-linked immunosorbent assay – ELISA

Epithelial to Mesenchymal Transition - EMT

Ethylenediaminetetraacetic acid – EDTA

FCS – Fetal Calf serum

Fibroblast to mesenchymal transition – FMT

Foetal bovine serum - FBS

Forced vital capacity – FVC

Fos-related antigen 2 transgenic mice - Fra-2 mice

Graft versus Host disease - cGvHD

Hematoxylin and eosin - H&E

Heritable pulmonary arterial hypertension – HPAH

Human Tissue Act – HTA

Hypochlorous acid - HOCl

Idiopathic pulmonary arterial hypertension – IPAH

Idiopathic pulmonary fibrosis – IPF

Immunoflourescence- IF

Immunohistochemistry – IHC

Interferon gamma – IFN-ϒ

Interleukin – IL

Interstitial lung disease – ILD

Intraperitoneally – IP

Matrix metalloproteinase – MMPs

Monocrotaline – MCT

Normal lung fibroblasts – NLF

Pericyte to Mesenchymal Transition - PeMT

Phosphate buffered saline – PBS

Plasminogen activator inhibitor -1 PAI-1

Platelet derived growth factor BB – PDGFBB

Pro–B-type natriuretic peptide - NT-proBNP

Pulmonary arterial endothelial cells – PAECs

Pulmonary arterial hypertension – PAH

Pulmonary arterial smooth muscle cells – PASMCs

Pulmonary artery wedge pressure – PAWP

Pulmonary fibrosis – PF

Pulmonary hypertension – PH

Quantitative polymerase chain reaction – qPCR

Right heart catheterisation – RHC

Right heart catheterisation – RHC

Right ventricular hypertrophy (right ventricle: left ventricle plus septum ratio - RV/LV+S

Scleroderma – SSc

Scleroderma associated pulmonary arterial hypertension – SSc-PAH

Scleroderma lung fibroblasts – SLF

Scleroderma renal crisis – SRC

Scleroderma renal crisis – SRC

Single nucleotide polymorphisms - SNPs

Specific pathogen free – SPF

Sugen – SU5416

Tight skin 1- mutation - Tsk-1

Tissue inhibitors of metalloproteinases – TIMP

Transforming growth factor-beta – TGFβ

Tumour necrosis factor – alpha – TNF-α

Tumour necrosis factor-alpha - TNF-α

TβRIIΔK, Kinase deficient type-II transforming growth factor-β receptor mice.

Vascular endothelial growth factor receptor – VEGFR

Von Willebrand Factor – vWF

Wildtype – WT

Wnt10b overexpressing mice - Wnt10b

World Health Organization – WHO

1. Introduction

1.1 Pulmonary hypertension

1.1.1 Pulmonary hypertension

Pulmonary Hypertension (PH) is defined by an elevated mean resting pulmonary arterial pressure (mPAP) greater than or equal to 25 mmHg at rest [1]. Pulmonary Hypertension (PH) is currently classified into five major groups based upon shared pathological, clinical features and treatment regimens (Table 1) [2]. The classification of PH was first determined at the inaugural World Health Organization's (WHO) scheme in 1973 [3]. The first major revision in 1998, divided PH into five separate groups based on clinical features and pathobiology [4]. Further revisions were made in 2003 leading to changing the term primary pulmonary hypertension to idiopathic pulmonary arterial hypertension (IPAH). The most recent WHO meeting took place in 2013 and no changes were made to the current classifications. The definition of PH will remain the same and experts decided there is still insufficient data to introduce the term "borderline PH" for patients with mPAP levels between 21 and 24 mm Hg [5]. However some debates continued mainly around whether the definition should be remain as resting mean mPAP greater than 25 mmHg at rest or should it defined as resting mean mPAP greater than 20 mmHg and should the term borderline PH be introduced for patients with an mPAP between 21 and 24 mmHg. Another question around the definition was should pulmonary vascular resistance be introduced to the definition of PH/PAH and is a pulmonary artery wedge pressure (PAWP) of 15 mmHg be appropriate to distinguish between pre-capillary and post-capillary PH and should PAWP be required to distinguish pre-capillary and post-capillary PH [6].

Group 1 is comprised of a diverse group of diseases and is termed pulmonary arterial hypertension (PAH), this group can be further sub-divided into IPAH; heritable PAH (HPAH) if there is a family history of PAH of which greater than 70% of patients have mutations in bone morphogenetic protein receptor 2 (BMPRII) [7]; or associated PAH (APAH) where other diseases are present such as the connective tissue disease systemic sclerosis (scleroderma/SSc). Group 2 is PH due to left heart failure, which previously has been reported to be the most frequent cause of PH, however this is now thought to be that associated with

schistosomiasis infection [8-11]. Group 3 is PH owing to lung disease and/or hypoxia. This includes chronic obstructive pulmonary disease (COPD), as well as interstitial lung diseases including idiopathic pulmonary fibrosis (IPF) and SSc. Group 4 is composed of chronic thromboembolic pulmonary hypertension (CTEPH) whereby obstruction of the pulmonary vasculature occurs due to thromboembolism, and may be revered by surgical intervention. Finally Group 5 is PH with unclear or multi-factorial etiologies. The pathological characteristics of PH are multifactorial and include, increased pulmonary arterial blood pressure, vascular remodelling of the pulmonary small arteries, right ventricular hypertrophy and ultimately, right ventricular failure [2].

1.1.2 Diagnosis

PH is suspected in any patient with unexplained dyspnea, breathlessness during minimal exercise and any sign of right ventricular dysfunction. PH is diagnosed by right heart catheterisation (RHC) because this method can determine if elevated PAP is due to increased precapillary resistance or postcapillary resistance [5]. Echocardiography cannot determine these differences but it can be used as an initial screening tool, to follow disease progression and response to therapy. The combination of the measuring biomarkers and the 6-minute walking test can be used to measure response to treatments in longitudinal trials and to manage disease progression [5].

Echocardiography continues to be the most commonly used non-invasive technique to suspect the development of PAH. One major problem with IPAH is the failure to detect the onset of disease for >2 years after the development of initial symptoms [12, 13]. Family screening occurs in patients with HPAH but due to low penetrance of BMPRII mutations there are some concerns about screening [14]. Patients with connective disease, HIV, congenital heart disease and liver disease are all screened for the development of PAH. There has been no new study based around these indications except for in SSc where the use of a two-step algorithm is improving the diagnosis of PAH in SSc [15]. The first step used in the DETECT study is to test patients for telangiectasia, anticentromere antibodies, right axis deviation on electrocardiogram, and reduced diffusing lung capacity for carbon monoxide (DLCO) and important serum biomarkers, urate and N-terminal pro–B-type natriuretic peptide (NT-proBNP). The second step in this study is the use of

echocardiography in patients with increased risk, followed by RHC to determine if the patient has PAH. Using this methodology, the number of missed PAH cases was 4% compared with 29% previously reported leading to earlier diagnosis and better treatment for patients [15].

1.1.3 Pathophysiology of PAH

PAH is characterised by excessive pulmonary vasoconstriction and vascular remodelling that can lead to the formation of concentric lesions, reduced blood flow, right heart failure and ultimately death. Alteration in cellular processes can contribute to this remodelling, altered proliferation and apoptotic resistance occurs in both endothelial cells and vascular smooth muscle cells (VSMCs) [16, 17]. It is also believed that changes in the microenvironment by increased secretion of the pro-inflammatory cytokines interleukin-6 (IL-6) and interleukin-8 (IL-8), increased levels of platelet derived growth factor two B chains (PDGFBB) and connective tissue growth factor (CTGF) may all contribute to the differentiation of pulmonary arterial smooth muscle cells (PASMCs) from a healthy to a disease relevant cell [18-20]. These changes in the microenvironment can induce these altered cellular responses and the production of extracellular matrix (ECM) [21]. The fibroblast also acquires a myofibroblast phenotype that exhibits increased proliferation and migration, these altered responses contribute to cells migrating and proliferating into the lumen of the pulmonary artery [22]. In healthy individuals there is a tightly regulated balance of locally released and circulating constrictive and dilatory agents. However in PAH, there is a rise in the levels of vasoconstrictors, for example endothlein-1 and serotonin and a decrease in vasodilators, for example prostaglandins and nitrous oxide [23].

It is also believed that the impact of BMPRII mutations and or a reduction in the receptors functionality can also contribute to remodelling. PASMCs isolated from control donors undergo apoptosis in response to bone morphogenetic protein (BMP) 2, 4 and 7 however patients harbouring BMPRII mutations are resistant to apoptosis [24]. It has also been reported that proliferation responses in PASMCs from HPAH patients and in the BMPRII (+/-) mouse model are altered. BMPRII reduction consistently conferred insensitivity to growth inhibition by transforming growth factor-beta 1 (TGF-β1) in both models in this study [17]. In comparison to PASMCS, BMP4 induced migration and tubule formation in endothelial cells, in PAH it is

hypothesised that survival of endothelial cells leads to occlusion of the lumen in the artery and the formation of concentric rings [25]. It has been shown that BMPs protect endothelial cells from apoptosis suggesting that a reduction in BMPRII contributes to the early endothelial dysfunction in PAH [26]. All of these different factors ranging from cellular switching, secretion of cytokines and altered cellular responses contribute to pathogenesis and development of PAH in patients.

1.1.4 The genetics of PAH

The genetics of PAH is constantly evolving with a host of germline mutations being reported to date. Initial work in the 1990s and early 2000s highlighted that altered BMPRII signalling is a major risk factor for the development of PAH via BMPRII gene mutations [27, 28]. The exact rate of BMPRII mutations in the general population is not known but it is believed to be quite low, in HPAH it is reported that around 70% of patients display BMPRII mutations. BMPRII mutations are also reported in IPAH and around 15% of IPAH patients have BMPRII mutations [27].

These studies highlighted the importance of the TGFβ superfamily and signalling and focused future studies to investigate this pathway in more detail. These genetic studies also highlighted that ALK-1, endoglin and Smad 9 mutations are also linked to the development of PAH and all of these mutations are members of the TGFβ superfamily.

The development of screening technologies has also led to the discovery of other mutations associated with PAH, for example the KCNK3 gene (Potassium channel, subfamily K, member 3) and the caveolin-1 gene (CAV-1) [27, 29]. The number of CAV-1 mutants with PAH is low but there is still an association and increased risk of developing PAH. Interestingly a reduction of caveolin-1 expression has been previously reported in the lungs of PAH patients and caveolin-1 has been reported to alter TGFβ signalling and reduce BMPRII signalling [30]. This mutation again highlights the importance of the TGFβ superfamily in the development of PAH.

Group 1: *Pulmonary arterial hypertension (PAH)*	Idiopathic (IPAH)	
	Heritable (HPAH)	Bone morphogenetic protein receptor type 2 (BMPR2) Activin receptor-like kinase 1 gene (ALK1), endoglin Unknown
	Drug- and toxin-induced	
	Associated with (APAH)	Connective tissue diseases
		Persistent pulmonary hypertension of the new-born (PPHN)
		Human immunodeficiency virus (HIV) infection
		Portal hypertension
		Congenital heart disease (CHD)
		Schistosomiasis
	Chronic haemolytic anaemia	
Group 2: *PH due to left heart diseases*		
Group 3: *PH due to lung diseases and/or hypoxia*	Chronic obstructive pulmonary disease (COPD)	
	Interstitial lung disease (ILD)	
	Sleep-disordered breathing	
	Alveolar hypoventilation disorders	
	Chronic exposure to high altitude	
	Other pulmonary diseases with mixed restrictive and obstructive pattern	
Group 4: *Chronic thromboembolic PH (CTEPH)*		
Group 5: *Haematological disorders*		

Table 1.1 The Nice 2013 disease classification of pulmonary hypertension

1.2 Scleroderma

Systemic sclerosis (SSc), also referred to as scleroderma is a complex heterogeneous autoimmune disease characterised by autoantibodies and pathological remodelling of connective tissues, which affects the skin and internal organs [18]. The most evident signs of SSc are manifested in the skin and it is to this that the disorder owes its original name, scleroderma (Greek: *skleros*, hard, and *derma*, skin). The most commonly adopted clinical classification for SSc is based upon the extent of clinical involvement of the skin, serological markers and natural history associations [31]. Clinically affected areas of skin are often referred to as involved, and regions clinically unaffected on the same patient as uninvolved. The classification based on skin involvement essentially divides the systemic disease into limited cutaneous SSc (lcSSc) and diffuse cutaneous SSc (dcSSc). In lcSSc fibrosis is mainly restricted to the extremities; whereas in dcSSc the skin involvement is more widespread, affecting the trunk as well as the hands, face and feet [32].

Pathologically SSc is divided into several processes: 1) microvascular injury; 2) inflammation and the development of autoantibodies; 3) accumulation of ECM and tissue fibrosis; 4) atrophy. Tissue fibrosis is almost universally preceded by microvascular dysfunction and inflammation in the development of the disease suggesting these phases represents an early stage in the disease process [32]. In SSc patients virtually all organ systems can be affected by fibrosis to varying degrees, however of major clinical significance are the heart, gastrointestinal tract, kidneys and lungs (Figure 1.1).

1.2.1 Auto-antibodies in SSc

Autoantibodies are present in the majority of patients with SSc, and may be used as an important diagnostic tool. Three major autoantibody groups anti-topoisomerase I (ATA), anti-centromere (ACA) and anti-RNA polymerase (ARA), have been described to be associated with different forms of SSc [33]. For example patients with ATA are associated with dcSSc [34], whereas ACA are more commonly associated with lcSSc patients [35]. A host of autoantibodies specific to SSc have been reported to be associated with, but not unique to, PAH, including ACA and anti-U3 ribonucleoprotein [36].

1.2.2 Epidemiology

The prevalence of SSc ranges from 30 to 300 cases per 1 million persons, and the incidence ranges from 2.3 to 22.8 cases per 1 million per year. Women are also at much higher risk of developing SSc than men with a slight increase in susceptibility for those of African heritage [32]. The overall survival rate in SSc patients is 60-83% at 5 years and 40-75% at 10 years depending on disease subset [37]. The cumulative frequencies of organ based complications from a cohort of SSc patients at the Royal Free are shown in Figure 1.1. A major cause of mortality currently associated with SSc patients are pulmonary complications, including pulmonary fibrosis (PF) and PH (Figure 1.1). The incidence of pulmonary fibrosis is significantly higher in dcSSc compared to lcSSc, whereas the incidence of PH is comparably in both disease subsets [38].

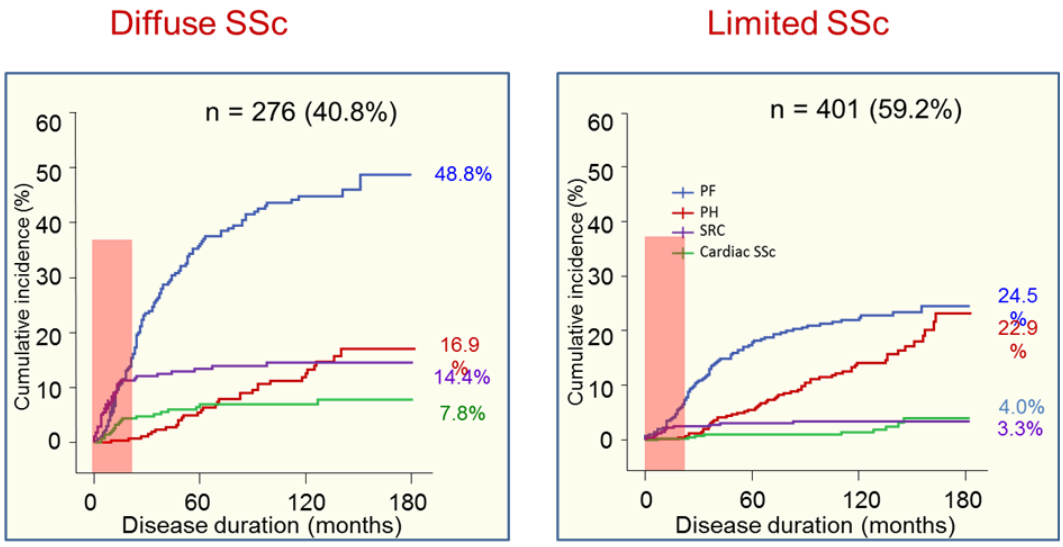

Figure 1.1. Organ based end-points in scleroderma (SSc) disease sub-sets: Kaplan Meir one minus survival curve of organ based complications in SSc, Adapted from [38].

These graphs highlight the cumulative incidence organ based complications including pulmonary fibrosis (PF, blue), pulmonary hypertension (PH, red), scleroderma renal crisis (SRC, purple) and cardiac SSc (green) in diffuse cutaneous systemic sclerosis (dcSSc) and limited cutaneous systemic sclerosis (lcSSc).

1.2.3 Pathophysiology of SSc

The pathophysiology of SSc is quite a complex process with vascular injury causing increased production of pro-inflammatory cytokines, for example interleukin-1 beta IL-1β, IL-6, IL-8 and growth factors like CTGF and type-1 collagen have all been previously reported to be elevated in SSc [39-43]. The changes in the microenvironment contribute to altered cellular responses and excessive deposition of ECM which can disrupt the tissue's architecture and phenotype leading to the development of fibrosis and atrophy [32]. SSc patients can develop complications in a host of different organ systems (Figure 1.1). The excessive deposition of ECM proteins that leads to fibrosis, the loss of tissue architecture, and ultimately the loss of function is also seen in the skin of patients. In the skin, fibrosis is initiated in the lower dermis and upper subcutaneous layer and leads to a decrease in appendages in the skin, loss of microvasculature and loss of reticular structure. The dermis is thickened in SSc due to the excessive accumulation of ECM [44]. The main focus of our work is based around pulmonary complications and the development of PAH in patients with SSc.

1.2.4 Vascular changes

Vascular injury represents the earliest disease manifestation in SSc, and consists of endothelial cell damage and the recruitment of leukocytes. Causing inflammation through the release of inflammatory mediators such as tumour necrosis factor-alpha (TNF-α), the release of degradative enzymes including matrix metalloproteinase (MMPs) and the production of reactive oxygen species [45]. A significant number of SSc patients exhibit vascular abnormalities; for example, Raynaud's phenomena is present in over 90% of SSc patients [46]. Vasculopathy can affect a number of tissues, including the digital vascular bed (digital ulcers), the kidney (SRC) and lung (PAH) [47]. In fibrotic human skin apoptotic endothelial cells have been detected in the inflammatory stage of disease [48]. Anti-endothelial cell antibodies, present in the serum of SSc patients, induce endothelial cell apoptosis *in-vitro* and may represent a link between immune dysfunction and vascular damage [48].

1.3 Pulmonary complications in SSc

Pulmonary complications of SSc are the leading cause of mortality in SSc. The major pathological complications associated with the lungs of SSc patients are PF and PH.

1.3.1 Pulmonary fibrosis in SSc

PF is observed in dcSSc and lcSSc with higher incident rates observed in the dcSSc group [38]. PF is characterised by excessive deposition of ECM proteins in the interstitium [18], and the loss of alveolar spaces and tissue architecture thereby preventing efficient gas exchange. It is a progressive disease which eventually leads to respiratory failure and premature death [49]. Idiopathic pulmonary fibrosis (IPF) is another form of fibrosis in the lung, IPF has a poor median survival from diagnosis of 3-5 years and an incidence in the United Kingdom of 4.6 per 100,000 people, and quite astonishingly the incidence between 1991 and 2003 increased each year by 11% [50]

Increased expression of proteoglycans and fibrillins are typical observed in the early stages of fibrosis whilst in later stages, type I collagen is the archetypal marker [32]. A key cell in the development of fibrosis is the fibroblast. Activation of this cell type plays a major role in the excessive deposition of ECM including fibronectin and collagen type I [18]. Activated fibroblasts present in wound healing are termed myofibroblasts and the activation of a fibroblast to a myofibroblast is potently induced by mediators such as TGF-β and PDGFBB which are two factors that are upregulated in SSc [51]. Interestingly, the kinase-deficient human type II TGFβ receptor (TβRIIΔk-fib) murine model, which has perturbed TGFβ signalling in explants of dermal and lung fibroblasts, represents a model of SSc exhibiting clinical and biochemical similarities to SSc patients [52-57].

1.3.2 Pulmonary hypertension in SSc

PH is defined as elevation in the blood pressure in the arties of the lung; greater than 25 mmHg at rest and is sub-divided into a number of groups. PAH (Group 1) results from specific vascular changes in the structure of vessels that in turn leads to the enhanced pressures. In contrast, the development of PAH associated to other underlying pathologies, such as the connective tissue diseases can be far more complex. SSc patients may develop elevated pulmonary pressures as a result of

clinically significant (20% of lung is fibrotic) PF, termed PH-SSc (Group 3; Table 1) or independently of major pulmonary fibrotic complications termed SSc-PAH (Group 1; Table 1). It is currently considered that around 15% of SSc patients develop PAH (Royal Free cohort). The overall prevalence of all types of PAH is estimated to be 30-50 cases per million [58]. Of these, the HPAH form of PAH represent a relatively small component of cases, 2-3 per million per year [58, 59]. The incidence of all PAH has been estimated to be between 6-60% of all patients [60]. SSc-PAH exhibits similar pathological changes to other forms of PAH including excessive pulmonary vasoconstriction, vascular remodelling and occlusion of the lumen and the occurrence of plexiform lesions [16, 61]. These processes that affect the intima, media and adventitia, lead to the narrowing of the lumen. These changes are associated with cellular changes in smooth muscle cell morphology, apoptosis of endothelial cells and proliferation of vascular cells including PASMCs endothelial cells and fibroblasts [16]. Collectively these processes lead to the narrowing and occlusion of the pulmonary arterioles.

Survival studies have shown patients with SSc-PAH have a particularly poor prognosis compared to those with PAH alone, with 1-year survival estimated at 55% compared to 84% in HPAH patients [62, 63].

1.3.3 Treatment of pulmonary fibrosis in SSc

Pulmonary fibrosis occurs in 48% of dcSSc and 25% of lcSSc patients and their prognosis is poor [38]. Immunosuppressive therapy is selected for patients with severe and progressive PF, cyclophosphamide is one drug of choice and has been shown to improve patient's forced vital capacity (FVC) and mycophenolate mofetil also exhibits efficacious results in patients with SSc-ILD [64-66]. Other therapies of choice are N-acetylcysteine, this drug has exhibited beneficial effects when added to standard treatment of azathioprine and prednisone, compared to that treatment alone. In end-stage cases and severe disease, lung transplantation can be considered [67-69]. Until recently there was no treatments have been approved for pulmonary fibrosis recent clinical trials have shown that pirfenidone and nintedanib has had significant improvements for patients [70]. Pirfenidone is a novel anti-fibrotic, anti-inflammatory drug that has demonstrated efficacy and safety in IPF patients. The mechanism of this drug is not completely understood but it is believed it exerts its

action by inhibiting fibroblast proliferation. Nintedanib is a tyrosine kinase inhibitor that has also been approved for the treatment of IPF patients [71].

1.3.4 Treatment of pulmonary hypertension in SSc

Survival studies have shown patients with SSc-PAH have a particularly poor prognosis compared to those with PAH alone, with 1-year survival estimated at 55% compared to 84% in HPAH patients [62]. General treatment of the PH involves diuretics, anticoagulation, oxygen and Digoxin for the treatment of heart failure with exercise also proving beneficial [72]. The specific therapies available to patients are divided into three main classes the phosphodiesterase-5 inhibitors (sildenafil and tadalafil), endothelin receptor antagonists (bosentan, ambrisentan and recently macintentan) and the prostanoids (iloprost and treprostinil) [73].

1.4 Vascular muscularisation in the development of PAH

A cardinal feature of SSc-PAH is the remodelling of blood vessels that leads to the occlusion of the vessel and contributes to a rise in pulmonary pressures [74]. The migration and proliferation of α-SMA positive cells including both fibroblasts (myofibroblasts) and PASMCs are the main mediators of pulmonary vascular remodelling.

1.5 The fibroblast in SSc

The connective tissue confers a structural scaffold that facilitates organ function. Composed of ECM, the most common cell found in the connective tissues are spindle shaped cells termed ‘fibroblasts’. These cells express vimentin, but not desmin or α-SMA are found in the majority of organs, and are essential for connective tissue homeostasis [75]. An imbalance in the deposition of ECM proteins including collagen type I and III leads to the pathological changes observed in SSc. Fibroblasts are highly active cells and each cell synthesises approximately 3.5 million pro-collagen molecules per cell per day [76]. Fibroblasts regulate matrix turnover through the expression of MMPs, which degrade ECM, and inhibitors of MMPs - tissue inhibitors of metalloproteinases (TIMP). Consistent with increased ECM deposition in SSc patients, serum levels of TIMP in dcSSc and lcSSc are significantly raised compared to healthy controls [77]. This supports the hypothesis that fibroblast regulated matrix accumulation occurs through an imbalance in turnover of the ECM and this plays a pivotal role in SSc [77].

Fibroblasts are also key contributors to fibrosis in patients with SSc. In healthy individuals fibroblasts are protected from stress by the surrounding ECM, during connective tissue diseases the damaged fibroblasts are no longer protected causing the fibroblasts to attach to the ECM [78]. Upon tissue injury, fibroblasts migrate towards the wound and due to the presence of growth factors released by immune and blood cells the fibroblasts differentiate into a secretory myofibroblasts that are involved in repair during wound healing [18].

1.5.1 Fibroblast to myofibroblast transition

In response to tissue injury mesenchymal cells of fibroblastic lineage accumulate at the wound site and deposit and remodel new ECM and contract the wound site. The main fibroblastic cells responsible for this process are termed myofibroblasts and exhibit specific markers and phenotypic properties that are suited to this role. Normally as wounds repair and resolve myofibroblast are lost from the site of injury, whereas in fibrotic pathologies such as SSc, they remain [79-83]. The persistent and accumulation of large numbers of myofibroblasts in connective tissues is responsible for the exaggerated and uncontrolled production of ECM during the development and progression in fibrotic pathologies such as SSc [75, 80]. Myofibroblasts can arise from resident fibroblasts in a process termed fibroblast to myofibroblast transition or fibroblast to mesenchymal transition (FMT) as shown in Figure 1.2 [75]. More recently it has become recognised myofibroblasts can arise from different cellular sources, including pericytes, smooth muscle and epithelial cells via a number of biological processes.

Histological analysis of SSc skin has shown an abundance of myofibroblasts involved in lesional skin and fibrotic areas of the visceral organs from SSc patients [75, 84]. Gene expression profiling studies demonstrate a number of genes are differentially regulated in wound healing fibroblasts to those derived from fibrotic regions of SSc patients [85]. Furthermore, comprehensive transcriptional analysis of skin biopsies has demonstrated differences in the gene expression profile of dermal fibroblasts from SSc patients into subsets including inflammatory and TGFβ gene signatures [86, 87]. The different gene expression profiles exhibited by fibroblasts from SSc patients may reflect the diverse origins of the cells that contribute to the formation of myofibroblasts. It remains unclear if SSc fibroblasts arising from these diverse cellular pools will respond to similar therapeutic interventions, and future

studies will be needed to explore the relevance to the pathological development of fibrosis in SSc patients [88-90].

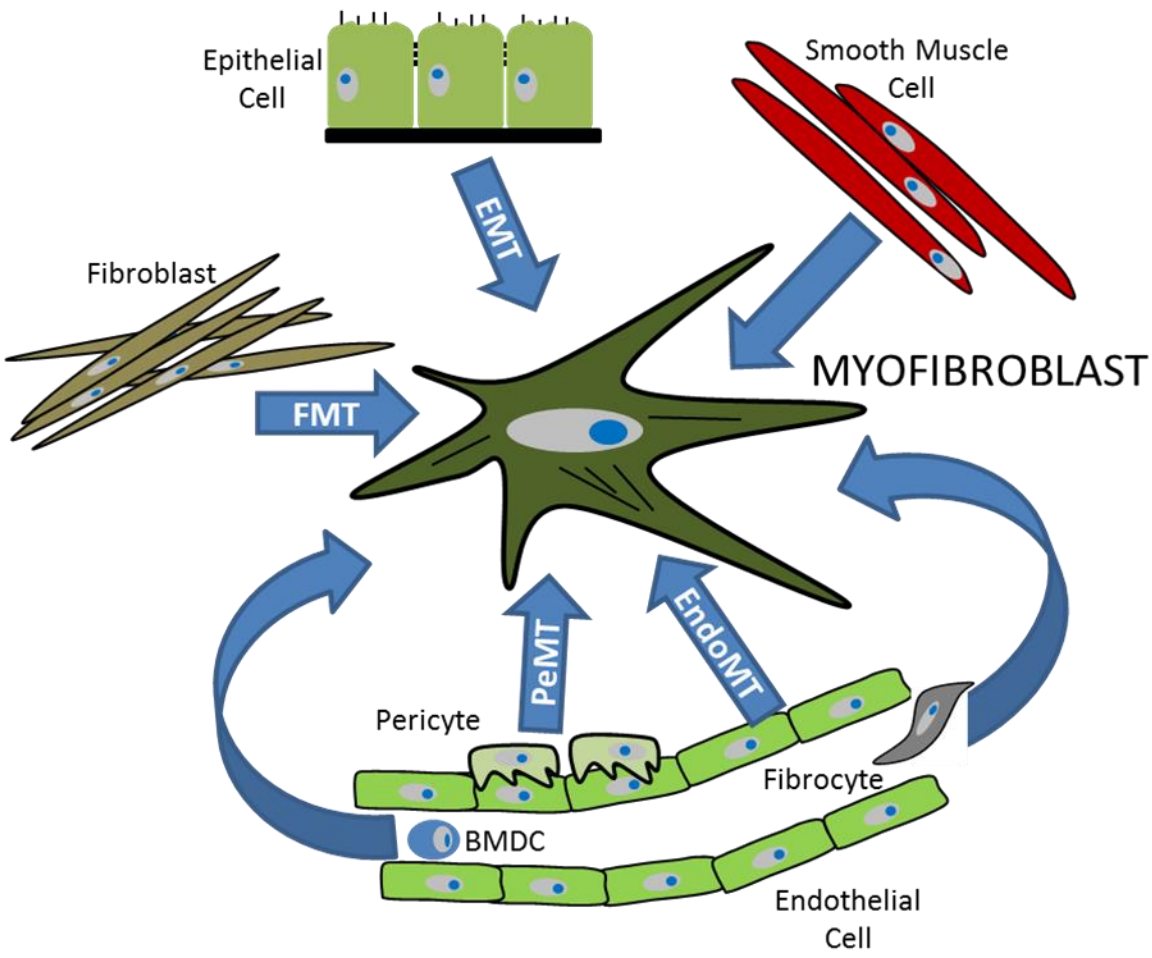

Figure 1.2 – The cellular origins of 'activated' fibroblasts and myofibroblasts

Myofibroblasts may arise from a number of cellular sources. The differentiation and activation of tissue resident cells: Fibroblast to, myofibroblast transition (FMT); Endothelial to Mesenchymal Transition (EndoMT); Epithelial to Mesenchymal Transition (EMT); Pericyte to Mesenchymal Transition (PeMT); Smooth muscle cell differentiation. The recruitment and differentiation of circulating bone marrow derived cells (BMDC) and fibrocytes may also contribute to the myofibroblast population.

1.5.2 Positional identity of fibroblasts – relevance to SSc

Fibroblasts isolated from different tissues display similar morphology, however exhibit diverse functional properties. For example, the capacity of fibroblasts from different anatomical sites to migrate, or express extracellular matrix proteins varies [91]. These differences are consistent with the wide variety of biological and physical environments these cells are found in. Chang *et al* elegantly highlighted the 'positional memory' of fibroblasts in gene expression profiling studies of fibroblasts from a variety of anatomical sites in the adult and foetus [92]. A striking feature in this study was the distinct and characteristic transcriptional patterns displayed by fibroblasts, including genes associated with lipid metabolism, the TGFβ and Wnt cell signaling pathways, as well as fate determination [92]. This study highlighted the context dependent activity of fibroblasts to generate appropriate extracellular microenvironments. For example, foetal lung and skin fibroblasts expressed high levels of the basement membrane protein type IV collagen in the skin and lung alveoli. In contrast, skin not lung fibroblasts, expressed significant levels of type I and V collagen that confers the tensile strength in the dermis [92]. Consistent with the different anatomical environmental requirements of organs, fibroblasts exhibit distinct immune-modulatory effects on leukocytes including recruitment [91]. The mechanism(s) by which fibroblasts acquire their positional identify remains unclear; however it is likely epigenetic mechanisms play a significant role [18, 93]. It remains to be investigated if SSc fibroblasts lose their positional identity and if this in turn promotes the development of a pro-fibrotic environment. It is plausible that location-specific signatures for fibroblasts and other cell types explain the diverse patterns of fibrosis between and within different subsets of SSc [18].

1.5.3 Origin of fibroblasts in SSc: resident cells, trans-differentiation, and circulating fibrocytes

The origin of activated fibroblasts or myofibroblasts in fibrotic tissues was, until comparatively recently believed to result from the expansion and activation of resident fibroblasts [75, 94]. However, recent studies have highlighted the potential for other tissue resident and blood borne cells to contribute to the pool of myofibroblasts that arise in fibrotic tissues [95-97]. A number of tissue resident cells including endothelial, epithelial and SMCs can differentiate into fibroblast like cells [95, 96, 98, 99]. In addition to tissue resident cells, blood borne cells such as

fibrocytes also contribute to the heterogeneity of these myofibroblasts (Figure 1.3) [100].

The differentiation of resident cells has been proposed as an important mechanism that contributes to the development of tissue fibrosis in SSc (Figure 1.3). For example, endothelial to mesenchymal transition (EndoMT) was thought to be a rare phenomenon confined to embryonic development, however Arciniegas *et al* elegantly demonstrated the capacity of adult endothelial cells to lose vascular markers such as E-cadherin and acquire myofibroblast markers, including α-SMA and type I collagen [96]. Consistent with a putative pathological role of EndoMT in SSc, the bleomycin murine model of pulmonary SSc suggests lung capillary endothelial cells have been shown to contribute to the pool of myofibroblasts/fibroblasts present in the bleomycin model of pulmonary SSc [95]. Like EndoMT, epithelial cells in a process termed epithelial to mesenchymal transition or EMT is induced by TGF-β [95].

EMT has been linked to cellular differentiation and tumour invasion for a number of years [14]. More recently EMT has become strongly associated with renal and pulmonary fibrosis in pre-clinical models [101]. However, it remains contentious the contribution of EMT in the development of fibrotic pathologies including SSc. During EMT, epithelial cells down regulate epithelial markers, such as E-cadherin and acquire mesenchymal/myofibroblast markers including α-SMA [75, 97]. EMT, like EndoMT are likely to lead to significant loss of the functional capacity of these cells to act as biological barriers, and contribute further to the development of fibrosis. EMT can be induced by a number of secreted factors including TGFβ, CTGF and fibroblast growth factor-2 FGF-2 all of which have been implicated in remodelling diseases as well as SSc [102]. For example, in SSc patients TGFβ is elevated in serum and several studies have demonstrated activation of components of the canonical and non-canonical TGFβ signalling pathway. Studies from our own group have further highlighted a cellular link between microvascular damage and fibrosis via pericyte trans-differentiating into myofibroblasts (PeMT) [103]. The presence of activated pericytes in dcSSc skin and the capability of these cells to transition into myofibroblasts when activated, further support their likely contribution dermal fibrosis in SSc [104].

In addition to local precursors, circulating cells are also able to contribute to the myofibroblasts that populate fibrotic tissues. For example, TGFβ promotes fibroblast to myofibroblast transition (FMT); endothelial to mesenchymal Transition (EndoMT); epithelial to mesenchymal Transition (EMT); pericyte to mesenchymal Transition (PeMT); and smooth muscle cell differentiation. In addition ET-1 promotes the recruitment and differentiation of circulating fibrocytes which are likely to contribute to the SSc fibroblast population. (Figure 1.3). Fibrocytes were initially described in early 1990s as blood borne collagen-producing cells, with antigen presenting capability [105]. Since then, they have been associated with a broad range of fibrosing disorders including SSc, sickle cell lung disease, asthma, PH and atherosclerosis, [106-110] Although the cell surface markers that identify fibrocytes remains ambiguous, it is widely accepted that these cells share immune and mesenchymal cell surface markers [111] and migrate to sites of tissue injury [112]. The pre-clinical bleomycin insult model, which serves as a model of SSc fibrosis, exhibits enhanced fibrocyte recruitment in the dermis and lung, supporting the notion that fibrocytes play a key role in SSc [101, 107]. Previous studies have demonstrated mice dosed with adenosine A_{2A} (A_{2A}) antagonists were protected from the development of bleomycin induced lung fibrosis [113]. The use of these A_{2A} antagonists also halted lung fibrocyte recruitment, suggesting that these receptors are involved in fibrocyte recruitment and supporting the contribution of fibrocytes in the development of pulmonary fibrosis [107]. Consistent with fibrocyte recruitment to sites of tissue injury, these cells express a number of chemokine receptors, including chemokine receptor type 4 (CXCR4). Analysis of SSc patients demonstrated the presence of CXCR4+/collagen type I + cells only in SSc-ILD patients. Furthermore, the expressions of CXCR4, and its ligand stromal cell-derived factor 1 (CXCL12), were also highly upregulated in SSc lung compared to healthy controls [27]. The SSc lungs that overexpress CXCR4 also lack caveolin-1 (Cav-1), and display enhanced monocyte migration compared to controls. In the bleomycin model the use of caveolin scaffolding domain (CSD) diminishes fibrocyte accumulation in the lung and may represent a novel therapy in SSc [109].

The cellular origin of the mesenchymal cells that contribute to the excessive accumulation of ECM and loss of tissue architecture in SSc fibrosis remains unclear. Indeed the contribution through the cellular processes that give rise to these cells,

including expansion of resident tissue fibroblasts, EMT, FMT and accumulation of bone marrow–derived and circulating fibrocytes that have been reported may vary in an organ specific manner (Figure 1.3). Future studies will be required to assess the relative contribution and therapeutic relevance in SSc.

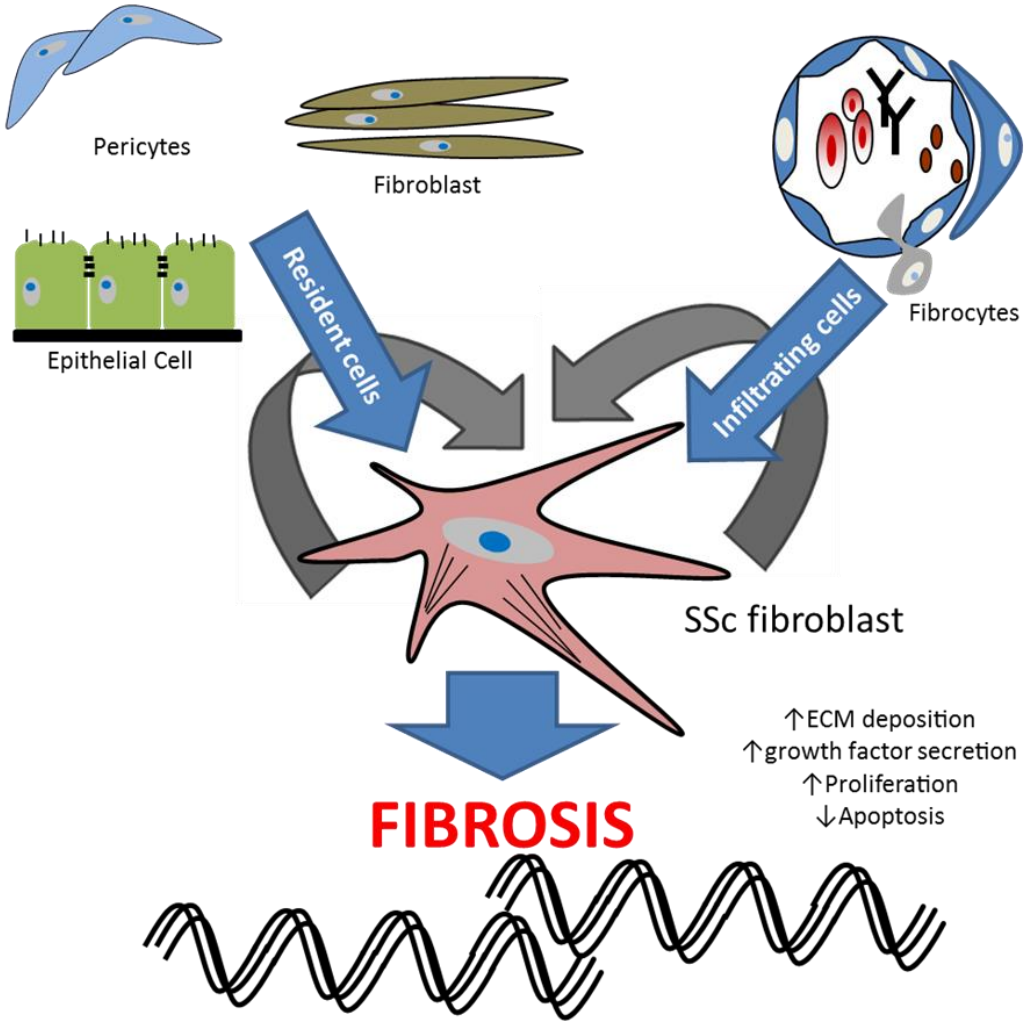

Figure 1.3 – SSc fibroblasts promote a pro-fibrotic microenvironment

SSc fibroblasts secrete elevated growth factors, chemokines and cytokines including endothelin-1 (ET-1), transforming growth factor-beta (TGFβ) and connective tissue growth factor (CTGF), which promote a pro-fibrotic microenvironment that can act in an autocrine and paracrine manner to expand the pool of pro-fibrotic fibroblasts in lesions

1.6 Smooth muscle cells

Vascular smooth muscle cells (VSMCs) are essential for normal vascular functions, and pathological changes are associated with a number of diseases including PAH [21, 114]. PASMCs in mature adults are predominantly involved in the contraction of the pulmonary arterioles and maintenance of normal blood flow and pressure [21]. In comparison to both skeletal or cardiac muscle which are terminally differentiated, VSMCs are unique due to their plasticity and their ability to undergo reversible changes in response to changes in stimuli from their local environment which normally maintain a contractile phenotype [21, 115].

1.6.1 Factors that contribute to SMC differentiation in SSc-PAH

In adults SMCs can adopt two different phenotypes known as contractile and synthetic SMCs and it is believed that these PASMCs play a key role in vascular remodelling in SSc-PAH [16]. PASMCs play an essential role in the maintenance of the vasculature [16]. Under normal circumstances PASMC are maintained in a contractile phenotype, however under pathological conditions these cells may de-differentiate into a synthetic phenotype. Contractile and synthetic SMCs differ in their cellular activities. For example, contractile SMCs are less proliferative and migratory than synthetic SMCs [21], whereas synthetic SMCs deposit more matrix proteins such as collagen-type I [21]. The switching of a contractile SMC to a synthetic cell type plays a key role in PAH by promoting vascular remodelling and occlusion of the vessel [21]. The maintenance of a healthy contractile cell is determined by a host of factors including hypoxia, cell-to-cell contact, growth factors and cellular injury. It has been previously highlighted that BMPs promote a contractile SMC phenotype which is characterised by the up-regulation of the contractile marker α-SMA; while the addition of PDGFBB in culture to PASMCs reduces the expression of α-SMA promoting a synthetic SMC phenotype (52). In HPAH, 70% of patients have mutations in the BMPRII gene (53), which leads to a reduction in the expression of functional BMPRII receptors on the cell surface and reduced responsiveness to BMP ligands. This dysregulation of BMP signalling in patients with HPAH is likely to play a role in the normal homeostasis of PASMCs and their phenotypic modulation promoting differentiation from a contractile to synthetic phenotype [20].

1.7 Animal models of SSc

1.7.1 Transgenic models of SSc

A number of animal models have been extensively used to explore the pathological mechanisms of SSc, perhaps the most well studied being the bleomycin insult model and the tight skin mouse (TSK; Table 1.2). However these models lack the pathological changes associated to SSc-PAH. More recently a number of transgenic models have sought to recapitulate the systemic features of SSc. A transgenic model is a model that has been genetically modified, for example by the transfer of a gene to create a phenotype that is similar to a disease of interest. Genetics in biology is the study of genes and genetic variation in organisms. The alteration of gene expression in transgenic models similar to genetic mutations in humans can lead to the development of disease. For example the TβRI^{CA}/Cre-ER and TβRIIΔk-fib transgenic mouse models have sought to modulate the TGFβ pathway and exhibit many of the pathophysiological changes observed in SSc patients (Table 2). The fos-related antigen (FRA-2) [116] and TβRIIΔk-fib transgenic mouse models of SSc develop pulmonary vasculopathies independently of pulmonary fibrosis, and thus represent a Group I SSc-PAH model. In contrast the bleomycin model develops raised right ventricular systolic pressure (RVSP) as a result of pulmonary fibrosis and more closely represents a more Group 3 PH-SSc model [117].

The TβRIIΔk-fib transgenic mouse model expresses, under the control of the collagen 1α2 enhancer/promoter, a kinase-deficient TβRII gene. These animals exhibit a paradoxical enhancement in TGFβ signalling, including activation of the canonical Smad signalling pathway, Smad2/3 [52]. Consistent with the observed phenotype of the TβRIIΔk-fib transgenic mouse model, Loeys-Dietz syndrome patients who possess TβR-II mutations exhibit increased expression of collagen and CTGF, as well as increased phosphorylated Smad2 in the nuclei, which is indicative of increased TGFβ signalling [118].

The TβRIIΔk-fib transgenic mice exhibit increased expression of latent TGFβ in the ECM and develop dermal fibrosis, as well as fibrosis in a number of internal organs, including the gut and lung [54, 57]. Furthermore, intratracheal administration of

bleomycin to these mice induced the appearance of myofibroblasts, and increased apoptosis of type II alveolar epithelial cells [55]. Interestingly these mice exhibit vascular defects in the lung independently of pulmonary fibrosis [56].

The administration of SU5416 (a VEGR2 antagonist) further enhanced the vasculopathy of this model including more severe vascular remodelling and a further enhancement in RVSP [119]. SU5415 also contributes to a further increase in TGFβ activity with increased phosphorylated Smad2/3 positive nuclei similar to that observed in PAH patients. Collectively this suggests the TβRIIΔk-fib transgenic mouse model may represent a good model to understand the molecular mechanisms that contribute to the development SSc-PAH.

The FRA-2 transgenic mouse model is another model of SSc that exhibits a pulmonary vasculopathy. These mice also exhibit dermal and lung fibrosis which is highlighted in histological studies by an increase in ECM (Table 2.1). FRA-2 is also overexpressed in patients with pulmonary fibrosis and this suggests that this model is representative of this cohort of patients [120]. In another study the FRA-2 mice were used alongside the chronic Graft versus Host disease (cGvHD) and tight skin 1-mutation (TSK-1) models to determine the best model of cardiac complications in SSc patients. Histological analysis highlighted accumulation of collagen in the hearts of SSc patients and FRA-2 mice in comparison to no rise in collagen expression in the cGvHD and Tsk-1 models suggesting the FRA-2 model better represents cardiac complications in SSc [121].

The Cav-1 transgenic mice are another example of murine model of SSc and these mice develop skin and lung fibrosis due to Cav-1 deficiency as highlighted in (Table 1.1). The loss of caveolae leads to the initiation of fibrosis that is observed histologically in the lungs with marked hypertrophy of type II pneumocytes [122, 123].

In terms of all the transgenic models of SSc, each individual model offers different platforms for different cohorts of patients. The FRA-2 mouse seems to replicate the best model for cardiac complications in SSc with these mice displaying loss of capillaries due to endothelial cell apoptosis similar to patients [121]. But the TβRIIΔK model of SSc and SSc-PAH is a representative model of patients with SSc-PAH due to similarities observed in vascular remodelling and pulmonary

vasculopathy [119]. Due to the heterogeneity of SSc each model offers differential benefits depending on the disease characteristics each patient displays.

1.7.2 Spontaneous models of SSc

The TSK models, TSK has a spontaneously occurring dominant mutation of the fibrillin-1 gene which results in a partial inframe duplication of fibrillin-1 leading to an altered phenotype that exhibits skin and lung fibrosis. In the skin cutaneous, fibrosis is observed and the mice also produce autoantibodies to SSc specific antigens [124]. Interestingly a genetic study identified single nucleotide polymorphisms (SNPs) in the fibrillin-1 gene in Japanese and Choctaw populations that increased the risk of developing SSc [125]. Microarray studies comparing the TSK-1 mouse to WT controls showed no difference in pro-fibrotic genes, nor activation in the TGFβ axis suggesting there is some weakness in this model [126]. A recent comparative study between TSK-1 and WT mice, exhibited an increase in collagen in the hearts of TSK-1 mice compared to WT. Interestingly, the collagen content of hearts from TSK-1 and WT males was amplified in comparison to their relative female mice. However no significant differences in collagen content were observed in the lung or kidney between the TSK-1 and WT mice [127]. The TSK2/+ mouse has also been proposed as a murine model of SSc. These mice only demonstrate skin fibrosis (Table 1.1), which can be seen by increased collagen synthesis and accumulation in the dermis. There is also evidence of mononuclear cell infiltration into the dermis of these mice. Furthermore, the TSK2/+ mouse has numerous auto-antibodies within its plasma, some of which are common to patients of SSc [128].

1.7.3 Chemical injury models of SSc

The bleomycin model is a model of skin and lung fibrosis and also a model of PH-SSc [117, 129, 130]. The bleomycin model is one of the most extensively used models in SSc research and provides many of the key features associated with SSc. This model exhibits both skin and lung fibrosis (Table 1.1) depending on the route of administration of the bleomycin. The administration of repeated subcutaneous injections of bleomycin leads to a model of skin fibrosis that recapitulates many key features of SSc: increase in collagen deposition, vascular thickening and inflammatory infiltrates [131]. It was also observed that there was an upregulation of TGFβ receptors and a rise in cytokines like IL-6 in serum [131]. The administration

of intratracheal bleomycin induces lung fibrosis in mice. Histological analysis of the lung highlighted an increase in collagen content and an increase in inflammatory infiltrate [132]. It has also been published that bleomycin induced lung fibrosis leads to enhance RVSP and a reduction in BMPRII levels suggesting it represents a strong model of PH-SSc as well as SSc alone [133].

Table 2.1. Murine models of SSc fibroblast dysfunction: Comparison of mouse models of SSc that exhibit fibroblast driven pathophysiology.

	Model	Skin	Lung	Kidney	Heart	Gut	Vessels
SSc Murine Models	**Transgenic**						
	TβRIIΔK	✓ [52]	✓ [52]			✓ [57]	✓ [56]
	TβR1^{CA};Cre-ER	✓ [134]	✓ [134]	✓ [134]			✓ [134]
	COL1α2-CTGF	✓ [135]	✓ [135]	✓ [135]			✓ [135]
	Fra-2	✓ [120]	✓ [120]		✓ [121]		
	Caveolin-1	✓ [123, 136]	✓ [123, 136]				✓[123, 136]
	Relaxin	✓ [137]	✓ [137]	✓ [137]	✓ [137]		
	Wnt10b	✓ [138]					
	Spontaneous						
	Tsk-1	✓ [124]	✓ [124]				
	Tsk-2	✓ [128]					
	Insult models						
	Bleomycin	✓ [131]	✓ [95]				
	HCLO	✓ [139]	✓ [139]				

TβRIIΔK, Kinase deficient type-II transforming growth factor-β receptor mice. **TβR1^{CA} Cre-ER**, constitutively active transforming growth factor-β receptor 1 mice. **COL1α2-CTGF**, Collagen type-1,alpha-2,connective tissue growth factor mice. **Fra-2**, fos-related antigen 2 transgenic mice. **Caveolin-1**, caveolin-1 deficient mice. **Relaxin**, relaxin knockout mice. **Wnt10b**, Wnt10b overexpressing mice. **Tsk-1**, tight-skin mice 1. **Tsk-2**, tight skin mice 2. **HCLO**, hypochlorous acid.

1.8 Animal models of pulmonary hypertension

A number of rodent models have been developed to model the development of pulmonary hypertension, the most commonly used models are the monocrotaline (MCT), the chronic hypoxic model and the combination of hypoxia and the systemic administration of the tyrosine kinase inhibitor, SU5416 (Sugen; Sigma Chemicals,UK) to C57BL/6 mice maintained in hypoxia. All of these models have been shown to recapitulate many of the features of PAH [140, 141].

1.8.1 Chronic hypoxia

Chronic hypoxia (10% O_2) is a common model of PH, both normobaric and hypobaric hypoxia and has been used to induce PH in many different animals including murine, rodent and bovine models [142-145]. The hypoxia model is a robust model of PH and shows high reproducibility between age matched animal strains however there is inter species variation [144]. The most common models used for PH research are the mouse and rat models, where the rodents are exposed to hypoxia for 21 and 14 days, respectively. These models display muscularisation and expansion of α-SMA positive cells, myofibroblasts and SMCs [144, 146]. The changes in the microenviroment induced by chronic hypoxia leads to hyperplasia and anti-apoptotic features in SMCs [147-150]. BMP ligands play a key role in regulating apoptosis in the pulmonary artery and the reduction of BMPRII at both a protein and gene level contributes to apoptotic resistance in SMCs, because BMP ligands are unable to induce their normal apoptotic effect [151]. In concordance with a reduction in BMPRII, an increase in plasminogen activator inhibitor-1 (PAI-1) gene expression is observed in the lung and histological analysis also shows a rise in phosphorylated Smad 2/3 levels, which is indicative of enhanced TGFβ signalling [146]. Direct comparisons between the hypoxia and MCT model have suggested that the MCT model exhibits a more exacerbated response with greater TGFβ activity and reduction in BMPRII [146]. These features are similar to what is observed in PAH patients with a reduction in BMPRII expression and enhanced phosphorylated Smad2/3 levels observed in muscularised vessels and concentric lesions [152]. In terms of muscularisation there is a rapid increase in thickening of the pre-capillary pulmonary arteries due to the expansion and hypertrophy α-SMA positive cells. It is also believed that this model is a pro-inflammatory model with an increase in cytokines and mononuclear inflammatory cells observed in the lung [153]. It has

been noted that there is thickening in the larger proximal arteries are observed in rats and after 2 weeks there is approximately a doubling in RVSP with very little studies reported RV failure [154]. Although this model recapitulates some features of PH, there is very little endothelial dysfunction observed akin to patients with severe PH, so a double hit model involving hypoxia and agents that induce endothelial dysfunction were investigated.

1.8.2 Sugen/hypoxia model

The sugen/hypoxia model is a recently developed model of severe pulmonary hypertension with enhanced vessel musculurisation and endothelial cell dysfunction compared to hypoxia alone [141, 155]. The addition of a vascular endothelial growth factor (VEGF) receptor antagonist sugen to the hypoxia model led to endothelial dysfunction due to uncontrolled proliferation of endothelial cells [140]. Hypoxia alone caused expansion of α-SMA positive cells but in combination with sugen more profound muscularisation was observed. The first study using this model was reported by Taraseviciene-Stewart *et al* and this pilot study investigated different dosing regimens of sugen to initially optimise the model [140]. Sugen was administered as a single dose 200 mg/kg at the commencement of the experiment or multiple doses of 200 mg/kg or 20 mg/kg once weekly for 3 weeks. Rats in all three groups exhibited a significant increase in RVSP with very little difference observed in each of the three groups. Histological analysis using α-SMA confirmed expansion of smooth muscle cells and a reduction in VEGFR2 staining in and an increase in caspase-3 staining in the sugen/hypoxia group suggested endothelial cell death and dysfunction leading to muscularisation of the pulmonary artery [141]. Other studies using this rodent model explored signalling pathways that are relevant to patients with PAH. Interestingly the addition of sugen to the hypoxia model has no additive effect to the reduction of BMPRII induced by hypoxia but it does lead to a further enhancement of TGFβ signalling due to an increase in phosphorylated Smad2/3 and PAI-1 expression in whole lung [140, 141, 155] This study used mice rather than rats, muscularisation observed in mice was not as severe as in rats but medial wall thickening and concentric lesions were still observed [140]. Although some components of this model are shared with PAH patients, such as reduced BMPRII and increased TGFβ signalling; gene-array studies showed that modification in a mere four genes were shared between lungs isolated from this model and lungs from

patients with PAH [156]. There have been other doubts in this model as previous publications have reported that sugen exerts its effect on the lung alone and does not cause changes to other organs [144].

1.8.3 Monocrotaline model

MCT, a plant alkaloid was first shown in 1967 to induce muscularisation of the small and medium arteries, an increase in the number of cells positive for α-SMA, in addition to increased pulmonary pressures of up to 80 mmHg in rats [157, 158]. Similarly, prolonged exposure to hypoxia induces elevated pulmonary pressures in both mice and rats and vascular muscularisation, although the latter is less pronounced in mice [144]. However, the MCT and hypoxia models lack some of the pathological changes observed in patients such as endothelial cell dysfunction [159]. There have been some reports to suggesting that there might be some endothelial cell dysfunction but pulmonary arterial medial hypertrophy is the main way in which the model has been characterised. It still remains unclear whether MCT induced endothelial cell damage leading to uncontrolled proliferation of SMCs or whether the MCT is inducing endothelial-mesenchymal transition. These ambiguities by which MCT induces PH is another limitation of the model and the understanding of the initial endothelial cell damage leading to SMC hypertrophy needs to be better understood [159, 160]. There has also been report of toxicity in other organs with changes observed in veins, liver and kidney as well as reports of myocarditis which affects both the left and right ventricle [161], There has been extensive publications reporting that more than 30 potential treatments/agents of PH are able to reverse or prevent PH in the MCT model which does not recapitulate in human PH, suggesting further limitations as a pre-clinical model of PH [144, 161].

1.8.4 BMPRII knock out and hypoxia model

As previously discussed BMPRII mutations play a key role in the development of some forms of HPAH and IPAH, however it has been reported that not all people with BMPRII mutations develop PAH [162, 163]. This suggests that BMPRII mutations alone do not cause PAH but they predispose patients to the development of the disease in combination with other factors. Since BMPRII mutations are important in the disease, animal models that are BMPRII centric are essential to recapitulate this specific cohort of patients. One group of HPAH patients have

heterozygous mutations in the BMPRII protein so mice harbouring this mutation were generated to investigate the effect of these mutations on the vasculature. Initially mice were generated with global deletion of BMPRII but these mice were not viable and lethal so heterozygous mice were used. Studies have shown that mice with heterozygous mutations in the BMPRII develop mild PAH and impaired response to hypoxia [164]. This study also compared BMPRII $^{(+/-)}$ with WT mice in normoxic conditions, showing that BMPRII $^{(+/-)}$ mice have an increased pulmonary vascular resistance and PAP, increased wall thickness of the muscularised pulmonary arteries and an increased number of alveolar capillary units [164]. However other studies using this model have not reported such differences between WT and BMPRII $^{(+/-)}$ mice questioning the robustness of this model [146].

Other transgenic approaches have also been used because another group of patient's have reported BMPRII mutations in coding and non-coding regions of the gene, and collectively these mutations result in lower levels of BMPRII and reduced functionality of the receptor. Mice expressing dominant negative forms of BMPRII, either a kinase-dead dominant negative form of BMPRII, or clinically relevant functional mutations in the BMPRII gene also develop pulmonary vascular remodelling and PH. BMPRII mutations are quite common in the tail domain of the receptor, so BMPR2^{R899X} mice are another transgenic model of PAH. Around one third of these mice develop increased RVSP, extensive vascular pruning, muscularisation of small pulmonary vessels, and development of large structural pulmonary vascular changes. This study reports that the phenotypic result of BMPRII tail domain mutations in smooth muscle causes vascular pruning leading to elevated RVSP [26]. This model is also associated with early dysregulation in multiple pathways which are relevant to PAH patients. This model could represent a platform for interrogating the early molecular pathways and phenotypic changes that contribute to the development of PAH [26].

Conditional knock outs of BMPRII have also suggested that BMPRII plays a key role in vascular function in the endothelium with mice and pulmonary endothelial cells (PAECs) expressing reduced levels of BMPRII. These mice exhibit an increase in permeability in cell based assays suggesting that reduction of BMPRII is contributing to an increase in vascular leak and leukocyte recruitment. These mice

also demonstrate RV hypertrophy and some common histological defects to that of PAH patients [165].

Although it is clearly evident that mutations or reduced levels of BMPRII increase patient's susceptibility to the development of PAH the current animal models do not recapitulate disease in patients as effectively as other models. One success of these models is delineating that BMPRII is linked to vascular defect by contributing to a rise in vascular leak and the production of pro-inflammatory cytokines, for example IL-8. Other pre-clinical models of PAH, the Sugen/hypoxia and the TβRIIΔK transgenic model could also be used to investigate the role of BRMPRII in PAH. These models report reduced levels of BMPRII, enhanced TGFβ signalling and histological changes that exhibit a more representative phenotype to that of patients. However experts might argue that these models only recapitulate non-heritable forms of the disease and can't be used for the genetic cohort of patients.

In conclusion the MCT, chronic hypoxia, the combination of hypoxia and SU5416 and BMPRII knock out model all represent useful tools to investigate and understand the development of PAH. The advantage of the hypoxia model is that the mechanism by which these rodents develop PAH is similar to the pathology observed in humans. The MCT model recapitulates many key features of the disease; however the addition of a chemical is a unique mechanism that is not observed in patients. The advantage of the SU5416 hypoxia model is that the rodents display much more severe muscularisation which is similar to patients, gene-array studies showed that modification in just four genes were shared between lungs isolated from this model and lungs from patients with PAH [156]. This suggests that each model has both advantages and disadvantages and to understand the mechanism of novel therapeutics in PAH more than one *in-vivo* model in combination with *in-vitro* studies are essential.

1.8.5 TβRIIΔk-fib model of associated PAH

As discussed in section 1.7.1 the TβRIIΔk-fib transgenic mouse model expresses, under the control of the collagen 1α2 enhancer/promoter, a kinase-deficient TβRII gene. These animals exhibit a paradoxical enhancement in TGFβ signalling, including activation of the canonical Smad signalling pathway, Smad2/3 [52].

Consistent with the observed phenotype of the TβRIIΔk-fib transgenic mouse model, Loeys-Dietz syndrome patients who possess TβR-II mutations exhibit increased expression of collagen and CTGF, as well as increased phosphorylated Smad2 in the nuclei, which is indicative of increased TGFβ signalling [118]. The TβRIIΔk-fib model exhibits a constitutive pulmonary vasculopathy with medial thickening, a perivascular proliferating chronic inflammatory cell infiltrate, and mildly elevated pulmonary artery pressure, which resembles the chronic hypoxia model of PAH.

The hypothesis that the TβRIIΔk-fib model is susceptible to the development of PAH, following the administration of SU5416 this model recapitulated many key features of SSc-PAH which enhanced RVSP, further expansions of SMCs and endothelial dysfunction leading to the development of the concentric lesions in the pulmonary artery [119]. Sugen also contributes to a further increase in TGFβ activity with increased pSmad2/3 positive nuclei similar to that observed in PAH patients. Collectively this suggests the TβRIIΔk-fib transgenic mouse model may represent a superior model to understand the molecular mechanisms that contribute to the development SSc-PAH.

1.9 The TGFβ/BMP superfamily

1.9.1 Canonical and non-canonical signalling in the TGFβ/BMP pathway

TGFβ is the founding member of the TGFβ superfamily comprised of over 30 peptide cytokines in mammals including activins, [166], inhibins [167] BMPs [168], and TGF-βs [51]. Members of the TGFβ superfamily are characterised by a cysteine 'knot' of six of these residues at the carboxyl terminal. TGFβs are synthesised by many cell types including macrophages and fibroblasts as large inactive precursor proteins, which are modified intracellularly and secreted as a latent complex [169, 170]. Although still poorly understood several factors have been shown to promote the release of bioactive TGF-β from this latent complex including MMPs and thrombospondin-1 (TSP-1) [171] The resultant bioactive TGF-β regulates several hundred target genes in fibroblasts promoting a variety of cellular effects including proliferation and differentiation in addition to promoting matrix deposition and reducing matrix turnover [172].

The effects of all the TGF-β superfamily members are transmitted from membrane to nucleus through the activation of serine-threonine (Ser-Thr) kinases (Figure 1.4). The TGFβ ligand binds to the constitutively active serine/threonine kinase TβRII and in turn TβRI (ALK5) is recruited, forming a heterotetrameric complex (59). This leads to the activation of the canonical Smad signalling pathway via Smads 2 and 3. In contrast BMP ligands bind the BMPRII receptor and in turn recruit either ALK3 or ALK6, leading to the activation of Smads 1, 5 and 8. In addition to the activation of the 'canonical' Smad signalling pathway by members of the TGF-β superfamily, non-canonical' signalling pathways include members of the mitogen-activated protein kinases (MAPKs), such as p38 MAPK, p42/44MAPK (ERK1/2), and c-Jun-N-terminal kinase (JNK) are activated by members of this family (64).

1.9.2 The TGFβ superfamily in SSc and PAH

TGFβ has been implicated in fibrosis research for over the last decade and enhanced signalling and increased expression of TGFβ regulated genes and proteins have been extensively published in renal, lung, liver and skin fibrosis [45].

Previous reports have highlighted that PASMCs isolated from HPAH patient's exhibit a pro-proliferative response to TGFβ compared to healthy donors [17]. The pro-proliferative effect of TGFβ in PASMCs was also replicated in mice harbouring a nonsense BMPRII mutation [173]. Interestingly in SSc phosphorylated levels of Smads 2 and 3 are increased and more localised to the nucleus which is indicative of enhanced TGFβ signalling and this phenomenon is also seen in concentric lesions of PAH patients [152, 174]. Although no studies have investigated BMPRII expression in SSc lungs it has been published that BMPRII is reduced in SSc skin and microvascular endothelial cells, whereas there were no significant differences in the expression levels of BMPRIA and BMPRIB [175] suggesting a reduction in BMPRII may play a key role in patients with SSc developing PAH. This phenomenon of enhanced TGFβ signalling in PAH and SSc is also reported in pre-clinical models of the disease. Increased TGFβ signalling has been observed in the monocrotaline rat model, the hypoxia model in rodents, the hypoxia Sugen model in rodents, the bleomycin PH model and the aortopulomnary shunt model in lambs in concordance with a reduction in BMPRII levels [133, 141, 146, 176].The reduction in cell surface associated BMPRII levels in HPAH SMCs leads to a reduction in BMP activation of Smad1 and 5 and this dysregulated signalling is replicated in preclinical models [24,

177].This imbalance that lies in TGFβ/BMP signalling may contribute to the development of PAH in SSc.

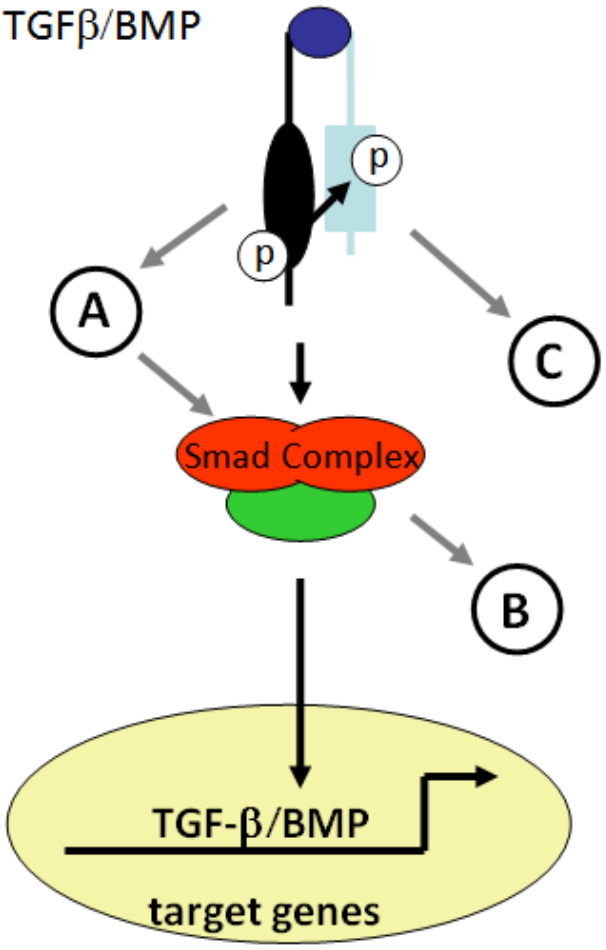

Figure 1.4. Schematic of the direct and modifying effects of the non-Smad signalling pathways

TGF-β and BMP ligand-receptor complex activates the canonical Smad signalling pathway (TGF-β activates Smad 2/3 and BMP activates Smad 1/5/8) and target genes in the nucleus (Black arrows). Non-Smad (non-canonical) signalling (p-38, ERK 1/2, JNK) mechanisms are shown in grey arrows. The TGF-β/BMP receptor complex directly activates protein A, which modulates the activity of the Smad pathway (A); the activated Smad complex activates protein B, which then transmits further signals into the nucleus (B); The TGF-β/BMP receptor complex directly activates protein C, which signals independently of Smads (C). Modified from Moustakas *et al*. [178].

2 Materials and methods

2.1 Generation of genetically modified mice

2.1.1 Generation of TβRIIΔk-fib transgenic mice

The generation and characterisation of TβRIIΔk-fib transgenic mouse model of SSc have been described previously by colleagues in the Department of Rheumatology [52, 54]. The cDNA encoding the extracellular and transmembrane portion of the human type II TGFβ receptor (comprising amino acids 24–184 of human TβRII) was subcloned into the Sal1 site of the pCD3 expression vector. The vector also includes the intron and polyadenylation signal from the murine protamine-1 gene. An internal ribosome entry site from the encephalomyocarditis virus was subcloned at the 5′-end of the Escherichia coli β-galactosidase (LacZ) gene. It was then excised as a NcoI-ClaI fragment from the internal ribosome entry site-LacZ-containing plasmid pWH8 and introduced into the pRM-6kb-LacZ plasmid using directional cloning between the same restriction sites. Progeny were backcrossed with wildtype (WT) mice to establish lines. Founders were previously shown to demonstrate consistent transgene expression in fibroblastic tissues and littermate WT C57BL/6 mice were used as controls [52].

2.1.2 Conditional genetic recombination

Methods for conditional alteration of gene expression add further refinement to gene targeting. For instance in TGFβ gene and receptor knockouts, where constitutive deletion proves fatal, it allows gene targeting to occur at predetermined time points. The Cre-lox mechanism was discovered in the P1 bacteriophage, where the virus uses Cre-lox recombination to circularize and facilitate replication of its genomic DNA when reproducing. This recombination strategy has been developed as a technology for genome manipulation-commonly gene deletion occurs in mice and other organisms and cells. It requires the Cre recombinase enzyme to catalyse recombination between two loxP sites: a specific sequence consisting of an 8-bp core sequence, where recombination takes place, and two flanking 13-bp inverted repeats. Inducible postnatal deletion of TβRII in fibroblasts of mice was achieved using this approach.

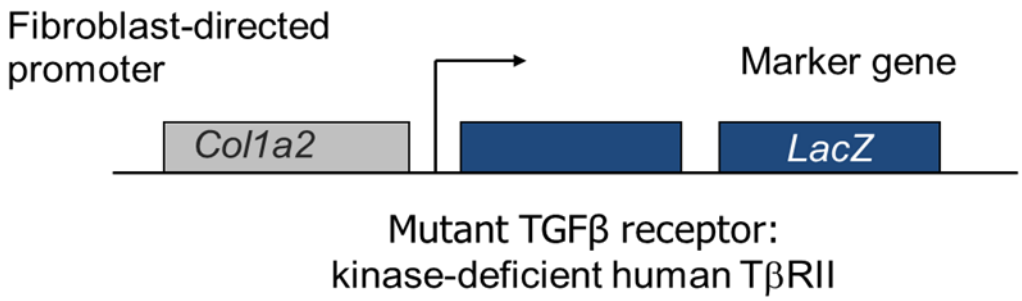

Figure 2.1 - Generation of TβRIIΔk-fib transgenic mice (Adapted from Derrett Smith, 2013).

2.1.3 Identification of genetically modified transgenic groups.

Neonatal pups were genotyped by polymerase chain reaction (PCR) analysis of genomic DNA extracted from ear-clip specimens. DNA was extracted using the HotSHOT DNA extraction method, 1470 µl of distilled H_20 ($_dH_20$) was added to 50x stock solutions of - 1.25M NaOH, 10mM EDTA at pH12 (#1) and 2M Tris-HCL at pH2 (#2). 75 µl of #1 was added to each tube and placed in PCR machine at 95°C for 30 minutes. 75 µl of #2 was added to #1 and mixed.

PCR expansion of genomic DNA from TβRIIΔk-fib mice was performed using Qiagen fast PCR kit (Qiagen) including primers specific for the β-galactosidase reporter gene (5'-CGGATAAACGGAACTGGAAA-3' and 5'-TAATCACGACTCGCTGTATC-3') (Sigma-Genosys, Haverhill, UK) to create a 500 bp product, primers specific for fabpi-200 as an internal control (5'-TGGACAGGACTGGACCTCTGCTTTCCTAGA-3' and 5'-TAGAGCTTTGCCACATCACAGGTCATTCAG-3'.) with a product size of 194 bp and water as negative control. Amplification was undertaken by 30 cycles of 3 mins of annealing at 68 °C, and 20s of extension at 96°C. Samples were run on a 2% agarose gel in 0.5% tris, boric acid and ethylenediaminetetraacetic acid (EDTA) (TBE) buffer with 0.05ul/ml Sybr safe (Sigma,UK) for 60 minutes at 120V. Negative samples were identified by presence of 1 band corresponding to internal control, positive samples were identified by 2 bands, 1 corresponding to internal control and one to target gene when viewed under ultraviolet light (Bio Spectrum, AC Imaging System, CA,USA) (Figure 2.2). The water sample acted as a negative control and no bands appeared on the gel (Figure 2.2).

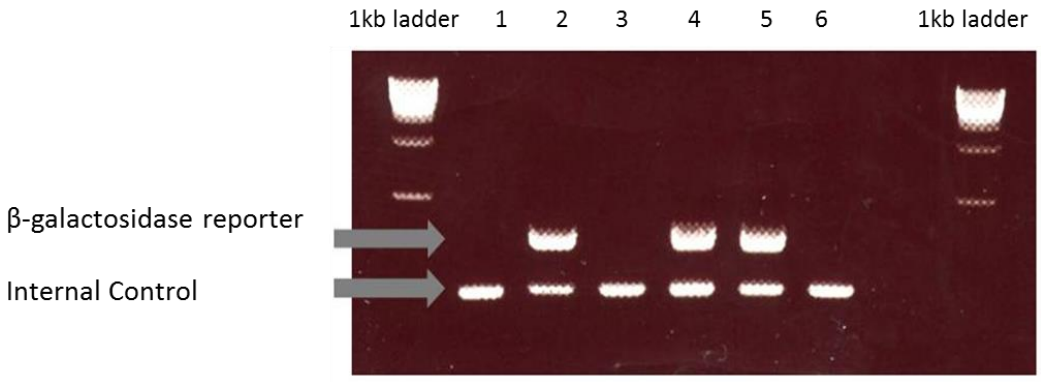

Figure 2.2: Genotyping results for TβRIIΔk-fib transgenic mice

2.2 Animal Procedures

2.2.1 Animal housing

All animals were bred in a specific pathogen free (SPF) facility and housed after weaning in a clean conventional colony, exposed to a 12 hour dark/light cycle, with access to food and water *ad libitum*. Strict adherence to institutional guidelines was practiced and full local ethics and Home Office approval were obtained prior to all animal procedures.

2.2.2 In-vivo measurement of mean arterial blood pressure and right ventricular systolic pressure

Ten to twelve week old TβRIIΔk-fib and WT littermate mice (20–25g) were anaesthetised with 1.5% isofluorane and placed on a thermostatically controlled heating blanket at 37°C. Hemodynamic measurements of right ventricular systolic pressure (RVSP) and mean arterial blood pressure (MABP) were obtained from the animals after six weeks of hypoxia exposure and relevant drug treatment. The animals were anaesthetised with 1.5% isofluorane and placed supine onto a heating blanket that was thermostatically controlled at 37^{o}C. First the right jugular vein was isolated and a pressure catheter (Millar mouse SPR-671NR pressure catheter with a diameter of 1.4F, Millar Instruments, UK) introduced and advanced into the right ventricle to determine RVSP. Second, MABP was measured by isolating the left common carotid artery and a pressure catheter introduced. Both RVSP and MABP were recorded onto a precalibrated PowerLab system (ADInstruments, Australia). The animal was euthanised via isofluorane anaesthetic overdose, the heart was removed, and individual chamber weights were measured to evaluate right

ventricular hypertrophy (right ventricle: left ventricle plus septum [RV/LV+S] ratio). Lungs were perfused with 10ml of saline via the right ventricle. The left lung was fixed by inflation with 10% formalin before paraffin embedding and sectioning. The whole blood was centrifuged (220 x g; 2 min), plasma removed and stored at -80^{o}C for further analysis. All measurements were made by observers blinded to genotype or treatment category. These experiments were performed by Dr S Trinder, Centre for Rheumatology and Connective Tissue Diseases, University College London.

2.2.3 Drug administration procedures

Pharmacological agents were administered orally (in chow) or via intraperitoneally (IP) injection. For studies investigating endothelial stress in the pulmonary circulation, SU5416 (3-(3,5-dimethyl-1H-pyrrol-2-ylmethylene)-1,3-dihydroindol-2-one: Sigma chemicals, UK), a small molecule tyrosine kinase inhibitor with specificity for vascular endothelial growth factor receptor 2 (VEGFR2) was administered IP in carboxymethylcellulose vehicle (0.5% carboxymethylcellulose sodium, 0.9% NaCl, 0.4% polysorbate, 0.9% benzyl alcohol in deionized water) to adult transgenic and wildtype littermate mice. The treatment protocol of SU5416 was a single injection (50 mg/kg) at the beginning of the 3 week experiment as published previously [140, 141].

For studies investigating the effects of JQ1 on the TβRIIΔk-fib, Animals were fed with either rodent Chow #5001 mixed with JQ1 and a coloring dye to identify the correct formulation for each group (Ssniff, Spezialdiaten, GmbH, Soest). The two formulations contained 999.392 g of Chow, 0.458 g of JQ1, and 0.15 g Green Dye to achieve a daily dose of 55 mg/kg or control Chow diet, 0.15 g Blue Dye. These doses were calculated on the assumption that the mice would consume 2.5 g per day and food consumption was monitored. Animals remained on this diet every day until the end of the study. At day 21 mice were sacrificed and RVSP, MABP and RV/LV+S ratios were recorded. Hearts, lungs and serum were collected and stored in appropriate manner for analysis (detailed in section 2.3).

2.3 Sample Collection

2.3.1 *In-vivo* serum collection

Animals under terminal anaesthetia were bled from the inferior vena cava and blood was collected in microcentrifuge tubes. The collected blood was allowed to clot then spun down at 5000 pm for 5 minutes, serum removed and stored at -80°C until analysed.

2.3.2 Post mortem collection

Animals were sacrificed using increasing concentrations of CO_2 and death was confirmed by cervical dislocation. Lungs were collected, divided and either snap frozen for protein analysis, immersed in 4% formaldehyde (Cell Path, UK) containing 10% saline for histological analysis, or stored in RNAlater for 24 hours before being placed in -80°C for RNA quantification.

2.4 Histology

2.4.1 Routine Histology

Before staining, sections were de-waxed in xylene (VWR, France) and passed through a graded ethanol (VWR, France) series to water. Lung architecture and degree of inflammation was determined by staining with haematoxylin and eosin (H&E) as per standard protocols. Collagen deposition was detected by sequential staining with the Lillie-Mayer's sequence followed by picrosirius red. Following staining slides were rinsed in water and dehydrated through an ethanol to xylene gradient and mounted with a coverslip using DPX. Staining was visualised using the Carl Zeiss Axio Vision microscope (Carl Zeiss GmbH, Jena, Germany).

2.4.2 Immunohistochemistry

Immunohistochemical analysis was performed on paraffin embedded lung sections from WT, TβRIIΔk-fib mice, control and scleroderma patients. Sections were deparaffinised using a xylene to ethanol gradient followed by rehydration, followed by methanol block for 10 minutes and running water for 5 minutes. Antigen retrieval was performed in pre heated citrate buffer (pH 6.0) for 10 minutes and slides washed for 5 minutes except in the case of BMPRII where antigen retrieval was performed by placing the slides in proteinase K (20 µg/ml in PBS, Dako,UK) for 20minutes at

room temperature. Slides were washed in PBS and blocked with the appropriate serum (20%) for 30 minutes followed by incubation in primary antibody or IgG control for 1 hour at room temperature (Table 2.3). PBS was repeated followed by a 30 minute incubation of secondary antibody (Table 2.3). Sections were incubated in Vectastain Elite ABC (Vector Laboratories) for 30 minutes, washed in PBS before being incubated for up to 10 minutes in DAB Peroxidase Substrate Kit, 3, 3'-diaminobenzidine (DAB) (Vector Laboratories). Slides were again washed in PBS and counterstained in Mayer's haematoxylin for 5 minutes and then dipped in acid alcohol and placed in blueing solution for 5 minutes. Sections were rinsed in water and dehydrated through an ethanol to xylene gradient and mounted with a coverslip using DPX. Staining was visualised using the Carl Zeiss Axio Vision microscope (Carl Zeiss GmbH, Jena, Germany).

Table 2.1 – Primary Antibodies used in IHC

Antigen	Species	Source	Catalogue No	Dilution
BMPRII	Rabbit	Abcam	Ab78422	1:200
Phospho-Smad 2/3 (Ser423/425)	Goat	Santa Cruz	sc-11769	1:300
α-SMA	Mouse	Sigma Aldrich	A2547	1:100
Von Willebrand Factor	Rabbit	Dako	A0082	1:200
Phospho-Smad 1	Rabbit	Abcam	Ab63439	1:100

2.5 Patient Samples

2.5.1 Sample Collections

Lung post mortem samples were collected from patients at the Royal Free Hospital Scleroderma Unit. Additional clinical information was determined including patient date of birth, age, gender and organ complications. Age and gender matched controls were obtained (Novartis, Horsham). Lung post mortems were sub-divided into four regions: One section was placed in an eppendorf tube and snap frozen in liquid nitrogen, and stored at -80°C for subsequent protein analysis; The second region for RNA extraction was stored with RNAlater™ RNA stabilisation reagent (Ambion,

Austin, Tx) according to manufacturer's guidelines. The third region was immersed in 10% formal saline containing 4% formaldehyde (CellPath, UK) for histological processing.

The final remaining portion was collected in Dubecco's Modified Eagle Medium (DMEM; with 2mM L-glutamine and 1 mM sodium pyruvate; Invitrogen) and cut into 2-3 mm^2 pieces using scalpels and placed in 75cm flasks. Lung tissue was allowed to adhere and then covered in fibroblast growth medium, DMEM; supplemented with 10 % (v/v) foetal bovine serum (FBS, Biosera) and 1 % (v/v) Penicillin-Streptomycin (Gibco). Cells were grown in 75cm flasks in a temperature controlled, humidified incubator with 5% CO_2 at 37°C. Outgrowths of fibroblasts were determined by morphological assessment and immunofluorescence staining for fibroblast growth factor-2 (FGF-2) were observed after 7-10 days and medium was changed every 2-3 days. Upon reaching 90% confluence cells were passaged using 0.25% Trypsin-EDTA solution (Sigma). Subsequen t experiments were performed on cells between passages 2 and 4. Prior to being exposed to treatments fibroblasts were serum starved in 0.1% FCS DMEM medium (low serum).

2.5.2 Ethical Approval and consent

Consent forms for post mortems followed the guidelines of the NHS trusts to meet requirements of the Human Tissue Act (HTA) 2004. The HTA 2004 covers England, Wales and Northern Ireland and was formed to regulate activities concerning the removal, storage, use and disposal of human tissue. Consent is the main principle of the act and underpins the lawful removal, storage and use of body parts, organs and tissue. In relation to post-mortems the HTA provides the necessary guidelines to ensure these examinations on deceased people are treated with dignity and respect. These include the essential consent and communication; the coroner's post-mortem examination; the hospital post-mortem examination and the relevant storage of tissue, tissue blocks and slides.

2.6. *In-vitro* tissue culture

2.6.1 Explant culture of murine lung fibroblasts

Whole lungs were isolated from WT and TβRIIΔk-fib mice. Lungs were washed in Dubecco's Modified Eagle Medium (DMEM; Invitrogen 2mM L-glutamine and 1

mM sodium pyruvate) and cut into 2-3 mm^2 pieces using scalpels and placed in 75cm flasks. Explant cultured fibroblasts were established as described in section 2.5.1.

2.6.2 Culture of human pulmonary arterial smooth muscle cells

Pulmonary arterial smooth muscle cells (PASMCs) (Promocell) were maintained in contractile SMC medium (Promocell) supplemented with 5 % (v/v) FBS and 1 % (v/v) Penicillin-Streptomycin (Gibco). Smooth muscle cell (SMC) medium supplemented with 15% (v/v) of FBS (Biosera), which promoted synthetic smooth muscle cell de-differentiation. Cells were grown in 75cm flasks in a temperature controlled, humidified incubator with 5% CO_2 at 37°C. Culture medium was changed every 2-3 days and cells were passaged by washing cell monolayer in phosphate buffered saline (PBS;Gibco) followed by trypsinisation (Sigma). Experiments were performed on cells between passages 3 and 6.

2.6.3 Immunostaining of cells

Explant cultured lung fibroblasts and PASMCs were seeded at 5 x 10^3 cells per well of a four well chamber slide and grown to 40% confluence. Cells were then fixed in an ice-cold methanol and acetone mixture (1:1 ratio) at -20^{o}C for 4 minutes. Chamber slides were then washed 3 times at room temperature for one minute in PBS and stored at 4^{o}C overnight. The following day slides were incubated for 30 minutes in PBS containing 10% serum of the host of the secondary antibody. Primary antibodies were diluted in PBS as shown in Table 2.2, and 350 µl was added to each chamber slide and incubated overnight at 4^{o}C. The following day, chamber slides were washed three times for 5 minutes in 0.05% (v/v) PBS-Tween (PBS-T). An appropriate Alexa Fluor® fluorescent secondary antibodies against primary antibody species IgG heavy and light chain (Invitrogen, UK) were incubated at 1:200 for 30 minutes followed by a wash for 5 minutes in 0.05% (v/v) PBS-T. Slides were mounted using Vectashield mounting medium with DAPI (Vector Laboratories) and Fluorescence signal was detected using AxioSkop2 fluorescence microscope and Axiovision v4.8 software (both Carl Zeiss GmbH, Jena, Germany).

Table 2.2 – Primary Antibodies used in immunostaining

Antigen	Species	Source	Catalogue No	Dilution
α-SMA	Mouse	Sigma	A2547	1:75
Calponin	Rabbit	Abcam	ab46794	1:250
Type 1 Collagen	Goat	Millipore	ab758	1:200
CTGF	Rabbit	Abcam	ab6992	1:400
Smoothelin	Mouse	Abcam	ab8969	1:300
Phospho-Smad1	Rabbit	Cell Signalling	#9516	1:80

2.6.5 Cell migration assay

Explant cultured fibroblasts and human PASMCs (PASMCs) were seeded at 2 $x10^4$ cells per well of a 96-well plate overnight in the appropriate culture medium to ensure a confluent monolayer. The following day medium was replaced with low serum DMEM supplemented with 1% (v/v) FBS and 1 % (v/v) penicillin-streptomycin for a further 24 hrs. Using a 96 well floating pin (V&P Scientific Inc) array a uniform scratch was applied to each well and the scratch confirmed by visual inspection. The medium was replaced with 1% (v/v) FBS and 1 % (v/v) penicillin-streptomycin in the presence of 10 μg/ml mitomycin (Calbiochem) and treatments. Treatments used were 10 ng/ml PDGF BB (Peprotech,USA), or 50 ng/ml BMP4 (Stemgent, UK), or 1 μM JQ1 (Sigma, UK). The extent of wound closure was assessed after 24 hours. Cellular wound closure was visualized on the Olympus Ck2 microscope and images stored for analysis using Carl Zeiss Axio Cam software (Carl Zeiss GmbH, Jena, Germany). Data was analysed by quantifying the percentage of area covered by treatment groups compared to area of wound at time zero.

2.6.6 Cell proliferation assay

PASMCs and explant cultured lung fibroblasts were seeded at $5x10^3$ cells per well of a 96 well plate. After 24 hours, media was supplemented with low serum medium alone or in the presence of 50 ng/ml PDGFBB (Peprotech, USA) or a concentration range of JQ1. After 24 and 72 hours cell proliferation was determined by crystal violet incorporation. Briefly, a media was removed from the cells at the times specified and washed twice in PBS. 50 μl of the prepared crystal violet solution (0.025% (w/v) crystal violet, 10% (v/v) methanol (VWR, USA)) was added to each well, and incubated at room temperature for 10 minutes. The crystal violet solution

was then removed, and the plate washed with $_{d}$H2O to remove non-cell bound crystal violet. The plate was dried for 3 hours and crystal violet was solubilised with the addition of 50ul of 10 % acetic acid (Sigma,UK) solution, and the absorbance at 560nm determined using a plate reader (Mithras LB940).

2.6.7 Cell apoptosis assay

Contractile and synthetic PASMCs were seeded at $5x10^3$ cells per well for 24 hours. Medium was removed from cells and washed with sterile PBS. Contractile and synthetic PASMCs were treated with 0, 0.5, 5 and 50 ng/ml of BMP4 (Stemgent,UK) and BMP7 (Stemgent,UK) dissolved in low serum FBS. Cells were incubated with BMP ligands. After 8 hours Caspase-Glo® 3/7 Reagent (comprising Caspase-Glo® 3/7 buffer (Promega) was mixed with the Caspase-Glo® 3/7 Substrate (Promega) in a 1:1 ratio) was added to each well in a 1:1 ratio. The plate was sealed with a plate sealer and mixed using a plate shaker at 300–500rpm for 30 seconds. Readings were taken between 1 and 3 hours after Caspase Glo was added; with 2 hours giving the optimum results. The luminescence of each sample was determined using using a plate reader (Mithras LB940).

2.6.8 Gel contraction assay

To study collagen gel contraction, fibroblasts were cultured within three-dimensional (3-D) collagen lattices (fibroblast populated collagen lattices; FPCL). 24-well tissue culture plates (Costar) were pre-coated with sterile 2% BSA (w/v) in PBS (2ml/well) and incubated at 37^{o}C overnight, and were then washed three times with sterile PBS. For FPCL, neutral collagen solution (containing one part of 0.2 M HEPES, pH8.0; four parts collagen (Vitrogen-100, 3 mg/ml, Celltrix, Santa Clara, CA) and five parts DMEM medium were prepared. Solutions were mixed with cells, to bring the final concentrations to 80,000 cells and 1.2mg collagen/ml alone or in the presence of 5 ng/ml TGFβ, 50 ng/ml BMP4 (Stemgent,USA) and 1 μm JQ1.The collagen-cell suspension (1 ml) was added to each well, and allowed to gel for 1 hour. After polymerisation, 1 ml of medium was added to each well, causing detachment of the FPCL from the tissue culture plastic. Contraction of the gel was quantified by loss of gel weight and decrease in gel diameter over a 24-h period.

2.6.9 FITC-albumin permeability assay

Pulmonary arterial endothelial cells (PAECs) were seeded at $1x10^5$ cells, into 3µm pore transwell inserts (VWR, 734-0037) and allowed to reach confluence after 24 hours. Monolayers were then exposed to conditioned medium from contractile and synthetic SMCs grown in complete EGM-2 for 24 hours with 800µl in the bottom well and 200µl in the transwell insert. After 24 hours 200µl was removed from the lower and replaced with 5mg/ml BSA, and 200 µl was removed from the top of the insert and replaced with 0.5% w/v (5mg/ml) FITC-albumin (Sigma, A9771). 20µl was removed from the lower well after 0.5, 1, 2 and 4 hours, and fluorescence determined on a plate reader at an 485nm and absorbance of 535nm (Mithras LB940).

2.6.10 Neutrophil migration assay

PAECs were seeded at $1x10^5$ cells per insert and exposed to conditioned medium from contractile and synthetic PASMCs as described in 2.6.9. Peripheral blood mononuclear cells (PBMCs) were isolated from peripheral blood using ficoll-paque. PBMCs were isolated by Mr Robert Good, Centre for Rheumatology and Connective Tissue Diseases, University College London. PBMCs were re-suspended in PBS/2%FCS at a concentration of $5x10^6$ cells/ml. 200µl of medium was removed from the lower well and replaced with 200µl 2%FCS in PBS. 200µl was removed from the insert and replaced with 200µl containing $1x10^6$ PBMCs to each insert. Neutrophil transmigration was determined after 2 hours by removing the inserts from the wells and washing off any attached neutrophils to the lower surface using PBS. Medium was removed and added into eppendorfs and centrifuged at 7000rpm for 5 minutes. Medium was aspirated and neutrophils resuspended in 100µl PBS and counted using a haemocytometer.

2.6.11 Enzyme-linked immunosorbent assay

Enzyme-linked immunosorbent assay (ELISA) was performed on conditioned medium from contractile and synthetic hPASMCs, explant cultured control and scleroderma fibroblasts in the presence or absence of recombinant proteins and inhibitors. Levels of human IL-6 Duoset ELISA kit (R&D Systems®, MN, USA), Human IL-8 Duoset ELISA kit (R&D Systems®, MN, USA) and Human CTGF Standard ELISA development kit (Peprotech, USA) were determined in conditioned

media as per manufacturer's protocol. Capture antibodies were prepared to appropriate concentrations and 100 µl added to each well in a 96 well microplate.
The microplate was sealed and allowed to incubate overnight at room temperature. Following overnight incubation, the capture antibody was removed, and the wells were washed to ensure complete removal of liquids. Plates were then blocked using 100µl per well of 0.2µm sterile-filtered 1% bovine serum albumin (BSA) in PBS (pH 7.4) for 1 hour at room temperature. Blocking solution was aspirated, and the wells washed. A seven-point standard curve was prepared using two fold dilutions and 100 µl of standards and sample were added to each well in duplicate and incubated at room temperature for 2 hours. Standards and samples were discarded and the wells were washed again. Detection antibody was prepared and 100 µl applied to each well for 2 hours at room temperature followed by washing. 100 µl streptavidin horseradish peroxidase (HRP) was added to each well for 20 minutes at room temperature followed by washing. Glo Substrate Reagent (R&D systems®, MN, USA) used as directed by manufacturer's protocol by mixing one part of Glo substrate reagent A (luminol) with two parts of Glo substrate reagent B (hydrogen peroxide) and 100 µl was added to each well. Plates were incubated in the dark for 5 minutes and the luminescence determined using a microplate reader (Mithras LB940). IL-6, IL-8 and CTGF concentrations of each sample were calculated using a standard curve of known concentrations.

2.7 RNA quantification and analysis

2.7.1 RNA isolation from tissue and cells

Whole lung lysates were prepared from WT and TβRIIΔk-fib mice stored at -80°C in RNAlater. Lung samples were ground to fine powder using a dry ice cooled pestle and mortar. Lung homogenates were re-suspended in RLT buffer and homogenised using an automated homogeniser (IKA, Ultra Turrax T8). Explant cultured fibroblasts were lysed by adding 350 µl of RLT buffer to each well and lysing with needle and syringe. Using spin-column technology 350 µl of 70% ethanol was added to the homogenised lung or cell lysate and mixed well by pipetting.700 µl of the sample was transferred to a RNeasy spin column placed in a 2ml collection tube and centrifuged for 15s at 10,000 rpm. The flow through was discarded and 700 µl buffer

RW1 was added to the spin column and centrifuged for 15s at 10,000 pm. Flow through was discarded and 500 µl buffer RPE was added to the RNeasy spin column and centrifuged for 15s at 10,000 pm. Flow through was discarded and 500 µl buffer RPE was added to the RNeasy spin column and centrifuged for 2 minutes at 10,000 pm. Spin column was replaced with a new collection tube and spun at max speed for 1 minute and in a another new collection tube 30-50 µl RNase-free water was added directly to the spin column membrane and centrifuge for 1 minute at 10,000 rpm to elute the RNA.

2.7.2 RNA quantification

RNA was quantified using a Nanodrop ND-8000 spectrophotometer (Thermo-Scientific). Briefly, 1µl samples were placed on the spectrophotometer and measured for quantity and purity judged by 260/280 ratio and this was repeated three times to ensure accuracy. The minimum 260/280 ratio accepted was 1.90. The quality of the isolated RNA was determined using an Agilent 2100 Bioanalyzer (Agilent Technologies UK Limited) using the Agilent RNA 6000 nano kit and chips according to manufacturer's instructions. The RNA integrity algorithm was used to determine integrity and values ranged from 8 to 10 (Figure 2.3).

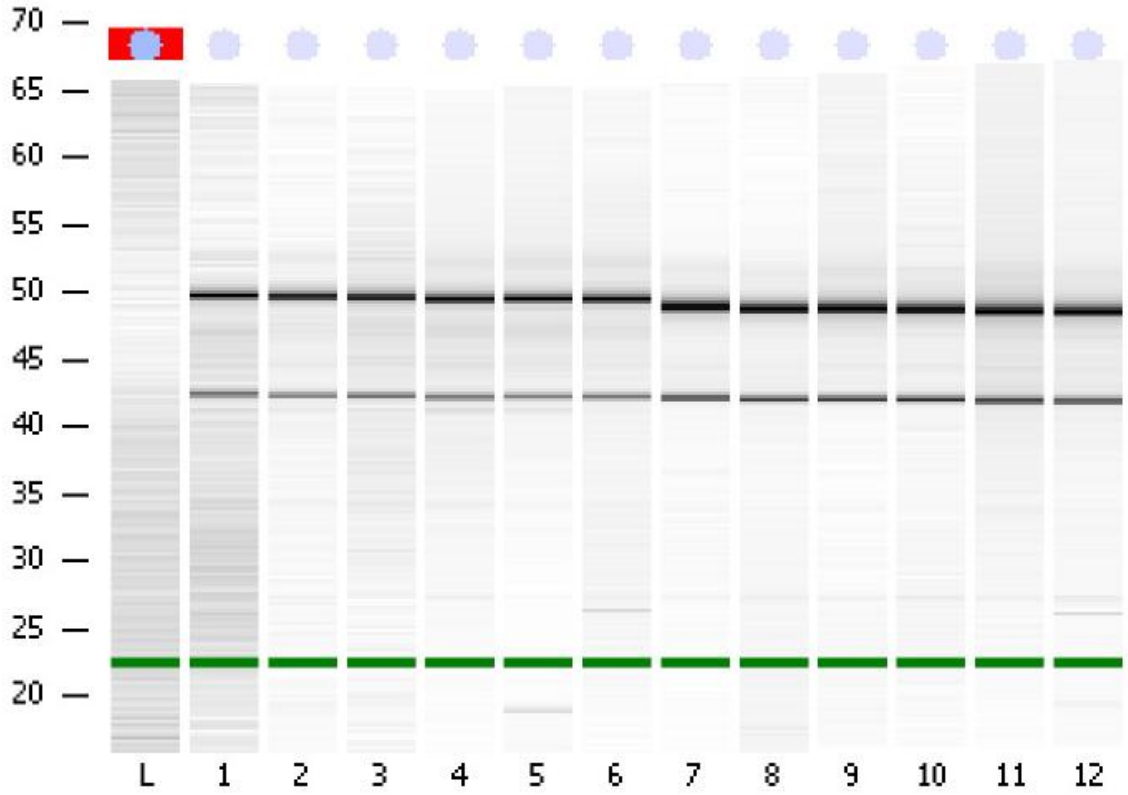

Figure 2.3 – Agilent NA 6000 Nano chip assay results for explant cultured fibroblasts and hPASMCs

2.7.3 Primer Design

Primers were designed using Roche Universal Probe library software and mouse accession numbers. Intron-spanning amplicons placed towards the 3' end of the gene of interest were preferred. Sequences were analysed for nearest neighbour melting points, GC content and GC clamps to ensure that primers were not self-annealing using a sequence manipulation site (bioinformatics.org/sms2/pcr_primer_stats.html). GC content of 40-60, and a difference of <2^{o}C in Tm were considered acceptable. Ideal amplicon length was 70-140 bp. In order to ensure specificity, primer sequences were then subjected to BLAST analysis (http://blast.ncbi.nlm.nih.gov/Blast.cgi). Specificity was confirmed using melt curve.

2.7.4 cDNA synthesis

500 ng or 1 µg of total RNA was reverse transcribed using the Quantitect reverse transcription kit (Qiagen). Briefly, this first involves a genomic DNA elimination step, followed by reverse transcription using a mix of random and oligoDT primers. The completed cDNA reaction was diluted five-fold with tRNA 0.2 µg/mL.

2.7.5 qPCR

2μl of diluted cDNA was used for real-time quantitative RT-PCR in a 10 μL reaction volume using Sensimix NoRef in a SYBR green-based assay (Quantace, London, UK) on a Rotorgene-6000 (Corbett Life Sciences, Sydney, Australia) under the following conditions (unless primer design required otherwise): 95^{o}C for 10 min, followed by 40 cycles of 95^{o}C for 10s, 57^{o}C for 15s and 72^{o}C for 5s. Primer dimers were excluded by melt curve analysis. The four most stable reference genes were identified and normalisation factors were obtained using geNorm (Vandesompele et al, 1999). Gene of interest copy numbers were corrected using these normalisation factors.

Table 2.3 – Primers used for qPCR

Reference Genes			
Primer Name	Gene	Forward	Reverse
mSdha	Mus musculus succinate dehydrogenase complex, subunit A	5'-TGTTCAGTTCCACCCCACA-3'	5'-TCTCCACGACACCCTTCTGT-3'
mRpl13	Mus musculus 60S ribosomal protein L13	5'-CAGTGAGATACCACACCAAGGTC -3'	5'–GTGCGAGCCACTTTCTTGT-3'
Gene Targets			
Primer Name	Gene	Forward	Reverse
mBMPRII	Mus musculus bone morphogenetic protein receptor, type II	5'-GAGCCCTCCCTTGACCTG -3'	5'-GTATCGACCCCGTCCAATC-3'
mSerpine-1	Mus musculus serpine peptidase inhibitor	5'-GACGTTGTGGAACTGCCCTA-3'	5'-AGCTGCTCTTGGTCGGAAAG-3'
mGrem1	Mus musculus gremlin 1	5'-CCACGGAAGTGACAGAATGA-3'	5'-GGGCATTTCCGACCATCTGA-3'
mCTGF	Mus Musclus connective tissue growth facor	5'-TGACCTGGAGGAAAACATTAAGA -3'	5'-AGCCCTGTATGTCTTCACACTG-3'

2.8 Western Blotting

2.8.1 Preparation of cell lysates for Western Blotting

Monolayers of fibroblasts (murine and human) maintained in DMEM medium and PASMCs maintained in either synthetic or contractile media SMC media were grown to 60-80 % confluence in 6-well plates. Cell monolayers were washed in 1x PBS and lysed in 120 µl lysis buffer comprising Radio Immuno Precipitation Assay (RIPA) buffer (Sigma) containing (150 mM NaCl, 50mM Tris pH 7.4; 1mM PMSF; 1% PMSF; 1% NP-40; 1% Sodium deoxycholic acid; 0.1% SDS; 10% complete, Mini, EDTA-free protease inhibitor cocktail (Roche) and phosphatase inhibitor cocktail 3 (serine/threonine protein phosphatases and L-isozymes of alkaline phosphatase inhibitor (Sigma,UK). Protein concentrations were determined using the BCA Protein Assay kit (Pierce # 23225), and 15 µg of protein mixed with 4x SDS Loading Buffer (8% SDS, 250mM Tris HCl pH 6.8, 20% glycerol) and 5% β-mercaptoethanol were denatured at 96°C for 5 minutes.

2.8.2 Preparation of tissue for Western blotting

Whole lung lysates were prepared from snap frozen lungs from WT and TβRIIΔk-fib mice. Lung samples were ground to fine powder using a dry ice cooled pestle and mortar. Lung homogenates were re-suspended in lysis buffer supplemented EDTA-free Protease Inhibitor Cocktail (Roche) and phosphatase inhibitor cocktail 3 (Serine/Threonine Protein phosphatases and L-Isozymes of Alkaline Phosphatase inhibitor, Sigma) and homogenised using an automated homogeniser (IKA, Ultra Turrax T8) Protein concentrations were determined using the BCA Protein Assay kit (Pierce # 23225).

2.8.3 Electrophoresis and transfer of protein samples for Western blotting

Protein samples (15 µg per sample) were resolved on pre-cast 4-12% Tris-Glycine gel (Invitrogen), alongside a Novex Sharp pre-stained protein standard (Invitrogen) at 200V, until the dye front had reached the bottom of the gel (approximately 45 minutes). Each gel was removed from its casing and placed within a transfer set-up using chromatography paper and Hybond C+ (Amersham) cut to 8cm by 6cm. All these components had previously been soaked in 1x Transfer buffer (Invitrogen), containing 20% (v/v) methanol (VWR, France). The transfer set-up was then

carefully placed within a transfer module (Invitrogen) and put into an electrophoresis tank (Invitrogen), and completely submerged in 1x transfer buffer. To prevent overheating, spaces surrounding the transfer module were filled with cold water. The transfer was then allowed to proceed at 35V for 1½ hours. After this time membranes were rinsed with Ponceau Red (Sigma) solution to confirm protein transfer to the Hybond™ membrane. Membranes were then washed 3 times in 0.5% PBS-T for 10 minutes each before immunoblotting (2.8.4).

2.8.4 Immunoblotting

Membranes were incubated in 10 ml of blocking buffer 5% (w/v) Marvel dried skimmed milk in 0.5% PBS-T, for 1 hour at room temperature to block non-specific protein binding to the membrane. The blots were washed for ten-minutes for three times in 0.5% PBS-T with constant agitation. Primary antibodies were diluted at concentrations as shown in Table 2.1 in blocking buffer and incubated at 4°C overnight. Membranes were then washed as before and an appropriate HRP linked secondary antibody diluted in blocking buffer added for further 1 hour at room temperature. The membranes were subsequently washed and proteins detected using an ECL Detection Kit (GE healthcare). The blot was exposed to ECL-specific film (GE healthcare), for between 5 seconds and 5 minutes and developed using Xograph Imaging Systems Compact x4 Western blotting machine.

Table 2.4 – Primary Antibodies used in Western blots

Antigen	Species	Source	Catalogue Number	Working dilution
BMPRII	Rabbit	Thermo Scientific	PA5-11863	1:500
BMPRIA	Rabbit	Santa Cruz	sc-20736	1:1000
Smad 1	Rabbit	Cell Signalling	#9512	1:1000
Phospho-Smad1 (Ser 206)	Rabbit	Cell Signalling	#5753	1:1000
Phospho-Smad 2/3 (Ser 423/425)	Goat	Santa Cruz	sc-11769	1:1000
Smad 2	Mouse	BD Transduction	610842	1:1000
p-p38 MAPK	Rabbit	Cell Signalling	9211	1:1000
p38 MAPK	Rabbit	Cell Signalling	9212	1:1000
p-p44-42 MAPK	Rabbit	Cell Signalling	9101	1:2000
p42 MAPK (ERK)	Mouse	Santa Cruz	sc-1647	1:1000
CTGF	Goat	Santa Cruz	sc-14939	1:1000
α-SMA	Mouse	Sigma Aldrich	A2547	1:2000
Smoothelin	Rabbit	Santa Cruz	sc-28562	1:1000
Calponin	Rabbit	Abcam	ab46794	1:500
Type 1 Collagen	Goat	Millipore	ab758	1:1000
SM-22	Goat	Abcam	ab10135	1:1000
GAPDH	Mouse	Abcam	ab9484	1:50,000
β-tubulin	Rabbit	Abcam	ab6046	1:50,000
Anti-Rabbit IgG HRP	Goat	Cell Signalling	#7074	1.1000
Anti-Mouse IgG HRP	Horse	Cell Signalling	#7076	1.1000
Anti-Goat IgG HRP	Rabbit	Dako	P0160	1:1000

2.9 Statistical Analysis

Statistical tests and graphs for both *in-vitro* and *in-vivo* studies were generated using GraphPad Prism 6.0 (GraphPad Software, La Jolla, CA). Results were expressed as mean ± S.E.M, $P<0.05$ denoted significance using the Mann-Whitney Test.

For *in-vivo* studies variation in MABP, RVSP, LV/RV ratio and muscularisation of arteries were analysed by one-way analysis of variance (ANOVA) with Bonferroni post-hoc analysis. Results were expressed as mean ± S.E.M, $P<0.05$ denoted significance.

3. Aberrant BMP signalling may contribute to pulmonary arterial hypertension in a TGFβ dependent murine model of scleroderma.

3.1 Introduction

A number of transgenic and insult based animal models have been used to better understand the biological processes that contribute to the development of SSc [18]. As outlined in chapter 1, (Table 2.1) a number of these models have been shown to develop pulmonary vascular remodelling including the Fra-2, and COL1α2-CTGF (Holmes *et al* unpublished observations). The TβRIIΔk-fib transgenic mouse model exhibits many of the complications associated with that of SSc patients [52, 54]. Furthermore, these mice exhibit a more severe response to intratracheal administration of bleomycin elevated myofibroblast numbers, and increased apoptosis of type II alveolar epithelial cells [55]. These mice display enhanced TGFβ signalling characterised by activation of the canonical Smad signalling pathway, Smad2/3 [52].

Consistent with the observed phenotype of the TβRIIΔk-fib transgenic mouse model, Loeys-Dietz syndrome patients which possess TβR-II mutations exhibit increased expression of collagen and CTGF, as well as increased phosphorylated Smad2 in the nuclei. [118]. Interestingly these mice also exhibit vascular defects in the lung independently of pulmonary fibrosis [56]. This led to the hypothesis that the TβRIIΔk-fib model may be more susceptible to the development of PAH. Recently Derrett-Smith *et al.* demonstrated the TβRIIΔk-fib transgenic mouse model of SSc spontaneously develops raised right ventricular systolic pressures (RVSP) and vascular remodelling [119]. The TβRIIΔk-fib mouse model displays a modest but significant elevation in RVSP and moderate vascular remodelling, but no change in the Fulton index [119]. However administration of the VEGF receptor antagonist SU5416, led to a further enhancement in RVSP and more extensive vascular remodelling with associated muscularisation of vessels and endothelial apoptosis [119]. Collectively this suggests the TβRIIΔk-fib transgenic mouse model may represent a novel model to explore the molecular mechanisms that contribute to the development SSc-PAH.

The expression of BMPRII in the TβRIIΔk-fib model has not been previously investigated but BMPRII reduction is a mechanism that is shared with other models of lung fibrosis and PAH. The bleomycin model has previously demonstrated a reduction in BMPRII gene expression. It has also been demonstrated that other models of PAH, for example the SU5416/hypoxia rat model, the hypoxia rodent model and the MCT model have also previously demonstrated a reduction in BMPRII in concordance with enhanced TGFβ activity.

As discussed earlier vascular remodelling can occur through the expansion of smooth muscle cells and fibroblasts. The final step was to examine the effect of PDGFBB on the proliferation and migration and explant cultured lung fibroblasts from TβRIIΔk-fib and WT controls. PDGFBB is known mitogen that can induce proliferation and migration; it has also been previously demonstrated to be implicated in SSc [179].

3.2 Aims

To investigate the relevance of the BMP receptor BMPRII in SSc-PAH, this work initially sought to assess the expression of this and associated downstream signalling pathways within the context of the TβRIIΔk-fib mouse model of SSc. This chapter investigates expression of components of the BMP signalling cascade including BMPRII in whole lung tissues using histological and molecular techniques. Using lung fibroblasts cultured from these mice, the expression of components of the BMP signalling cascade was assessed and the cellular response of these cells to the BMPRII ligand BMP4 determined. Vascular remodelling in part results from increases in resident cells, including fibroblasts and PDGFBB can promote proliferation and migration in fibroblasts [180]. Extending these studies the response of TβRIIΔk-fib fibroblasts to PDGFBB was assessed.

3.3 Results

3.3.1 VEGFR inhibition exacerbates the hypertensive phenotype in the TβRIIΔk model.

The TβRIIΔk-fib mouse model displays a modest but significant elevation in RVSP and moderate vascular remodelling spontaneous at eight to twelve weeks of age. The administration of the VEGFR antagonist SU5416 under normoxic conditions induces extensive pulmonary vascular remodelling with further elevation in RVSP and right ventricular hypertrophy [119]. 10 pulmonary arterioles (100 μm) per section were scored and blinded to the source of tissue (n=3). Each vessel was scored as either nonmuscularised or non-inflamed (0), partially muscularised or inflamed(1), or fully muscularised or inflamed (2).

Immunohistological staining for the smooth muscle cell marker α-SMA (brown) and the endothelial cell marker vWF (brown) displayed increased vessel wall thickening. There were no cardinal features of advanced or severe PAH such as plexiform lesions observed in TβRIIΔk-fib vessels (Figure 3.1A). In contrast the addition of SU5416 to WT mice induced a mild muscularisation with minimal vessel thickening, whilst and in the TβRIIΔk-fib SU5416 induced extensive pulmonary vascular remodelling and the formation of concentric lesions (Figure 3.1A). Quantification highlighted a significant increase in muscularisation in the TβRIIΔk-fib group alone compared to WT mice. The addition of SU5416 led to a significant rise in the degree of muscularisation in WT and TβRIIΔk-fib compared to control mice (Figure 3.1B).

Hematoxylin and eosin (H&E) staining highlights a slight increase perivascular inflammatory cell infiltrate and medial thickening in the TβRIIΔk-fib mice group compared to wild-type controls (Figure 3.1C). The addition of SU5416 in WT mice led to a mild inflammatory phenotype whereas SU5416 to TβRIIΔk-fib mice led to enhanced perivascular inflammatory cell infiltration compared to TβRIIΔk-fib alone and a more extensive medial thickening and obliteration of some smaller vessels (Figure 3.1C). Quantification of this inflammation showed that there was a significant rise in the degree of inflammation in WT and TβRIIΔk-fib compared to control mice (Figure 3.1D).

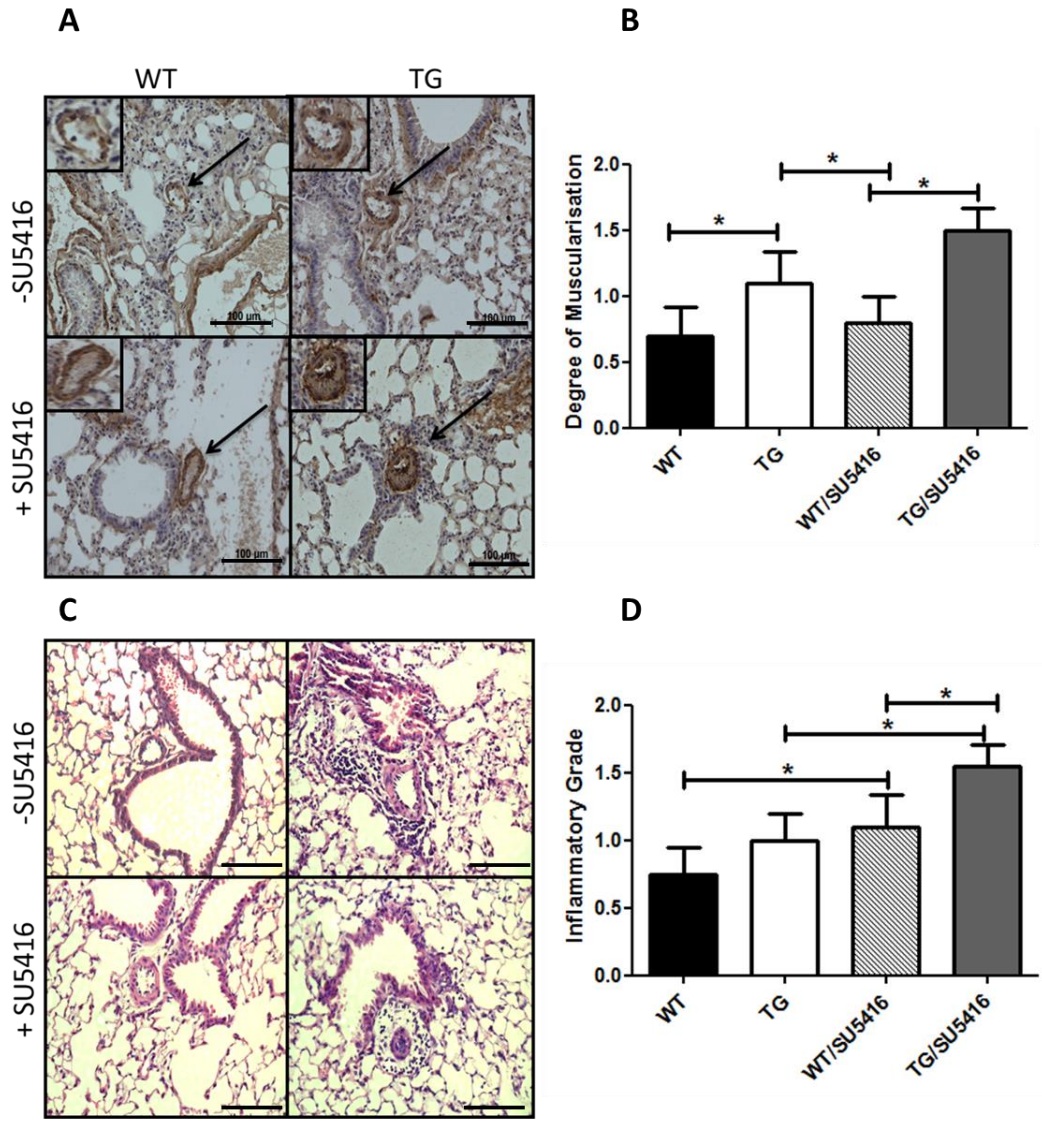

Figure 3.1 – VEGFR inhibition enhances vascular remodelling and medial thickening in TβRIIΔk-fib mice

Immunohistochemical staining for alpha-smooth muscle actin (α-SMA) and von-Willebrand factor (vWF) (A) and Hematoxylin and eosin (H&E) (D) on paraffin embedded formalin fixed lung sections from wild type (WT), TβRIIΔk-fib mice exposed *in-vivo* to SU5416 or vehicle alone. 10 pulmonary arterioles (100 µm) per section were scored and blinded to the source of tissue (n=3). Each vessel was scored as either nonmuscularised or non-inflamed (0), partially muscularised or inflamed(1), or fully muscularised or inflamed (2) (B,D). Black line indicates 100 µm and magnification x20 using the Carl Zeiss microscope. *$p<0.05$ Mann Whitney Test.Black line indicates 100 µm and magnification x20 using the Carl Zeiss microscope.

3.3.2 Investigation expression of BMPRII and downstream signalling components of the TGFβ superfamily in whole lung tissues.

To initially assess expression of components of the TGFβ superfamily in TβRIIΔk-fib transgenic mouse model of SSc-PAH whole lungs were isolated from WT and TβRIIΔk-fib mice following administration of SU5416 or vehicle control. Using lung homogenates the expression of BMPRII, and downstream signalling components of the TGFβ superfamily was assessed by Western blot (Figure 3.2). Lung homogenates from TβRIIΔk-fib exhibited a marked and significantly lower levels of BMPRII compared to that of WT mice ($p<0.05$; Figure 3.2A). Treatment of WT mice with SU5416 led to a significant ($p<0.05$; Figure 3.2A) reduction of BMPRII compared with vehicle, whereas TβRIIΔk-fib mice treated with SU5416 led to no further significant reduction in BMPRII expression (Figure 3.2 B).

In contrast, no significant change was observed in phosphorylation of the downstream BMP activated canonical signalling pathway, Smad 1, 5 and 8 (Figure 3.2 A, B). Whereas the addition of SU5416 induced a tread in increased total Smad1, 5 and 8 compared to TβRIIΔk-fib (Figure 3.2 A, B).

Lung homogenates of the TβRIIΔk-fib were assessed for expression of the TGFβ activated downstream canonical signalling pathways Smad 2 and 3. TβRIIΔk-fib mice exhibited enhanced phosphorylation of Smad2/3 compared to WT controls ($p<0.05$). The addition of SU5416 to WT mice led to a significant increase in phosphorylated-Smad 2/3 levels compared to vehicle treated WT mice but SU5416 did not have a significant effect on TβRIIΔk-fib mice (Figure 3.2 A, B).

Assessment of the phosphorylation of the non-canonical signalling pathway, demonstrated a significant increase in phosphorylated ERK 1/2 in vehicle treated TβRIIΔk-fib mice compared to WT controls ($p<0.05$). Treatment of WT controls with SU5416 led to rise in phosphorylated ERK 1/2 compared to vehicle treated controls which failed to reach significance. No significant effect of SU5416 was observed on TβRIIΔk-fib treated animals. No significant difference in phosphorylated or total p38 was observed in any of the four groups tested (Figure 3.2 A, B).

Confirmation of BMPRII and phosphorylated Smad2/3 was sought using immunohistochemistry (IHC) on sections from paraffin embedded lungs from WT and TβRIIΔk-fib mice treated with SU5416 or vehicle control. Lungs from WT mice exhibited BMPRII staining around vascular structures (Figure 3.3A). TβRIIΔk-fib

mice exhibited reduced BMPRII staining compared to WT controls. *In-vivo* administration of SU5416 led to a marked reduction of BMPRII expression in WT mice compared to vehicle treated animals. However *in-vivo* administration of SU5416 in the TβRIIΔk-fib mice had no overt effect on BMPRII expression compared to vehicle controls (Figure 3.3A). Consistent with Western blot analysis (Figure 3.2A), IHC assessment of phosphorylated Smad2/3 expression demonstrated enhanced levels in the TβRIIΔk-fib lungs compared to WT controls (Figure 3.3 B). Furthermore, *in-vivo* administration of SU5416 in WT and TβRIIΔk-fib mice induced an increase in phosphorylated Smad2/3 levels in both groups (Figure 3.3B).

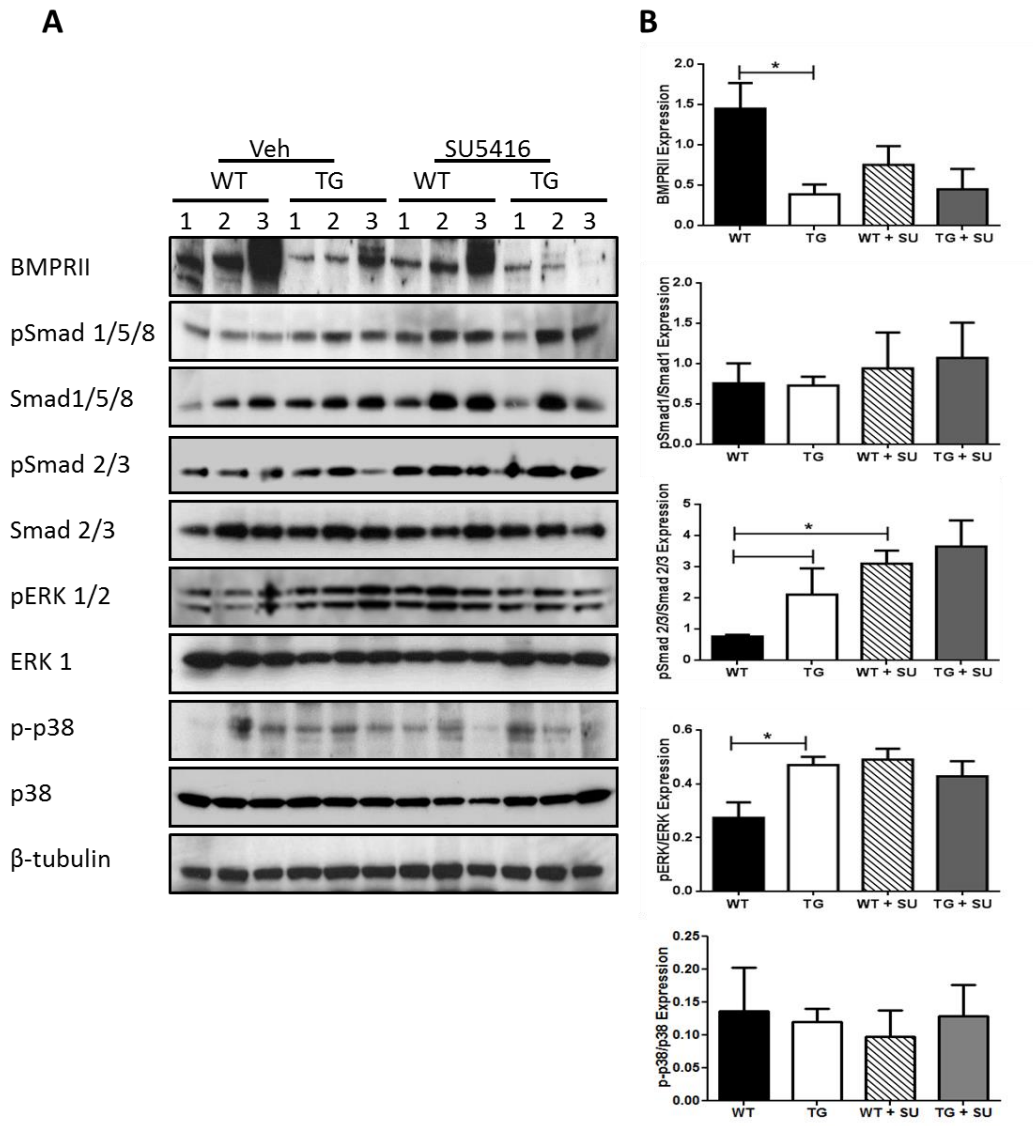

Figure 3.2 – BMPRII expression is reduced in the TβRIIΔk-fib model of SSc-PAH

Western blots were performed on protein extracts prepared from whole lungs isolated from wild type (WT) and TβRIIΔk-fib mice exposed *in-vivo* to SU5416 or vehicle (n=3). Blots were probed for expression of BMPRII, phospho-Smad2/3 (pSmad2/3), Smad3, phospho-Smad 1 (pSmad 1), Smad 1, phospho-ERK 1/2 (pERK 1/2), ERK 1/2, phospho-p38 (p-p38) and p38. Protein loading was determined by β-tubulin levels and representative blots are presented above (A). Densitometry was performed and the mean ± SEM expression of BMPRII normalised to β-tubulin expression and plotted (B) pSmad 1/5/8, pSmad2/3, pERK 1/2 1/2 and p-p38 was normalised to each of their total proteins and plotted (n=6) (B). *p<0.05 using Mann-Whitney Tests. (B).

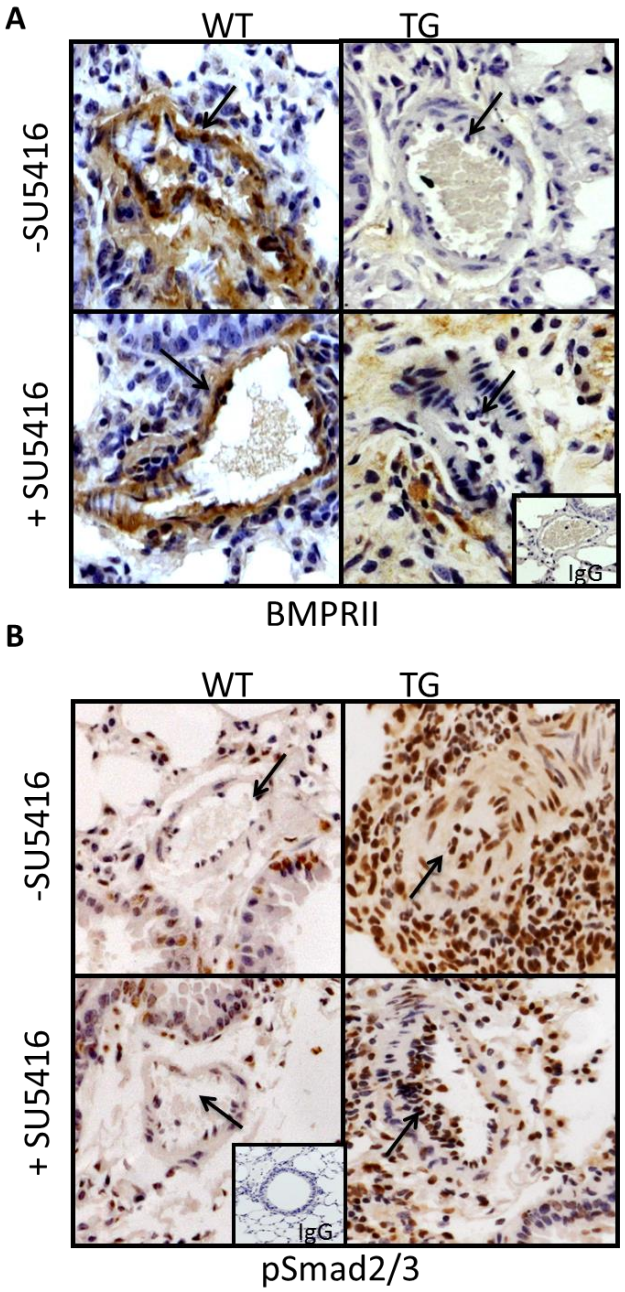

Figure 3.3 – Immunohistochemical expression of components of the TGFβ superfamily in the lung of TβRIIΔk-fib model of SSc-PAH

Immunohistochemical staining for BMPRII (A) and phopho-Smad2/3 (pSmad2/3) (B) on paraffin embedded formalin fixed lung sections from wild type (WT) and TβRIIΔk-fib mice exposed *in-vivo* to SU5416 or vehicle alone. Representative images shown of 10 images per mouse, n=3 per group. Magnification x40 using Carl Zeiss microscope.

3.3.3 Investigation of expression of BMPRII and downstream signalling components of TGFβ superfamily in fibroblasts

A number of cell types have been implicated in vascular remodelling associated with the development of PAH, including fibroblasts. The expression of BMP receptors and downstream signalling components of the TGFβ superfamily was assessed in fibroblasts established from the lungs of WT and TβRIIΔk-fib mice (Figure 3.4).

Initially expression of the BMP type I and II receptors, BMPRIA and BMPRRII was assessed by Western blot. Expression of BMPRIA was unchanged in TβRIIΔk-fib mice fibroblasts, compared to WT controls. Whereas BMPRII expression was significantly reduced TβRIIΔk-fib mice compared to WT controls ($p<0.05$; Figure 3.5 A, B). Gene expression of BMPRII was assessed by qPCR and expression normalised to succinate dehydrogenase complex, subunit A. In contrast to protein, no significant difference in BMPRII gene transcript levels was observed between TβRIIΔk-fib mice fibroblasts, compared to WT controls (Figure 3.5 B).

There was no significant difference observed in phosphorylation of the downstream BMP activated canonical signalling pathways, Smad 1,5 and 8 (Figure 3.5 A).

Assessment of the phosphorylation of the non-canonical signalling pathway ERK1/2, demonstrated a significant increase in fibroblasts from TβRIIΔk-fib mice compared to WT controls ($p<0.05$; Figure 3.5). No significant difference in total levels of ERK1/2 was observed. TβRIIΔk-fib mice exhibited a significant increase in phosphorylated p38 levels compared to WT controls ($p<0.05$; Figure 3.5). In addition total levels of p38 were significantly elevated in TβRIIΔk-fib mice compared to WT controls ($p<0.05$; Figure 3.4).

Lung fibroblasts of the TβRIIΔk-fib were further assessed for expression of the TGFβ activated downstream canonical signalling pathways Smad 2 and 3. Fibroblasts from TβRIIΔk-fib mice exhibited enhanced phosphorylation of Smad2/3 compared to WT controls ($p<0.05$; Figure 3.5 A), whereas total Smad2/3 was unchanged.

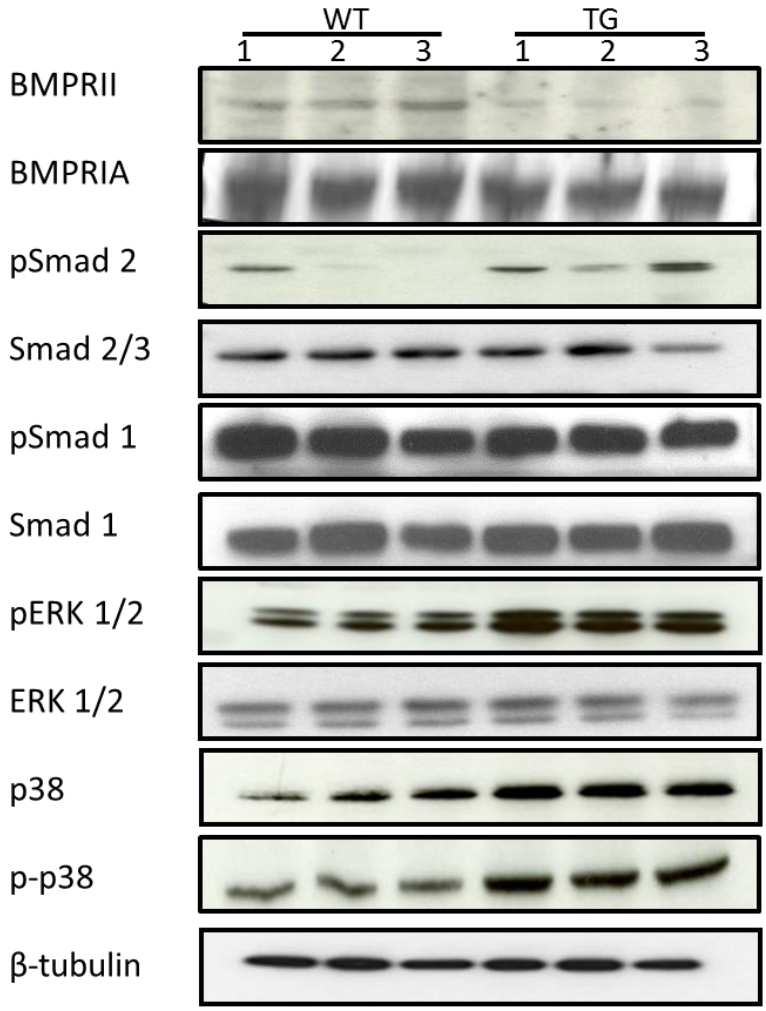

Figure 3.4 – Expression of components of the TGFβ superfamily and downstream signalling pathways in explants cultured lung fibroblasts from WT and TBRIIΔK-fib mice

Protein was isolated from confluent monolayers of explant cultured murine lung fibroblasts from WT and TβRIIΔk-fib (TG) mice (n=3). Western Blots were performed and probed for expression of BMPRII, BMPR1A, phospho-Smad 2/3 (pSmad 2/3),Smad 2/3, phospho-Smad1 (pSmad1), Smad1, phosphor-ERK 1/2 (pERK 1/2), ERK 1/2, phosphorylated p38 (p-p38) and p38. Protein loading was determined by β-tubulin levels representative blots are presented above (A). Protein loading was determined by β-tubulin levels (A).

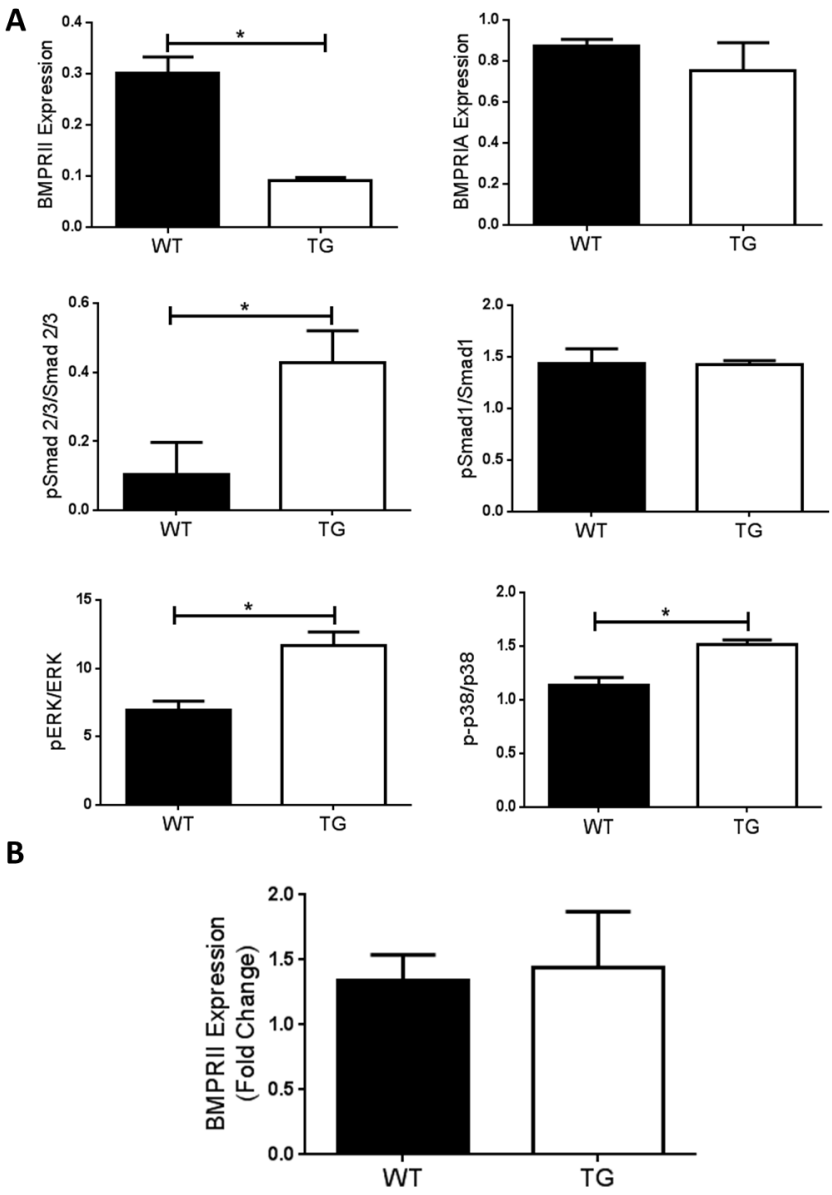

Figure 3.5 - Expression of components of the TGFβ superfamily and downstream signalling pathways in explant cultured lung fibroblasts from WT and TBRIIΔK-fib mice.

Densitometry was performed and the mean ± SEM expression of BMPRII, was normalised to β-tubulin expression and fold change plotted (n=6) (A). pSmad 2/3, pSmad 1, pERK 1/2 and p-p38 was normalised to their respective total proteins. *$p<0.05$ using Mann-Whitney Test (B). BMPRII gene expression was determined by quantitative polymerase chain reaction (qPCR) of RNA from explant cultured fibroblasts and expression normalised to the succinate dehydrogenase complex, subunit A (Sdha) gene (C).

3.3.4 TβRIIΔk-fib fibroblasts exhibit a blunted response to BMP4

BMPs acting via the receptor BMPRII activate a number of downstream signalling pathways including Smad1. To investigate the functional effect of reduced BMPRII highlighted in 3.3.3, the induction of phosphorylated Smad1 in response to the BMP ligand, BMP4 was assessed.

Initially the optimal dose and time dependent induction of phosphorylated Smad1 in response to BMP4 was assessed in WT murine fibroblasts. Induction of phosphorylated Smad1 by BMP4 (50 ng/ml) was assessed at 0.25, 0.5, 1, 2, and 24 hours (Figure 3.6A). Phosphorylated Smad1 was significantly increased compared to base line at 0.25, 0.5, 1, 2 hours, returning to base line after 24 hours in response to BMP4. Fibroblasts exhibited a maximal ~3 fold induction at 0.5 hours (Figure 3.6A). Having established maximal temporal induction of phosphorylated Smad1 to occur at 0.5 hours, a dose response of lung fibroblasts to BMP4 was investigated. Significant induction of phosphorylated Smad1 by BMP4 was observed in lung fibroblasts at 5 and 50ng/ml, with maximal ~2 fold induction observed at the 5ng/ml treatment with BMP4 ($p<0.05$; Figure 3.6B).

Using these optimised conditions I assessed the induction of phosphorylated Smad1, phosphorylated ERK 1/2 and phosphorylated p38 levels by BMP4 in fibroblasts isolated from TβRIIΔk-fib mice (Figure 3.7 A, B). TβRIIΔk-fib fibroblasts exhibited a significantly blunted induction of phosphorylated Smad1 ($p<0.05$) consistent with the reduced expression of BMPRII. Consistent with this, induction of phosphorylated ERK 1/2 and phosphorylated p38 by BMP4 was significantly ($p<0.05$) reduced in TβRIIΔk-fib fibroblasts compared to WT controls (Figure 3.7 A, B).

Confirmation of the blunted responses to BMP4 exhibited by TβRIIΔk-fib fibroblasts was confirmed by assessing nuclear translocation of phosphorylated Smad1 in response to BMP4 (Figure 3.8 A). Consistent with reduced BMPRII expression, fibroblasts from the TβRIIΔk-fib model exhibited a significant reduction in phosphorylated Smad1 positive nuclei in fibroblasts compared to WT controls was observed ($p<0.05$; Figure 3.8, B).

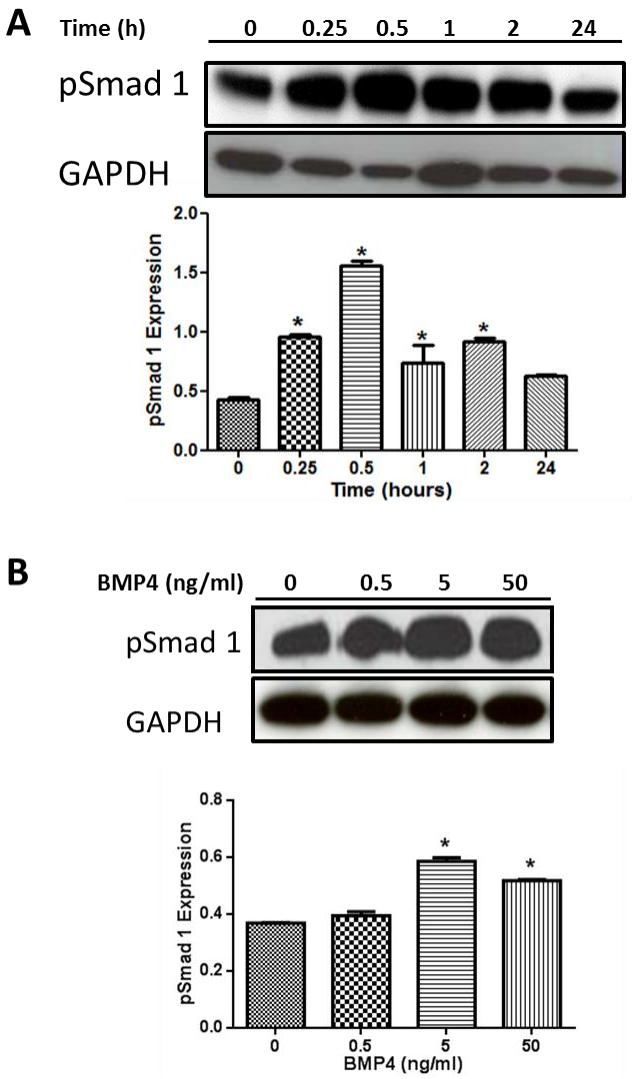

Figure 3.6 – BMP4 temporal and dose dependent induction of phosphorylated-Smad1 in lung fibroblasts by BMP4

Monolayers of explant cultured fibroblasts established from WT mice were stimulated with BMP4 and phosphorylated-Smad1 (pSmad1) levels determined by Western blot. The temporal induction of pSmad1 in response to 50 ng/ml BMP4 at 0, 0.25, 0.5, 1, 2 and 24 hours was determined (A).Induction of pSmad 1 stimulated with 0, 0.5, 5 and 50ng/ml of BMP4 for 0.5 hours was determined (B). Representative blots of three independent experiments (n=3). Densitometry was performed and the mean ± SEM expression of pSmad1 was normalised to GAPDH expression and plotted (A) and (B). *$p<0.05$ using Mann-Whitney Tests (A and B).

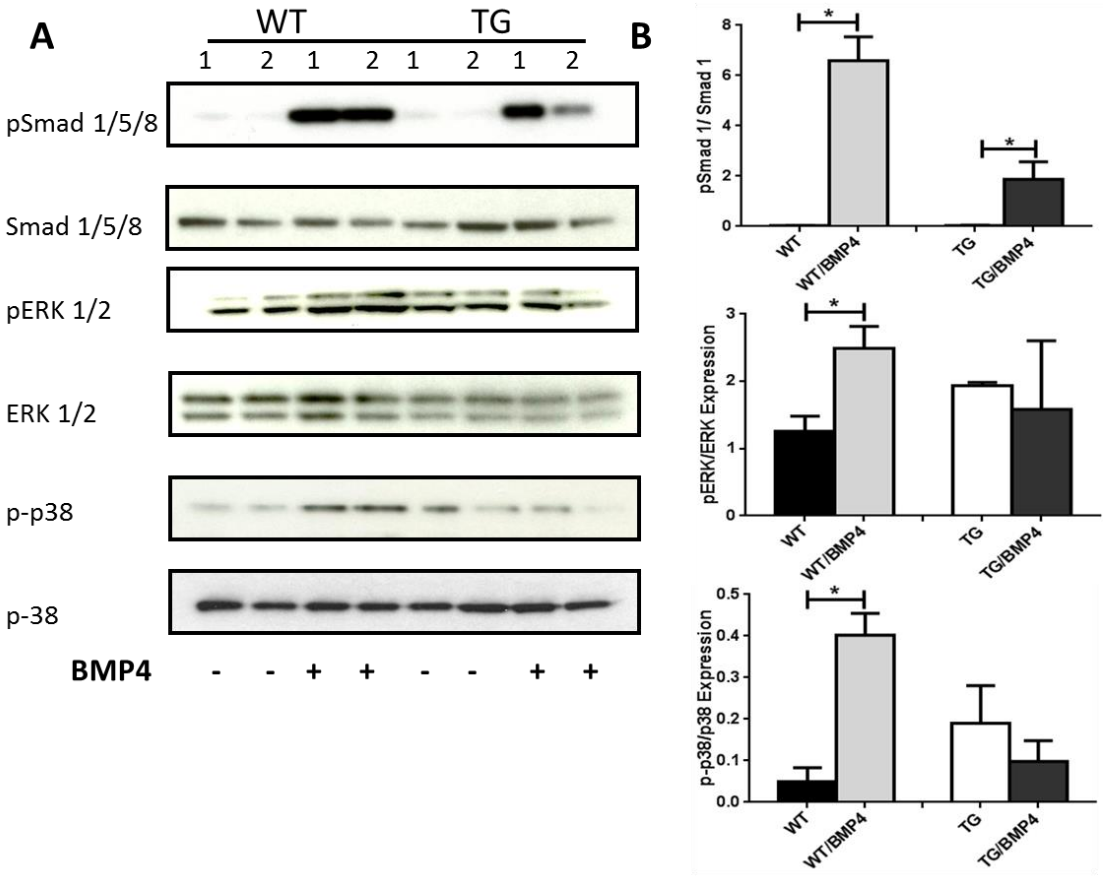

Figure 3.7 – Altered phosphorylation of downstream signalling pathways in response BMP4 in TβRIIΔk-fib fibroblasts

Monolayers of explant cultured fibroblasts established from WT and TβRIIΔk-fib mice were stimulated with BMP4 (5 ng/ml) for 0.5 hours in three independent experiments and phosphorylated-Smad1 (pSmad1), phosphorylated-ERK 1/2 (ERK 1/2) and phosphorylated-p38 (p-p38) levels determined by Western blot. p-Smad1, pERK 1/2 and p-p38 protein levels were determined by Smad1, ERK 1/21/2 and p38 levels (A) (n=6). Densitometry was performed and the normalised mean ± SEM expression ratio of phosphor/total protein Smad1, ERK 1/2 and p38 was normalised and representative blots were plotted (B). *$p<0.05$ using Mann-Whitney Tests.

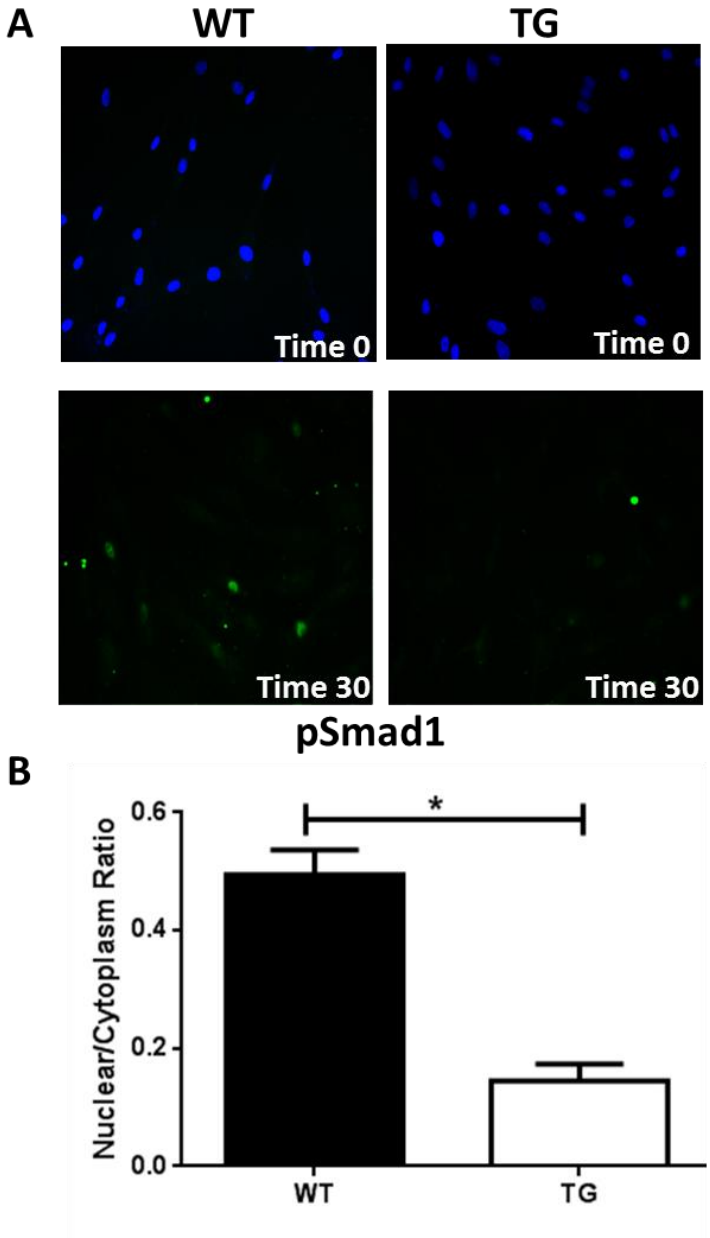

Figure 3.8 – Altered phosphorylation of phosphorylated-Smad 1 in response to BMP4 in TβRIIΔk-fib fibroblasts.

Monolayers of explant cultured fibroblasts established from WT and TβRIIΔk-fib mice were stimulated with BMP4 (5 ng/ml) for 0.5 hours in three independent experiments and three biological replicates and total and phosphorylated-Smad1 (pSmad1) (green) positive nuclei was determined (A) by immunoflouresence (IF). Magnification x20 using the Carl Zeiss microscope. The ratio of pSmad 1/Smad 1 was determined and the mean ± SEM plotted (B). *$p<0.05$ using Mann-Whitney Tests.

3.3.5 Investigation of fibroblast proliferation and migration in the TβRIIΔk-fib model.

Proliferation and migration are two key characteristics that can contribute to vascular remodelling in SSc-PAH [18]. Fibroblasts that exhibit enhanced migration and proliferation can contribute to medial thickening and muscularisation in pulmonary vessels [143,147,150,181,182]. The effect of PDGFBB, a potent inducer of fibroblast migration and proliferation on TβRIIΔk-fib fibroblasts was assessed.

Confluent monolayers of TβRIIΔk-fib and WT fibroblasts were scratched and treated with either 1% FCS alone or supplemented with 10ng/ml of PDGFBB in the presence of the anti-proliferative Mitomycin-C (10 ug/ml) and migration assessed after 48 hours (Figure 3.9A, B). PDGFBB induced migration in both WT and TβRIIΔk-fib explant cultured fibroblasts. TβRIIΔk-fib fibroblasts exhibited a significant increased capacity to migrate across the scratched monolayer compared to WT controls in response to PDGFBB treated ($p>0.05$; Figure 3.9C).

The proliferative response of TβRIIΔk-fib fibroblasts to PDGFBB was next assessed. WT and TβRIIΔk-fib fibroblasts were seeded at equal cell density in the presence or absence of PDGFBB (50 ng/ml) and cell number determined using the crystal violet proliferation assay at 72 hours. PDGFBB induced cell numbers were normalised to media alone controls and plotted as indicated in Figure 3.9C. A significant increase in TβRIIΔk-fib fibroblast cell number in response to PDGFBB compared to WT controls was observed ($p>0.05$; Figure 3.9A).

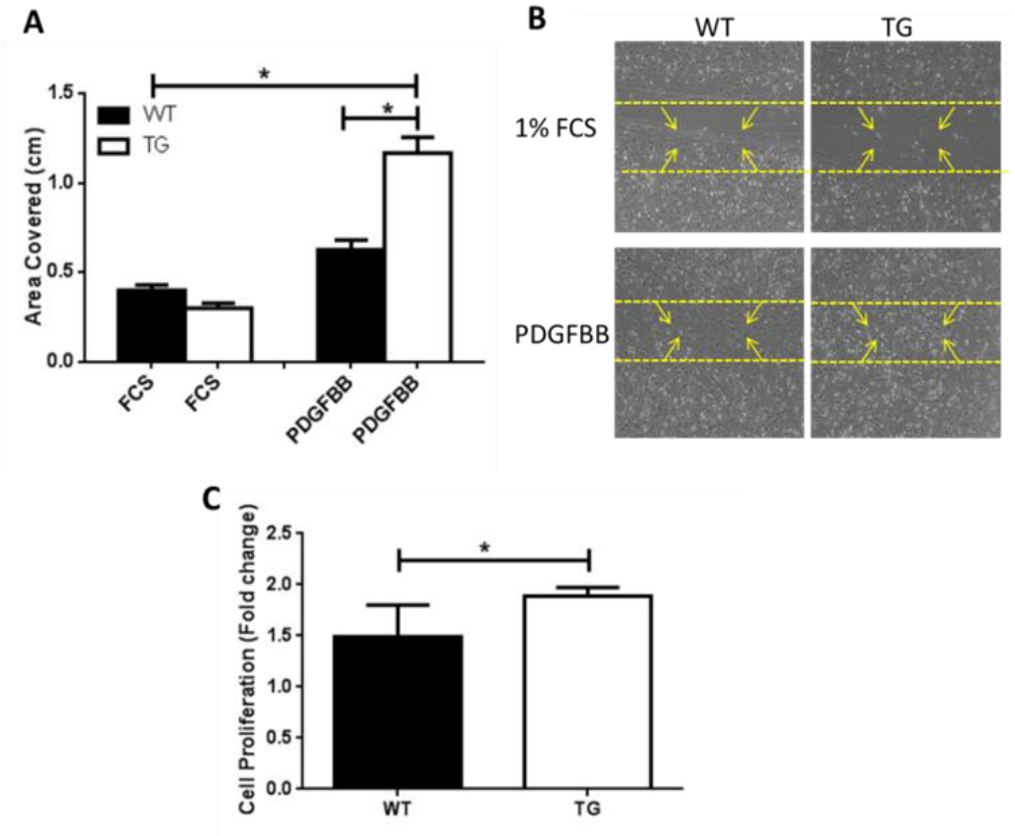

Figure 3.9 – TβRIIΔk-fib lung fibroblasts exhibit increased proliferative and migratory response to PDGFBB

Platelet derived growth factor (PDGFBB) mediated proliferation in wildtype (WT) and TβRIIΔk-fib mice explant cultured fibroblasts was examined. Data represent the fold proliferation induced by PDGFBB compared to vehicle controls and are expressed as a mean of three donors. Proliferation was assessed after 72 hours (A). *p<0.05, Unpaired T-test (A).Confluent monolayers of WT and TβRIIΔk-fib lung fibroblasts were scratched and migratory responses assessed in response to 1% FCS (FCS) and 10 ng/ml of PDGFBB (PDGF) in the presence of 10 μg/ml Mitomycin C for 48 hours. Experiments were performed on three mice per group in triplicate. (B). Migration was assessed after 24 hours, images were taken using the Olympus CDK2 microscope and data analysed using Axio Vision software. *p<0.05, Mann-Whitney Test (C).

3.4 Discussion

It has been previously reported that the TβRIIΔk-fib transgenic mouse model of SSc spontaneously develops an enhancement of RVSP and many key features PAH. These animals exhibit a paradoxical enhancement in TGFβ signalling, including activation of the canonical Smad signalling pathway, which is conveyed in elevated levels of phosphorylated Smad2/3 [52]. Consistent with the observed phenotype of the TβRIIΔk-fib transgenic mouse model, Loeys-Dietz syndrome patients who possess TβR-II mutations exhibit increased levels of phosphorylated Smad2 in the nuclei. In SSc similar phenotypes have been observed with increased levels of phosphorylated Smad2 reported in the skin of SSc patients [118]. There are also three other variants of disease with mutations also observed in TGFβ-R2, TGFβ2 and Smad 3.

TβRIIΔk-fib transgenic mice display increased expression of latent TGFβ in the ECM and develop dermal fibrosis, as well as fibrosis in a number of internal organs [54, 57]. The administration of bleomycin to these mice induced the appearance of myofibroblasts, and increased apoptosis of type II alveolar epithelial cells suggesting that these mice have an increased susceptibility to injury [55]. The TβRIIΔk-fib mice develop a more much severe fibrotic phenotype than wildtype mice. Interestingly these mice exhibit vascular defects in the lung independently of pulmonary fibrosis [56].

In this study key recent findings related to clinical aspects of SSc associated PAH have been elucidated and observations using a mouse model of SSc that is induced by targeted genetic perturbation of TGFβ signalling in fibroblasts. These mice have been reported to develop enhanced RVSP and vascular remodelling compared to wildtype controls [119].

This mouse model has recently been found to be highly sensitive to a pharmacological inhibitor of VEGF signalling (SU5416), the administration of SU5416 leads to the pharmacological induction of a phenotype reminiscent of SSc-PAH. The background of these mice is similar to SSc patients and these mice also spontaneously develop mild PAH and in this context, observation that SU5416

induced PAH in the TβRIIΔk-fib model of SSc provided an opportunity to explore potential mechanisms of susceptibility that may be relevant to human SSc. As highlighted in Figure 3.1 the TβRIIΔk-fib mice display mild PAH but the addition of SU5146 leads to the formation of concentric lesions, further elevation of RVSP, medial wall thickening and inflammatory infiltrate [56, 119].

In figure 3.2 and 3.3 it is demonstrated that that the TβRIIΔk-fib mice display elevated levels of phosphorylated Smad2/3, phosphorylated ERK 1/2 and phosphorylated p38 expression in lung fibroblasts These mice also display an increase in phosphorylated Smad 2/3 in whole lung tissue compared to wild type controls [52]. Furthermore this data suggests a key role for heightened activity of the TGFβ pathway in driving this process in SSc-PAH. Several reports have demonstrated enhanced TGFβ responsiveness in PASMCs from HPAH patient's with BMPRII mutations, including elevated secretion of inflammatory chemokines [13] and an enhanced pro-proliferative response, a phenomena replicated in mice harbouring nonsense BMPRII mutations [13, 14]. Enhanced TGFβ signalling has previously been reported in IPAH vessels [15-17]. A number of groups have also demonstrated that preclinical models of PAH exhibit enhanced TGFβ activity including the monocrotaline rat, hypoxia and hypoxia SU5416. [10-12]. A plethora of studies have demonstrated pharmacological antagonists of the TGFβ signalling pathway can inhibit and reverse the development of PAH in preclinical models which exhibit genetically independent reduction in BMPRII levels in tissues [17]. Consistent with this the TβRIIΔk fib model of SSc which exhibits enhancement in TGFβ signalling including phosphorylated levels of Smads 2 and 3, develops PAH under normoxic conditions [1, 7]. Collectively these studies and this thesis support the notion that enhanced TGFβ signalling contributes to the development of PAH and SSc-PAH.

Previously studies have shown the reduction of functional cell surface expression of BMPRII in patients is strongly associated with the development of HPAH and IPAH [183, 184]. The next investigation was to examine if TβRIIΔk-fib mice that spontaneously develop PAH also have reduced BMPRII protein levels. In figure 3.2 and 3.3 it has been highlighted that the TβRIIΔk-fib mice display a reduction of functional BMPRII in both whole lung tissue and lung fibroblasts and this may represent a common susceptibility mechanism in HPAH, SSc-PAH and IPAH

patients. There was no change in phosphorylated Smad 1 levels in either whole lung tissue or lung fibroblasts in the TβRIIΔk-fib model. A number of groups have also demonstrated that preclinical models of PAH, including the monocrotaline rat, hypoxia and hypoxia SU5416 also exhibit reduction in BMPRII levels [141,146, 176]. This suggests along with the observations in the TβRIIΔk-fib model that a reduction in BMPRII may lead to an increased susceptibility of developing PAH.

Following on from these observations the next experiment was to investigate the impact of the reduction in BMPRII levels in the TβRIIΔk model on the BMP activated canonical and non-canonical signalling pathways. Explant lung fibroblasts from WT controls exhibited a robust phosphorylation of Smad1 in response to BMP4. In contrast, fibroblasts isolated from TβRIIΔk mice were less responsive, consistent with reduced BMPRII receptor expression, and previously reported studies in patients with HPAH harbouring defined BMPRII gene mutations [24, 177]. This disrupted BMP signalling is another parallel mechanism between the TβRIIΔk model and PAH patients.

To assess the functional effects of reduction of BMPRII protein in TβRIIΔk mice, relevant functional assays in explants cultured lung fibroblasts were examined Migration and proliferation are key pathological features in PAH by which fibroblasts contribute to the remodelling and occlusion of pulmonary vessels [143, 147, 150, 181, 182]. PDGFBB is a potent mitogen for fibroblasts and PASMCs, and expression of the PDGFA, PDGFB, PDGFR-α, and PDGFR-β have been reported to be increased in patients with severe PAH [185, 186]. Furthermore, PASMCs isolated from HPAH patients with functional mutations in the BMPRII gene exhibit impaired migration (Holmes *et al*, unpublished observations). Building on this work the migratory responses of fibroblasts isolated from the TβRIIΔk model of SSc was investigated. Fibroblasts isolated from the TβRIIΔk-fib model, which express less BMPRII than WT fibroblasts exhibited enhanced response to PDGF-BB leading to increased fibroblast migration. Fibroblasts from the TβRIIΔk model also display enhanced proliferation compared to WT controls suggesting that fibroblasts from this model exhibit a phenotype that can contribute to more vascular remodelling. It has been previously demonstrated that fibroblasts that are exposed to hypoxia display elevated levels of phosphorylated-p38 and that this increase in expression is linked to

enhanced proliferation [187, 188]. This suggests that the elevated phosphorylated-p38 levels in fibroblasts from the TβRIIΔk model might be contributing to the enhanced proliferation in this model. These changes have also been reported in IPAH and IPF where fibroblasts display increased proliferation and migration, two cellular processes that can contribute to vascular remodelling [22, 189].

These results have made a link between an enhanced TGFβ environment that may contribute to a reduction in BMPRII. The hypoxia, SU5146/hypoxia and MCT models of PAH have also demonstrated a reduction of BMPRII and an increase in phosphorylated Smad 2/3 levels in the lungs of these animals [141, 144, 164, 190]. This is the first time these results have been demonstrated in an SSc model and the link between a reduction in BMPRII in a model of SSc and the development of PAH. The TβRIIΔk model can provide a platform that might provide a better understanding to the mechanism by how SSc patients develop PAH. This model represents a model to represent SSc patients that exhibit enhanced TGFβ activity and a reduction in BMPRII can allow us to investigate novel therapeutics that targets this signalling axis. The bleomycin model of SSc-PH also exhibits a reduction in BMPRI and this raises the question do other SSc models, for example the FRA-2 model display a reduction in BMPRII that may be increases the susceptibility of these mice developing PAH.

3.5 Conclusion

The TβRIIΔk mouse model of SSc develops a mild PAH phenotype and following exposure to the VEGFR antagonist SU5416 these mice develop a more severe pulmonary vasculopathy, enhance RVSP and increased infiltration of immune cells into vascular lesions [119]. These transgenic mice exhibit enhanced TGFβ activity, highlighted by elevated phosphorylated Smad 2 and 3 expression in the lungs in concordance with a reduction in BMPRII protein levels in both whole lung tissues and fibroblasts.

Mutations in the BMPRII gene which lead to the reduction of functional BMPRII at the cell surface have been strongly implicated in the susceptibility of developing PAH in HPAH and IPAH patients [7, 14, 17, 24, 26, 28, 183, 184, 191, 192]. A number of studies have shown in pre-clinical insult models of PAH a reduction in protein levels of BMPRII is associated with enhanced TGFβ activity [141, 144, 146, 193, 194]. Collectively supporting the notion that imbalance in TGFβ/BMP pathway is a key component in the development of PAH. TβRIIΔk mice exhibit reduced BMPRII expression in the lung, which is further reduced by the *in-vivo* administration of SU5416. Fibroblasts from these mice also display reduced BMPRII expression, dysregulated BMP signalling and blunted responses to BMP ligands. Functionally TβRIIΔk fibroblasts exhibited increased rates of proliferation and migration, two features that can contribute to occlusion of the lumen in the pulmonary arteries.

Future studies will seek to assess the relevance of these observations in the context of SSc patients.

4. Reduction of BMPRII in patients with scleroderma may increase susceptibility to the development of PAH

4.1 Introduction

SSc is a heterogeneous autoimmune rheumatic disease characterised by vascular dysfunction and fibrosis that leads to pathological remodelling of tissues [18]. PAH is an important complication occurring in up to 10% of SSc cases [195]. The risk of developing PAH persists through the disease and is time dependent, suggesting that SSc operates as a susceptibility factor [38]. SSc-PAH patients have a significantly poorer prognosis compared to those with idiopathic and heritable forms of the disease [196, 197]. A number of gene mutations are associated with heritable PAH and are discussed extensively in chapter 1. Many of these reported mutations are associated with genes in the TGFβ superfamily and downstream signalling pathway. The most prevalent gene mutated being in the type II BMP receptor BMPRII. A number of mutations in this gene have been identified and lead to the reduction in expression or loss of function of BMPRII at the cell surface [102]. In contrast, genetic studies on SSc and SSc-PAH patients have not detected mutations in the BMPRII gene [198]. Wang *et al* demonstrated that heightened DNA methylation of the BMPRII promoter contributes to a reduction in BMPRII expression in dermal microvascular endothelial cells of patients with SSc [175]. In addition to this a number of studies have also highlighted non-genetic mechanisms that can lead to reduced BMPRII protein levels, including ubiquitination and proteasomal degradation mediated by Smurf1, K5 and E3 ligase and Itch [17, 190]. Collectively non-genetic mechanisms may also contribute to a reduction in BMPRII expression and therefore a predisposition to the development of PAH.

A number of studies have highlighted the key role for TGFβ in the development of PAH [146, 192] and speculated that imbalance between the BMP and TGFβ axes contributes to the development of PAH [17, 102]. A significant body of evidence has implicated TGFβ in the development of SSc. Consistent with the importance of the TGFβ superfamily, in chapter three, a pre-clinical model of SSc (TβRIIΔk-fib mouse strain) which develops pathological remodelling of lung and raised right ventricular systolic pressures due to upregulation of TGFβ signalling in fibroblasts and an

aberrant BMP signalling axis [57, 101]. Further lungs and fibroblasts from these mice exhibited reduced expression of BMPRII

In chapter three the role of altered BMPRII expression and signalling in determining susceptibility to PH in the TβRIIΔk-fib murine model of SSc was explored and the aim was to translate these key findings to human SSc lung samples. Results have shown constitutive reduction in BMPRII expression in the lung of the TβRIIΔk-fib strain and the aim was to investigate BMPRII expression in lung tissue and explants cultured fibroblasts from donor controls and SSc-PAH patients. It will be interesting to investigate if impaired BMP signalling is observed in SSc patients which would elude to a fundamental susceptibility mechanism for the development of PAH associated with SSc. The TβRIIΔk-fib model displayed no change in mRNA expression of BMPRII suggesting that post-translational modifications that affect protein turnover may be contributing to a reduction in BMPRII expression. This mechanism of proteasomal degradation was also investigated in SSc patients.

Proteasomal degradation and regulation has been linked to pulmonary fibrosis and the ubiquitin-proteasome system has been linked to cellular protein turnover [199]. The proteasome is located in both the cytoplasm and nucleus with a 20s barrel like structure that has 19s regulatory proteins at both ends [199]. The proteasome has two main functions, scaffold and proteinase that are ATP dependent [200]. Different sites on the proteasome has different functions, the threonine residues are the active site and the hydroxyl groups function as catalytic nucleophils that have three separate cleavage partialities that are known as chyotryptic, tryptic and caspase like [199]. Proteasomal inhibitors, for example MG132 and bortezomib target these functions and exert their effects by binding to one or more for these sites, for example MG132 can inhibit chyotryptic and tryptic enzymatic activites and bortezomib only inhibits chyotryptic activity. In the proteasome there is the regulatory 19s complex that recognises, bind and unwinds proteins and together with the 20s core forms the 26s proteasome [201]. In relation to TGFβ signalling which is of interest to this work and SSc-PAH both protein degradation and ubiquitin are believed to modulate this pathway [202, 203]. As mentioned earlier a number of papers have also highlighted non-genetic mechanisms that lead to reduced BMPRII protein levels, including ubiquitination and proteasomal degradation mediated by Smurf1, K5 and E3 ligase and Itch [17, 190]. KSHV has been shown to downregulate BMPRII and it is

believed that this occurs through the expression of the ubiquitin ligase K5, this work shows that expression of K5 can dowregulate BMPRII through ubiquitation and lysosomal degradation leading to aberrant BMP signalling [204]. Following on from this work the same group showed that by inhibiting lysosomal degradation using chloroquine that the development and progression of PH in MCT rats was prevented. In addition using the MCT model of PH where BMPRII levels are significantly reduced, chloroquine, elevated BMPRII expression in the lung of MCT rats compared to vehicle controls. *In-vitro* chloroquine increased BMPRII expression suggesting that lysosomal degration of BMPRII might contribute to the development of PH and that inhibition of the lysosome may be a novel approach in the treatment of PAH [205].

Due to this alteration in BMPRII protein turnover in the TβRIIΔk-fib model and patients, MG132 a proteasomal degradation inhibitor was investigated. Bortezomib is another example of a proteasomal degradation inhibitor which is currently FDA approved for the treatment of patients with multiple myeloma [206].In animal models, proteasomal inhibition has demonstrated an ability to alleviate liver fibrosis, cardiac fibrosis, renal fibrosis and myelofibrosis [207-210]. Interestingly bortezomib has already demonstrated efficacy in the bleomycin model of fibrosis, it promoted normal wound healing and prevented the development of skin and lung fibrosis. Bortezomib significantly reduced collagen content in the lung and skin thickness in the bleomycin model and also significantly reduced TGFβ induction of α-SMA and CTGF in lung fibroblasts [132]. This study highlights the potential for proteasomal inhibition in pulmonary complications of SSc however another study reported conflicting data. This study showed that neither bortezomib nor MG132 demonstrated efficacy in the bleomycin model of lung fibrosis or the in the TSK-1/+model of skin fibrosis [211].

4.2 Aims

In the TβRIIΔk-fib model of SSc, BMPRII expression and downstream signalling pathways were altered, suggesting dysfunctional expression of BMPRII and altered phosphorylation of signalling proteins that comprise the TGFβ superfamily signalling pathways. Building on these observations the aim of this chapter was to explore the relevance in SSc patients. Expression of BMPRII and components of the TGFβ superfamily signalling pathways was assessed in whole lung tissues and explant cultured fibroblasts from SSc patient. Downstream signalling BMP pathways are altered in the TβRIIΔk-fib model, and using SSc explant lung fibroblasts the donor controls and SSc fibroblasts were exposed to BMP4 treatment to assess the activation of downstream signalling pathways. Following on from interrogating the TGFβ and BMP signalling pathways the aim was to demonstrate functional changes in explant cultured lung fibroblasts that might contribute to the development of PAH and vascular remodelling.

4.3 Results

4.3.1 SSc lung exhibits enhanced TGFβ activity in both whole tissue and explant cultured fibroblasts.

Initially I sought to determine whether the TGFβ/BMP axis imbalance observed in the lungs of the TβRIIΔk-fib mouse model of SSc had clinical relevance to SSc patients. Using Western blot, the expression of components of the TGFβ superfamily downstream signalling pathway was assessed in explant cultured lung fibroblasts established from SSc patients and compared these to control lung fibroblasts. The expression profile of the TGFβ superfamily from explant cultured lung fibroblasts from patients with SSc and healthy controls was assessed by Western blot (Figure 4.1 A). Lung fibroblasts from SSc patients demonstrated significantly elevated levels of phosphorylated-Smad 2/3 and phosphorylated-ERK 1/2 ($p<0.05$; Figure 4.1 A). There was no significant change in expression of phosphorylated Smad 1 and phosphorylated-p38 in explant cultured lung fibroblasts from SSc patients (Figure 4.1 A). There was no significant difference in Smad 1, Smad 2/3, ERK 1/2 and p38 protein expression in normal fibroblasts compared to fibroblasts from SSc patients (Figure 4.1).

Given the enhanced phosphorylation of Smad 2/3 expression in explant lung fibroblasts, a number of classically TGFβ regulated genes were assessed by qPCR in explant cultured lung fibroblasts. Expression of PAI-1, CTGF and the BMP antagonist Gremlin-1 (Figure 4 C) demonstrated elevated basal expression, however this failed to reach statistical significance (Figure 4 C). Collectively suggesting the TGFβ signalling pathway may be elevated in SSc lung fibroblasts. Interestingly enhanced TGFβ activity has been observed in skin fibroblasts from SSc patients suggesting that heightened TGFβ activity might be a shared mechanism in both the skin and lung of SSc patients [174].

Fibroblasts are a key cell type involved in the SSc and SSc-PAH but the expression of TGFβ and BMP patways in whole lung tissue was also of interest. From this the the expression of TGFβ superfamily and downstream signalling pathways in whole lung tissue were investigated. Interestingly results in whole lung tissue was similar to explant cultured fibroblasts, Lung tissue from SSc patients demonstrated significantly elevated levels of phosphorylated-Smad 2/3 and phsphorylated-ERK

1/2 ($p<0.05$;Figure 4.2 A). There was no significant change in expression of phosphorylated-Smad 1 and phosphorylated-p38 in whole lung tissue from SSc patients (Figure 4.2 A). There was no significant difference in Smad 1, Smad 2/3, ERK 1/2 and p38 protein expression in normal fibroblasts compared to fibroblasts from SSc patients (Figure 4.2A).

Immunohistochemistry (IHC) was used to explore the expression and distribution of phosphorylated-Smad 1 and phosphorylated-Smad2/3 in paraffin embedded lungs from control lung tissue and lung tissue from SSc-PAH patients. Lungs from both controls and SSc-PAH patients exhibit similar staining patterns for phosphorylated-Smad 1 (Figure 4.3A). IHC assessment of phosphorylated-Smad2/3 expression demonstrated enhanced levels in the SSc-PAH lungs compared to controls (Figure 4.3B).

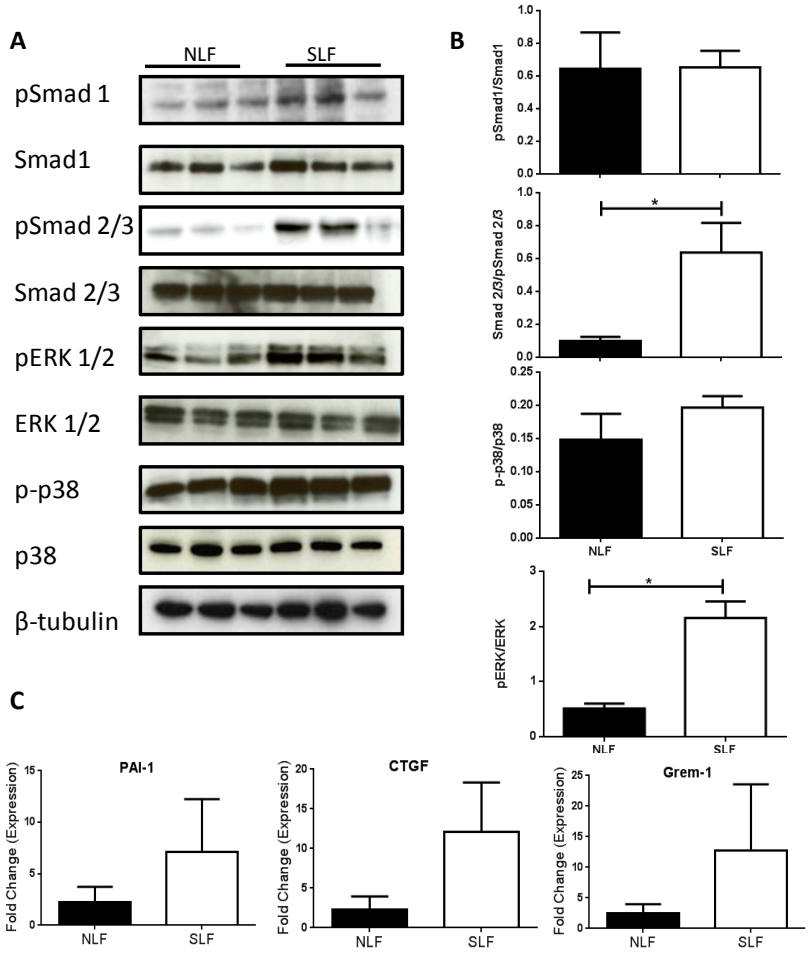

Figure 4.1 – Expression of components of the TGFβ superfamily and downstream signalling pathways in explant cultured fibroblasts

Western blots were performed on proteins isolated from confluent monolayers of explant cultured lung fibroblasts from control (NLF) and SSc (SLF) patients (n=6). Blots were probed for expression of phosphorylated-Smad 2/3 (pSmad 2/3), Smad 2/3, phosphorylated-Smad1 (pSmad1), Smad1, phosphorylated-ERK 1/2 (pERK 1/2), ERK 1/2, phosphorylated-p38 (p-p38) and p38 (A). Protein loading was determined by β-tubulin levels and representative blots are shown above (A). Densitometry was performed and the mean ± SEM expression of p-Smad 2/3, Smad2/3, pSmad1, Smad1, pERK 1/2, ERK 1/2, p-p38 and p-38 was normalised to β-tubulin expression and plotted (B). Quantitative polymerase chain reaction (qPCR) of RNA from NLF and SLF explant cultured fibroblasts (n=6) for TGFβ regulated genes PAI-1, connective tissue growth factor (CTGF) and Gremlin-1 and expression was normalised to succinate dehydrogenase complex, subunit A (Sdha) gene and the mean ± SEM plotted (C). *$p<0.05$ using Mann-Whitney Tests (C).

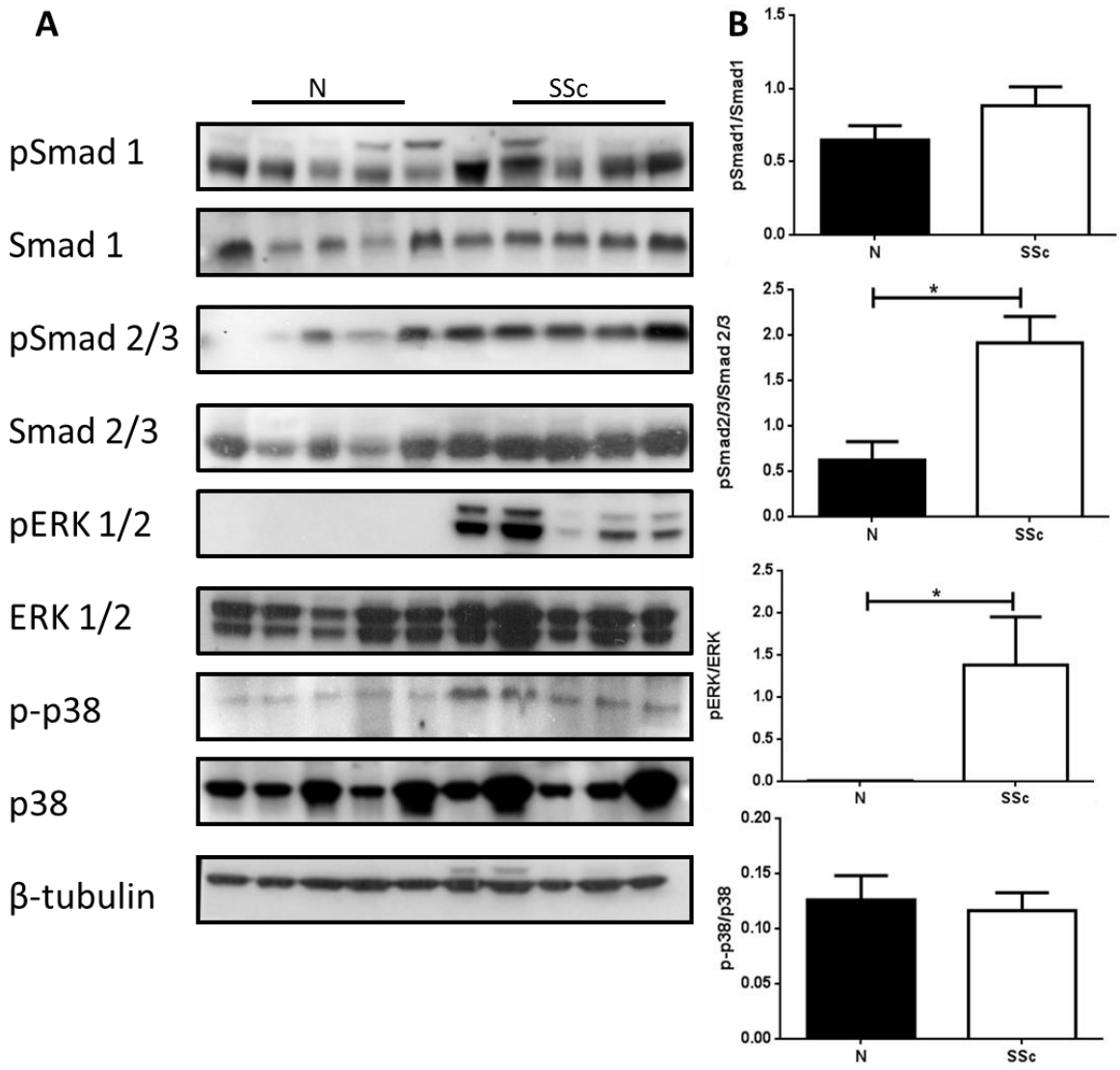

Figure 4.2 – Expression of components of the TGFβ superfamily and downstream signalling pathways in whole lung tissue

Western blots were performed on proteins homogenates of whole lung tissue from control (N) and SSc patients (n=6). Blots were probed for expression of phosphorylated-Smad 2/3 (pSmad 2/3), Smad 2/3, phosphorylated-Smad1 (pSmad1), Smad1, phosphorylated-ERK 1/2 (pERK 1/2), ERK 1/2, phosphorylated-p38 (p-p38) and p38 (A). Protein loading was determined by β-tubulin levels and representative blots are displayed above (A). Densitometry was performed and expression normalised to β-tubulin levels and the ratio of the mean ± SEM expression of p-Smad 2/3 to Smad2/3, p-Smad1 to Smad1, p-ERK 1/2 to ERK 1/2, p-p38 and p-38 plotted (B). *$p<0.05$ using Mann-Whitney Test.

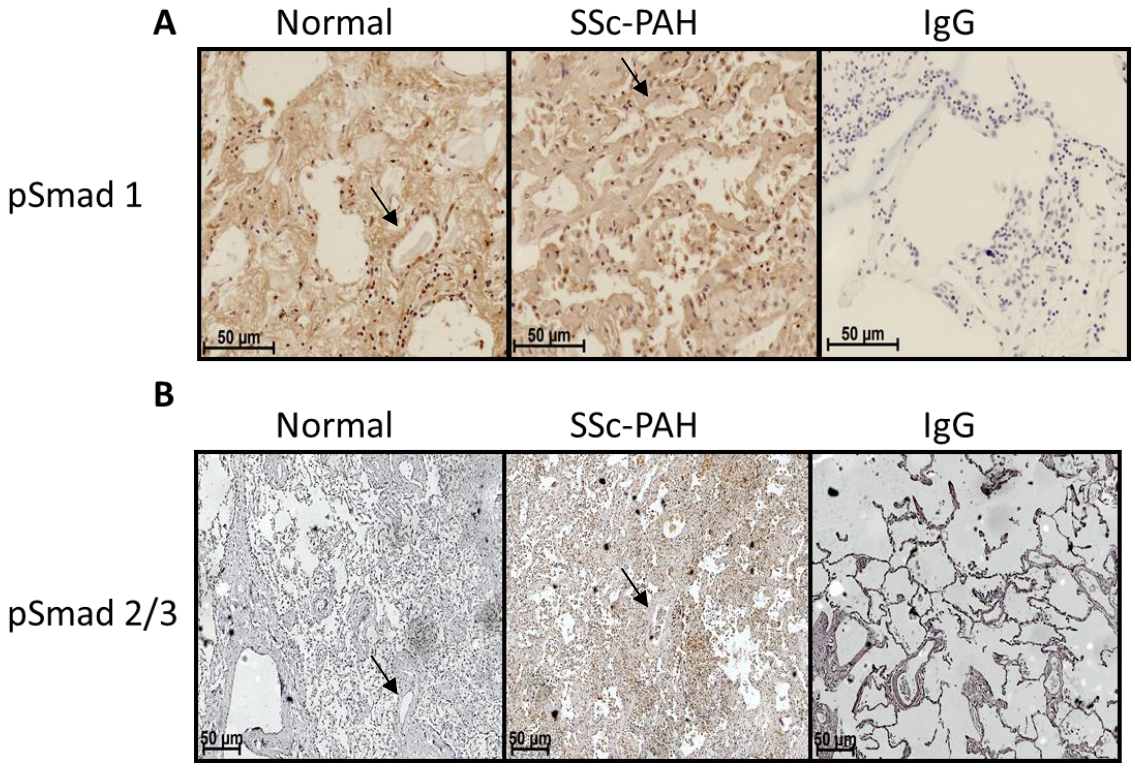

Figure 4.3 – Immunohistochemistry of phosphorylated-Smad 1 and phosphorylated-Smad 2/3 in SSc-PAH lung

Immunohistochemical staining for phosphorylated-Smad 1 (pSmad1) (A) and phosphorylated-Smad2/3 (pSmad2/3) (B) on paraffin embedded formalin fixed lung sections from control lung (Normal) and SSc-PAH patients was performed. Representative images shown of n=3 per group. Black arrow indicates vascular staining. Magnification x20. Images were taken using the Carl Zeiss microscope.

4.3.2 A reduction in BMPRII in SSc lung may be a susceptibility factor to the development of PAH in SSc patients

The expression of BMPRII in whole lung tissue and fibroblasts from SSc patients was investigated to examine if BMPRII reduction was observed in concordance with enhanced TGFβ activity. Using Western blot analysis the expression of BMPRII was assessed from confluent explant cultured lung fibroblasts and homogenised whole lung tissue from SSc patients and patients from other diseases with no lung involvement (Figure 4.4 A, C). SSc-PAH explant cultured lung fibroblasts exhibited a significant reduction in BMPRII expression compared to healthy controls ($p<0.05$; Figure 4.4 C.)

BMPRII protein expression in whole lung tissue was investigated by Western blot analysis, there was a significant reduction in BMPRII expression in whole lung tissue in SSc-PAH patients compared to control lung ($p<0.05$; Figure 4 B, D).

IHC confirmed a reduction in BMPRII in SSc-PAH patients, normal unaffected lung displayed BMPRII expression around vascular structures as indicated by black arrows compared to control tissue (Figure 4.4F).

The levels of BMPRII gene transcripts were then investigated by qPCR. Whereas BMPRII protein levels were significantly reduced, BMPRII gene expression was elevated and was trending towards significance (Figure 4.4 E); suggesting that post transcriptional effects are responsible for the reduction in BMPRII protein expression. Proteasomal degradation and ubiquition that has previously been implicated in pulmonary fibrosis and PAH and this suggests there might be a similar mechanism in SSc and the development of PAH in these patients.

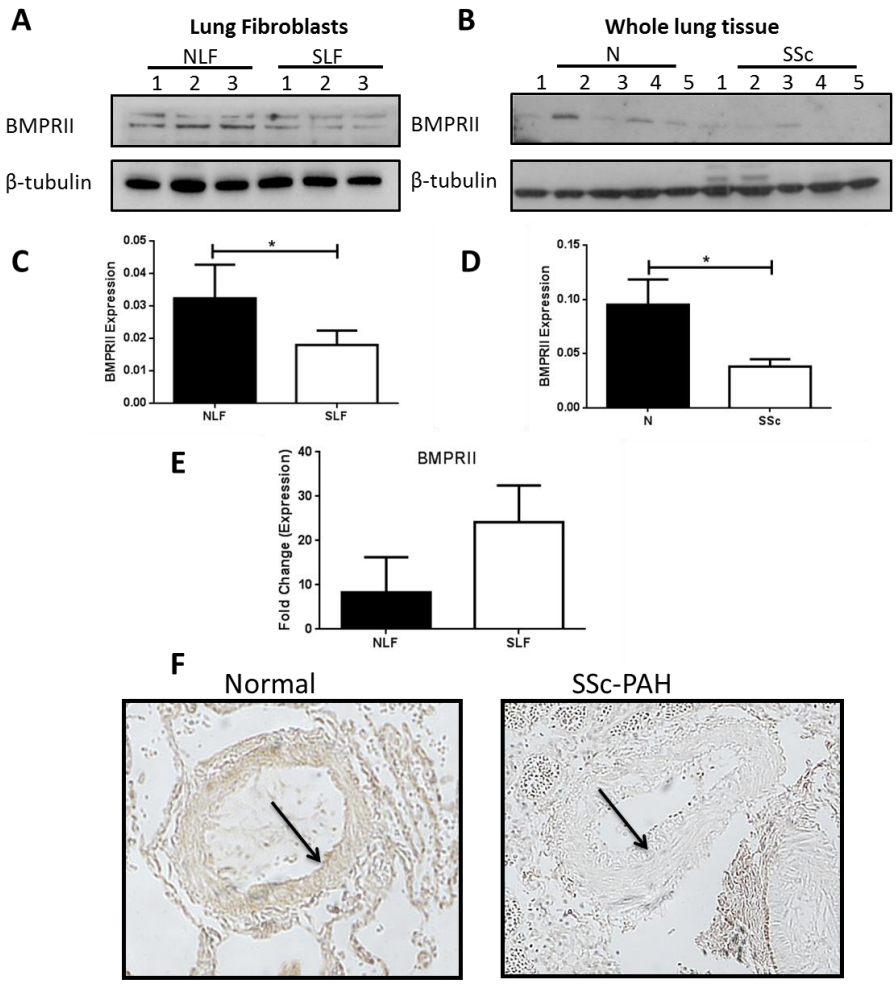

Figure 4.4 – Expression of BMPRII in explant cultured fibroblasts and whole lung.

Western blots were performed on proteins isolated from confluent monolayers of explant cultured lung fibroblasts from control (NLF) and SSc (SLF) patients and whole lung tissue from control (normal) and SSc-PAH patients (n=3). Blots were probed for expression of BMPRII (A, B). Protein loading was determined by β-tubulin levels (A, B). Densitometry was performed and the mean ± SEM expression of BMPRII was normalised to β-tubulin expression and plotted (C, D). *$p<0.05$ using Mann-Whitney Test. BMPRII expression levels was determined by quantitative polymerase chain reaction (qPCR) of RNA isolated from explant cultured fibroblasts from NLF and SLF and expression normalised to succinate dehydrogenase complex, subunit A (Sdha) gene (n=6) (E). Immunohistochemical staining for BMPRII on paraffin embedded formalin fixed lung sections from normal and SSc patients. Black arrow indicates vascular staining. Representative images shown (n=3). Magnification x100 using Carl Zeiss Microscope, (F).

4.3.3 SSc fibroblasts exhibit an aberrant response to BMP ligands

BMP's acting via the receptor BMPRII activates a number of downstream signalling pathways including the canonical signalling pathways Smad 1, 5 and 8 as well as non-canonical signalling pathways ERK 1/2 and p-38.

To assess if the reduced expression of BMPRII in SSc fibroblasts resulted in a functional reduction in response to BMP ligands, the effect of BMP4 on phosphorylation of downstream signalling proteins was assessed. Explant cultured fibroblasts from SSc-PAH and control patients were serum starved for 24 hours followed by stimulation with BMP4 (5 ng/ml) for 30 minutes to assess the phosphorylation of Smad1 and ERK 1/2 and p38 proteins. Explant cultured fibroblasts from SSc-PAH fibroblasts exhibited similar basal levels of phosphorylated-Smad 1. Control donors exhibited significantly higher induction of phosphorylated Smad1 in response to BMP4 compared with SSc-PAH fibroblasts, which displayed a blunted induction of phosphorylated Smad1 levels in response to BMP4, ($p>0.05$; Figure 4.5A, B).

Assessment of explant cultured fibroblasts from SSc-PAH fibroblasts demonstrated a significant elevation in basal levels of phosphorylated-ERK 1/2 compared to healthy controls. Stimulation of control donor fibroblasts with BMP4 induced a significant induction of phosphorylated-ERK 1/2, whereas SSc-PAH fibroblasts displayed a blunted response to BMP4 with no significant induction of phosphorylated-ERK 1/2 levels observed, ($p>0.05$; Figure 4.5A, B).

Explant cultured fibroblasts from normal and SSc-PAH fibroblasts exhibited similar basal levels of phosphorylated p38 and no significant induction of phosphorylated-p38 by BMP4 was noted in healthy control or SSc fibroblasts.

Taken collectively, these results suggest that a reduction in BMPRII expression leads to a blunted response to BMP 4 in SSc fibroblasts.

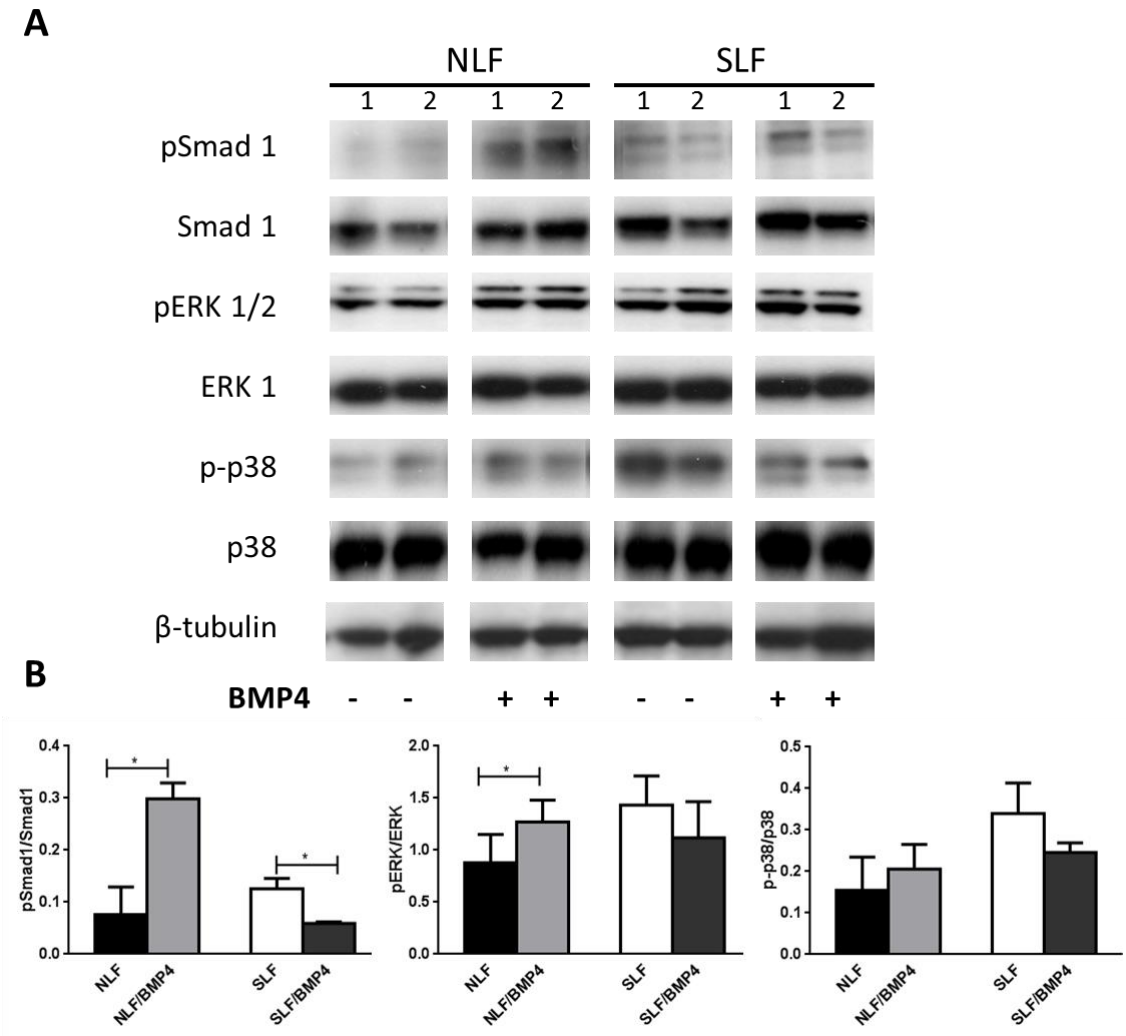

Figure 4.5 - SSc lung fibroblasts exhibit a blunted response to BMP4 which results in a perturbed BMP signalling profile

Monolayers of explant lung fibroblasts established from control (NLF) and SSc patients (SLF) were stimulated with BMP4 [5 ng/ml] for 0.5 hours in three independent experiments and phosphorylated-Smad1 (pSmad1), Smad1, phosphorylated-ERK 1/2 (pERK 1/2), ERK 1/2, phosphorylated-p38 (p-p38) and p38 levels determined by Western blot (A). Densitometry was performed and the mean ± SEM expression of pSmad1, pERK 1/2 and p-p38 normalised to Smad 1, ERK 1/2 and p38 expression and plotted (B). *$p<0.05$ using Mann-Whitney Test.

4.3.4 Proteasomal degradation inhibitor MG132 can upregulate BMPRII expression and restore responses to BMP ligands.

Previously ubiquitination and proteasomal degradation of BMPRII have been proposed to contribute to further reduction of BMPRII protein levels in HPAH patients [190, 204]. To investigate the effect of proteasomal degradation on the reduced BMPRII protein expression in lung fibroblasts established from SSc patients the effect of the inhibitor MG132 was assessed.

Explant cultured lung fibroblasts were serum starved for 24 hours followed by exposure to MG132 (1 μM) or vehicle control for a further 16 hours and expression of BMPRII was assessed by Western blot. Consistent with 4.3.3, there was a significant reduction in BMPRII expression in SSc fibroblasts compared to healthy controls. The addition of MG132 led to a significant increase in BMPRII protein levels both in healthy control and SSc fibroblasts ($p<0.05$; Figure 4.6 A, B).

As highlighted in figure 4.5 explant cultured fibroblasts display a blunted response to BMP4 stimulation. To establish if elevation in BMPRII levels in response to MG132 led to a composite restoration of cellular responses to BMP4, phosphorylation of Smad1 was assessed. Serum starved explant cultured lung fibroblasts exposure to 1 μM of MG132 or vehicle control for 16 hours were exposed to BMP4 (5 ng/ml) for 30 minutes and phosphorylated Smad1 assessed by Western blot. Pre-treatment of lung fibroblasts from control and SSc donors with MG132 resulted in an increase in BMP4 ligand induction of phosphorylated Smad1 compared with BMP4 treatment alone. MG132 exhibited significantly greater effects on phosphorylation of Smad1 in fibroblasts derived from SSc patients compared to healthy donor controls ($p<0.05$; Figure 4.6 C).

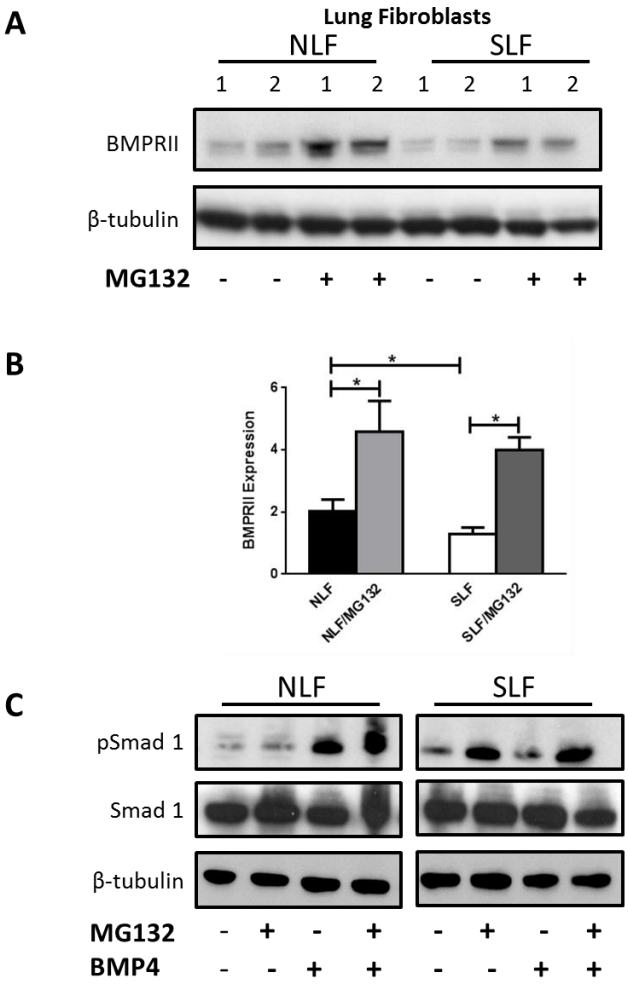

Figure 4.6 – The proteasomal inhibitor MG132 enhances BMPRII levels in explant cultured fibroblasts in normal and SSc patients

Western blots were performed on proteins isolated from confluent monolayers of explant cultured lung fibroblasts from normal and SSc patients (n=3). Blots were probed for expression of BMPRII. Protein loading was determined by β-tubulin levels (A). Densitometry was performed and the mean ± SEM expression of BMPRII normalised to β-tubulin expression and representative blots plotted (B). Monolayers of explant lung fibroblasts established from normal and SSc patients were stimulated with FCS (0.1%), MG132 (1 μM) for 16 hours followed by BMP4 (5 ng/ml) for 0.5 hours in three independent experiments and phosphorylated-Smad1 (pSmad1) determined by Western blot. p-Smad1, protein levels was determined by β-tubulin levels (C). Densitometry was performed and the mean ± SEM expression of pSmad1 was normalised to β-tubulin expression and plotted (D). *$p<0.05$ using Mann-Whitney Tests.

4.3.5 SSc fibroblasts display pro-migratory and proliferative properties

Proliferation and migration are two key characteristics that can contribute to vascular remodelling in SSc-PAH. Fibroblasts that exhibit enhanced migration and proliferation may contribute to medial thickening and muscularisation in pulmonary vessels.

The ability of explant cultured fibroblasts from normal and SSc patients to migrate in response to stimulation with FCS (1%) or PDGFBB (10 ng/ml) was assessed. Confluent monolayers of fibroblasts were scratched and treated with either 1% FCS alone or 10ng/ml of PDGFBB in the presence of the anti-proliferative Mitomycin-C (10 μg/ml) and migration assessed after 48 hours (Figure 4.7 A). Migration was observed in both normal and SSc explant cultured lung fibroblasts in the presence of PDGFBB. However fibroblasts from SSc patients demonstrated a significant increased ability to migrate across the scratched monolayer in response to PDGFBB treatment compared to normal lung fibroblasts ($p<0.05$; Figure 4.7 B).

To assess the ability of explant cultured fibroblasts to proliferate, lung fibroblasts were treated with FCS (1%) or PDGFBB (10 ng/ml). Lung fibroblasts from SSc patients demonstrated a significant increase in cell numbers compared to normal fibroblasts in response to FCS (1%) or PDGFBB (10 ng/ml). PDGFBB exhibited greater rates of proliferation in both normal and SSc fibroblasts compared to 1% FCS ($p<0.05$; Figure 4.7 C). Collectively these results suggest that SSc fibroblasts exhibit an increased capacity to migrate and proliferate in response to PDGFBB and suggest that this is a potential mechanism that contributes to vascular remodelling in SSc-PAH.

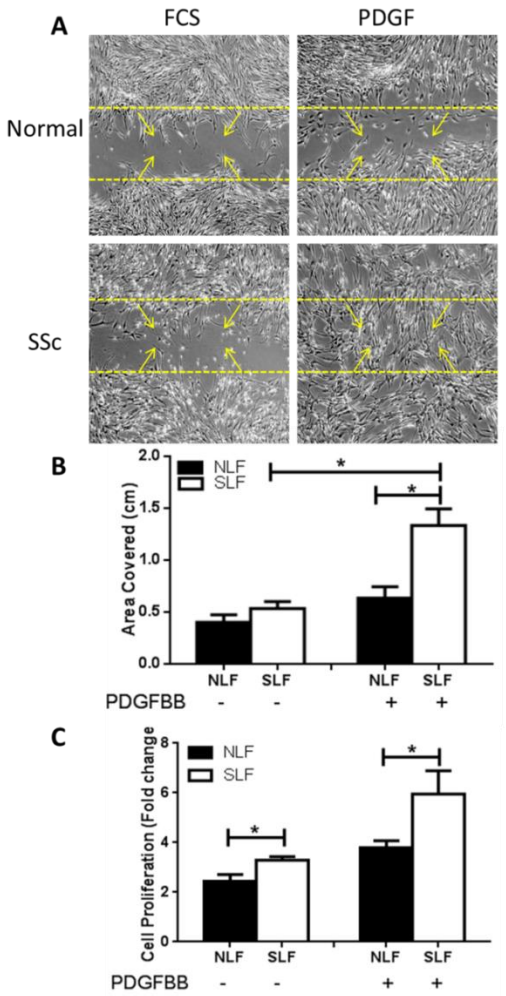

Figure 4.7 – SSc lung fibroblasts exhibit increased migratory and proliferative capacity compared to healthy donors in response to PDGFBB

Confluent monolayers of scleroderma (SLF) and control donor lung fibroblasts (NLF) were scratched and migratory responses assessed in response to 1% FCS and 10 ng/ml of Platelet derived growth factor (PDGFBB) in the presence of 10 μg/ml Mitomycin C for 48 hours (A). Experiments were performed on three patients per group in triplicate. Migration was assessed after 24 hours, images were taken using the Olympus CDK2 microscope and data analysed using Axio Vision software. *$p<0.05$, Mann-Whitney Test (B). Basal and 50 ng/ml PDGFBB mediated proliferation in NLF and SLF. Data represents the fold proliferation induced by PDGFBB compared to vehicle controls and are expressed as the mean of three donors. Proliferation was assessed after 72 hours (C). *$p<0.05$, Mann-Whitney Test (C).

4.4 Discussion

Clinical observations suggest that SSc provides a permissive phenotype in which PAH can occur, but that this may be independent of other manifestations of the disease. For example, PAH occurs from around 36 months of disease duration and with equal frequency in the two major SSc subsets suggesting it is does not reflect skin involvement. Also, unlike other cardio-respiratory manifestations that tend to occur early in the disease, PAH develops in 1-2 percent of cases throughout follow up and represents a time dependent risk [38]. Thirdly, borderline elevation of mean pulmonary artery pressure confers a higher risk factor for the development of PAH suggesting that there is progressive pulmonary haemodynamic change in SSc patients that can in some cases progress to PAH [212]. Since it has been shown previously highlighted that a reduction of functional cell surface expression of BMPRII is strongly associated with the development of HPAH and IPAH, I wanted to investigate BMPRII expression in the lung of SSc patients [183, 184]. In this chapter it is highlighted that patients with SSc have a reduction of BMPRII in whole lung tissue and explant cultured lung fibroblasts and this may represent common susceptibility mechanism in HPAH, SSc and IPAH patients. Furthermore this data suggests a key role for heightened activity of the TGFβ pathway in driving this process in SSc.

Previous reports have demonstrated PASMCs from HPAH patients with BMPRII mutations exhibit enhanced responsiveness to TGFβ1, including elevated secretion of inflammatory chemokines and enhanced pro-proliferative response, a phenomenon replicated in mice harbouring nonsense BMPRII mutations [17, 173]. Enhanced TGFβ signalling has previously been reported in IPAH vessels [152,174,194]. Indicative of enhanced TGFβ signalling, in both whole lung tissue and lung fibroblasts from SSc patients elevated phosphorylated levels of Smads 2/3 was observed. Consistent with this a number of groups have demonstrated that preclinical models of PAH exhibit enhanced TGFβ activity including the monocrotaline rat, chronic hypoxia and hypoxia SU5416 models, and in concordance with a reduction in BMPRII levels [141,146,176]. A number of studies have demonstrated pharmacological antagonists of the TGFβ signalling pathway can inhibit and reverse the development of PAH in preclinical models which exhibit a non-genetic reduction in BMPRII levels in tissues [194]. Consistent with this the TβRIIΔk fib model of

SSc which exhibits enhancement in TGFβ signalling including phosphorylated levels of Smads 2/3, spontaneously develops PAH under normoxic conditions. Collectively these studies support the notion that enhanced TGFβ activity and downstream signalling contributes to the development of PAH. These results support the role of TGFβ signalling in the development of PAH both in SSc and other forms of PAH.

Previous studies have demonstrated PASMCs with reduced BMPRII expression exhibit altered responses to TGFβ [17, 177]. There is a marked reduction in pulmonary vascular BMPRII expression in both whole lung and lung fibroblasts from TβRIIΔk fib mice compared to wildtype controls as discussed in chapter three. In this chapter BMPRII expression was found to be reduced in both lung fibroblast and whole lung tissue from SSc patients. Interestingly BMPRII transcripts were not significantly different in control or SSc lung fibroblasts, suggesting the reduction in BMPRII may result from changes in protein turnover or dysfunctional protein stability.

It has also been implicated that a reduction in BMPRII in PASMCs from PAH patients is associated with a blunted induction by BMP ligands of downstream signalling pathways [23]. Similarly, as shown in chapter three, fibroblasts isolated from the TβRIIΔk fib model exhibited reduced BMPRII expression and a blunted response to BMP ligands. Consistent with this BMP4 induced a significant increase in phosphorylated Smad1 and phosphorylated ERK 1/2 in healthy control fibroblasts, whereas little or no effect on the induction of phosphorylated-Smad1 or phosphorylated-ERK 1/2 was observed in SSc lung fibroblasts. This suggests that the reduction in BMPRII protein levels in SSc lung may be contributing to aberrant BMP signalling.

A number of studies have demonstrated that non-genetic mechanisms can impact on expression of BMPRII [190, 213]. A recent study demonstrated reduction of protein and mRNA of BMPRII in microvascular endothelial cells and skin of SSc patients resulted from epigenetic repression [175]. Other studies have demonstrated a putative role for ubiquitination and subsequent degradation of BMPRII [213]. Kaposi sarcoma-associated herpesvirus (KSHV) has been implicated as an etiological agent promoting the development of PAH. Durrington *et al.* revealed that

the KSHV expressed protein K5, ubiquitinates the cytoplasmic domain of BMPRII, leading to lysosomal degradation [204]. Further, overexpression of Smurf1 reduces steady-state levels of BMPRII through ubiquitination and subsequent proteasomal and lysosomal degradation [17, 190]. Consistent with this Smurf1 mRNA levels are elevated in SSc lung fibroblasts (Personal communication, A Holmes). These findings suggest that enhanced protein degradation may be responsible for reduced BMPRII expression in SSc.

Using the proteasomal inhibitor MG132 which has previously been reported to reverse bleomycin-induced fibrosis in mice suggesting that MG132 has therapeutic efficacy in the lung [132]. BMPRII protein expression in fibroblasts from SSc patients was up-regulated in the presence of MG132, although not to those levels observed in healthy controls. Consistent with the partial restoration of BMP signalling, treatment of SSc fibroblasts with MG132 and the subsequent addition of BMP4 led to a significant induction of phosphorylated-Smad1. This suggests that proteasomal inhibitors may reduce the risk of SSc patients developing PAH and may be a potential protective mechanism in patients that are borderline PAH.

Interestingly explant cultured fibroblasts from SSc patients exhibited increased migratory and proliferative capacity compared to healthy controls. The proliferation and expansion of α-SMA positive cells in vascular remodelling suggest that the activated fibroblast in SSc patients could contribute to vascular remodelling and occlusion of the lumen. Interestingly Hummers and colleagues has shown PDGFBB to be elevated in the serum of SSc patients, and thus contribute to remodelling in SSc patients [214].

4.5 Conclusion

In conclusion, experiments in this chapter have shown a reduction in BMPRII protein in lung tissue and fibroblasts from patients with SSc. This was associated with enhanced activation of downstream components of the TGFβ signaling pathway. In contrast to HPAH and IPAH patients, where a significant proportion harbour mutations in the BMPRII gene, data suggests that the blunted response of SSc lung fibroblasts to BMP ligands results from post-transcriptional events that lead to reduction in the levels of BMPRII protein, and that this could be partially restored *in-vitro* using the proteasomal inhibitor MG132. Collectively these results suggest SSc may act to phenocopy HPAH by promoting an environment where BMPRII protein levels and downstream signalling is reduced and promotes increased susceptibility to the development of PAH in the background of SSc.

5. Differentiated PASMCS may resemble PASMCs isolated from patients with non-heritable forms of PAH

5.1 Introduction

PH is defined as elevated blood pressure in the arteries of the lung; greater than 25mmHg at rest and is sub-divided into a number of groups (Table 1.1). PAH (Group 1) results from specific vascular changes in the structure of the pulmonary vessels that in turn leads to the increased pulmonary vascular resistance and elevated mean PAP [16]. It is believed that PASMCs are a cell type that can contribute to the development of PAH in both HPAH and SSc-PAH. In the development of PAH associated with other underlying pathologies, such as the connective tissue diseases like SSc the disease is more diverse since it may fall into Group I or other Groups of pulmonary hypertension. SSc patients may develop elevated pulmonary pressures as a result of pulmonary fibrosis, termed SSc-PH (Group 3; Table 1) or independently of major pulmonary fibrotic complications termed SSc-PAH (Group 1; Table 1). The work in chapter three and chapter four have focused on the role of fibroblasts in the development of SSc-PAH and in this chapter the work focuses on the potential role of PASMCs another key cell type involved in PAH pathology.

It is currently considered that the majority of SSc patients with increased develop SSc-PAH which was highlighted in the recent DETECT study [15]. The overall prevalence of all types of PAH is estimated to be between 30-50 cases per million [58]. Of these, the heritable forms of PAH represent a relatively small component of cases, 2-3 per million per year [58, 59]. The incidence of all PAH in SSc patients has been estimated to be between 6-60% of all patients [60]. Survival studies have shown patients with SSc-PAH have a particularly poor prognosis compared to those with PAH alone, with 1-year survival estimated at 55% compared to 84% in HPAH patients [62].

The more severe prognosis of SSc-PAH compared PAH alone suggests that comparing the PAH pathobiology in non-heritable forms of PAH in patients with IPAH and SSc-PAH may provide further information into disease prognosis and elucidate factors that are different or the same in these diseases. There has been extensive research based around PASMCs in PAH but in SSc, the main body of *in-vitro* research is based around the transition of the fibroblast to a myofibroblast; and

more recently the role circulating progenitor cells for example fibrocytes in SSc [109].

SSc-PAH exhibits similar pathological changes to other forms of PAH including excessive pulmonary vasoconstriction, vascular remodelling and occlusion and the occurrence of plexiform lesions [16]. These processes that affect the intima, media and adventitia, lead to the narrowing of the lumen. These changes are associated with cellular changes in smooth muscle cell morphology, apoptosis of endothelial cells and proliferation of vascular cells including SMCs endothelial cells and fibroblasts [16]. Collectively these processes lead to the narrowing and occlusion of the pulmonary arterioles.

The major focus of this study was PASMC differentiation and alterations in the microenvironment, for example increased secretion of pro-inflammatory cytokines, IL-6, IL-8, PDGFBB and CTGF may also contribute to the differentiation of PASMCs from a contractile to synthetic cell [16, 17] Furthermore, contractile PASMCs are less proliferative and migratory than synthetic PASMCs [21], whereas synthetic PASMC deposit more matrix proteins such as collagen-type I [114]. The switching of a contractile PASMC to a synthetic cell type plays a key role in PH by promoting vascular remodelling and occlusion of the vessel [21]. The maintenance of a healthy contractile cell that controls these factors discussed above is determined by a host of factors including hypoxia, cell-to-cell contact, growth factors and cellular injury [21]. When these changes occur a contractile cell differentiates into a synthetic PASMC and cellular responses are altered.

It has been previously highlighted that BMPs promote the maintenance contractile SMC phenotype which is characterised by the up-regulation of the contractile marker α-SMA, while the addition of PDGFBB in culture to PASMCs reduces the expression of α-SMA promoting a synthetic SMC phenotype [20]. In HPAH, 70% of patients have mutations in the BMPRII gene [2], which leads to a reduction in the expression of functional BMPRII receptors on the cell surface and reduced responsiveness to BMP ligands. This dysregulation of BMP signalling in patients with HPAH is likely to play a role in the normal homeostasis of PASMCs and their phenotypic modulation, promoting differentiation from a contractile to synthetic phenotype [20]. Moreover, mechanistic studies involving BMP4 and miR-21 have

highlighted a key mechanism by which PASMC differentiation occurs and potentially contributes to the development of PAH. The addition of BMP4 to PASMCs leads to Smad signalling, association with primary transcripts of miR-21 and the knockout of a negative regulator of contractile gene expression, programmed cell death 4 (PDCD4). Furthermore, PDGFBB induces miR-221, which leads to uncontrolled cell proliferation and down regulation of contractile genes [215]. *In-vivo* it has been reported that miR-21 is unregulated in the distal small arteries in the lungs of the hypoxia murine model of PAH [216]. It has been reported a number of times that in patients with atherosclerosis that their aortic SMCs located in the intima compared to both the media and adventitia have increased expression of PAI-1 and phosphorylated-Smad2. The expression of these markers suggests in atherosclerosis the aortic SMC phenotype displays enhanced TGFβ activity [217]. Interestingly it has been reported that in PAH there is an increase in phosphorylated-Smad 2/3 expression in concentric lesions suggesting that the synthetic PASMC might also be contributing to this enhanced activity [152].

5.2 Aims

The aim of this chapter was to develop a robust assay of PASMC differentiation to better assess the contribution of this cell to the development of SSc-PAH. During the development of PAH changes in the cellular microenvironment leads to alterations in proliferation, migration, and apoptosis rates in vascular cells including fibroblasts, PAECs and PASMCs [16, 217-220]. These changes contribute to the differentiation of contractile PASMCs to the more disease relevant 'synthetic' PASMCs. The aim of this chapter was to develop a robust assay of PASMC differentiation to better assess the contribution of this cell to the development of SSc-PAH. I initially sought to compare the functional differences of contractile and synthetic PASMCs extending these studies to investigate BMPRII expression and TGFβ signalling. Finally the impact of PASMCs differentiation on the capacity of PAECs to form a functional barrier was assessed.

5.3 Specific methods

5.3.1 PASMC differentiation *in-vitro*

PASMCs (Promocell) were maintained in contractile PASMC medium (Promocell) supplemented with 5 % (v/v) FBS (Gibco) and 1 % (v/v) Penicillin-Streptomycin (Gibco). PASMCs were removed from the monolayer by trypsinisation (Trypsin-EDTA, Sigma) and counted using the trypan-blue method. The trypan blue method is used for determining cell number and the assay is based on the fact that non-viable cells turn blue due to loss of their membrane integrity while the viable cells do not absorb the trypan blue because there membrane remains intact. 10 µl of cell suspension was transferred into an eppendorf along with 10µl of trypan blue. A cover slip was placed on top of the haemocytometer and 10 µl of the mix was added to the cover slip to fill the counting chambers. The cells were then counted using a Carl Zeiss Axio Cam microscope. Contractile PASMCs were seeded at 2 x 10^4 cells per well of a 6 well plate for 24 hours. After 24 hours medium of each well was replaced with fresh medium, supplemented with 5 % (v/v) FBS and 1 % (v/v) Penicillin-Streptomycin (Gibco) for contractile and 15 % (v/v) FBS and 1 % (v/v) Penicillin-Streptomycin (Gibco) for synthetic PASMCs. Contractile PASMCs were observed to be spindle like cells and synthetic cells were a more rhomboid shape. The increased concentration of FCS with increased growth factors may be contributing to the differentiation observed and an example of one growth factor that may be inducing this differentiation is PDGF. At each time point day 3, day 7, day 10 and day 14 the PASMCs were serum starved in 0.1% FCS for 24 hours and medium collected. Cell monolayers were washed in 1xPBS and lysed in 120 µl lysis buffer comprising Radio Immuno Precipitation Assay (RIPA) buffer (Sigma) containing 150 mM NaCl, 50mM Tris pH 7.4; 1mM PMSF; 1% PMSF; 1% NP-40; 1% Sodium deoxycholic acid; 0.1% SDS; 10% complete, Mini, EDTA-free protease inhibitor cocktail (Roche) and phosphatase inhibitor cocktail 3 serine/threonine protein phosphatases and L-isozymes of alkaline phosphatase inhibitor (Sigma,UK). Protein concentrations were determined using the BCA Protein Assay kit (Pierce # 23225), and 15 µg of protein mixed with 4x SDS Loading Buffer (8% SDS, 250mM Tris HCl pH 6.8, 20% glycerol) 5% β-mercaptoethanol and denatured at 96°C for 5 minutes.

5.4 Results

5.4.1 PASMC differentiation leads to changes in morphology and protein markers of contractile PASMCs.

Pathological changes in PASMCs are believed to be a key feature in the development of PAH [16]. The switching of the contractile PASMC phenotype to a synthetic SMC phenotype is believed to be a feature of vascular remodelling in a number of diseases including PH [16]. Initial experiments sought to define conditions to promote differentiation of PASMCs cells from contractile to synthetic phenotype and assess this using a series of techniques, including Western blotting and immunofluorescence (IF). Based upon previous studies on SMC differentiation the effects of increased serum and, cell to cell contact on contractile PASMCs and synthetic PASMCs morphology and markers was assessed. Contractile PASMCs exhibit a more spindle like morphology, whilst synthetic PASMCs differentiate into a more rhomboid like cell (Figure 5.1 A). α-SMA was identified as a contractile marker and was mostly highly expressed at day 3 in contractile PASMCs with a significant reduction observed in synthetic PASMCs from day 3 to 7, 10 and 14 ($p<0.05$). Smoothelin expression was elevated in contractile PASMCs at day 3, whilst a reduction was observed in synthetic PASMCs with significance achieved at day 14 (Figure 5.1 B, C; $p<0.05$). Expression of calponin and SM-22-alpha did not change significantly in contractile nor synthetic PASMCs. CTGF expression was elevated in synthetic PASMCs compared to contractile PASMCs at day 3, 7 and 10 with significant elevation of CTGF expression at day 14 in synthetic PASMCs (Figure 5.1; $p<0.05$). Type-1 collagen expression was elevated in synthetic PASMCs compared to contractile PASMCs at day 3, 7 and 10 with significant elevation of type-1 collagen expression observed at day 14 in synthetic PASMCs (Figure 5.1 B, C; $p<0.05$). IF studies echoed these observations, α-SMA and smoothelin expression (Figure 5.2 A) was elevated in contractile PASMCs compared to synthetic PASMCs, whilst type-I collagen and CTGF expression was elevated in synthetic PASMCs compared to contractile PASMCs (Figure 5.2 B).

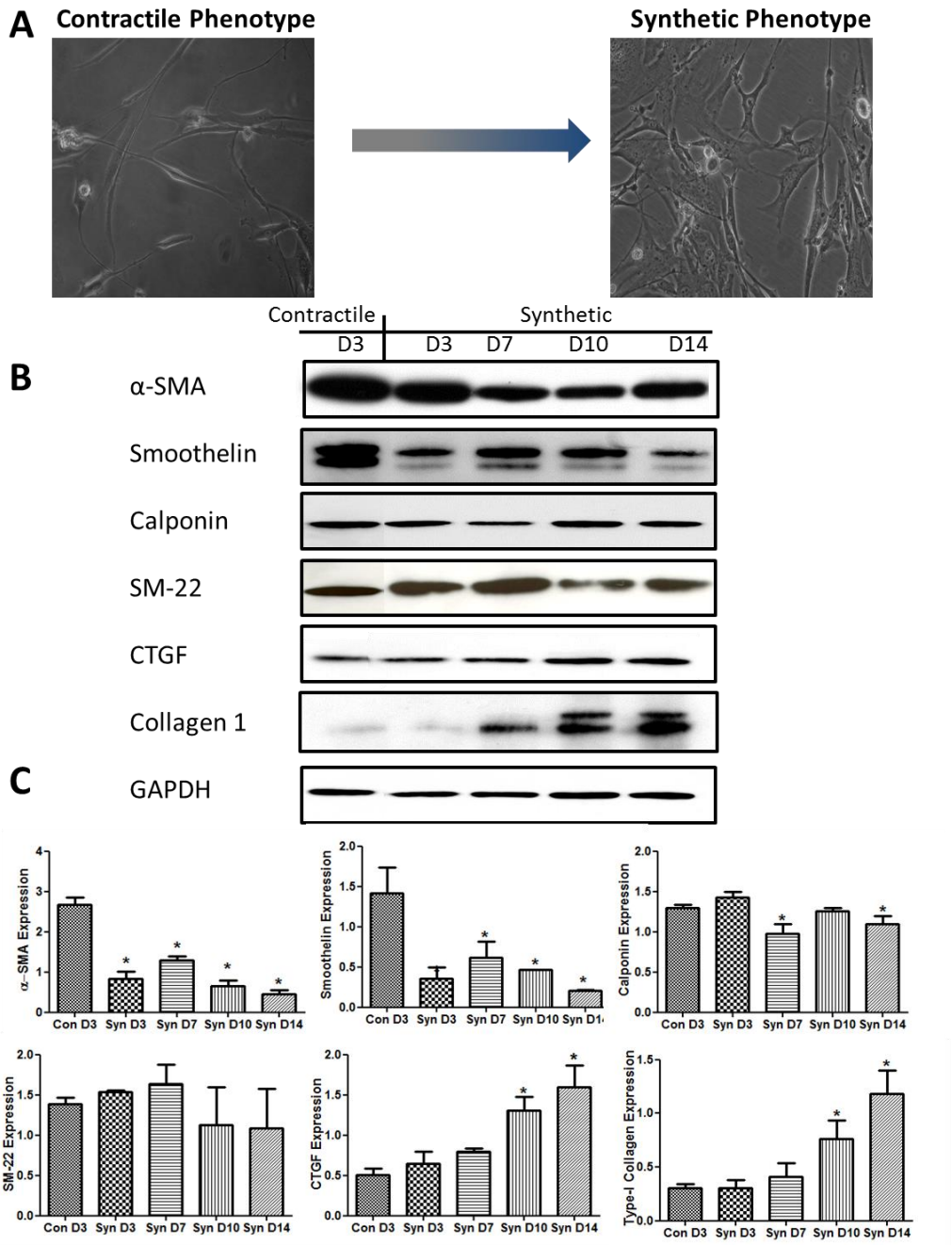

Figure 5.1 - Protein markers of contractile and synthetic PASMCs

Representative images of contractile and synthetic PASMCs after 10 days in culture (A). Western blot analysis was performed on protein extracts from contractile and synthetic PASMCs at different timepoints day (D) 3,7,10 and 14. Blots were probed for the expression of α-SMA, smoothelin, calponin, SM-22, CTGF and type-I collagen (n=3) (B) Protein loading was determined by GAPDH expression. Densitometry was performed and the mean ± SEM expression of α-SMA, smoothelin, calponin, SM-22, CTGF and type I collagen plotted (C). *$p<0.05$ using Mann Whitney Test.

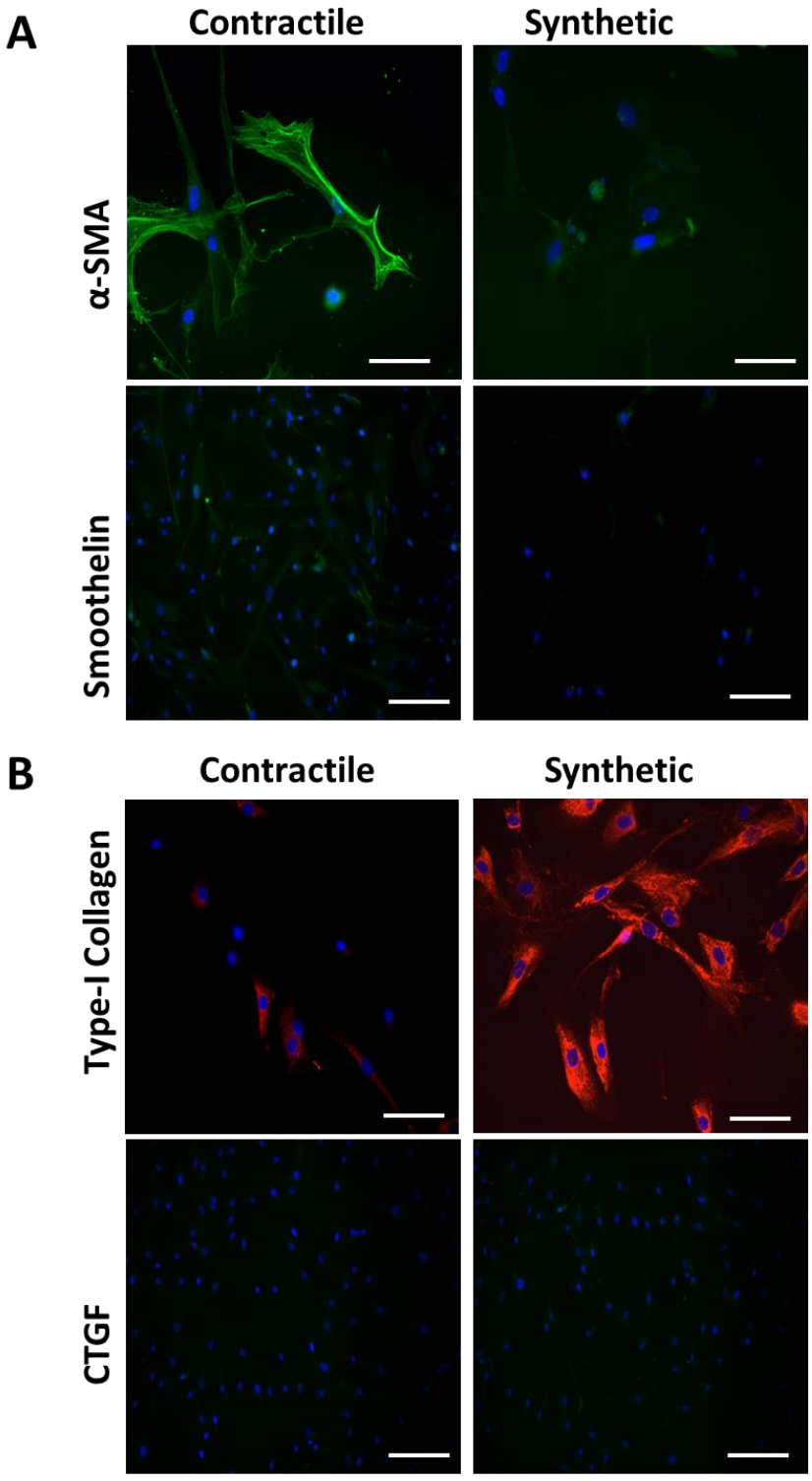

Figure 5.2 - Immunofluorescence staining of contractile and synthetic PASMCs
Immunofluorescence staining was performed on contractile and synthetic PASMCs for α-SMA, smoothelin, CTGF and type-I collagen. Images were taken using the Carl Zeiss Axiovison microscope and representative images of 3 independent experiments shown. White line indicates 100 µM using the x 40 magnification.

5.4.2 PASMC differentiation leads to changes in secreted inflammatory proteins.

Elevated levels of circulating pro-inflammatory proteins have been reported in the sera of PAH patients, and in the conditioned media from PASMCs isolated from patients [218]. The secretion of a number of these factors was assessed in conditioned serum free medium from contractile and synthetic PASMCs. PASMCs were either maintained as contractile PASMCs or differentiated into synthetic PASMCs, growth medium for both cell types was replaced with serum free medium. Conditioned media was collected after 24 hours and the concentration of a series of pro-inflammatory proteins assessed using a multiplex system. Contractile and synthetic PASMCs secreted detectable levels of IL-1β, IL-6, IL-8, and TNF-α and TNF-β. Synthetic PASMCs demonstrated increased secretion of IL-6, IL-8 and TNF-β compared to contractile conditioned medium. Only synthetic PASMCs demonstrated detectable levels of IL-10 and INF–γ. There was no significant difference in secreted levels of IL1-β or TNF-α in contractile or synthetic PASMCs (Figure 5.3A).

To further assess the secretion of pro-inflammatory cytokine secretion, a temporal secretion of IL-6 and IL-8 in synthetic conditioned medium by ELISA was performed. IL-6 secretion was significantly elevated on day 3, 7, 10 and 14 in synthetic PASMCs compared to contractile PASMCs but maximal secretion occurred at day 14 ($p>0.05$; Figure 5.3B). IL-8 secretion was also significantly elevated on day 3, 7, 10 and 14 in synthetic PASMCs compared to contractile PASMCs. However maximal secretion occurred at day 7 with a temporal reduction observed at day 10 and 14 ($p>0.05$; Figure 5.3B).

A

Fold change	IL-1β	IL2	IL-4	IL-5	IL-6	IL-8	IL-10	IL-12	INFγ	TNFα	TNFβ
Contractile	1	-	-	-	1	1	-	-	-	1	1
Synthetic	1	-	-	-	3	4	5	-	5	1	2.7

B

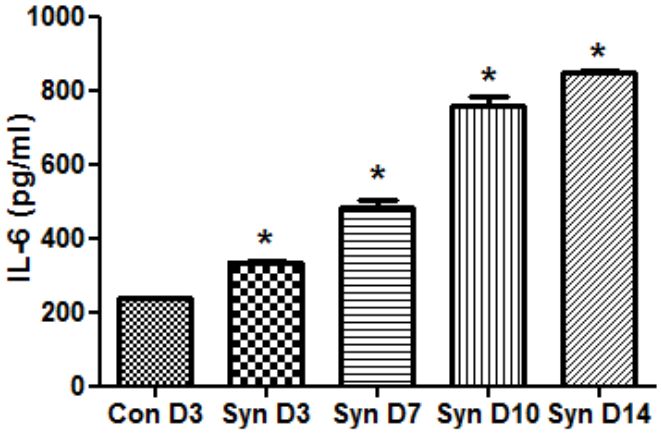

C

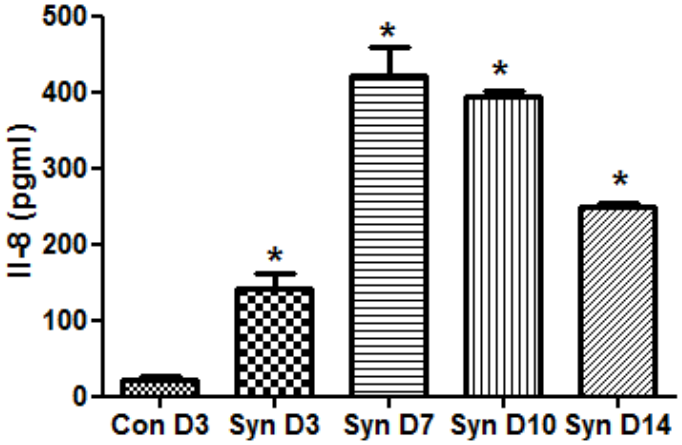

Figure 5.3 – Secreted markers of PASMC contractile and synthetic switching

Conditioned medium from contractile and synthetic PASMCs was collected at day (D) 3, 7, 10 and 14. Multiplex analysis was performed on the conditioned medium for inflammatory mediators and fold change determined of detectable proteins (A). Levels of interleukin-6 (IL-6) (B) and interleukin-8 IL-8 (C) were determined by ELISA Secretion was normalised to protein levels in the cell monolayer. The mean ± SEM of 3 independent experiments were plotted (B and C). *$p<0.05$ compared to contractile PASMCs, Mann-Whitney Test.

5.4.3 Functional differences between contractile and synthetic PASMCs.

As demonstrated in figure 5.1, 5.2 and 5.3 contractile and synthetic PASMCs exhibit differences in protein and secretion profiles that may contribute to the development of PAH and vascular remodelling. The literature has also reported functional changes in PASMCs from patients of PAH so using this assay it was important to compare functional responses in these cells. Migration is a key cellular activity in the pulmonary artery that contributes to the formation of concentric lesions in the artery. The capacity of contractile and synthetic PASMCs to migrate in response to stimulation with PDGFBB was assessed. Confluent monolayers of PASMCs were scratched and treated with either 1% FCS as a negative control or 50ng/ml of PDGFBB and migration assessed after 48 hours (Figure 5.4A). These experiments were performed in the presence of an anti-proliferative Mitomycin-C (10 μml). Migration was observed in both contractile and synthetic PASMCs but a significant increase in migration in response to PDGFB was observed in contractile PASMCs compared to synthetic PASMCs ($p<0.05$).

Pooled data from a series of independent experiments and donors of contraction assays using type-1 collagen lattices show that contractile PASMCs were significantly more contractile than synthetic PASMCs ($p<0.05$; Figure 5.4 B). Contractile and synthetic PASMCs were exposed to 10% FCS for 24 hours and results showed that this condition induced further contraction in contractile PASMCs compared to synthetic PASMCs ($p<0.05$). Contraction was assessed by measuring the diameter of each individual gel or the gel weight.

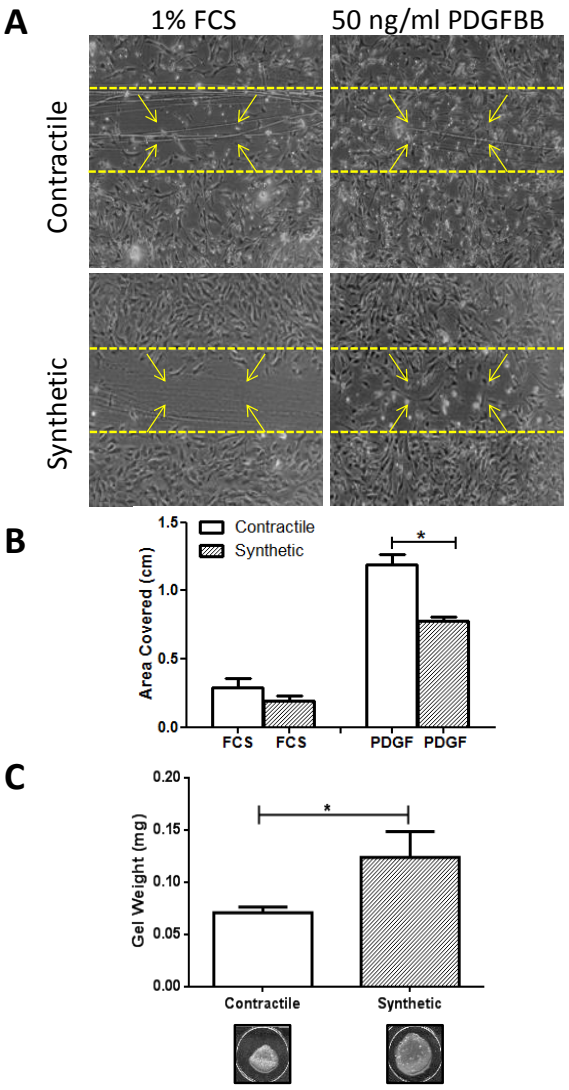

Figure 5.4 – Contractile PASMCs displays increased migration and collagen gel contraction compared to synthetic PASMCs

Confluent monolayers of contractile and synthetic PASMCs were scratched and migratory responses assessed in response to 1% FCS alone or supplemented with PDGFBB (50 ng/ml). All experiments were performed in the presence of 10 µg/ml Mitomycin C in three independent experiments in triplicate. (A). Migration was assessed after 48 hours, images were taken using the Olympus CDK2 microscope and data analysed using Axio Vision software to determine area covered by each treatment group and the mean ± SEM plotted (B). Contractile and synthetic PASMCs were seeded in to type I collagen gels and treated with 10% FCS and gel contraction after 48 hours was assessed by measuring gel weight and the mean ± SEM plotted (C) (n=3). *$p<0.05$ Mann Whitney Tests.

5.4.3 Synthetic PASMCs display a reduction in BMPRII similar to that observed in PASMCs from IPAH patients.

Previous work has suggested the importance of BMPRII and downstream signalling pathways in PASMCs in patients with PAH. Expression of BMPRII and the impact of the BMPRIIl signalling pathway were investigated in contractile and synthetic PASMCs. A significant reduction in BMPRII protein expression was observed in synthetic compared to contractile PASMCs ($p<0.05$, Figure 5.5A), however there was no significant change in phosphorylated-Smad1 protein expression in contractile and synthetic PASMCs. qPCR studies were also performed to investigate BMPRII and Gremlin gene expression. There was a reduction in BMPRII gene expression and an increase in Gremlin expression in synthetic PASMCs which echoes observations in PASMCs from HPAH and IPAH patients (Figure 5.5B). The observation of reduced BMPRII, led us to investigate how both contractile and synthetic PASMCs respond to BMP ligands. It has been previously reported that BMP ligands induced apoptosis in PASMCs, to assess the implication of reduced BMPRII in PASMCs the effect of 0, 5, 50 and 500 ng/ml of BMP4 and BMP7 on cellular apoptosis was investigated [24, 151, 219, 220]. Results highlighted that at baseline there was reduced apoptosis in synthetic PASMCs compared to contractile PASMCs, the addition of BMP4 and 7 at varying concentrations displayed a blunted response in synthetic PASMCs but these ligands induced apoptosis in contractile PASMCs ($p<0.05$, Figure 5.6 A).

Pooled data from a series of independent experiments and donors of contraction assays using type-1 collagen lattices show that contractile PASMCs promoted significantly more contraction than synthetic PASMCs. Exogenous addition of 50 ng/ml of BMP4 significantly induced further contraction in contractile PASMCs but had little or no effect in synthetic PASMCs. Contraction was assessed by measuring the diameter of each individual gel or the gel weight (Figure 5.6 B).

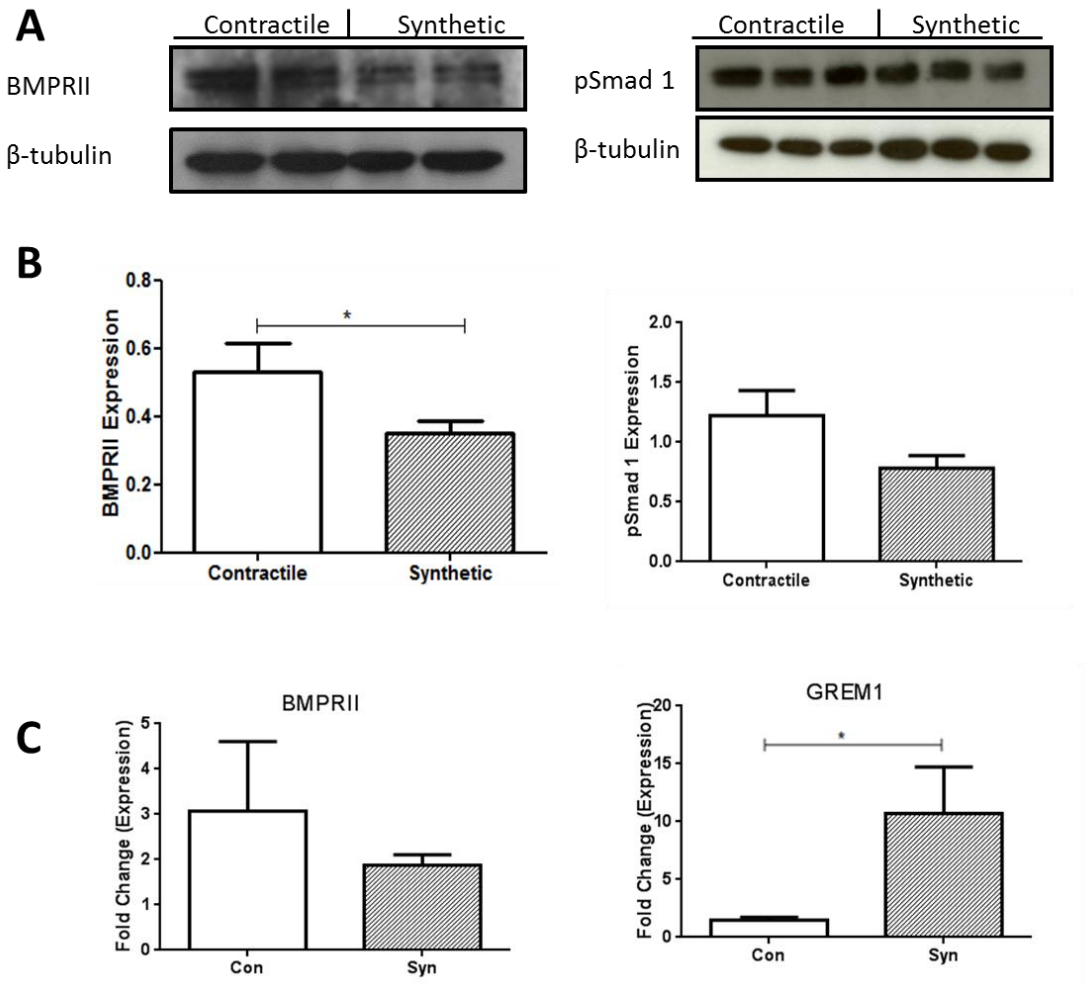

Figure 5.5 – Protein and gene expression of BMPRII in PASMCs and downstream signalling factors

Western blots were performed on protein isolated from both contractile and synthetic pulmonary arterial smooth muscle cells (PASMCs) (n=3). Blots were probed for expression of BMPRII and phosphorylated-Smad1, protein loading was determined by β-tubulin levels (A). Densitometry was performed and the mean ± SEM expression of BMPRII and phosphorylated-Smad1 was normalised to β-tubulin expression and plotted (B). *$p<0.05$ using Mann Whitney Tests. (B). Quantitative polymerase chain reaction (qPCR) of RNA for BMPRII and Gremlin 1 (C).

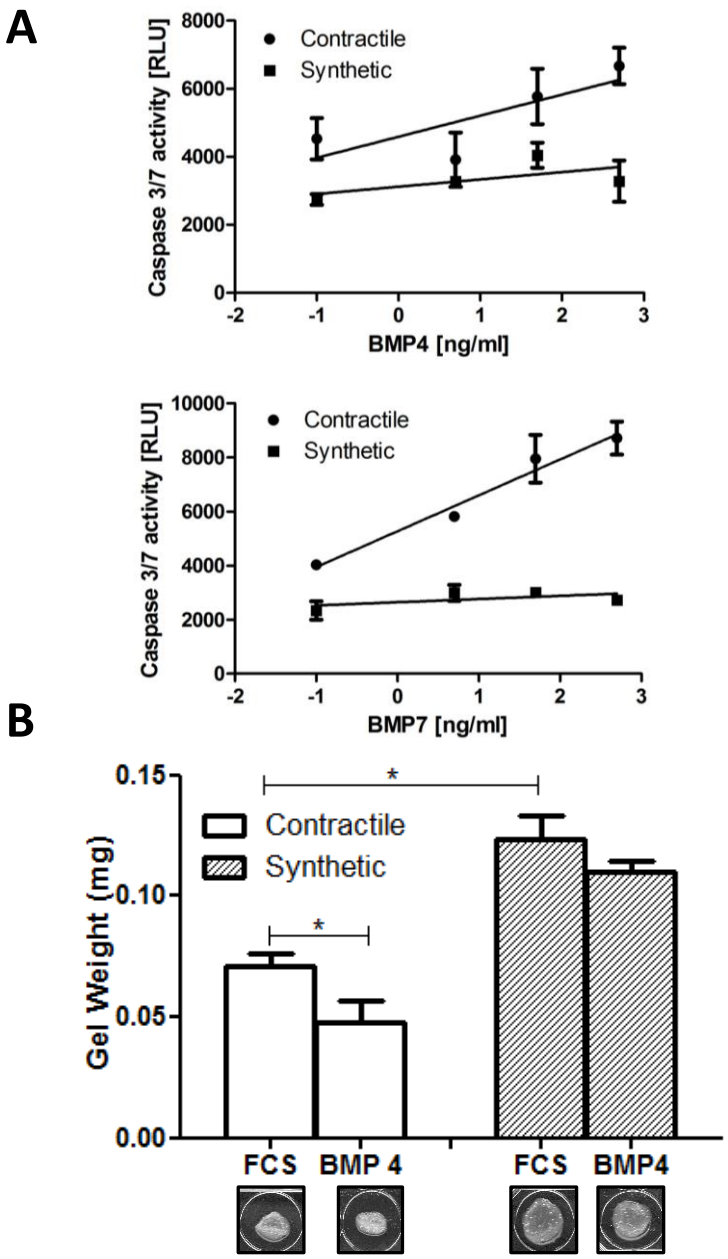

Figure 5.6 – Synthetic PASMCs displayed a blunted response in to BMP ligands leading to altered functional responses

Contractile and synthetic PASMCs were seeded and exposed to 0, 5, 50, and 500 ng/ml of BMP4 and BMP7 for 8 hours. Caspase-Glo® 3/7 reagent was then added in a 1:1 ratio to BMP4 and 7 and incubated for 2 hours. Plates were then read by luminescence to assess apoptosis (A).

Contractile and synthetic PASMCs were treated with either 0.1% FCS or 50 ng/ml BMP4 for 48 hours and gel contraction was assessed by measuring gel weight (n=3). *p<0.05 using Mann Whitney Tests (C).

5.4.4 Contractile and synthetic PASMCs display differential responses to TGFβ.

Previous studies have highlighted differences in control and HPAH PASMCs ability to respond to TGFβ; using the *in-vitro* assay of differentiation, the ability of contractile and synthetic PASMCs to respond to TGFβ was assessed [17]. There was no significant difference in phosphorylated-Smad2 protein levels in either contractile or synthetic PASMCs (Figure 5.7A). qPCR was used to investigate gene expression of TGFβ regulated genes, both TGFβ regulated genes CTGF and PAI-1 were elevated in synthetic PASMCs that was trending towards significance [221].

Pooled data from a series of independent experiments and donors of contraction assays using type-1 collagen lattices show that contractile PASMCs promoted significantly more contraction than synthetic PASMCs, furthermore TGFβ (5 ng/ml) significantly induces further contraction in both contractile and synthetic PASMCs compared to untreated PASMCs($p<0.05$; Figure 5.7 B). Contraction was assessed by measuring the diameter of each individual gel or the gel weight.

As previously highlighted, levels of the pro-inflammatory cytokine IL-6 were elevated in synthetic PASMCs ($p<0.05$; Figure 5.3B). However the exogenous addition of TGFβ (5 ng/ml) did not affect the IL-6 levels in contractile PASMCs, but led to a further significant increase in synthetic PASMCs which has been reported in PASMCs from HPAH patients [17].

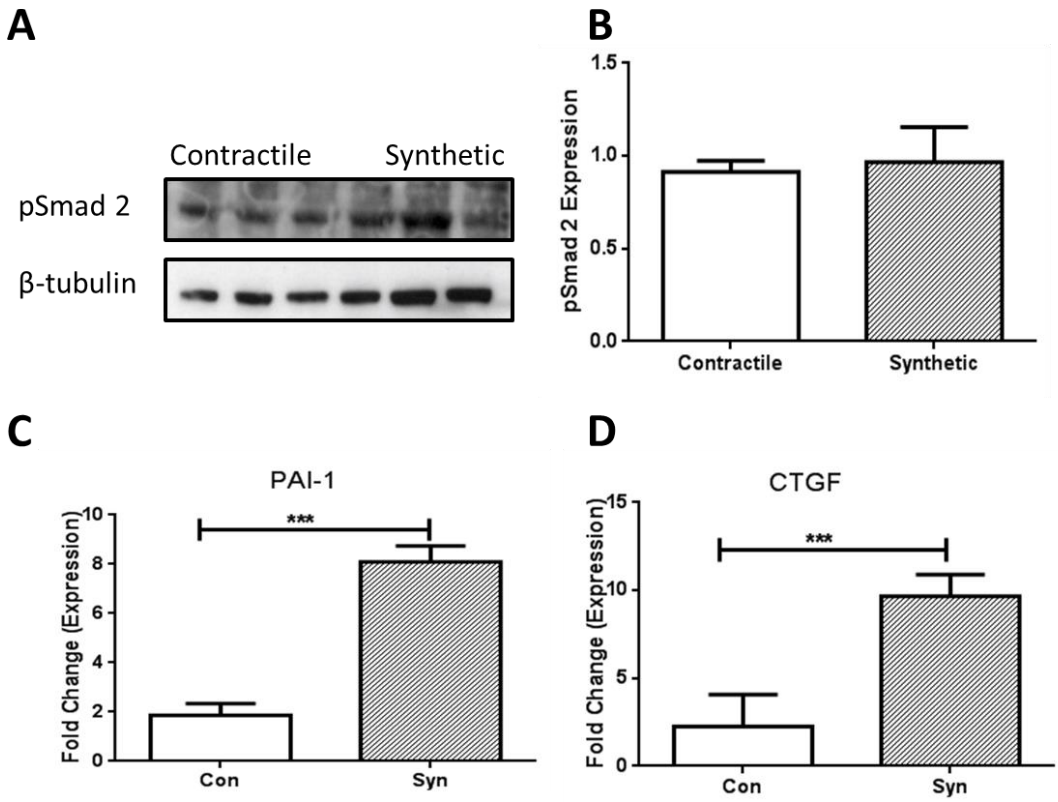

Figure 5.7– Enhanced TGFβ activity in synthetic PASMCs

Western blots were performed on protein isolated from monolayers of contractile and synthetic PASMCs (n=3). Blots were probed for expression of phosphorylated -Smad2 (pSmad2), protein loading was determined by β-tubulin levels (A). Densitometry was performed and the mean ± SEM expression of pSmad2 was normalised to β-tubulin expression and plotted (A). 60 % confluent contractile and synthetic PASMCs were serum-starved (n=3) and total RNA was isolated from each sample and reverse-transcribed, cDNA was subjected to real-time PCR analysis PAI-1 and CTGF and expression was normalized to succinate dehydrogenase complex, subunit A (Sdha) gene (C,D). Data are expressed as fold induction.. *$p<0.05$, using Mann Whitney Tests (C, D).

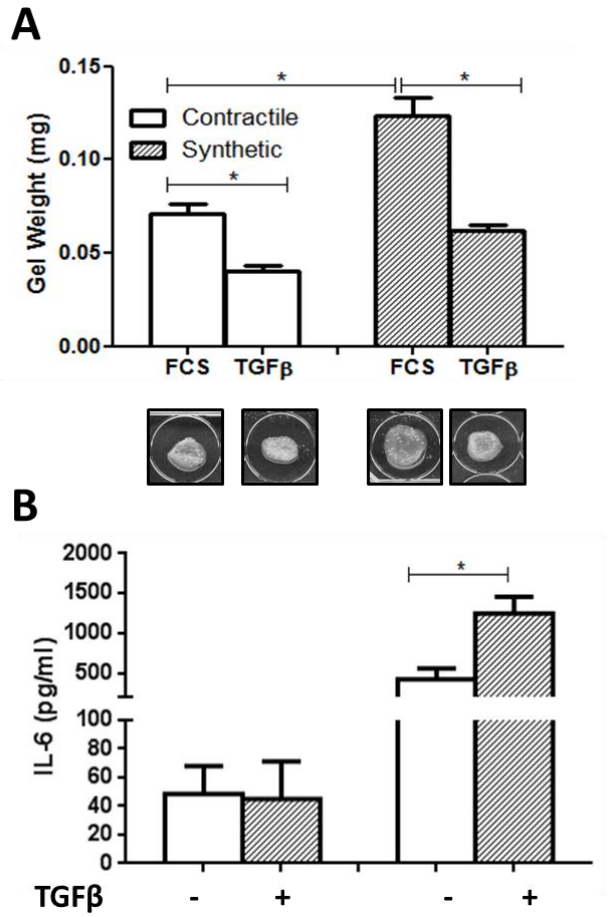

Figure 5.8 – TGFβ induces increased contraction and IL-6 secretion in synthetic PASMCs.

Contractile and synthetic PASMCs were treated with either 0.1% FCS or 2 ng/ml TGFβ for 48 hours and gel contraction was assessed by measuring gel weight (n=3) (A). Conditioned medium from contractile and synthetic PASMCs was collected and secretion was normalised to protein levels in the cell monolayer. Levels of IL-6 was measured by ELISA in three independent experiments (n=3) (B). (A-B). *$p<0.05$, using Mann Whitney Tests.

5.4.5 The influence of contractile and synthetic PASMCs on endothelial cells.

The paracrine interaction between PASMCs and PAECs is essential for maintaining haemostatic levels of migration and proliferation of medial SMCs, and the integrity of the endothelial barrier [222]. In healthy individuals this complex interaction is tightly regulated which results in an efficient endothelial barrier and controlled PASMC proliferation. However in patients with PAH and/or SSc, 'healthy' PASMCs differentiation into synthetic 'disease' like phenotypes, can become uncontrolled and lead to a reduction in endothelial barrier integrity and medial hyperplasia [223-225].

60% confluent contractile and synthetic PASMCs were serum starved for 24 hours in basal EMG-2 medium with 2% FCS, medium collected. $1x10^5$ PAECs were seeded into 24 well, 3µm pore transwell inserts and allowed to form a confluent monolayer for 24 hours. Conditioned medium from contractile and synthetic PASMCs was added to the inserts for 24 hours. Endothelial permeability was assessed by adding 5mg/ml FITC-albumin into the insert and measuring fluorescence of the medium in the bottom of the well at 535nm to quantify permeability after one hour. Contractile PASMCs had no effect on endothelial cell permeability compared to control medium, in contrast synthetic PASMCs significantly increased endothelial cell permeability ($p<0.05$; Figure 5.8A).

The effect of PASMCs on immune cell endothelial transmigration was measured by adding $1x10^6$ freshly isolated PBMCs to the inserts after incubation with the conditioned medium for 24 hours. Cells were counted in the bottom of the well after 2 hours of transmigration (Figure 5.8B). Contractile PASMC medium had no significant effects on endothelial immune cell transmigration, however synthetic PASMC medium significantly elevated the immune cell movement across the endothelial barrier ($p<0.05$; Figure 5.8). In contrast to these findings, neither contractile nor synthetic SMC conditioned medium had an effect on PAEC migration or proliferation rates ($p<0.05$; Figure 5.9).

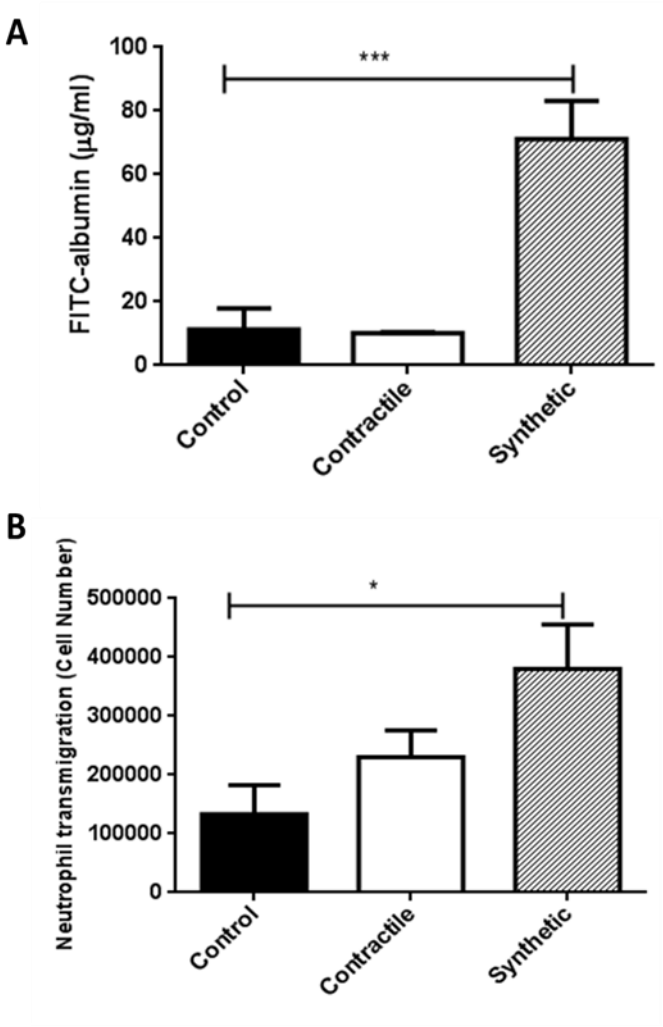

Figure 5.9 – Synthetic PASMCs increase endothelial permeability and neutrophil transmigration

Control endothelial cell medium and conditioned medium from contractile and synthetic PASMCs was added to a confluent layer of PAECs to investigate the effect of PASMCs on endothelial cells. Contractile PASMCs exhibit no effect on FITC albumin leak whereas synthetic PASMCs exert a significant effect on FITC albumin leak equating to increased endothelial cell barrier leak (n=3) (A).Contractile PASMCs exhibit no effect on neutrophil transmigration whereas synthetic PASMCs exert a significant effect on neutrophil transmigration (n=3). *$p<0.05$ using Mann Whitney Tests. (A-B).

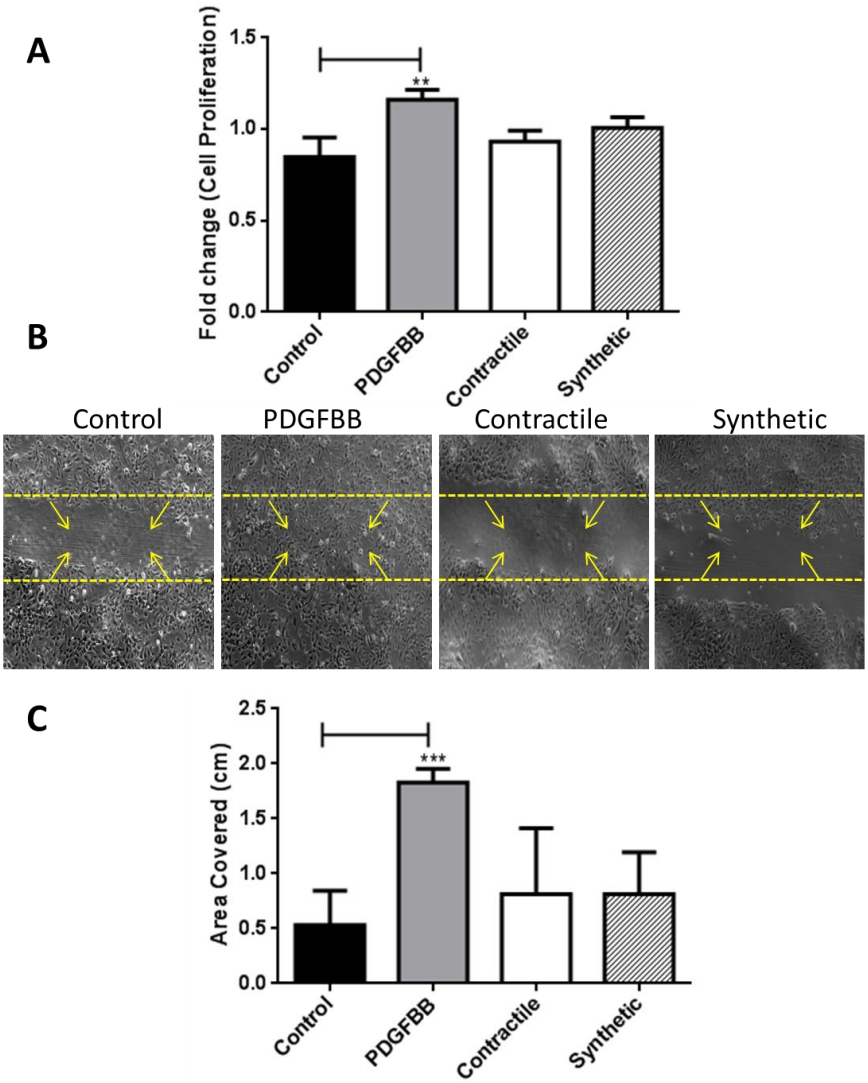

Figure 5.10 – Contractile and synthetic PASMCs have no effect on endothelial cell migration or proliferation

Confluent monolayers of PAECs were exposed to 1% FCS, 50 ng/ml PDGFF-BB and conditioned medium from contractile and synthetic PASMCs to assess the effect of PASMCs on PAEC proliferation using the crystal violet cell proliferation method. Experiments were performed on three independent donors in triplicate. *p<0.05, using a Mann Whitney Test (n=3) (A).

Confluent monolayers of PAECs were scratched and migratory responses assessed in response to 1% FCS, 50 ng/ml of PDGFBB and conditioned medium from contractile and synthetic PASMCs. All experiments were performed in the presence of 10 μg/ml Mitomycin C for 48 hours. Experiments were performed on three independent donors in triplicate. (B). Migration was assessed after 48 hours, images were taken using the Olympus CDK2 microscope and data analysed using Axio Vision software. *p<0.05, Mann Whitney Test (C).

5.5 Discussion

Pathological changes in PASMCs are believed to be a key feature in the development of PAH [16, 21]. The loss of a 'normal' contractile phenotype to that of a 'disease' synthetic phenotype is a feature of vascular remodelling in a number of diseases including PAH [21]. The differentiation of a SMC from a contractile to a synthetic cell induces a change in morphology and functionality of the cell, with the synthetic cell possessing increased proliferative and anti-apoptotic qualities [21]. As discussed earlier, in HPAH, 70% of patients have BMPRII mutations [2] and this perturbation of BMP signalling in patients of IPAH may play a key role in the homeostasis of a PASMC and their phenotypic modulation. Initial experiments were performed to investigate and establish robust markers of a contractile and a synthetic cell with a particular focus on PASMCs. The maintenance of a healthy contractile cell is determined by a host of factors, hypoxia, cell to cell contact, growth factors and cell injury all contribute to PASMC differentiation, therefore conditions were established that would promote differentiation of a contractile cell to a synthetic phenotype [21]. The hypothesis that increased serum and cell to cell contact would promote differentiation to a synthetic cell was confirmed and this allowed us to establish markers of each cell type. These markers were interrogated by both Western blot analysis and immunoflouresecent staining. α-SMA and smoothelin had previously been identified as contractile markers of SMCs [226, 227]. This work identifies α-SMA and smoothelin as markers specifically for contractile PASMC and Type-I collagen and CTGF were identified as protein markers of a synthetic PASMCs. These results are supported in the literature as it has been previously reported that a synthetic cell produces increased ECM and contributes to vascular remodelling [21].

In addition to identifying protein markers of both contractile and synthetic PASMCs, secreted factors from the conditioned medium of both cell types were also investigated. Multiplex analysis identified differences in secreted factors between contractile and synthetic PASMCs; IL-6, IL-8, IL-10, IFN-g and TNF-β levels were elevated in the synthetic phenotype. IL-6 and IL-8 were identified as key markers, because previous work has shown that both IL-6 and IL-8 serum levels are elevated in patients with both IPAH and HPAH [218]. In this study Kaplan-Meier curves

showed levels of IL-6 and IL-8 predicted survival in patients, 5-year survival rates for patients with IL-6 levels > 9 pg/ml was 30%, however patients with levels < 9 pg/ml fared better with survival at 63% [218].

Using functional assays it was possible to determine how contractile and synthetic PASMCs behave and how these changes in behaviour may contribute to the development of PAH via muscularisation in the pulmonary artery. Previous reports have suggested that synthetic PASMCs are more migratory but our data suggested the opposite to these reports [21, 226]. This result could be explained by increased expression of α-SMA in contractile PASMCs which might be contributing to the increased migratory capacity of the contractile PASMC. It may also be that in disease pathology the PASMC contributes more to endothelial dysfunction, whilst the fibroblast is the more migratory and proliferative cell that occludes the lumen. Contractile PASMCs exhibited increased contractility compared to synthetic PASMCs, and it has been previously reported that BMP signalling plays a key role in maintaining the contractile apparatus of the PASMC [215].

Having identified cellular proteins, secreted markers and functional changes that characterise both contractile and synthetic PASMCs, I investigated the TGF-β/BMP axis in PASMCs. BMPRII levels have been reported to be reduced in PASMCs from patients in IPAH with a blunted response to BMPs [24, 177]. The reduction of BMPRII levels in the synthetic 'disease' phenotype at both the protein and gene level suggests these cells appear similar to PASMCs from isolated IPAH patients. There was also a rise in the gene expression of the BMP antagonist gremlin 1. It has been previously reported that gremlin 1 has higher expression in the lung than any other organ. Furthermore, Gremlin 1 is also elevated in the lung of PAH patients and novel gremlin 1 antibodies can reverse PAH in the pre-clinical sugen/hypoxia model of PAH [155, 228]. Functional assays were then used to determine the impact of reduced BMPRII levels on the PASMC. The rate of apoptosis is essential in maintaining normal vasculature so the rate of apoptosis in contractile and synthetic PASMCs was investigated. Synthetic PASMCs exhibit an apoptotic resistance in response to BMP 4 and 7 due to the reduction of BMPRII which prevents BMP ligands exerting their anti-apoptotic effects. This can lead to a rise in the synthetic PASMC population contributing to the occlusion of the lumen and vascular

remodelling [24,151,219]. As discussed previously contractile PASMCs exhibit increased contractility compared to synthetic PASMCs, BMPs are involved in the regulation of contractility and results in this chapter confirm this [215]. BMP4 treatment induces contraction in the contractile PASMCs suggesting it plays a role in this cellular process; however synthetic PASMCs exhibit a blunted response to BMP4, and less contraction in synthetic PASMCs might be due to the reduction of BMPRII in synthetic PASMCs. These results suggest that the reduction of BMPRII in synthetic PASMCs leads to a dysregulation of cellular processes that contribute to vascular remodelling and the development of PAH. Suggesting the ability to upregulate BMPRII or restore BMP signalling in the PASMC could provide an attractive therapeutic approach to preventing PASMC differentiation and the development of PAH.

Previous reports have highlighted that enhanced TGFβ signalling in PAH may contribute to a reduction of BMPRII where patients with PAH have increased phosphorylated-Smad2/3 staining in concentric lesions in the lung [152]. In concert with the reduction of BMPRII in the TβRIIΔk fib model of SSc there is a possibility that this reduction of BMPRII may be a unifying mechanism and contributes to SSc-PAH. Synthetic PASMCs also exhibited a perturbed response to BMP ligands and the dysregulation of both TGFβ and BMP canonical signalling pathways observed in synthetic PASMCs is similar to previous reports in PASMCs in HPAH patients, where a reduction in phosphorylated-Smad1 after BMP4 treatment has also been observed [24, 177].

Enhancement of the TGFβ axis is observed alongside a reduction in BMPRII in PAH, and data in this chapter supports this trend. A significant increase in CTGF and PAI-1 gene expression, further corroborate the TGFβ/BMP axis imbalance, as they are markers of enhanced TGFβ activity. TGFβ does not affect IL-6 secretion in contractile PASMCs, however it significantly enhanced IL-6 secretion in synthetic PASMCs. It has been previously shown in PASMCs from HPAH patients that TGFβ treatment exhibits differential effects on control and HPAH PASMCs [17]. This study reported that HPAH PASMCs have enhanced transcription of IL-8 and IL-6 in response to TGF-β1 compared with control PASMCs. The regulation of these cytokines is dependent on the cell context and may differ between normal and

disease states [17]. There is substantial evidence in the literature supporting the role of inflammation in the development of PAH, it has been reported that pro-inflammatory cytokines, for example, IL-8, TNF-α and IL-6 are significantly elevated in HPAH patients [218,229,230]. IL-6 is also elevated in pre-clinical models of PAH suggesting it plays a key role in the development of the disease [231, 232]. This suggests that by neutralising IL-6 and IL-8 it is possible to restore the anti-proliferative effects of TGF-β1 on HPAH PASMCs [17]. Interestingly, anti-IL-6 therapies have been shown to be safe and efficacious in the treatment of rheumatoid arthritis and other disorders [233]. Administration of tocilizumab, a humanized anti-IL-6 monoclonal antibody, has improved PAH symptoms in patients with mixed connective tissue disease and severe PAH [234]. The data from our contractile and synthetic PASMCs and PASMCs from patients highlights the involvement of IL-6 in The interaction between PASMCs and endothelial cells is important in the development of PAH. Functional assays were performed to determine the effect of contractile and synthetic PASMCs on endothelial cells and their function on the vasculature. It has been previously shown that co-culture of SSc, but not control fibroblasts could induce transendothelial migration of U937 cells. It was also shown that conditioned medium from SSc fibroblasts had similar effects on Jurkat-6 (T lymphocyte) cells, and with peripheral blood mononuclear cells from a patient with dcSSc [235].This could be due to the increased levels of inflammatory cytokines and growth factors for example PDGF-BB in conditioned medium from SSc fibroblasts. This is similar to what is observed in synthetic PASMCs, these PASMCs have elevated levels of IL-6, IL-8 and CTGF. The anatomical location of endothelial and PASMCs in the artery suggests that their interaction could play a key role in the occlusion of the lumen and increased vascular leak. Conditioned medium from contractile PASMCs had no effect on endothelial cell leak suggesting in normal pulmonary artery there is not an imbalance in cytokines or growth factors that might contribute to this phenomenon. However during PASMC differentiation, the synthetic PASMC becomes a pro-inflammatory cell that significantly increases vascular leak. It has been previously reported that in the hypoxia rat model there is increased vascular permeability and leukocyte migration, implicating vascular permeability in the development of PAH [236]. Synthetic PASMCs secrete significantly more IL-6, IL-8 and TNF-α, and these pro-inflammatory cytokines are possibly contributing to increased endothelial cell leak and immune cell influx. IL-6

and IL-8 have previously been reported to be elevated in the serum of SSc patients [40, 237], and IL-6 has been found to have detrimental effects on endothelial barrier integrity [238]. In addition, IL-6 and IL-8 increase expression of ICAM-1, VCAM-1 and E-selectin, adhesion proteins known to increase the adherence and infiltration of immune cells [239, 240]. Similarly elevated IL-8 is known to activate endothelial cells and increase immune cell interactions as well as increase endothelial permeability [241-243]. Other groups have shown IL-8 reduces expression of tight junction proteins which again could contribute to increased leak [239]. Consistent with these studies the pro-inflammatory profile of synthetic PASMCs induces increased endothelial cell leak and immune cell influx compared to contractile PASMCs.

Finally, it was investigated if conditioned medium from contractile or synthetic PASMCs can influence endothelial cell proliferation or migration. PDGFBB induced endothelial proliferation and migration but neither contractile nor synthetic PASMC conditioned media had any effect [244, 245]. It has been previously shown that PASMCs can inhibit endothelial cell migration but it was observed that PASMCs were unable to influence endothelial cell migration [246]. Sato *et al* conducted their studies in bovine cells whilst this study used human cells so this could a factor that is contributing to variable observations. In order to investigate this further it would be essential to profile both contractile and synthetic PASMCs for known endothelial cell mitogens, or inhibitors of migration and proliferation to determine if they might have an effect. Synthetic PASMCs have a pro-inflammatory phenotype that may be contributing this, the increase in growth factors and cytokines may be inducing downregulation of tight junction proteins. This downregulation may be the mechanism by which synthetic PASMCs are inducing endothelial cell leak.

5.6 Conclusion

In conclusion this work has established and validated a novel assay to induce synthetic PASMC by promoting differentiation of contractile PASMCs through exposure to increased serum concentrations and cell-cell contact. Differentiated synthetic PASMCs display similar characteristics to PASMCs isolated from PAH patients, including enhanced secretion of pro-inflammatory chemokines. This study has highlighted a plethora of protein and pro-inflammatory markers to identify contractile and synthetic PASMCs. Smoothelin and α-SMA have been identified as robust markets of contractile PASMCs and type-I collagen and CTGF have been implicated as markers of synthetic PASMCs. IL-6 and IL-8 are pro-inflammatory cytokines that elevated in synthetic PASMCs. Furthermore synthetic PASMCs display reduced BMPRII expression and exhibit blunted responses to BMP ligands, whilst exhibiting enhanced responses to TGFβ, similar to PASMC from HPAH patients. Extending these observations further the effects on synthetic PASMCs on endothelial cell functions was investigated. Pro-inflammatory synthetic PASMC are also able to contribute to and influence vascular permeability, and immune cell influx, which are likely to contribute to the development of PAH. Given the challenges of obtaining PASMCs from SSc-PAH patients the generation of synthetic PASMCs cells *in-vitro* that shares many characteristics of PASMCs from PAH patients, will allow future studies to better understand the pathological mechanisms that contribute to the development of SSc-PAH.

6. The bromodomain inhibitor JQ1 can prevent the development of PAH in the TβRIIΔk-fib model of SSc-PAH

6.1 Introduction

The definition of epigenetics is contentious, currently there are a two definitions in the literature, one group defines it as: how genotypes create individual phenotypes during development that may be induced by differential environments and lifestyles endured by individuals [247]. However another group described epigenetics as all the (meiotically and mitotically) heritable changes that occur in gene expression that are not directly coded in the DNA sequence [248]. Epigenetic changes can occur through different processes know as histone modifications, acetylation, deacetylation and methylation. Histone acetyltransferases (HATs) act as writers and catalyse the addition of acetyl groups to lysine residues in histone tails, whereas histone deacetylases (HDACs) serve as erasers with opposing effects [249]. In general histone acetylation represents transcriptionally active regions whereas deacetylated residues can be found in transcriptionally inactive euchromatic or heterochromatic regions [250]. Histone methylation can be a marker for both active and inactive regions of chromatin. For example if methylation on lysine 9 on the N terminus of histone 3 (H3) it is associated with silent DNA, however if it occurs at lysine 4 of H4 it represents activity at a promoter region [249]. Human tumours were the first to show global hypomethylation which was followed by the discovery of hypermethylated tumour-suppressor genes (TSGs) and most recently the inactivation of microRNA (miRNA) by DNA methylation [251-256]. The low levels of DNA methylation in tumours is mainly due to hypomethylation of repetitive DNA sequences and, demethylation of coding regions and introns that allow transcription of mRNA [257]. The progression of normal skin through the different stages of carcinoma has displayed a progressive loss of DNA methylation in the lesions [258].

In TSGs hypermethylation of the regions of DNA where a cytosine nucleotide is located next to a guanine nucleotide in the linear sequence of bases (CpG islands) in promoter regions have been linked to the origin of many tumours. The initial reports of this were in the retinoblastoma (Rb) TSG and other reports have followed in the breast cancer susceptibility gene 1 (BRCA1) [253, 259]. This hypermethylation can

affect many cellular processes involved in the cell-cycle, for example DNA repair, apoptosis, cell-to-cell interaction and angiogenesis [257]. It is still unclear why hypermethylation is observed in some cancers but not in others; comprehension of this may lead to a better understanding of epigenetics in cancer. Methylation of BMPRII and the role of epigenetic changes have also been implicated in the skin of SSc patients. As mentioned earlier histone modifications through acetylation and deacetylation also contribute to the development of cancer through direct effects on nuclear processes, including gene transcription, DNA repair and replication [249]. In leukaemia and sarcomas, chromosomal translocations involve readers such as HATs, one example of this is histone methyltransferase in mixed-lineage leukaemia 1 (MLL1) [260].

Through a better understanding of the different epigenetic mechanisms that are contributing to cancers, novel-epigenetic inhibitors are currently being developed both pre-clinically and clinically for the treatment of cancers. Recently, two novel selective small molecule inhibitors that target the amino-terminal bromodomains (BRD) of BRD4 JQ1, and inhibitor of bromodomain extra terminal 762 (I-BET762), have been shown to exhibit anti-proliferative effects in a range of malignancies [261].

The major focus of the work in this chapter will be JQ1 and its role in SSc-PAH. JQ1 is a BRD inhibitor, BRD is a conserved member of the BET family of chromatin readers, BRD consists of four members BRD2, BRD3, BRD4 and BRD testis (BRDT). When JQ1 binds to the BRD pocket it leads to the displacement of BRD4 from active chromatin and the subsequent removal of RNA polymerase II from target genes [262, 263]. In SSc and SSc-PAH the pathological mechanisms that contribute to the development of pulmonary complications are not completely understood but it is believed that a plethora of processes and cell types are involved in the disease [18, 45]. The SSc-PAH myofibroblast and synthetic PASMC share many features to cancer cells including resistance to apoptosis, uncontrolled proliferation and migration [18,21,75,264-269]. Epigenetic inhibitors have demonstrated efficacy in pre-clinical models and safety in clinical trials for the treatment cancer [263, 270], and recently it was published that JQ1 was able to attenuate bleomycin induced lung fibrosis and significantly reduce inflammatory cell

infiltrate [189]. Furthermore, JQ1 inhibited TGFβ induced fibroblast to myofibroblast transition (FMT) by preventing the upregulation of α-SMA and type-I collagen [189]. Tang *et al* showed JQ1 inhibited PDGFBB migration, proliferation and contraction in fibroblasts from (IPF) patients [180]. These publications have highlighted the potential for JQ1 in the treatment of fibrosis, and suggest potential in their use for SSc, with the hope that epigenetic treatments could prevent the development of PAH in SSc. Previous studies have demonstrated that JQ1 inhibits myofibroblast differentiation and the fibrotic fibroblast phenotype. The hypothesis of this chapter was that inhibition of the BRD proteins using the pharmacological inhibitor JQ1 will attenuate the development of PAH in the TβRIIΔk-fib model of SSc-PAH and the SSc fibroblast phenotype. I have highlighted previously (Figure 4.4) that BMPRII is reduced in whole lung and explant cultured fibroblasts in SSc-PAH patients and it was hypothesised that a decrease in BMPRII might be a contributory risk factor for the development of PAH. Previous reports have shown that BMPRII is reduced in the skin and microvascular endothelial cells in SSc patients [175]. This study also showed that the use of epigenetic inhibitors, DNA methyltransferase inhibitor 5-Aza-2'-de-oxycytidine (5-AZA) and the histone deacetylase inhibitor trichostatin (TSA) had modest effects alone but in combination there was a significant rise in BMPRII expression in microvascular endothelial cells [175]. This suggests that the epigenetics may also modulate BMPRII expression in the lung of SSc patients. The epigenetic inhibitor JQ1 was used *in-vitro* and *in-vivo* to assess its role in modulating BMPRII expression in the lung of the TβRIIΔk-fib model and in explants cultured fibroblasts from SSc patients.

6.2 Aims

The aim of this chapter was to investigate the role of the epigenetic inhibitor JQ1 in the modulation of both fibroblasts and PASMCs disease phenotype. SSc fibroblasts have altered phenotypes compared to normal fibroblasts; the effect of the epigenetic inhibitor JQ1 was investigated to assess its effect on the expression of different disease like markers, functional assays and the secretion of pro-inflammatory cytokines. I went on to investigate if JQ1 treatment *in-vivo* would prevent the development of PAH in the TβRIIΔk-fib model of SSc-PAH. To determine the effect of JQ1, investigated examined RVSP, histological changes, protein expression in the lung and the secretion of pro-inflammatory cytokines in serum. SSc-PAH

Another aim based around other discoveries is that BMPRII expression might be modulated by the epigenetic inhibitor JQ1 and by upregulating BMPRII JQ1 might prevent the development of PAH in the TβRIIΔk-fib model.

6.3 Results

6.3.1 The effect of the epigenetic inhibitor JQ1 in the SSc fibroblast

SSc is a disease of unmet clinical need where pulmonary complications have a devastating effect [38]. The primary effector cell driving SSc in the lung is the myofibroblast which can be derived from fibroblasts, endothelial to mesenchymal transition, epithelial to mesenchymal transition or from circulating progenitor cells [18, 271].

Previous reports have highlighted that elevated type-I collagen and CTGF are associated with pulmonary complications and a disease like phenotype in SSc lung [42, 266, 268, 272]. These proteins are implicated in the deposition of ECM and and vascular remodelling.

Experiments were conducted to assess whether JQ1 had an effect on the expression of type-1 collagen and CTGF. To test this hypothesis, lung fibroblasts were treated with 1 μM JQ1 for 48 hours and assessed by Western blot to determine the effect of JQ1 on type-1 collagen and CTGF protein expression ($p<0.05$; Figure 6.1 A). Type-1 collagen expression was significantly elevated in lung fibroblasts from SSc patients compared to healthy controls and treatment with JQ1 significantly attenuated expression in both lung fibroblasts from SSc patients and healthy controls ($p<0.05$; Figure 6.1 B). CTGF was elevated in lung fibroblasts from SSc patients compared to controls and JQ1 reduced CTGF expression in lung fibroblasts from SSc patients suggesting that BRDs are playing a role in myofibroblast formation ($p<0.05$; Figure 6.1 C).

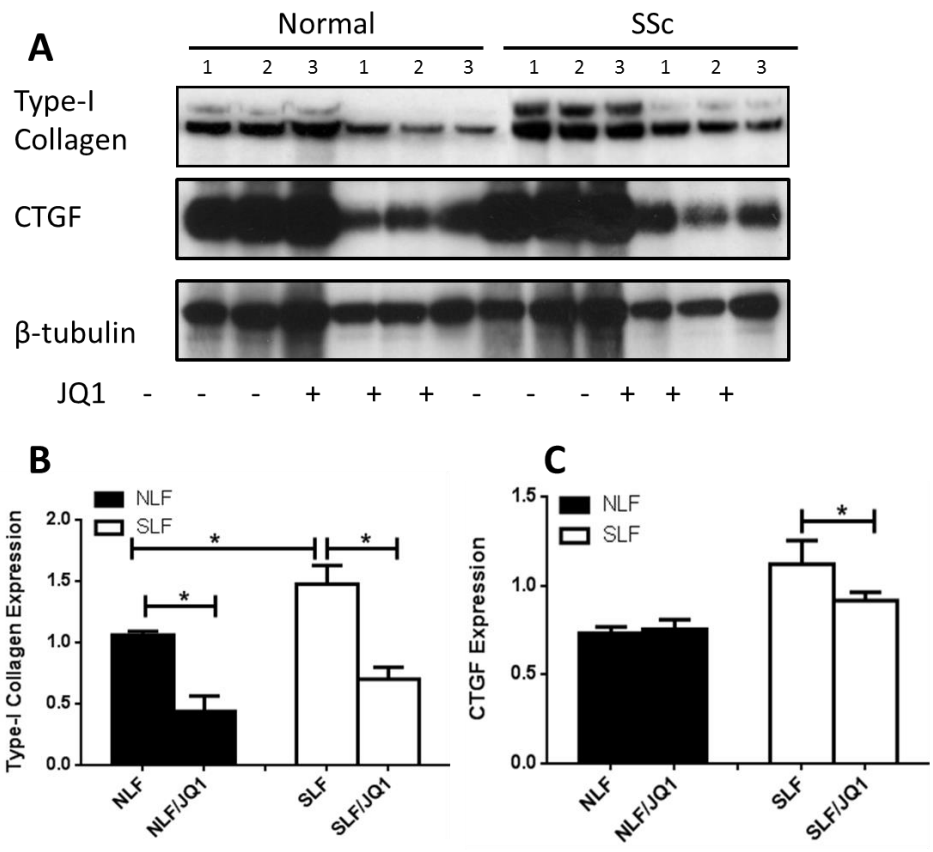

Figure 6.1- JQ1 inhibits elevated type-I collagen and CTGF expression in both normal and SSc lung fibroblasts

Western blots were performed on proteins isolated from confluent monolayers of explant cultured lung fibroblasts from control (NLF) and SSc (SLF) lung fibroblasts (n=3). Fibroblasts were maintained in the presence of either JQ1 (1uM) or vehicle control. Blots were probed for expression of type-I collagen and CTGF. Protein loading was determined by β-tubulin (A). Densitometry was performed and the mean ± SEM expression of type-I collagen (B) and CTGF (C) normalised to β-tubulin expression was plotted. *$p<0.05$ using Mann Whitney Test.

6.3.2 The epigenetic inhibitor JQ1 can arrest the myofibroblast phenotype of the SSc fibroblast.

Previously I have shown lung fibroblasts from SSc patients display increased migration, proliferation and contraction rates (Chapter 4), these are key processes that may contribute to the development of pulmonary pathologies in SSc patients such as PAH. To assess the functional involvement of bromodomain and extra terminal domain (BET) BRDs proteins phenotypic response assays were used to investigate the ability of JQ1 to inhibit migration, proliferation and contraction by lung fibroblasts from SSc patients. The initial aim was to investigate if inhibition of JQ1 can alter these processes that are thought/believed to contribute to the development of PAH in SSc (Figure 4.7). Both control lung fibroblasts and lung fibroblasts from SSc patients were treated with PDGFBB in the presence or absence of 1 μM JQ1 for 24 hours to assess the effect of JQ1 on fibroblast migration (Figure 6.2A). Confluent monolayers of fibroblasts were scratched and treated with either 1% FCS or 50 ng/ml PDGFBB in the presence and absence of 1 μM of JQ1. These experiments were also performed in the presence of the anti-proliferative mitomycin-C. Consistent with previously studies in chapter 4, PDGFBB induced migration was significantly increased in lung fibroblasts from SSc patients compared to controls. JQ1 significantly inhibited migration in control and SSc lung fibroblasts ($p<0.05$; Figure 6.2B).

The effect of JQ1 on PDGFBB induced proliferation of lung fibroblasts was assessed. Lung fibroblasts were incubated with 50 ng/ml PDGFBB and the effects of a range of JQ1 concentrations compared to vehicle controls were determined. PDGFBB treatment induced increased proliferation in lung fibroblasts from SSc patients, compared to control lung fibroblasts ($p<0.05$; Figure 6.3). Incubation with JQ1 led to a significant inhibition of PDGFBB-induced fibroblast proliferation in both normal and SSc lung fibroblasts in a concentration dependent manner ($p<0.05$; Figure 6.3).

Gel contraction was assessed using pooled data from a series of independent experiments and donors using type-1 collagen lattices, these contraction assays show that both 5 ng/ml TGFβ and 10% FCS significantly induced increased contraction rates in lung fibroblasts from SSc patients compared to controls ($p<0.05$; Figure 6.4

A and B). Experiments were also performed in the presence of 1 μM JQ1; JQ1 had no significant effects on gel contraction. Contraction was assessed by measuring the diameter of each individual gel or the each gel's weight (Figure 6.4 A and B).

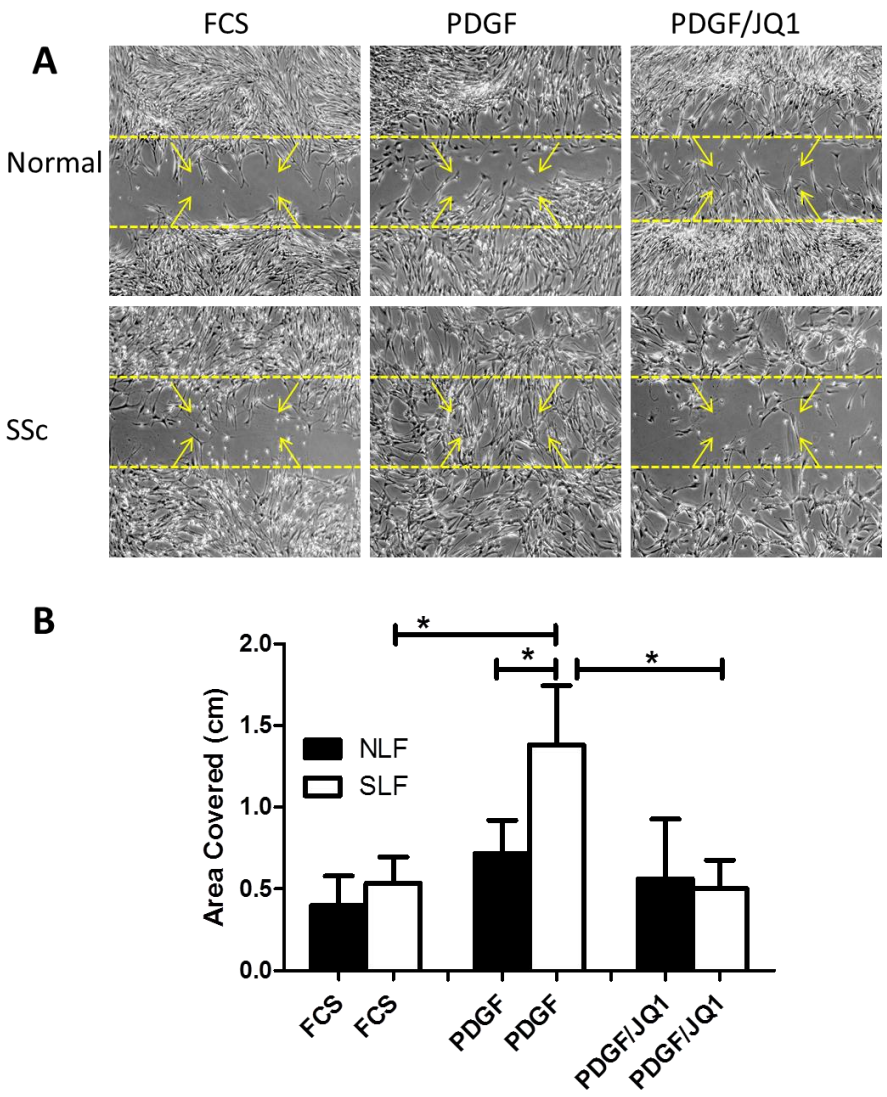

Figure 6.2 –PDGFBB induced migration is inhibited by JQ1 in SSc lung fibroblasts is by JQ1

Confluent monolayers of control (NLF) and SSc lung fibroblasts (SLF) were scratch wounded and cellular migration in response to 1% foetal calf serum (FCS), or 50 ng/ml PDGFBB in the presence of JQ1 (1uM) vehicle control assessed after 24hrs (A). Experiments were performed in the presence of 10 μg/ml mitomycin C on three independent donors in triplicate and the mean ± SEM plotted (B). *$p<0.05$, using Mann Whitney Test (B).

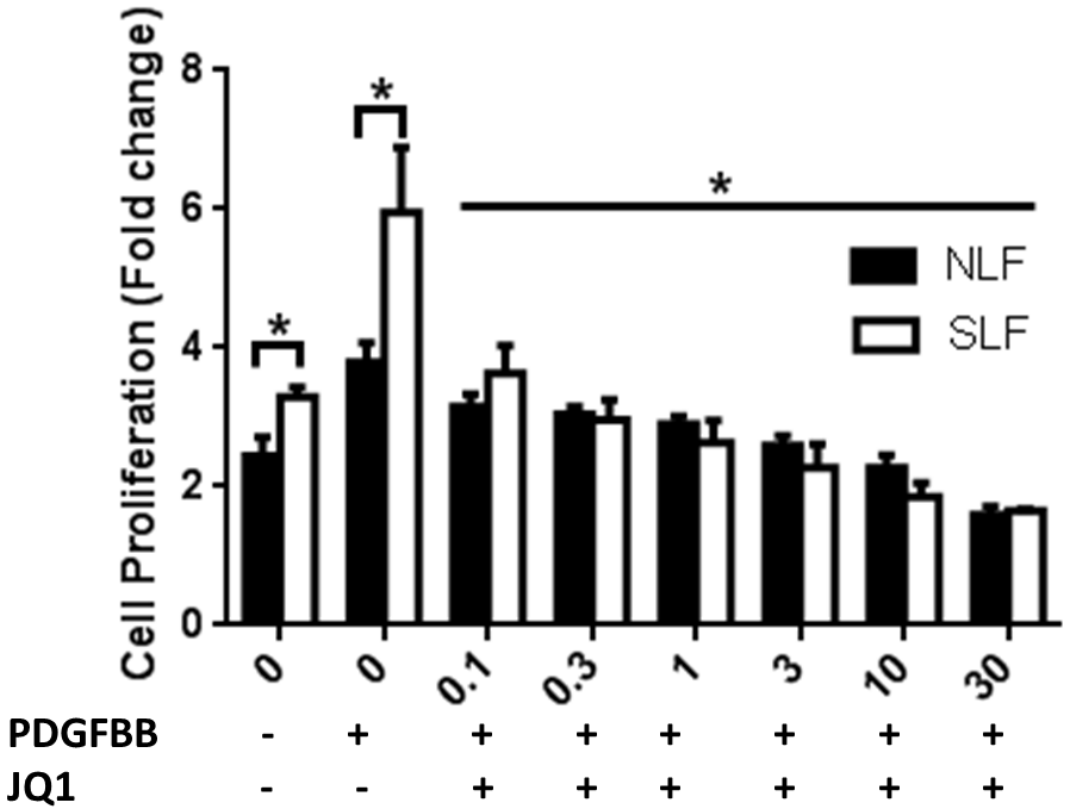

Figure 6.3 - JQ1 antagonises PDGFBB induced proliferation in SSc lung fibroblasts.

Control (NLF) and SSc (SLF) lung fibroblasts seeded at equal cell densities were stimulated with PDGFBB (50 ng/ml) and the dose dependent effects of JQ1 on cell numbers determined after 72 hours. Data represents the fold change in cell numbers after 72 hours to seeded cells and are expressed as the mean of three individual donors ± SEM. Proliferation was assessed after 72 hours. *$p<0.05$, Two-way analysis of variance (ANOVA).

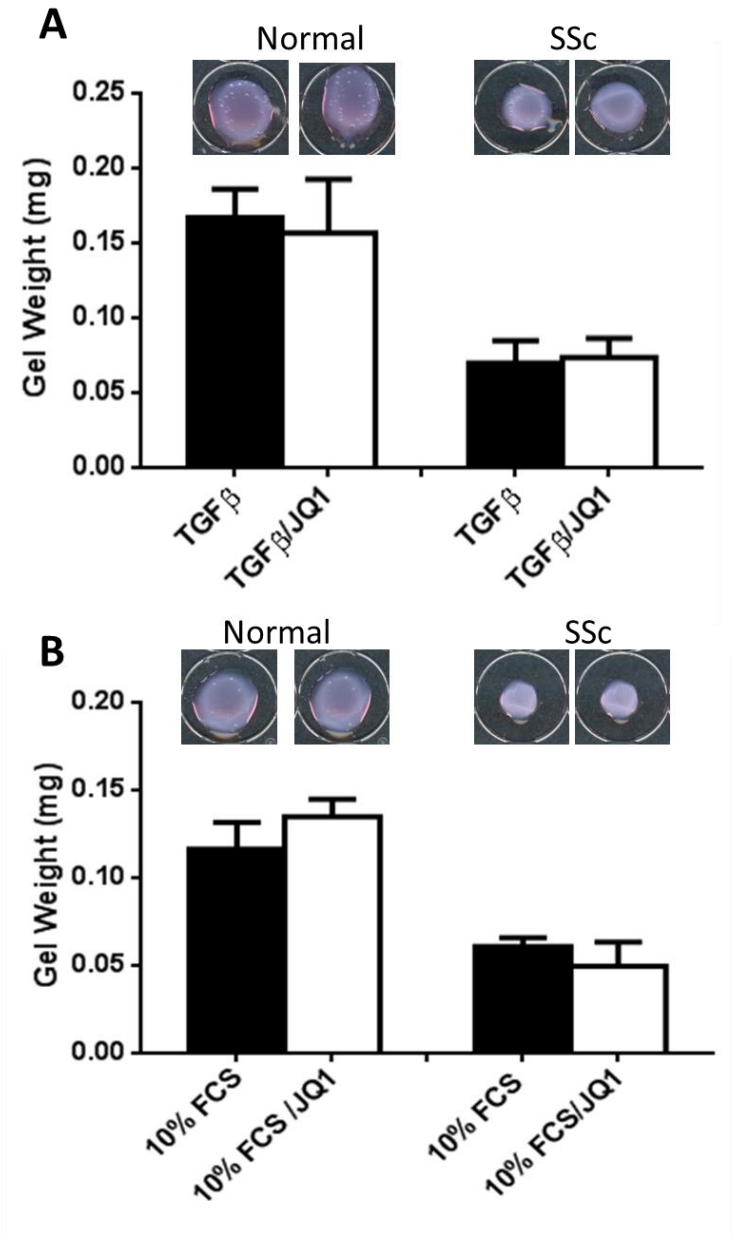

Figure 6.4 – JQ1 does not modulate SSc gel contraction.

Control (NLF) and SSc (SLF) lung fibroblasts were seeded at 2 x 10^4 in 24 well plates into collagen matrix and exposed to either 5 ng/ml TGFβ (A) or 10% FCS (B) in the presence or absence of 1 μM JQ1 or vehicle control. After 72 hours, gel contraction was assessed by measuring gel weights and the mean ± SEM of three cell lines plotted. *$p<0.05$ using Mann Whitney Test test (C).

6.3.4 The pro-inflammatory phenotype of SSc fibroblasts is reduced by treatment in JQ1.

Elevated levels of circulating pro-inflammatory cytokines have been reported in the sera of SSc and IPAH patients by many groups [218, 273]. A number of studies have demonstrated the SSc fibroblast secrete elevated levels of pro-inflammatory cytokines, for example IL-6. BRD inhibitors have previously been shown to modulate a number of inflammatory chemokines including IL-6. I sought to assess the effects of JQ1 on SSc fibroblast secretion of inflammatory chemonkines using the MSD multiplex array.

SSc lung fibroblasts secreted detectable levels of IL-2, IL-4, IL-10, and TNF-α, whilst levels secreted by healthy control lung fibroblasts were below the detectable limits of the array. IL-6 and IL-13 was detectable in control lung fibroblast conditioned media, however was significantly elevated in SSc lung fibroblast conditioned media ($p<0.05$; Figure 6.5) JQ1 had no significant effect effects on IL-2, IL-4, IL-10 and IL-13 secretion by SSc lung fibroblasts. In contrast IL-6 secretion was significantly inhibited by JQ1 in control and SSc lung fibroblasts levels were significantly increased in SSc lung fibroblasts compared to healthy controls ($p<0.05$; Figure 6.5A) and JQ1 significantly reduced IL-6 secretion in SSc lung fibroblasts ($p<0.05$; Figure 6.5 A). IL-8 secretion levels were significantly increased in SSc lung fibroblasts compared to healthy controls ($p<0.05$; Figure 6.5B) but JQ1 had no effect on IL-8 secretion in either normal or SSc lung fibroblasts.

A

	NLFs	NLF/JQ1	SLF	SLF/JQ1
IL-2	-	-	4¶	1.6
IL-4	-	-	1.1	0.8
IL-6	520	529	1190	555 *
IL-8	1493	2826	10053¶	7640
IL-10	-	-	3.0	1.2
IL-13	2.3	12.5	28.1¶	22.7
TNF-α	-	-	2.2	1.0

B C

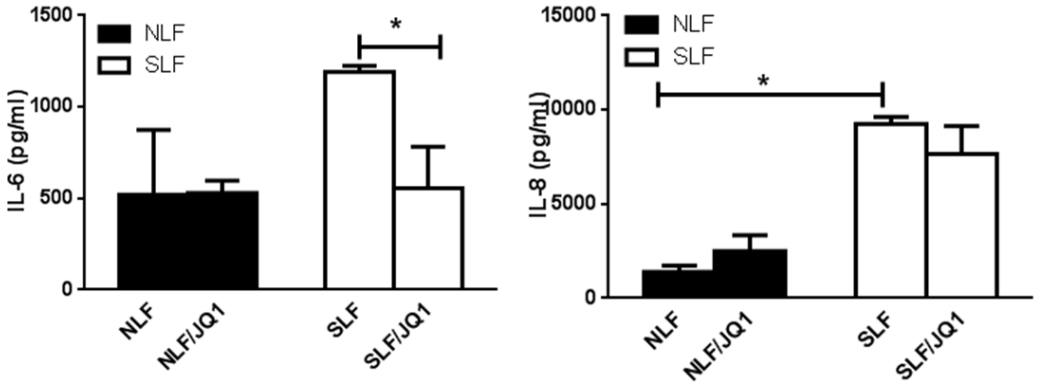

Figure 6.5 – SSc lung fibroblasts exhibit a pro-inflammatory profile compared to normal lung fibroblasts

Conditioned medium from normal lung fibroblasts (NLF) and SSc lung fibroblasts (SLF) was collected after 48 hours and secretion was normalised to protein levels in the cell monolayer. Multiplex analysis was performed on the conditioned medium for inflammatory mediators and concentrations (ng/ml) tabulated, IL-2, IL-6, IL-8 and IL-13 were significantly elevated in SLF compared to NLF (A). Levels of IL-6 (A) and IL-8 (B) were confirmed and values plotted ± SEM. *p<0.05, Unpaired T-test (A-C). * denotes significance between JQ1 treated and untreated groups. ¶ denotes significance between NLF and SLF.

6.3.5 Synthetic phenotype is modulated by the bromodomain inhibitor JQ1

The role of the PASMC is important in maintaining a healthy vasculature. Pathological differentiation from a contractile to synthetic PASMC is believed to be a key feature in vascular remodelling [21]. It has already demonstrated that the BRD inhibitor JQ1 can modulate disease characteristics of the fibroblast (Figure 6.1, Figure 6.2), the complexity of SSc and PAH suggest more than one cell type contribute to the development of SSc and PAH and another key cell type involved in these diseases is the PASMC.

Using contractile and synthetic PASMCs (as discussed in section 5.4.1) and PASMCS isolated from healthy controls and IPAH patients, I investigated the effect of JQ1 on protein and secreted markers of a synthetic PASMCs. Type-I collagen was established as a marker of synthetic PASMCs (Figure 5.1) and using Western blot analysis (Figure 6.6 A) and immunofluorescence (Figure 6.6 B), the effect of JQ1 on type-I collagen in synthetic PASMCs was assessed. The BRD inhibitor JQ1 was able to significantly reduce type-I collagen expression in synthetic PASMCs ($p<0.05$; Figure 6.6 C).

Synthetic PASMCs were also treated with PDGFBB and JQ1 to determine the effect of JQ1 on cell proliferation. PASMCs were incubated with 50 ng/ml PDGFBB alone and in varying concentrations of JQ1. PDGFBB treatment induced proliferation and in a concentration dependent manner JQ1 significantly inhibited proliferation of synthetic PASMCS ($p<0.05$; Figure 6.6 D).

PASMCs were then treated with JQ1 to examine the effect of JQ1 on pro-inflammatory cytokines that are elevated in the sera of PAH patients and correlate to patient survival [218]. PASMCs were maintained in either contractile or synthetic medium (section 5.4.1) and growth medium replaced with 0.1% FCS medium for serum starvation with or without 1 μM JQ1. After 24 hours medium was collected to determine the effect of JQ1 on pro-inflammatory cytokines After 24 hours IL-1β, IL-6, IL-10 and IL-13 were significantly elevated in synthetic compared to contractile PASMCs. JQ1 significantly inhibited secretion of IL-1β, IL-6, IL-10 and IL-13 in synthetic PASMCs ($p<0.05$; Figure 6.7 A-D).

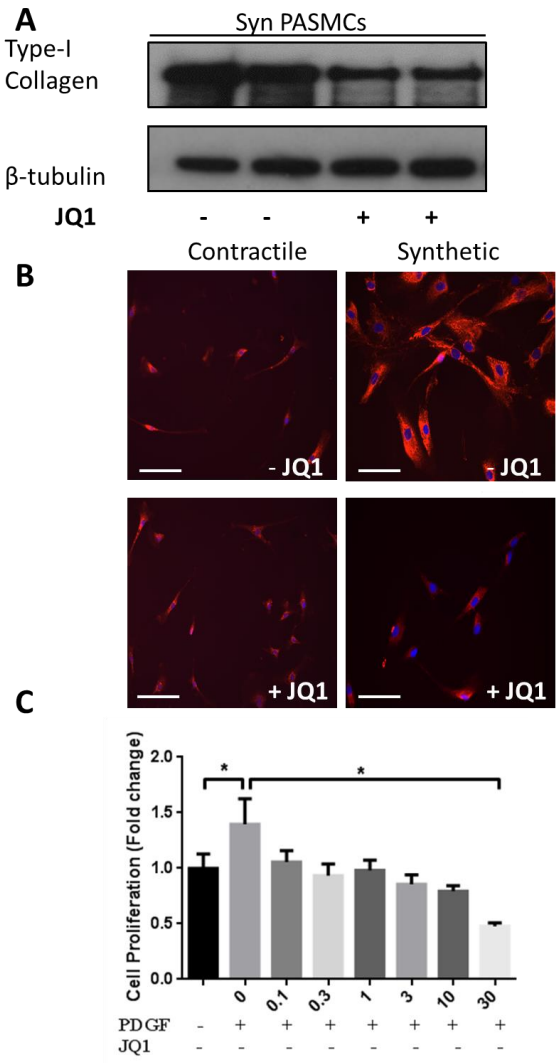

Figure 6.6 – Synthetic PASMC's phenotype is modulated by JQ1

Western blots were performed on proteins isolated from confluent monolayers of synthetic pulmonary arterial smooth muscle cells (PASMCs; n=3). Blots were probed for expression of type-I collagen. Protein loading was determined by β-tubulin (A). Immunofluorescence staining was performed on type-I collagen (B). Images were taken using the Carl Zeiss Axiovison microscope and images shown are representative of three independent experiments. Platelet derived growth factor (PDGFBB) mediated proliferation in synthetic PASMCs and JQ1 inhibits proliferation at 0.1 μM to 30 μM. Data represent the fold proliferation induced by PDGFBB compared to vehicle controls and are expressed as a mean of three donors. Proliferation was assessed after 72 hours (C). (*$p<0.05$, Two-way analysis of variance (ANOVA) (C). White line indicates 100 μM using the x 40 magnification.

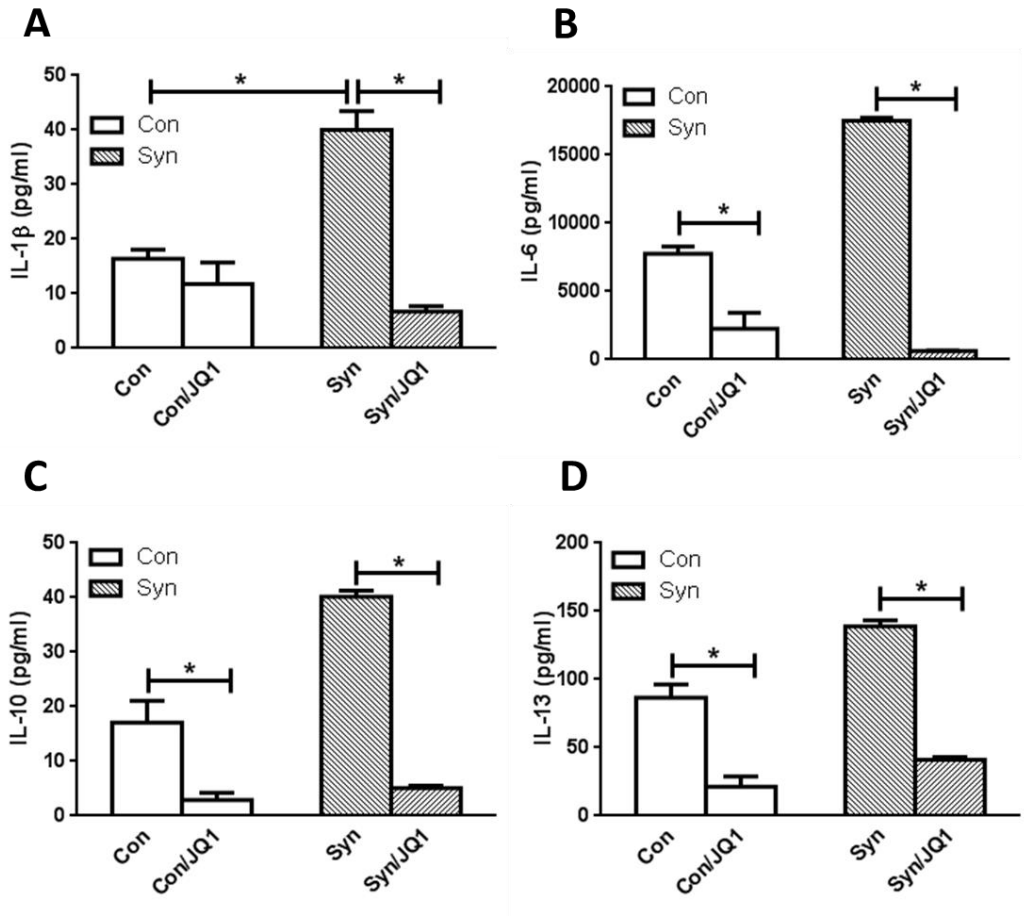

Figure 6.7 – Synthetic PASMCs display a pro-inflammatory phenotype that can be attenuated by JQ1

Conditioned medium from contractile and synthetic pulmonary arterial smooth muscle cells PASMCs was collected after 48 hours serum starvation. Secretion was normalised to protein levels in the cell monolayer. Multiplex analysis was performed using three individual donors in duplicate for IL-1β (A), IL-6 (B), IL-10 (C) and IL-13 (D). *$p<0.05$, Mann-Whitney Test (A-D).

6.3.6 IPAH PASMCS can be modulated by JQ1 to resemble control PASMCs

Using type-1 collagen which has been previously validated as a marker of synthetic PASMCs (Figure 5.1), I investigated the expression of type-I collagen in PASMCS isolated from IPAH patients.

Interestingly type-I collagen expression is also elevated in PASMCs from IPAH patients compared to healthy controls and JQ1 significantly reduced expression of type-I collagen in both control and IPAH patients (*$p<0.05$; Figure 6.7B).

Both control and IPAH PASMCs were serum starved in 0.1% FCS for 24 hours in the presence or absence of 1 μM JQ and IL-6 and IL-8 levels were measured by ELISA. Both IL-6 and IL-8 levels were significantly elevated in IPAH PASMCs compared to healthy controls, but JQ1 significantly reduced IL-6 secretion but had no effect on IL-8 (*$p<0.05$; Figure 6.8 C).

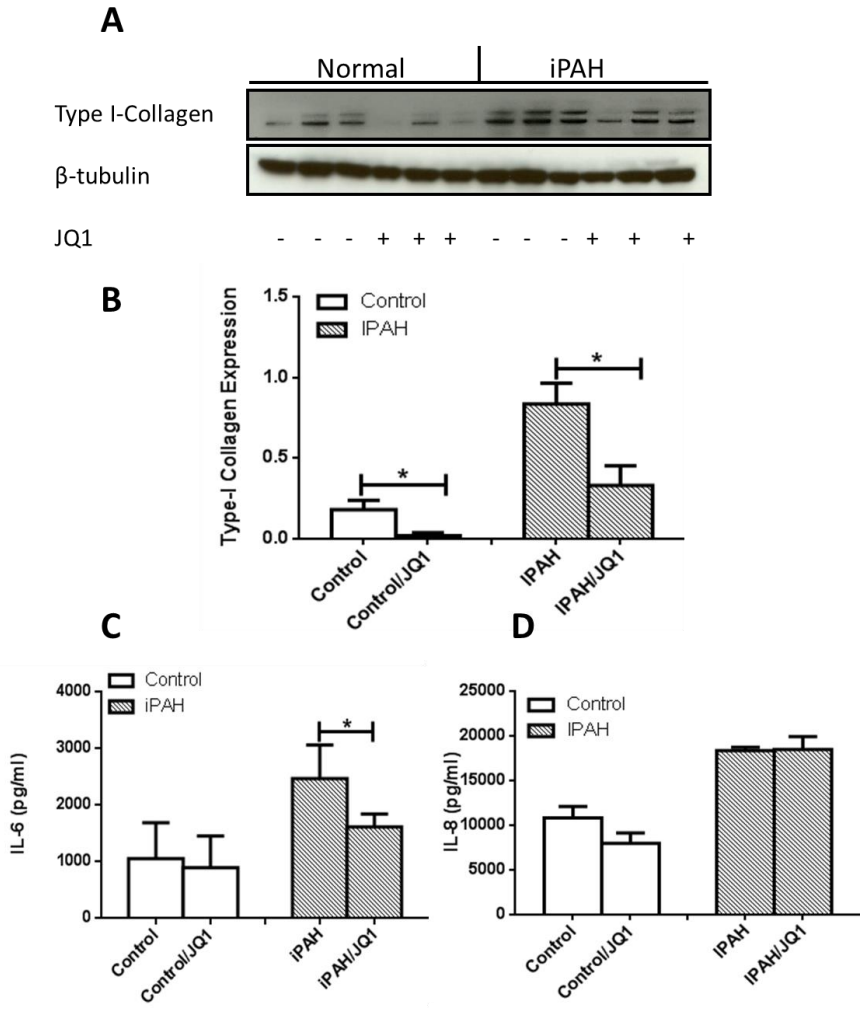

Figure 6.8 – IPAH PASMCS resemble synthetic PASMCs and JQ1 can inhibit their disease like phenotype

Western blots were performed on proteins isolated from confluent monolayers of control (n=3) and IPAH PASMCs (n=3) in the presence of JQ1 (1uM) or vehicle control. Blots were probed for expression of type-I collagen and protein loading determined by β-tubulin (A). Densitometry was performed and the mean ± SEM of type-I collagen expression normalised to β-tubulin expression plotted (B). Conditioned medium from control and IPAH PASMCs (n=3) treated with JQ1 (1uM) or vehicle control was collected after 48 hours in serum starvation medium and IL-6 and IL-8 levels determined by ELISA. Secreted IL-6 and IL-8 levels were normalised to β-tubulin protein levels and the mean ± SEM of IL-6 (C) and IL-8 (D) plotted. *$p<0.05$, Unpaired T Test.

6.3.7 TβRIIΔk-fib mice develop elevated RVSP that can be prevented by the administration of JQ1

It has been previously reported that TβRIIΔk-fib mice display constitutive pulmonary vasculopathy with medial thickening, a perivascular proliferating chronic inflammatory cell infiltrate, and significantly elevated pulmonary artery pressure compared to wild type controls [119].

Addition of the VEGFR antagonist SU5416 by intraperitoneal injection induced a pulmonary vascular phenotype that was more severe, with pulmonary arteriolar luminal obliteration by apoptosis-resistant proliferating endothelial cells. These changes resulted in right ventricular hypertrophy, confirming haemodynamically significant PAH [119]. This chapter investigateds how the TβRIIΔk-fib model spontaneously develops PAH and how the exposure to an epigenetic inhibitor JQ1 might prevent the development of PAH in these mice.

For this experiment the effect of the BRD inhibitor JQ1 in the development of mild PAH in the TβRIIΔk-fib model of SSc-PAH was investigated. JQ1 was infused in feed doses calculated based on the assumption that the mice would consume 2.5 g per day and food consumption was monitored. Animals remained on this diet every day 21 at the end of the study. Consistent with previous studies the TβRIIΔk-fib mice displayed a significant increase in RVSP compared to WT controls (*$p<0.05$; Figure 6.9A). JQ1 did not affect RVSP in WT mice but JQ1 significantly reduced RVSP in TβRIIΔk-fib mice (*$p<0.05$; Figure 6.9A). There was no difference in the RV mass index (Fulton index) between TβRIIΔk-fib and WT mice and JQ1 had no effect on RV mass index in either TβRIIΔk-fib or WT mice (Figure 6.9B).

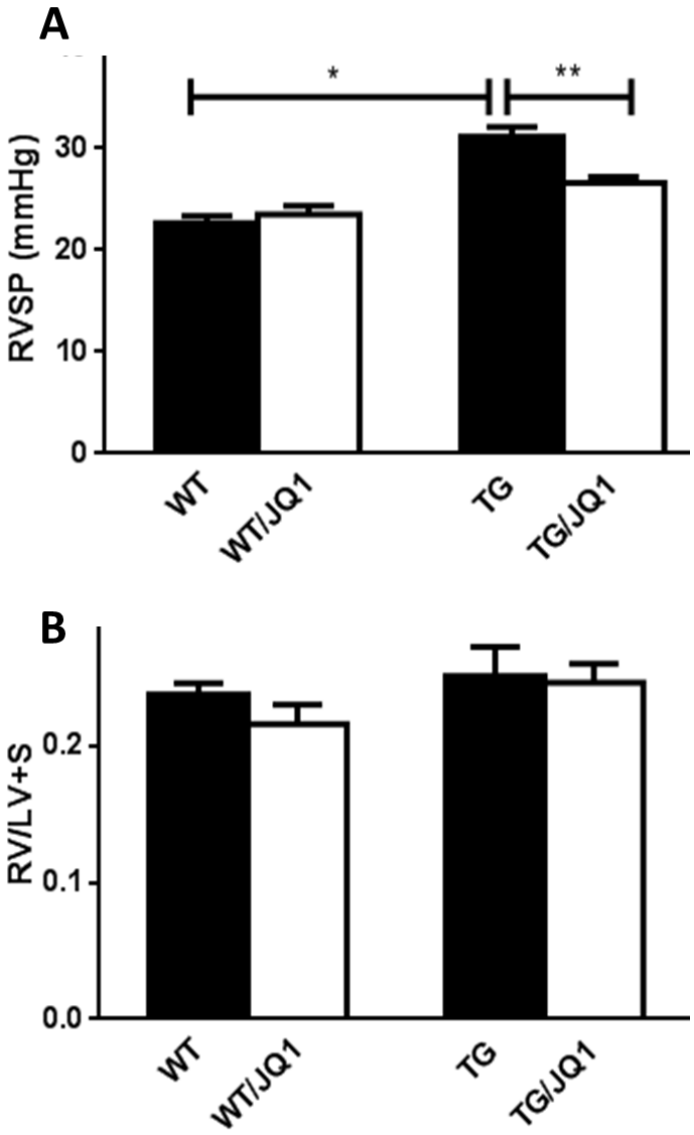

Figure 6.9 – The effect of JQ1 on RVSP and fulton index in the TβRIIΔk-fib model of SSc-PAH

Right ventricular systolic pressure (RVSP) (A) and right ventricle:left ventricle plus septum ratio (RV/LV+S) (Fulton Index) (B) in wildtype and TβRIIΔk-fib exposed to vehicle control or 20mg/kg JQ1 infused in feed (n=6). Data was analysed by one-way analysis of variance (ANOVA) with Bonferroni post-hoc analysis. Results presented are expressed as the mean ± S.E.M, *$p<0.05$; ** $p<0.01$.

6.3.8 TβRIIΔk-fib mice display a pulmonary structural vasculopathy that is attenuated by JQ1

In this experiment the TβRIIΔk-fib model is not exposed to the VEGR antagonist SU5416 which previously induced a more severe phenotype in the TβRIIΔk-fib model [119]. This work is investigating how the TβRIIΔk-fib model spontaneously develops PAH and how the exposure to an epigenetic inhibitor JQ1 might prevent the development of PAH in these mice. The TβRIIΔk-fib model of SSc-PAH displays muscularisation and the formation of concentric lesions in small pulmonary arteries of approximately 20 μm [119].

Immunohistological staining for the smooth muscle cell marker α-SMA (brown) and the endothelial cell marker vWF (brown) displayed increased vessel wall thickening. There were no cardinal features of advanced or severe PAH such as plexiform lesions observed in TβRIIΔk-fib vessels (Figure 6.10). The epigenetic inhibitor JQ1 was able to reduce muscularisation and vessel thickness in TβRIIΔk-fib mice compared to vehicle control treated mice (Figure 6.10).

Hematoxylin and eosin (H&E) staining highlights a slight increase perivascular inflammatory cell infiltrate and medial thickening in the TβRIIΔk-fib mice group compared to wild-type controls. JQ1 was able to reduce medial thickening and inflammatory cell infiltrate in TβRIIΔk-fib mice (Figure 6.11).

The examination of medial wall thickening in the lungs of TβRIIΔk-fib mice was performed by IF double staining. IF staining of α-SMA (red), vWF (green) and nuclear dapi (blue) was performed on paraffin embedded formalin fixed lung sections from WT and TβRIIΔk-fib mice exposed *in-vivo* to JQ1 or vehicle alone (Figure 6.12). Both WT and JQ1 treated mice displayed similar staining with a single layer of smooth muscle cells highlighted by red fluorescence and a single layer of endothelial cells highlighted by green fluorescence (Figure 6.12). However in the pulmonary artery of TβRIIΔk-fib the formation of concentric rings due to the expansion of smooth muscle cells is observed which may result from the increase in α-SMA positive cells. This vessel thickening is only seen in the media due to no endothelial cell dysfunction being reported in the pulmonary artery of TβRIIΔk-fib mice. In the TβRIIΔk-fib JQ1 treated group there is slight medial thickening but a decrease compared to TβRIIΔk-fib mice treated with vehicle (Figure 6.12).

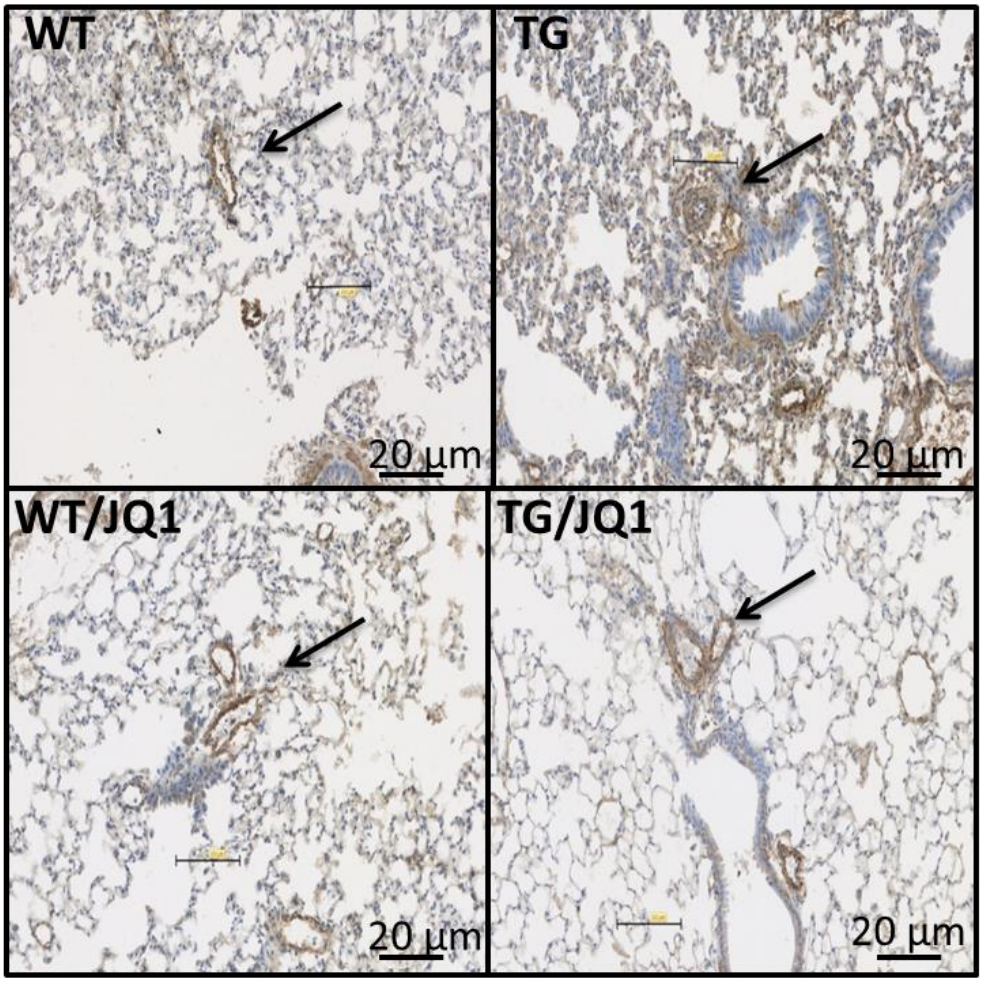

Figure 6.10 – JQ1 prevents the development of muscularisation in the TβRIIΔk-fib model of SSc-PAH

Immunohistochemical double staining for alpha-smooth muscle actin (α-SMA) and von Willebrand factor (vWF) on paraffin embedded formalin fixed lung sections from wild type (WT) and TβRIIΔk-fib mice exposed *in-vivo* to JQ1 or vehicle alone (n=6 mice per group). Representative images shown of n=6 mice per group. Magnification x20.

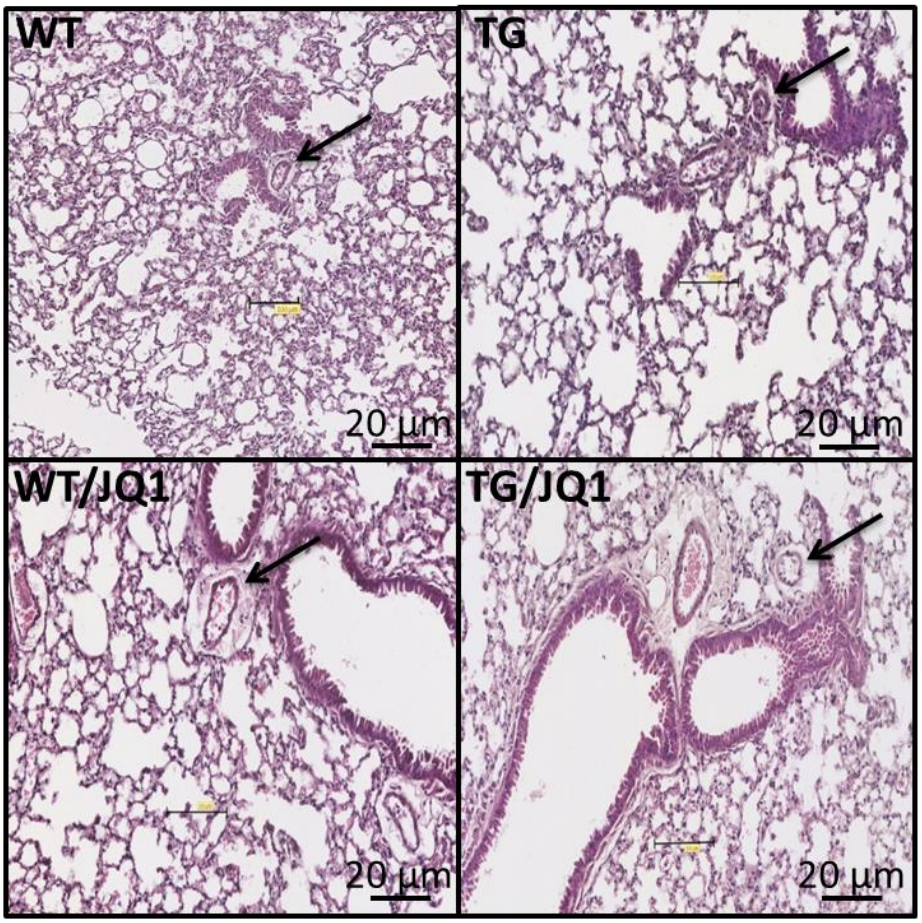

Figure 6.11 – JQ1 reduces medial thickening and inflammatory infiltrate in the TβRIIΔk-fib model of SSc-PAH

Hematoxylin and eosin (H&E) staining of paraffin embedded formalin fixed lung sections from wild type (WT) and TβRIIΔk-fib mice exposed *in-vivo* to JQ1 or vehicle alone (n=6 mice per group). Representative images shown; Magnification x20.

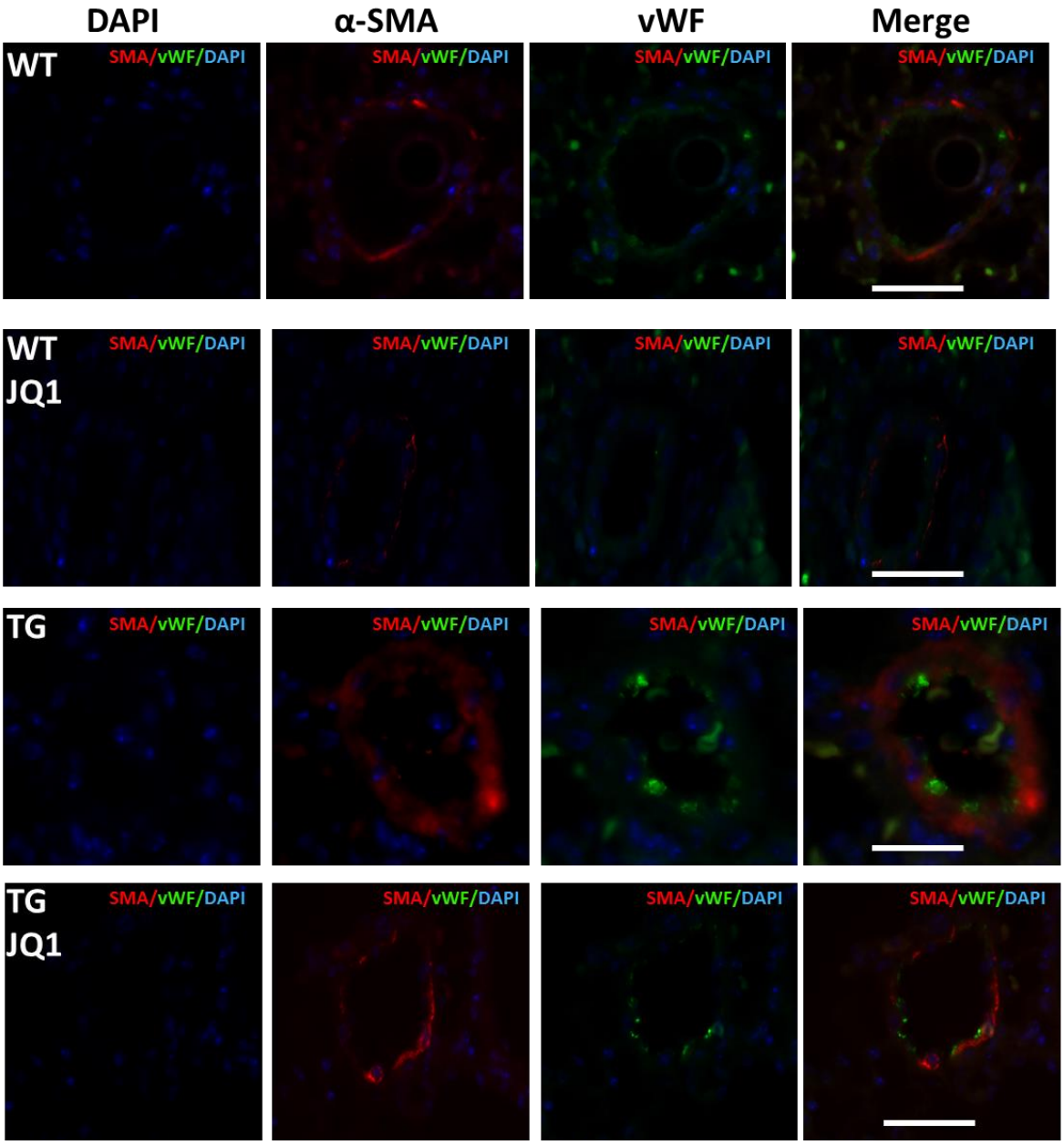

Figure 6.12 – JQ1 reduces muscularisation in the TβRIIΔk-fib model of SSc-PAH

Expression of alpha-smooth muscle actin (α-SMA; red), von Willebrand factor (vWF; green) and nuclear DAPI (blue) was determined by immunofluorescence on paraffin embedded formalin fixed lung sections from wild type (WT) and TβRIIΔk-fib mice exposed *in-vivo* to JQ1 or vehicle alone (n=6 per group). Representative images shown. White line indicates 20 μm. Magnification x20.

6.3.9 The effect of JQ1 on the TGFβ/BMP superfamily in the TβRIIΔk-fib model

The work of this thesis has highlighted the involvement of enhanced TGFβ activity and a reduction of BMPRII in the development of PAH in SSc patients. The next question was to investigate the role of JQ1 on the expression of components of the TGFβ superfamily in the TβRIIΔk-fib model of SSc-PAH.

Using whole lungs isolated from WT controls and TβRIIΔk-fib mice treated with JQ1 or vehicle, the protein expression of components of the TGF-β superfamily was explored and downstream signalling pathways in TβRIIΔk-fib mice (Figure 6.13).

Expression of BMPRII, BMPRIA phosphorylated-Smad2/3, Smad 2/3, phosphorylated-Smad 1, Smad 1, phosphorylated-ERK1/2, ERK 1/2, phosphorylated-p38 and p38 was determined in whole lung protein homogenates isolated from the WT controls and TβRIIΔk-fib treated with JQ1 or vehicle control by Western blot (Figure 6.13).

Lung homogenates from TβRIIΔk-fib and WT displayed no significant change in BMPRIA expression in TβRIIΔk-fib or WT either treated with JQ1 or vehicle control (Figure 6.13 A).

As previously demonstrated in figure 5.2 lung homogenates from TβRIIΔk-fib exhibited significantly lower levels of BMPRII compared to that of WT mice ($p<0.05$; Figure 6.13 B).Levels of BMPRII in the lungs from WT and TβRIIΔk-fib mice treated with JQ1 compared to vehicle treated mice exhibited a significant reduction in BMPRII expression ($p<0.05$; Figure 6.13 B).

Following examination of the BMPR proteins the assessment of the TGFβ/BMP canonical pathways were investigated. Lung homogenates from TβRIIΔk-fib and WT displayed no significant change in phosphorylated Smad1/Smad1 expression in TβRIIΔk-fib or WT either treated with JQ1 or vehicle control (Figure 6.13 A).

As previously demonstrated, levels of phosphorylated-Smad2/3/Smad 2/3 were elevated in TβRIIΔk-fib mice compared to WT controls ($p<0.05$; Figure 6.13 B). TβRIIΔk-fib mice treated with JQ1 exhibited a reduction in phosphorylated Smad2/3/Smad 2/3 that was trending but did not quite reach signifcance (Figure 6.13 D).

Finally lung homogenates of the TβRIIΔk-fib were assessed for the phosphorylation of the non-cannonical signalling pathway. TβRIIΔk-fib mice lung homogenates displayed an increase in the level of phosphorylated-ERK1/2/ERK1/2 but JQ1 had

no effect on phosphorylated-ERK1/2/ERK1/2 expression in JQ1 treated mice (Figure 6.13 E). TβRIIΔk-fib mice lung homogenates displayed an increase in the level of phosphorylated-p38/p38 and JQ1 significantly reduced p-p38/p38 expression in both WT and TβRIIΔk-fib mice (*$p<0.05$; Figure 6.13 F).

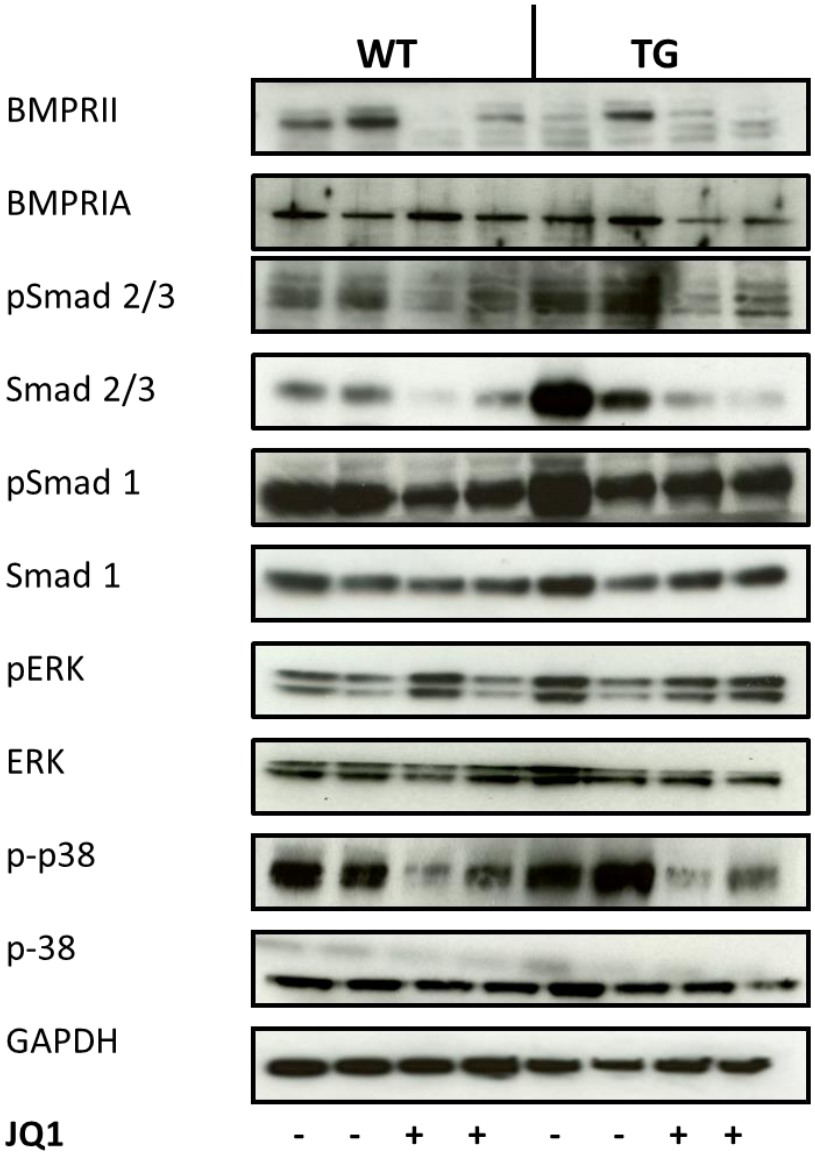

Figure 6.13 – The effect of the epigenetic inhibitor JQ1 on the BMP receptors and components of the TGFβ superfamily signalling pathways

Western blots were performed on protein extracts prepared from whole lungs isolated from wild type (WT) and TβRIIΔk-fib mice exposed *in-vivo* to JQ1 or vehicle controls (n=3). Blots were probed for expression of BMPRII, BMPR1A, phosphorylated Smad2/3 (pSmad2/3), Smad 2/3, phosphorylated Smad 1 (pSmad 1), Smad 1, phosphorylated ERK1/2 (pERK), ERK, phosphorylated p38 (p-p38) and p38. Protein loading was determined by GAPDH levels and representative blots show above (A).

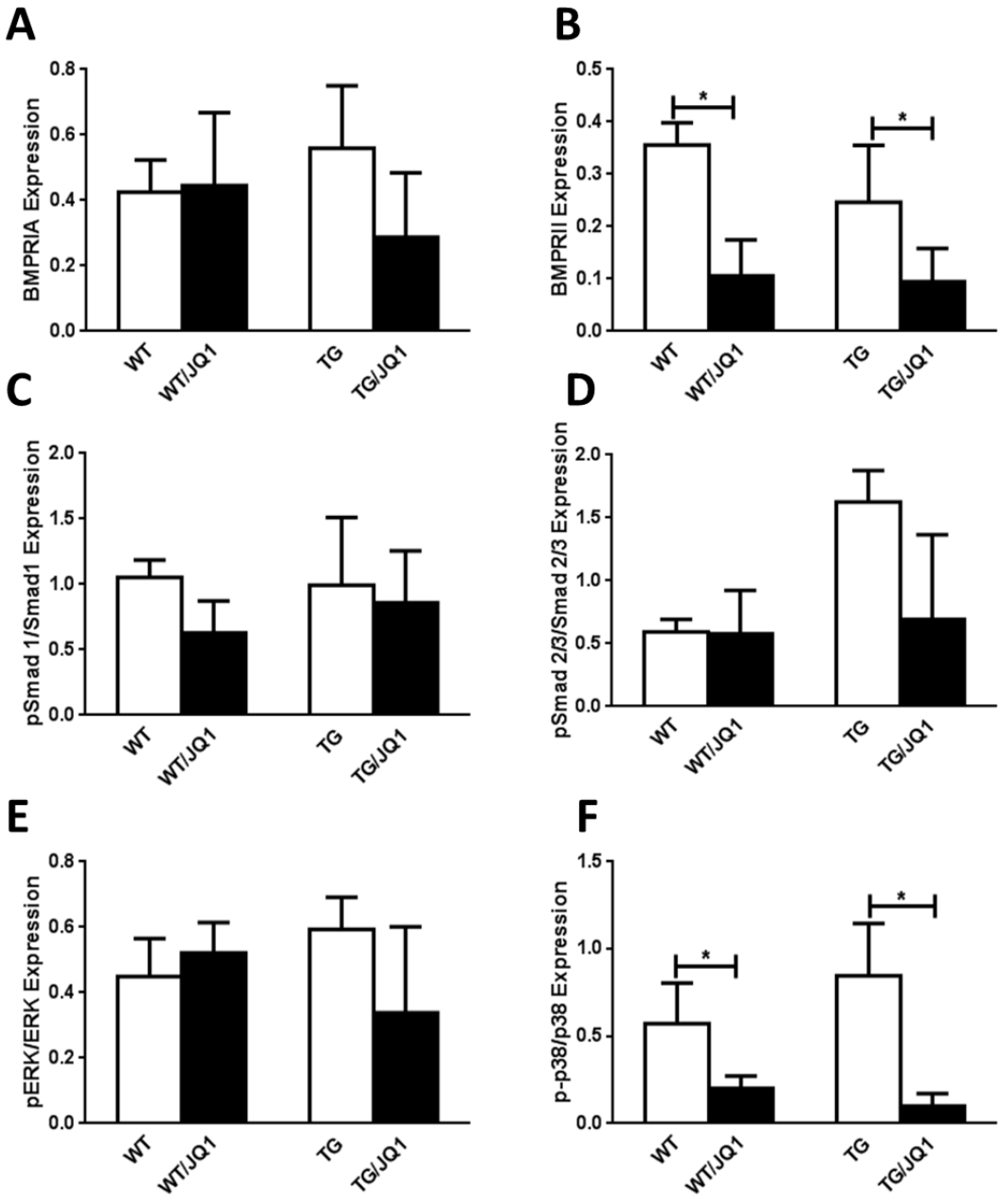

Figure 6.14 – Densitometry displaying the effect of the epigenetic inhibitor JQ1 on the TGFβ/BMP family and downstream signalling pathways

Densitometry was performed and the mean ± SEM expression of (A) BMPRII, (B) phospho-Smad2/3 (pSmad2/3), (C) Smad 2/3, phospho-Smad 1 (pSmad 1), (D) Smad 1, phospho-ERK1/2 (pERK), (E) ERK, phospho-p38 (p-p38) and (F) p38 plotted (n=3). *$p<0.05$ using Mann-Whitney Tests. (A-F).

6.4 Discussion

Several studies to date have been published around the role of JQ1 and BRD proteins in IPF, multiple myeloma and prostate cancer [180, 261, 263]. JQ1 has demonstrated the ability to inhibit fibrosis in the pre-clinical bleomycin model, attenuate fibroblast to mesenchymal transition and to exert anti-inflammatory effects *in-vitro* [180, 274]. These characteristics of JQ1 make it a suitable candidate to investigate the role of JQ1 in the development of PAH in the TβRIIΔk-fib model of PAH-SSc and to examine JQ1's effect on the SSc-PAH fibroblast. The BRD inhibitor JQ1 prevented the development of PAH in the TβRIIΔk-fib model and demonstrated an ability to reverse disease like phenotypes in scleroderma lung fibroblasts and IPAH PASMCs suggesting that BRD proteins might play a key role in the development PAH and provides a novel therapeutic for the treatment of PAH.

Previous studies from our group and others have highlighted the differences between normal lung fibroblasts and scleroderma lung fibroblasts. Fibroblasts isolated from patients display altered phenotypic responses that might be contributing to the development of PAH in SSc patients [18, 267-269, 275, 276]. During vascular remodelling fibroblasts undergo phenotypic changes that result in altered cellular responses. These changes have been reported in IPAH and IPF where fibroblasts display increased proliferation and migration, two cellular processes that can lead to remodelling by occlusion of the lumen in the pulmonary artery [22, 189]. These fibroblasts also exhibit an enhanced inflammatory phenotype which is highlighted by an increase in secretion of pro-inflammatory cytokines [153]. It has been previously reported that these cellular changes could be linked to epigenetic modifications such as histone acetylation, deacetylation or microRNA expression [22, 277].

This study highlights an essential role for BRDs in reprogramming an activated and epigenetically modified fibroblast and PASMC. These cells are characterised by abnormal cellular processes, inflammation and overproduction of ECM contributes to the development of PAH. SSc lung fibroblasts have previously been reported to express elevated levels of CTGF and type-1 collagen that contribute to increased ECM production [278-283], and this work demonstrates that type-1 collagen is elevated in PASMCs from IPAH patients. JQ1 is able to reduce the expression of CTGF and type-I collagen in both SSc lung fibroblasts and PASMCs isolated from

IPAH, suggesting that JQ1 can reduce the secretion of ECM in the lung and pulmonary artery. Functionally explant cultured lung fibroblasts from SSc display cellular activities that may contribute to vascular remodelling and the development of PAH. It has been previously reported that JQ1 can arrest cell proliferation in cancerous cells and fibroblasts from IPF patients [189, 284, 285]. Fibroblast proliferation and migration is elevated in SSc lung fibroblasts and one study has reported the expansion of α-SMA positive cells by increased rates of migration and proliferation in both SSc and IPAH cells may be potentially contributing to the occlusion of the lumen that is observed in patients with SSc-PAH and PAH [22]. To the best of my knowledge this is the first report that SSc-PAH fibroblasts isolated from the lung of SSc patients displayed elevated rates of proliferation and migration. Interestingly JQ1 had no significant effect on migration of normal fibroblasts and this may be due the normal fibroblasts exhibiting an unaltered epigenetic profile which prevents JQ1 from interacting with these normal fibroblasts. The inhibition of both proliferation and migration in SSc fibroblasts by the BRD inhibitor JQ1 is also a novel observation in SSc lung fibroblasts. This suggests that the anti-proliferative and migratory attributes of JQ1 might be able to contribute to slowing down the progression of vascular remodelling in SSc-PAH and PAH patients by epigenetically modifying the phenotype of the activated fibroblast. PASMCs play a key role in the development of PAH, JQ1 exhibited anti-proliferative effects on "disease" like synthetic PASMCs. Here it has been demonstrated that JQ1 can inhibit disease characteristics in two key cell types that contribute to the development of PAH [21].

Activated SSc lung fibroblasts, PASMCs from IPAH patients and "disease" like synthetic PASMCs exhibit an inflammatory phenotype that may contribute to the development of PAH. It has been previously reported that pro-inflammatory cytokines are elevated in SSc, for example IL-6 and IL-1β have been associated with disease involvement and progression [40, 286]. In PAH, previous work has shown that IL-1β, IL-6, IL-8, IL-10 and IL-13 serum levels are elevated in patients with both IPAH and HPAH [218, 230]. In this study Kaplan-Meier curves showed that levels of IL-6, IL-8 and IL-10 predicted survival in patients, 5-year survival rates for patients with IL-6 levels > 9 pg/ml was 30%, however patients with levels < 9 pg/ml fared better with survival at 63% [218]. IL-13 was also elevated in serum of IPAH and HPAH patients but this cytokine did not correlate with survival [218].

Histologically it has been highlighted that inflammation plays a key role in PAH, in SSc-PAH it has been reported that an increase in mononuclear inflammatory cells locate around affected vessels with concentric lesions and vascular remodelling, however unaffected areas of the lung seem to exhibit features of a normal lung [287-290]. In HPAH Tuder *et al* were the first to demonstrate the influx of inflammatory infiltrates in severe PAH [291]. The importance of inflammation in the disease has been highlighted by Savai et *al* and currently therapeutics that target cytokines are being investigated. One example of this is Tocilizumab the anti-IL6 monoclonal antibody that is currently undergoing pre-clinical and clinical studies in SSc and PAH [292-294].

By identifying inflammatory cytokines that are elevated in patient serum it provides inflammatory markers to examine that contribute to the development of PAH, in key cell types, for example the fibroblast and PASMC. Interestingly IL-6, IL-8 and IL-13 are elevated in SLF, IL-1β, IL-6, IL-8 IL-10 and IL-13 are elevated in "disease" like synthetic PASMCs compared to "healthy" contractile PASMCs. Since these inflammatory markers play a key role in PAH and correlate with survival so the effect of JQ1 on anti-inflammatory markers was investigated [218]. JQ1 exhibits attenuation of IL-6 in SSc lung fibroblasts and IPAH PASMCs but has no effect on IL-8 secretion, inhibiting the secretion of IL-6 is important due to its levels in serum correlating to survival in IPAH patients [218]. Interestingly there are also active clinical trials for the treatment of SSc with specific IL-6 antibodies; one example of this is Tocilizumab the anti-IL6 monoclonal antibody [292, 293]. Similar results were observed in fibroblasts in IPF patients with JQ1 inhibited elevated IL-6 levels. JQ1 also reduced IL-1β, IL-10 and IL-13 which are all cytokines that implicated in PAH [218]. The ability of JQ1 to attenuate the pro-inflammatory effects of cytokines that are key to PAH progression and survival suggest JQ1 demonstrates potential to be a novel therapeutic for SSc patients at risk of developing PAH. Our *in-vitro* data suggests that JQ1 can epigenetically modify the activated phenotype of key cells involved in the development of PAH by altering their functional abnormalities and inflammatory attributes.

Following on from positive *in-vitro* data, the role of JQ1 *in-vivo* was investigated and its effect on haemodynamics in the TβRIIΔk-fib model of SSc-PAH was

investigated. Initially I hypothesised that down regulation of BMPRII might be contributing to the development of PAH in this model and in patients in SSc-PAH.

JQ1 prevented the development of PAH in the TβRIIΔk-fib by reducing elevated RVSP's compared to TβRIIΔk-fib with vehicle control. There was no right ventricle hypertrophy observed in the TβRIIΔk-fib and JQ1 had no effect on this. Histologically it has been demonstrated that JQ1 can reduce the number of partial and fully muscularised arterioles in TβRIIΔk-fib mice and decrease mild perivascular inflammatory cell infiltrate and medial thickening. These histologically observations suggest a role for JQ1 and BRD inhibitors in preventing vascular remodelling in the TβRIIΔk-fib model. One possible mechanism for this might be the anti-proliferative and migratory properties JQ1 displayed *in vitro* as JQ1 has demonstrated these properties in other diseases, for example IPF and cancer [180, 189, 299]. These characteristics might be curtailing the expansion of α-SMA positive fibroblasts and PASMCs. The reduction of α-SMA red staining in the IF studies suggests that this might be a mechanism by which JQ1 arrests the development of PAH in the TβRIIΔk model.

In the TβRIIΔk-fib model (Figure 3.1 and 3.4.) BMPRII is reduced in whole lung and explant cultured fibroblasts and in clinical material from SSc-PAH BMPRII is also reduced (Figure 4.4). BMPRII mutations are associated with the development of HPAH and IPAH and this study shows by a non-genetic means BMPRII reduction is associated with PAH [14, 24, 26, 162, 183, 184, 295-298].Previous reports have shown that BMPRII is reduced in the skin and microvascular endothelial cells in SSc patients [175]. This study also showed that the use of epigenetic inhibitors, DNA methyltransferase inhibitor 5-Aza-2'-de-oxycytidine (5-AZA) and the histone deacetylase inhibitor trichostatin (TSA) had modest effects alone but in combination there was a significant rise in BMPRII expression in microvascular endothelial cells [175].

The aim of this work was that JQ1 might modulate BMPRII expression by epigenetically modifications. BMPRII protein expression in the TβRIIΔk-fib model is reduced compared to WT controls, however unexpectedly BMPRII levels were significantly reduced in both WT and TβRIIΔk-fib JQ1 treated groups. Our hypothesis was that JQ1 might increase BMPRII by binding to the acetylated lysine

of the BRD residues. As mentioned above this hypothesis stemmed from a previous study where BMPRII is reduced in the skin of SSc patients and the use epigenetic inhibitors significantly increased BMPRII expression [175]. These results show the opposite *in-vivo* suggesting that JQ1 is exerting it's affect by altering cellular phenotypes that contribute to vascular remodelling and by anti-inflammatory effects. This suggests that BMPRII increases the susceptibility of this model of PAH but is only one contributory factor in a complex disease. It also suggests that alone JQ1 might not be effective due to its specificity to BRD proteins but in combination with other epigenetic inhibitors might demonstrate an ability to upregulate BMPRII.

In concordance with a reduction in BMPRII an over activated TGFβ pathway is also associated with SSc-PAH and PAH. Enhanced TGFβ signalling has been previously observed in IPAH vessels [152, 174, 194]. Indicative of enhanced TGFβ signalling, whole lung tissue and explant cultured fibroblasts from SSc-PAH patients exhibited elevated levels of phosphorylated Smad 2 and 3.

The TβRIIΔk-fib model of SSc-PAH also displays enhanced TGFβ activity with increased levels of phosphorylated levels of Smads 2 and 3 [40, 52, 54]. Another aim of this study was to investigate if JQ1 could reduce enhanced TGFβ and downstream signalling pathways. JQ1 displayed an ability to inhibit TGFβ pathway activity, elevated levels of phosphorylated-Smad 2/3 have been associated with SSc and PAH with increased phosphorylated-Smad 2/3 levels staining in concentric lesions of PAH patients [152]. Here JQ1 demonstrates an ability to reduce phosphorylated-Smad 2/3 expression in whole lung tissue. A number of studies have demonstrated pharmacological antagonists of the TGFβ signalling pathway can inhibit and reverse the development of PAH in preclinical models which exhibit genetically independent reduction in BMPRII levels in tissues [194]. This study supports the notion that enhanced TGFβ signalling contributes to the development of PAH and SSc-PAH. JQ1 also demonstrated an ability to reduce phosphorylated -p38 levels but had no effect on phosphorylated ERK 1/2. It has been previously reported that p38 inhibitor FR167653 significantly attenuates the expression of inflammatory cytokines in the MCT model of PH, ultimately preventing the progression of PH [300]. These results suggest that p38 might play a key role in the molecular events that are involved in the development and progression of PH; this supports the mechanism by which JQ1

is having a protective effect on the development of PAH in the TβRIIΔk model [300].

6.5 Conclusion

This chapter highlights the benefit of a novel epigenetic inhibitor in preventing the development of PAH in a transgenic model of SSc-PAH. The BRD inhibitor JQ1 displays an ability *in-vitro* to decrease markers that contribute to increased ECM production, JQ1 also arrests the disease phenotype of fibroblasts and PASMCs by inhibiting migration, proliferation and excessive production of inflammatory cytokines. *In-vivo* JQ1 prevented the development of PAH in the TβRIIΔk model by reducing RVSP and also prevented muscularisation in some vessels, medial hypertrophy and inflammatory filtrates. Furthermore, JQ1 reduced phosphorylated Smad 2/3 and phosphorylated -p38 levels in the lungs of TβRIIΔk mice and both of these signalling proteins have been implicated in PAH. Previous reports have highlighted by targeting the TGFβ axis and inhibited phosphorylated-p38 prevents the development PAH in pre-clinical models suggesting benefits of JQ1's inhibitory effects on TGFβ [194, 300].

7. Final discussion and future studies

7.1 Final Discussion

In this thesis I have applied an integrated approach using *in-vivo* and *in-vitro* experimental studies to explore key biological pathways that underlie the development of PAH in SSc. A major focus has been the use of the TβRIIΔk-fib transgenic mouse model of SSc. This model provides a powerful tool for exploring the role of enhanced TGFβ activity, clinically implicated in the development of SSc and PAH, in the connective tissue microenvironment and on the relevance to the TGFβ superfamily receptor member, BMPRII and the downstream signalling pathways.

The central findings of the work provide a plausible unifying model for SSc susceptibility to PAH that involves a TGFβ dependent perturbation of BMP signalling due to reduced protein expression of the receptor BMPRII as highlighted in figure 7.1. Extrapolation into human tissue samples provides additional validation of this mouse model. This work also profiled changes in the lung architecture in the TβRIIΔk-fib model and confirmed the utility of explant lung fibroblasts from these mice in exhibiting a disease like phenotype. These observations lead us to examine how these characteristics displayed in the TβRIIΔk-fib model might also be found in SSc patients.

Extending the observation in the mouse model of reduced BMPRII expression and altered downstream signalling in components of the TGFβ/BMP pathways I assessed the relevance in clinically derived material. The TGFβ/BMP pathways in SSc and normal explant cultured fibroblasts were examined and functional differences in these fibroblasts were assessed. BMPRII protein expression was significantly reduced in SSc lung tissues and fibroblasts. In contrast BMPRII mRNA was elevated in SSc patient tissues compared to that of donor control tissues, suggesting that altered translation or enhanced protein degradation might be responsible for reduced BMPRII expression in SSc. To assess this the effects of the proteasomal inhibitor MG132, BMPRII protein expression and downstream signalling responses to the BMP ligands was assessed. MG132 led to a significant increase in BMPRII levels and concomitant increase in downstream signalling by SSc fibroblasts response to BMP4. Collectively these observations are supportive that enhanced proteasomal

degradation of BMPRII contributes to a reduction in BMPRII protein expression in SSc.

Whilst many IPAH and HPAH patients harbour mutations in the BMPRII gene, no such mutations have been reported in SSc-PAH patients [198]. SSc is a complex disease in which a number of cell types including PASMCs and fibroblasts contribute to the development of SSc-PAH vascular remodelling and the deposition of ECM, including PASMCs and fibroblasts. Extending these studies I explored the cellular mechanisms that may contribute to vascular remodelling. Initial I sought to develop and characterise PASMCs either maintained in a contractile 'healthy' state or PASMCs driven to a synthetic and more 'disease-like' phenotype. Synthetic PASMCs exhibited many of the features of SSc fibroblasts including elevated levels of CTGF, type-I collagen and pro-inflammatory cytokines such as IL-6 and IL-8. Assessing the expression of components of the TGFβ superfamily of receptors and downstream signalling pathways, synthetic PASMCs exhibited reduced BMPRII expression. Consistent with the reduction in functional cell surface expression of BMPRII, synthetic PASMCs demonstrated a blunted response to BMP ligands compared to contractile PASMCs.

Previous studies from our and other group have shown a key role for BRD proteins in modulating differentiation of fibroblasts into myofibroblasts and the SSc fibroblast phenotype [180, 189]. Using a novel epigenetic inhibitor of BRD proteins, JQ1 I sought to investigate the contribution of epigenetics in the SSc lung fibroblast and synthetic PASMCs phenotypes. JQ1 inhibited the SSc lung fibroblast and synthetic PASMC phenotype. Extending this further I investigated the effects of JQ1 on the development of PAH in the TβRIIΔk-fib model. In addition JQ1 attenuated the development of PAH in the TβRIIΔk-fib and reduced the formation of concentric lesions in the vessels of TβRIIΔk-fib mice.

7.1.1 Reduction of BMPRII in scleroderma lung

PAH is an important complication of SSc [195]. The risk of SSc patients developing PAH continues throughout the disease suggesting that SSc is the susceptibility factor [38]. SSc-PAH patients have a significantly poorer prognosis compared to those with IPAH or HPAH [196, 197]. Mutations that lead to a loss of expression or function of the BMPRII have been strongly implicated in the pathogenesis of HPAH and IPAH [102]. In contrast, genetic studies in SSc-PAH patients have not detected mutations in the BMPRII gene [198, 301]. Wang *et al* have recently demonstrated that BMPRII expression is reduced in the skin of SSc patients. The reduction of BMPRII has been linked to heightened DNA methylation of the BMPRII promoter [175].

In chapter three I demonstrated that the TβRIIΔk-fib model of SSc which spontaneously develops PAH exhibits a reduction in BMPRII protein expression in whole lung tissue and explant cultured fibroblasts. These observations in this pre-clinical model coincide with reduced BMPRII expression in the rodent hypoxic, rodent SU5415/hypoxic and MCT models suggesting that a reduction in BMPRII expression might increase the susceptibility to developing PAH [141, 146, 193]. These results from the TβRIIΔk-fib model and other pre-clinical models that reduced BMPRII by non-genetic means may contribute to the development of PAH. [119].

The observation that a reduction of BMPRII by a non-genetic means is observed in pre-clinical models of PAH and in the skin of SSc patients led us to examine BMPRII expression in the lung of SSc patients. BMPRII expression was reduced in whole lung tissue and explant cultured fibroblasts from SSc patients, whereas BMPRII mRNA expression was increased suggesting that enhanced protein degradation may be responsible for reduced BMPRII expression in SSc (Chapter four). One weakness of this study was that BMPRII is more highly expressed in PAECS and PASMCs compared to fibroblasts so it would be interesting to investigate BMPRII expression in both of these cell types. Interestingly our observations are in contrast to those of Wang et al who demonstrated reduction in both mRNA and protein levels of BMPRII in microvascular endothelial cells from SSc patients [175]. These results suggest that possibly different mechanisms by which BMPRII levels may be reduced in these cells or organ.

A number of studies have highlighted non-genetic mechanisms that lead to reduced BMPRII protein levels, including ubiquitination and proteasomal degradation mediated by Smurf1, K5 and E3 ligase and Itch [17, 190]. Collectively non-genetic mechanisms may also contribute to a reduction in BMPRII expression and therefore a predisposition to the development of PAH. The use of a proteasomal degradation inhibitor MG132 led to an increase BMPRII protein levels in control and SSc lung fibroblasts. Consistent with MG132 treatment restoring functional BMPR2 to the cell surface, BMP ligands induced activation of downstream signalling pathways in SSc lung. The rise in BMPRII levels in both control and SSc lung fibroblasts in response to MG132 suggests proteasomal degradation is a normal mechanism of turn-over of BMPRII receptors. Interestingly Smurf1 has recently been demonstrated to be elevated in SSc lung tissues (Holmes *et al*; personal communication). Suggesting this mechanism may be enhanced in SSc patients. Collectively this suggests that proteasomal degradation inhibitors might provide a novel therapeutic approach to prevent the reduction in BMPRII levels in SSc patients and the development of non-genetic forms of PAH (chapter 4).

PASMCs are another key cell type involved in vascular remodelling and the development of PAH and have been extensively investigated IPAH and HPAH, but not as frequently in SSc where access to PASMCs from patients has been limited. As highlighted in chapter five, I sought to use the differentiation of control PASMCs from contractile to synthetic forms to investigate this process and its relevance to SSc. The differentiation of PASMCs into a disease like synthetic phenotype led to a reduction in BMPRII and blunted responses to BMP ligands. BMPRII protein expression has previously been reported to be reduced in PASMCs from IPAH patients with defined BMPRII mutations and these cells exhibited dampened response to BMP ligands [24, 177]. The reduction of BMPRII levels in our synthetic 'disease' phenotype at the protein and transcript level suggests these cells exhibit a similar phenotype to those isolated from IPAH patients. Synthetic PASMCs also demonstrated a rise in the gene expression of the BMP antagonist gremlin 1. It has been previously reported that gremlin 1 has higher expression in the lung than any other organ. Furthermore, Gremlin 1 is also elevated in the lung of PAH patients and novel gremlin 1 antibodies can reverse PAH in the pre-clinical sugen/hypoxia model of PAH [155, 228]. Elevated gremlin 1 may represent a novel mechanism by which

responses to BMP ligands may be blunted in diseases such as SSc-PAH. Future work to assess the levels in SSc patient lung tissues and serum would be interesting to define the contribution to the development of SSc-PAH.

The development of vascular remodelling in the context of PAH involves a number of cell types. Consistent with this these results suggest that more than one cell type contributes to the development of PAH and the use of co-culture systems will be essential in gaining a better understanding of disease pathology, but also that a reduction of BMPRII is a shared mechanism between explant cultured lung fibroblasts and PASMCs. Interestingly both SSc lung fibroblasts and synthetic PASMCS display a blunted response to BMP similarly to PASMCs from IPAH patients [24, 177]. These results suggest that a reduction in BMPRII may predispose patients to the development of PAH and that more than one cell type can contribute to this.

7.1.2 Enhanced TGFβ activity in SSc lung

It has been previously reported that heightened TGFβ activity is observed in the skin of SSc patients, highlighted by a rise in phosphorylated Smad 2/3 protein expression and PAI-1 gene expression [174]. The TβRIIΔk-fib model has also displayed increased activity in explant skin and lung fibroblasts and now whole lung tissue with a rise in phosphorylated Smad 2/3 expression [40, 52, 54, 302]. As mentioned earlier these mice also develop PAH so this enhanced TGFβ activity might contribute to the development of PAH and SSc. Enhanced TGFβ signalling has previously been reported in IPAH vessels highlighted by an increase in phosphorylated Smad 2/3 staining [152, 174, 194]. Indicative of enhanced TGFβ signalling, our work also demonstrated elevated phosphorylated Smad 2/3 levels in whole lung tissue and explant cultured lung fibroblasts from SSc patients. A number of groups have also highlighted that preclinical models of PAH exhibit enhanced TGFβ activity including the MCT rat, hypoxia and hypoxia SU5416, and this observation is in concordance with a reduction in BMPRII levels [141, 146, 176]. This suggests that both a reduction in BMPRII and enhanced TGFβ activity are linked to a mechanism that is contributing to the development of PAH.

Further studies to elucidate the factors that drive the imbalance in TGFβ/BMP activity and how these pathways influence each other could be important in understanding the development of PAH. It seems that in the TβRIIΔk-fib model where TGFβ activity is elevated that may be a factor that causes a reduction in BMPRII. In the bleomycin lung model BMPRII is also reduced in both the inflammatory and active fibrosis phase suggesting that BMPRII reduction precedes the development of fibrosis in this model [133]. It raises another question that in early stages of SSc that a reduction in BMPRII might increase the risk of patients developing PAH. These observations suggest that a reduction in BMPRII and an enhanced TGFβ axis are observed in both SSc-PAH, HPAH and IPAH and may a unifying mechanism in the development of PAH as highlighted in figure 7.1

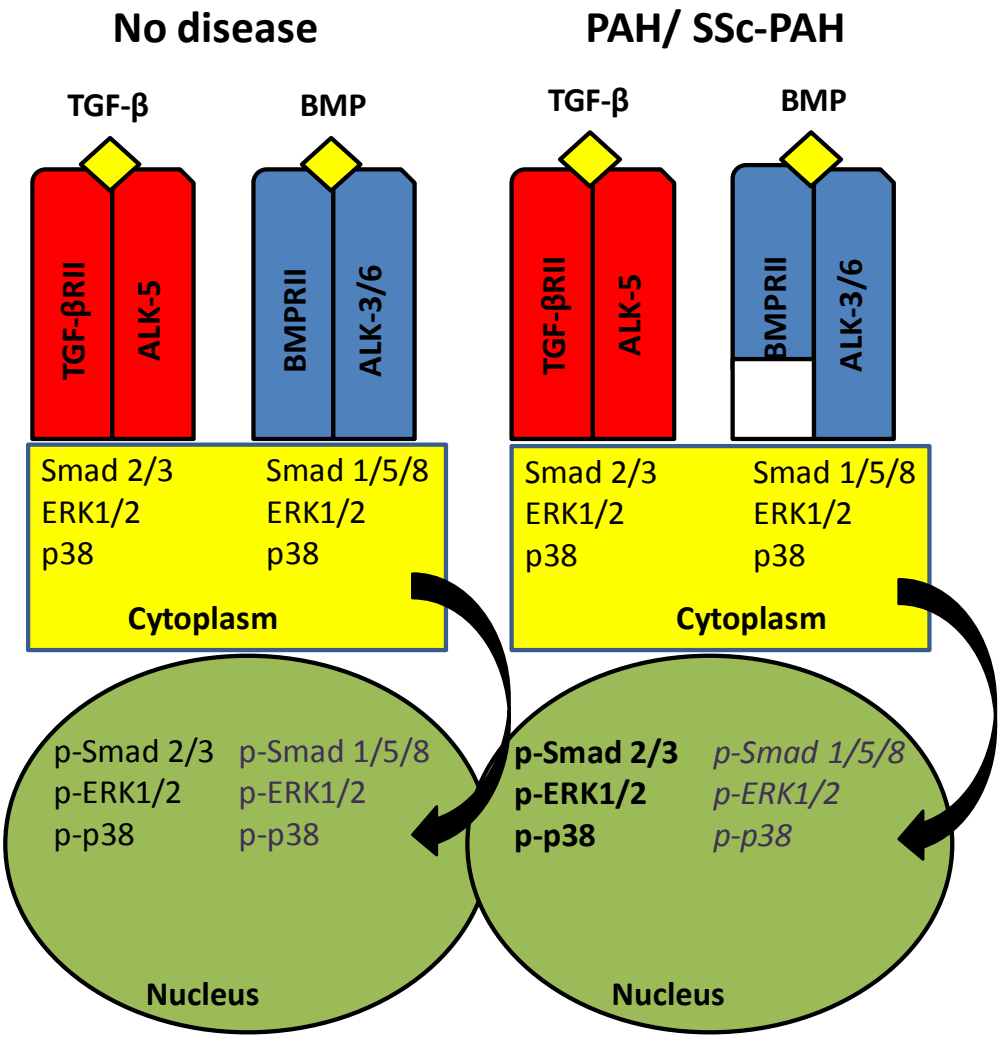

Figure 7.1 - TGFβ and BMP signalling in PAH and SSc-PAH patients compared to humans with no disease.

TGF-β and BMP ligand-receptor complex activates the canonical Smad signalling pathway inducing phosphorylation and translocation from the cytoplasm to the nucleus (Smad 2/3 and Smad 1/5/8). Non-Smad (non-canonical) signalling mechanisms are also activated (ERK 1/2, p38). (A) In healthy humans, The TGF-β/BMP receptor complex directly activates canonical and non-canonical pathways leading to phosphorylation and translocation from the cytoplasm to the nucleus. (B) In patients with PAH or SSc PAH due to a loss of BMPRII expression due to mutations or a reduction of protein on the cell surface there is a reduction of BMP activated canonical (pSmad 1) and non-canonical signalling pathways (p-ERK 1/2 and p-p38) (grey italics), and an increase in canonical TGFβ signalling (pSmad 2/3) and non-cannonical TGFβ signalling (p-ERK 1/2 and p-p38) (bold). It is believed that this imbalance increases the susceptibility to patients with SSc developing PAH.

7.1.3 The role of epigenetics in scleroderma

As discussed in chapter six the definition or meaning of epigenetics is interpreted differently by researchers [247] [248]. The major focus of chapter six was the role of JQ1 in SSc-PAH. JQ1 is a BRD inhibitor, BRD is a conserved member of the BET family of chromatin readers, BRD consists of four members BRD2, BRD3 and BRD testis (BRDT). When JQ1 binds to the BRD pocket it leads to the displacement of BRD4 from active chromatin and the subsequent removal of RNA polymerase II from target genes [262, 263]. Other groups have highlighted that BMPRII is reduced in the skin and microvascular endothelial cells in SSc patients [175]. This study also showed that the use of epigenetic inhibitors similar to JQ1, DNA methyltransferase inhibitor 5-Aza-2'-de-oxycytidine (5-AZA) and the histone deacetylase inhibitor trichostatin (TSA) that these inhibitors had humble effects individually but in combination there was a significant rise in BMPRII expression in microvascular endothelial cells [175].

The aim of this study was to investigate the role of JQ1 in PAH and delineate what pathways and cellular responses JQ1 affected. *In-vitro* JQ1 was able to reduce the secretion of ECM and pro-inflammatory cytokines from both SSc lung fibroblasts and PASMCs from IPAH patients.

In-vivo using the TβRIIΔk-fib model JQ1 was able to prevent the development of PAH in the TβRIIΔk-fib by reducing elevated RVSP's compared to TβRIIΔk-fib with vehicle control. In chapter three it was demonstrated that BMPRII protein expression is reduced in the TβRIIΔk-fib model, however unexpectedly BMPRII levels were significantly reduced in both WT and TβRIIΔk-fib JQ1 treated groups. The initial working hypothesis was that JQ1 might increase BMPRII expression by binding to the acetylated lysine residues of BRD 4. This was plausible because in a study where BMPRII is reduced in the skin of SSc patients epigenetic inhibitors increased BMPRII expression however in this study two epigenetic inhibits were required to significantly increase BMPRII expression [175]. The results in chapter six demonstrate the contrary *in-vivo* suggesting that JQ1 is exerting it's affect by altering cellular phenotypes that contribute to vascular remodelling and by anti-inflammatory effects.

JQ1 did display positive effects on the TGFβ pathway, elevated levels of phosphorylated Smad 2/3 and phosphorylated-p38 have been associated with SSc and PAH with increased phosphorylated Smad 2/3 levels staining in concentric lesions of PAH patients [152]. Here JQ1 demonstrates an ability to reduce elevated levels of phosphorylated Smad 2/3 expression in whole lung tissue and reduce and phosphorylated-p38 expresssion. A number of studies have demonstrated pharmacological antagonists of the TGFβ signalling pathway can inhibit and reverse the development of PAH suggesting that JQ1 might be exerting it's affecting indirectly through the TGFβ pathway [194].

7.2 Future studies

As well as providing fundamental insight into the mechanism by which the TβRIIΔk-fib model and SSc patients develop PAH, this thesis also provides a platform for future experimental studies. Although this work is consistent with other reports that enhanced TGFβ activity occurs in concordance with a reduction in BMPRII in the development of pulmonary diseases, but the mechanism by which these pathways interact require further elucidation. A number of experiments could be envisaged to assess this. For example, knockdown studies of BMPRII using shRNA or siRNA approaches on control lung fibroblasts or contractile PASMC, or complimentary overexpression BMPRII studies on SSc lung fibroblasts or synthetic PASMCs could be performed to assess effects on phenotypic changes in proliferation, migration and apoptosis. A previous study using pulmonary artery endothelial cells has reported that a loss of BMPRII lead to a rise in secretion in pro-inflammatory cytokines, increased endothelial cell permeability and transmigration of mononuclear cells and neutrophils [303]. Other studies demonstrate a reduction in BMPRII levels expression in PASMCs is associated with increased IL-6 secretion suggesting BMPRII plays a key role in regulating the inflammatory environment. It has also been highlighted that BMPRII heterozygous null mice don't display an overt PH phenotype unless an additional trigger is implemented [304-306]. This study again suggests that BMPRII reduction in the lung is a susceptibility factor but in order for PAH to develop, additional complications in combination with reduced BMPRII are required. These results and the work by Burton *et al* suggest that BMPRII may act to dampen inflammatory signals in the pulmonary vasculature and a reduction of BMPRII may predispose patients to an inflammation microenvironment and vascular damage. It would be interesting to repeat functional studies in PASMCs to gain a better understanding of the role of BMPRII in these cells.

7.2.1 Proteasomal inhibition as a novel potential therapy in SSc

MG132 demonstrated an ability to upregulate BMPRII expression in both normal and SSc lung fibroblasts and restoring SSc lung fibroblasts responses to BMP4, leading to restoration of normal phosphorylated Smad1 induction. This suggests that MG132 has potential as a novel therapeutic for non-genetic forms for PAH; however these are only preliminary studies.

As discussed in chapter four, bortezomib is a proteasomal degradation inhibitor which is currently approved for the treatment of patients with multiple myeloma. Future experiments to initially assess the effects of bortezomib on BMPRII and restoration BMP response and compare these MG132 effects would seek to confirm the suitability of this licenced therapy for SSc. Since BMPRII is expressed more highly in PASMCs and PAECs it would also be interesting to perform experiments in these cell types.

The effect of MG132 and bortezomib on pro-inflammatory cytokines, for example IL-6 and IL-8 that are implicated in the development of SSc and PAH could also be assessed. Another important experiment would be to investigate if bortezomib and MG132 can prevent the deposition of ECM, for example type-1 collagen expression and CTGF. As discussed earlier the interaction and phenomenon observed in SSc of enhanced TGFβ and reduced BMPRII expression needs to be elucidated further. The question would be if MG132 can inhibit the heightened TGFβ activity in SSc and how does it exert its effect.

In-vivo proteasomal inhibitors have demonstrated some positive but controversial results in models of lung, heart and kidney fibrosis so the exact role of these inhibitors is still unknown [132, 209-211].*In-vivo* it would be important to examine the role of MG132 and bortezomib in both the TβRIIΔk-fib model and the SU5416/hypoxia mouse model. Experimental readouts would initially be haemodynamic readouts, for example RVSP, MAP and Fulton index. Histologically it would be important to investigate if MG132 and bortezomib can reduce the number of muscularised vessels and the influx of inflammatory infiltrate in these models. It would also be interesting to collect serum and perform multiplex analysis to examine anti-inflammatory. *In-vivo* it would be important to investigate if MG132 and bortezomib can upregualte BMPRII and inhibit TGFβ signalling in the TβRIIΔk-

fib model of SSc-PAH and the SU5416/hypoxia mouse model of PAH as previously reported *in-vitro*.

7.2.2 Interaction between TGFβ/BMP signalling pathways

TGFβ and BMP signalling pathways demonstrate antagonistic activities during the development of many tissues. Although the crosstalk between BMP and TGFβ signalling pathways is well defined in bone development, it is poorly understood in the lung and in diseases like PAH and SSc [307]. The interaction between both TGFβ and BMP pathways can contribute to degradation of receptors and activity alterations in both pathways. The activity of type I and II TGFβ receptors can be altered by different methods, depshosphorylation of activated receptors, interfering with Smad signalling and proteasomal degradation. An example of this is how the inhibitory Smads (I-Smad) affect receptor Smads (R-Smad) activity but also by recruiting E3 ubiqutin ligases, for example Smurf 1 and 2 to the receptor complex. This leads to both ALK5 and TGFβR-II being ubiquitylated and degraded. Smad 7 has also been shown to direct Smurf1 to ALK6 with forms a heterodimer with BMPRII leading to ubiquitylation and degradation [308]. All of these mechanisms suggest that this interaction is important in disease development and potentially in PAH and SSc, Smad 7 is more common to target ALK6 and BMP signalling leading to a reduction in BMP signalling and an enhancement in TGFβ activity [308].

LMP-1 is a LIM domain protein that has also been highlighted to interact with Smurf 1, which in turn can prevent Smurf 1, mediated ubiquitylation of Smad 1/5, this interaction leads to enhanced BMP signalling. Interestingly both Smurf 1 and I-Smad 7 expression is elevated in the MCT and hypoxia model of PAH whereas BMPRII expression is downregulated suggesting that induction of Smurf 1 can downregulate BMPRII and suppress BMP signalling and may play a key role in the development of PAH [190]. Smurf 1 is also elevated in the lung of SSc patients suggesting that this mechanism might be contributing to the development of PAH (Holmes *et al*, unpublished).

However LIM kinase 1 (LIMK1) is a kinase that regulates actin by phosphorylating cofilin, which is an actin depolymerising factor. An elegant study has isolated a LIMK-1 interacting protein that encompasses the tail region of BMPRII. The tail region is not involved in BMP signalling but mutations in HPAH are found in this region. Further studies suggested that BMPRII is able to prevent LIMK1 from phosphorylating cofilin, however in HPAH this mechanism is prevented due to BMPRII mutations in the tail region leading to deregulation of actin dynamics. The complexity and balance of these pathways are essential for understanding the development of PAH and how BMPRII is down regulated in SSc [309].

7.2.3 The role of bromodomains and epigenetic modulation in SSc

The work on epigenetics in this thesis (Chapter six), investigated the effect of a bromdomain inhibitor JQ1 on the development of PAH in the TβRIIΔk-fib model and its effect on SSc lung fibroblasts and synthetic and IPAH PASMCs phenotypes.

Previous studies have demonstrated JQ1 can modulate the dermal SSc fibroblasts phenotype. Consistent with this we demonstrate JQ1 can modulate both the SSc lung fibroblasts and synthetic and IPAH PASMCs phenotypes, as determined by matrix deposition and inflammatory chemokine release. As discussed earlier JQ1 inhibits the BET family of chromatin readers, BRD which consists of four members BRD2, BRD3 and BRD testis (BRDT). When JQ1 binds to the BRD pocket it leads to the displacement of BRD4 from active chromatin and the subsequent removal of RNA polymerase II from target genes [262, 263]. Whilst we have demonstrated the efficacy of JQ1 *in-vitro* and *in-vivo* it remains unclear which of the family members contribute to the pathological phenotype of SSc lung fibroblasts and synthetic and IPAH PASMCs. To explore this further, future experiments to assess the effects on collagen type I expression and IL-6 of siRNA knockdown of members of the BRD family (BRD2, BRD3 and BRD4) could be performed. Although BRDT is restricted normally in its expression to the testis and ovaries, it remains unclear the spatial and temporal expression of other members of this family in SSc and SSc-PAH. Immunohistochemical studies to assess in SSc patient's lung the differential expression of these family members and in other SSc disease sub types may offer

insight into the mechanisms which Brd proteins contribute to the pathological differentiation of fibroblasts and PASMCs in SSc and specifically the development in PAH. It would also be interesting to examine BRD expression in the TβRIIΔk-fib model and SU5146/hypoxia model to investigate if BRD expression is elevated in these models compared to controls and attenuated in JQ1 treated groups.

It remains unclear the impact of chronic administration of epigenetic inhibitors for diseases such as SSc, and may have significant side effects for example effecting normal wound healing. Understanding the key members of the family that contribute to the development of SSc-PAH, will allow for the development of specific inhibitors of BRD family members. The development of specific inhibitors are likely to reduced side effects that would be expected with broad spectrum inhibitors.

7.3 Concluding remarks

PAH is a devastating complication of SSc and the outcome is significantly worse in SSc-PAH compared to both IPAH and HPAH. However despite this difference, work described in this thesis suggests that key biological processes may be similar between these forms of PAH. Observations from the lungs of TβRIIΔk-fib and SSc-PAH patients' show that a reduction is BMPRII is linked to SSc and the complex phenotype observed in SSc patient's phenocopies other types of PAH.

These observations in a pre-clinical model and clinically derived material provide further insight to SSc with bi-directional translation. The observation of a reduction in BMPRII in SSc lung validates the TβRIIΔk-fib model of SSc, whilst the model also allows us to gain greater insight into the disease. The increased TGFβ microenvironment in the TβRIIΔk-fib model due to genetic alterations leads to a potential link between enhanced TGFβ and a reduction in BMPRII. This mechanism is validated in the both the lungs of SSc-PAH and IPAH patients. However the mechanism of cross talk where by enhanced activity of the TGFβ pathway impacts the BMPRII regulated signalling pathways needs further exploration. In the end SSc providers a susceptibility phenotype for PAH and this may explain why the understanding of mechanism has been so challenging. This thesis shows that to understand complex pathologies pre-clinical models provide a platform to understand disease pathology and to understand the human disease it is important to explore different cell types and whole lung tissue.

8. Bibliography

1. Hoeper MM, Bogaard HJ, Condliffe R, Frantz R, Khanna D, Kurzyna M, Langleben D, Manes A, Satoh T, Torres F *et al*: **Definitions and Diagnosis of Pulmonary Hypertension**. *Journal of the American College of Cardiology* 2013, **62**(25, Supplement):D42-D50.

2. Simonneau G, Robbins IM, Beghetti M, Channick RN, Delcroix M, Denton CP, Elliott CG, Gaine SP, Gladwin MT, Jing ZC *et al*: **Updated clinical classification of pulmonary hypertension**. *Journal of the American College of Cardiology* 2009, **54**(1 Suppl):S43-54.

3. Hatano S, Strasser T, World Health Organization.: **Primary pulmonary hypertension : report on a WHO meeting, Geneva, 15-17 October 1973**. Geneva: World Health Organization; 1975.

4. Fishman AP: **Clinical classification of pulmonary hypertension**. *Clinics in chest medicine* 2001, **22**(3):385-391, vii.

5. Badesch DB, Champion HC, Sanchez MA, Hoeper MM, Loyd JE, Manes A, McGoon M, Naeije R, Olschewski H, Oudiz RJ *et al*: **Diagnosis and assessment of pulmonary arterial hypertension**. *Journal of the American College of Cardiology* 2009, **54**(1 Suppl):S55-66.

6. Simonneau G, Gatzoulis MA, Adatia I, Celermajer D, Denton C, Ghofrani A, Gomez Sanchez MA, Krishna Kumar R, Landzberg M, Machado RF *et al*: **Updated clinical classification of pulmonary hypertension**. *Journal of the American College of Cardiology* 2013, **62**(25 Suppl):D34-41.

7. Li W, Dunmore BJ, Morrell NW: **Bone morphogenetic protein type II receptor mutations causing protein misfolding in heritable pulmonary arterial hypertension**. *Proceedings of the American Thoracic Society* 2010, **7**(6):395-398.

8. Oudiz RJ: **Pulmonary hypertension associated with left-sided heart disease**. *Clinics in chest medicine* 2007, **28**(1):233-241, x.

9. Barnett CF, De Marco T: **Pulmonary hypertension associated with left-sided heart disease**. *Heart failure clinics* 2012, **8**(3):447-459.

10. Fernandes CJ, Jardim CV, Hovnanian A, Hoette S, Morinaga LK, Souza R: **Schistosomiasis and pulmonary hypertension**. *Expert review of respiratory medicine* 2011, **5**(5):675-681.

11. Lapa M, Dias B, Jardim C, Fernandes CJ, Dourado PM, Figueiredo M, Farias A, Tsutsui J, Terra-Filho M, Humbert M *et al*: **Cardiopulmonary manifestations of hepatosplenic schistosomiasis**. *Circulation* 2009, **119**(11):1518-1523.

12. Hoeper MM, Bogaard HJ, Condliffe R, Frantz R, Khanna D, Kurzyna M, Langleben D, Manes A, Satoh T, Torres F *et al*: **Definitions and diagnosis of pulmonary hypertension**. *Journal of the American College of Cardiology* 2013, **62**(25 Suppl):D42-50.

13. Brown LM, Chen H, Halpern S, Taichman D, McGoon MD, Farber HW, Frost AE, Liou TG, Turner M, Feldkircher K *et al*: **Delay in recognition of pulmonary arterial hypertension: factors identified from the REVEAL Registry**. *Chest* 2011, **140**(1):19-26.

14. Germain M, Eyries M, Montani D, Poirier O, Girerd B, Dorfmuller P, Coulet F, Nadaud S, Maugenre S, Guignabert C *et al*: **Genome-wide association analysis identifies a susceptibility locus for pulmonary arterial hypertension**. *Nature genetics* 2013, **45**(5):518-521.

15. Coghlan JG, Denton CP, Grünig E, Bonderman D, Distler O, Khanna D, Müller-Ladner U, Pope JE, Vonk MC, Doelberg M *et al*: **Evidence-based detection of pulmonary arterial hypertension in systemic sclerosis: the DETECT study**. *Annals of the rheumatic diseases* 2013.

16. Schermuly RT, Ghofrani HA, Wilkins MR, Grimminger F: **Mechanisms of disease: pulmonary arterial hypertension**. *Nature reviewsCardiology* 2011, **8**(8):443-455.

17. Davies RJ, Holmes AM, Deighton J, Long L, Yang X, Barker L, Walker C, Budd DC, Upton PD, Morrell NW: **BMP type II receptor deficiency confers resistance to growth inhibition by TGF-beta in pulmonary artery smooth muscle cells: role of proinflammatory cytokines**. *American journal of physiology Lung cellular and molecular physiology* 2012, **302**(6):L604-615.

18. Gilbane AJ, Denton CP, Holmes AM: **Scleroderma pathogenesis: a pivotal role for fibroblasts as effector cells**. *Arthritis research & therapy* 2013, **15**(3):215.

19. Chan MC, Hilyard AC, Wu C, Davis BN, Hill NS, Lal A, Lieberman J, Lagna G, Hata A: **Molecular basis for antagonism between PDGF and the TGFbeta family of signalling pathways by control of miR-24 expression**. *The EMBO journal* 2010, **29**(3):559-573.

20. Lagna G, Ku MM, Nguyen PH, Neuman NA, Davis BN, Hata A: **Control of phenotypic plasticity of smooth muscle cells by bone morphogenetic protein signaling through the myocardin-related transcription factors**. *The Journal of biological chemistry* 2007, **282**(51):37244-37255.

21. Owens GK, Kumar MS, Wamhoff BR: **Molecular regulation of vascular smooth muscle cell differentiation in development and disease**. *Physiological reviews* 2004, **84**(3):767-801.

22. Wang D, Zhang H, Li M, Frid MG, Flockton AR, McKeon BA, Yeager ME, Fini MA, Morrell NW, Pullamsetti SS *et al*: **MicroRNA-124 controls the proliferative, migratory, and inflammatory phenotype of pulmonary vascular fibroblasts**. *Circulation research* 2014, **114**(1):67-78.

23. Davies RJ, Morrell NW: **Molecular mechanisms of pulmonary arterial hypertension: role of mutations in the bone morphogenetic protein type II receptor**. *Chest* 2008, **134**(6):1271-1277.

24. Yang X, Long L, Southwood M, Rudarakanchana N, Upton PD, Jeffery TK, Atkinson C, Chen H, Trembath RC, Morrell NW: **Dysfunctional Smad signaling contributes to abnormal smooth muscle cell proliferation in familial pulmonary arterial hypertension**. *Circulation research* 2005, **96**(10):1053-1063.

25. Valdimarsdottir G, Goumans MJ, Rosendahl A, Brugman M, Itoh S, Lebrin F, Sideras P, ten Dijke P: **Stimulation of Id1 expression by bone morphogenetic protein is sufficient and necessary for bone morphogenetic protein-induced activation of endothelial cells**. *Circulation* 2002, **106**(17):2263-2270.

26. Teichert-Kuliszewska K, Kutryk MJ, Kuliszewski MA, Karoubi G, Courtman DW, Zucco L, Granton J, Stewart DJ: **Bone morphogenetic protein receptor-2 signaling promotes pulmonary arterial endothelial cell survival: implications for loss-of-function mutations in the pathogenesis of pulmonary hypertension**. *Circulation research* 2006, **98**(2):209-217.

27. Austin ED, Loyd JE: **The genetics of pulmonary arterial hypertension**. *Circulation research* 2014, **115**(1):189-202.

28. Best DH, Austin ED, Chung WK, Elliott CG: **Genetics of pulmonary hypertension**. *Current opinion in cardiology* 2014, **29**(6):520-527.

29. Ma L, Roman-Campos D, Austin ED, Eyries M, Sampson KS, Soubrier F, Germain M, Tregouet DA, Borczuk A, Rosenzweig EB *et al*: **A novel channelopathy in pulmonary arterial hypertension**. *The New England journal of medicine* 2013, **369**(4):351-361.

30. Zhao YY, Malik AB: **A novel insight into the mechanism of pulmonary hypertension involving caveolin-1 deficiency and endothelial nitric oxide synthase activation**. *Trends in cardiovascular medicine* 2009, **19**(7):238-242.

31. LeRoy EC, Medsger TA, Jr.: **Criteria for the classification of early systemic sclerosis**. *The Journal of rheumatology* 2001, **28**(7):1573-1576.

32. Gabrielli A, Avvedimento EV, Krieg T: **Scleroderma**. In: *New England Journal of Medicine.* vol. 360: Massachusetts Medical Society; 2009: 1989-2003.

33. Pakozdi A, Nihtyanova S, Moinzadeh P, Ong VH, Black CM, Denton CP: **Clinical and serological hallmarks of systemic sclerosis overlap syndromes**. *The Journal of rheumatology* 2011, **38**(11):2406-2409.

34. Reveille JD, Solomon DH, American College of Rheumatology Ad Hoc Committee of Immunologic Testing G: **Evidence-based guidelines for the use of immunologic tests: anticentromere, Scl-70, and nucleolar antibodies**. *Arthritis and rheumatism* 2003, **49**(3):399-412.

35. Hudson M, Fritzler MJ, Baron M, Canadian Scleroderma Research G: **Systemic sclerosis: establishing diagnostic criteria**. *Medicine* 2010, **89**(3):159-165.

36. Denton CP, Hachulla E: **Risk factors associated with pulmonary arterial hypertension in patients with systemic sclerosis and implications for screening**. *European respiratory review : an official journal of the European Respiratory Society* 2011, **20**(122):270-276.

37. Ioannidis JPA, Vlachoyiannopoulos PG, Haidich AB, Medsger Jr TA, Lucas M, Michet CJ, Kuwana M, Yasuoka H, van den Hoogen F, te Boome L *et al*: **Mortality in systemic sclerosis: An international meta-analysis of individual patient data**. *The American Journal of Medicine* 2005, **118**(1):2-10.

38. Nihtyanova SI, Schreiber BE, Ong VH, Rosenberg D, Moinzadeh P, Coghlan JG, Wells AU, Denton CP: **Prediction of pulmonary complications and long-term survival in systemic sclerosis**. *Arthritis & rheumatology* 2014, **66**(6):1625-1635.

39. Patrick MR, Kirkham BW, Graham M, Harrision LC: **Circulating interleukin 1 beta and soluble interleukin 2 receptor: evaluation as markers of disease activity in scleroderma**. *The Journal of rheumatology* 1995, **22**(4):654-658.

40. De Lauretis A, Sestini P, Pantelidis P, Hoyles R, Hansell DM, Goh NS, Zappala CJ, Visca D, Maher TM, Denton CP *et al*: **Serum interleukin 6 is predictive of early functional decline and mortality in interstitial lung disease associated with systemic sclerosis**. *The Journal of rheumatology* 2013, **40**(4):435-446.

41. Khan K, Xu S, Nihtyanova S, Derrett-Smith E, Abraham D, Denton CP, Ong VH: **Clinical and pathological significance of interleukin 6 overexpression in systemic sclerosis**. *Annals of the rheumatic diseases* 2012, **71**(7):1235-1242.

42. Holmes AM, Ponticos M, Shi-Wen X, Denton CP, Abraham DJ: **Elevated CCN2 expression in scleroderma: a putative role for the TGFbeta accessory**

receptors TGFbetaRIII and endoglin. *Journal of cell communication and signaling* 2011, **5**(3):173-177.

43. Southcott AM, Jones KP, Li D, Majumdar S, Cambrey AD, Pantelidis P, Black CM, Laurent GJ, Davies BH, Jeffery PK *et al*: **Interleukin-8. Differential expression in lone fibrosing alveolitis and systemic sclerosis**. *American journal of respiratory and critical care medicine* 1995, **151**(5):1604-1612.

44. Moinzadeh P, Denton CP, Abraham D, Ong V, Hunzelmann N, Eckes B, Krieg T: **Biomarkers for skin involvement and fibrotic activity in scleroderma**. *Journal of the European Academy of Dermatology and Venereology : JEADV* 2012, **26**(3):267-276.

45. Abraham DJ, Varga J: **Scleroderma: from cell and molecular mechanisms to disease models**. In: *Trends in Immunology- Autoimmunity special issue.* vol. 26; 2005: 587-595.

46. LeRoy EC: **Systemic sclerosis. A vascular perspective**. *Rheumatic diseases clinics of North America* 1996, **22**(4):675-694.

47. Fleming JN, Schwartz SM: **The pathology of scleroderma vascular disease**. *Rheumatic diseases clinics of North America* 2008, **34**(1):41-55; vi.

48. Sgonc R, Gruschwitz MS, Boeck G, Sepp N, Gruber J, Wick G: **Endothelial cell apoptosis in systemic sclerosis is induced by antibody-dependent cell-mediated cytotoxicity via CD95**. *Arthritis and rheumatism* 2000, **43**(11):2550-2562.

49. Coward WR, Saini G, Jenkins G: **The pathogenesis of idiopathic pulmonary fibrosis**. *Therapeutic advances in respiratory disease* 2010, **4**(6):367-388.

50. Gribbin J, Hubbard RB, Le Jeune I, Smith CJ, West J, Tata LJ: **Incidence and mortality of idiopathic pulmonary fibrosis and sarcoidosis in the UK**. *Thorax* 2006, **61**(11):980-985.

51. Leask A, Abraham DJ: **TGFβ signaling and the fibrotic response**. *The FASEB Journal* 2004, **18**(7):816-827.

52. Denton CP, Zheng B, Evans LA, Shi-wen X, Ong VH, Fisher I, Lazaridis K, Abraham DJ, Black CM, de Crombrugghe B: **Fibroblast-specific expression of a kinase-deficient type II transforming growth factor beta (TGFbeta) receptor leads to paradoxical activation of TGFbeta signaling pathways with fibrosis in transgenic mice**. *The Journal of biological chemistry* 2003, **278**(27):25109-25119.

53. Delgado JA, Al-Azzam O, Denton AM, Markell SG, Goswami RS: **A resource for the in silico identification of fungal polyketide synthases from predicted fungal proteomes**. *Molecular plant pathology* 2012, **13**(5):494-507.

54. Denton CP, Lindahl GE, Khan K, Shiwen X, Ong VH, Gaspar NJ, Lazaridis K, Edwards DR, Leask A, Eastwood M *et al*: **Activation of key profibrotic mechanisms in transgenic fibroblasts expressing kinase-deficient type II Transforming growth factor-{beta} receptor (T{beta}RII{delta}k)**. *The Journal of biological chemistry* 2005, **280**(16):16053-16065.

55. Hoyles RK, Khan K, Shiwen X, Howat SL, Lindahl GE, Leoni P, du Bois RM, Wells AU, Black CM, Abraham DJ *et al*: **Fibroblast-specific perturbation of transforming growth factor beta signaling provides insight into potential pathogenic mechanisms of scleroderma-associated lung fibrosis: exaggerated response to alveolar epithelial injury in a novel mouse model**. *Arthritis and rheumatism* 2008, **58**(4):1175-1188.

56. Derrett-Smith EC, Dooley A, Khan K, Shi-wen X, Abraham D, Denton CP: **Systemic vasculopathy with altered vasoreactivity in a transgenic mouse model of scleroderma**. *Arthritis research & therapy* 2010, **12**(2):R69.

57. Thoua NM, Derrett-Smith EC, Khan K, Dooley A, Shi-Wen X, Denton CP: **Gut fibrosis with altered colonic contractility in a mouse model of scleroderma**. *Rheumatology* 2012, **51**(11):1989-1998.

58. Peacock AJ, National Pulmonary Hypertension Services of UK, Ireland: **Treatment of pulmonary hypertension**. *Bmj* 2003, **326**(7394):835-836.

59. Anzai A, Anzai T, Nagai S, Maekawa Y, Naito K, Kaneko H, Sugano Y, Takahashi T, Abe H, Mochizuki S *et al*: **Regulatory role of dendritic cells in postinfarction healing and left ventricular remodeling**. *Circulation* 2012, **125**(10):1234-1245.

60. McGoon M, Gutterman D, Steen V, Barst R, McCrory DC, Fortin TA, Loyd JE, American College of Chest P: **Screening, early detection, and diagnosis of pulmonary arterial hypertension: ACCP evidence-based clinical practice guidelines**. *Chest* 2004, **126**(1 Suppl):14S-34S.

61. Becker MO, Kill A, Kutsche M, Guenther J, Rose A, Tabeling C, Witzenrath M, Kuhl AA, Heidecke H, Ghofrani HA *et al*: **Vascular Receptor Autoantibodies in Pulmonary Arterial Hypertension Associated with Systemic Sclerosis**. *American journal of respiratory and critical care medicine* 2014.

62. Koh ET, Lee P, Gladman DD, Abu-Shakra M: **Pulmonary hypertension in systemic sclerosis: an analysis of 17 patients**. *British journal of rheumatology* 1996, **35**(10):989-993.

63. Kawut SM, Taichman DB, Archer-Chicko CL, Palevsky HI, Kimmel SE: **Hemodynamics and survival in patients with pulmonary arterial hypertension related to systemic sclerosis**. *Chest* 2003, **123**(2):344-350.

64. Lota HK, Wells AU: **The evolving pharmacotherapy of pulmonary fibrosis**. *Expert opinion on pharmacotherapy* 2013, **14**(1):79-89.

65. Goldin J, Elashoff R, Kim HJ, Yan X, Lynch D, Strollo D, Roth MD, Clements P, Furst DE, Khanna D *et al*: **Treatment of scleroderma-interstitial lung disease with cyclophosphamide is associated with less progressive fibrosis on serial thoracic high-resolution CT scan than placebo: findings from the scleroderma lung study**. *Chest* 2009, **136**(5):1333-1340.

66. Hoyles RK, Ellis RW, Wellsbury J, Lees B, Newlands P, Goh NS, Roberts C, Desai S, Herrick AL, McHugh NJ *et al*: **A multicenter, prospective, randomized, double-blind, placebo-controlled trial of corticosteroids and intravenous cyclophosphamide followed by oral azathioprine for the treatment of pulmonary fibrosis in scleroderma**. *Arthritis and rheumatism* 2006, **54**(12):3962-3970.

67. Chakraborty S, Chopra P, Ambi SV, Dastidar SG, Ray A: **Emerging therapeutic interventions for idiopathic pulmonary fibrosis**. *Expert opinion on investigational drugs* 2014.

68. Fisichella PM, Reder NP, Gagermeier J, Kovacs EJ: **Usefulness of pH monitoring in predicting the survival status of patients with scleroderma awaiting lung transplantation**. *The Journal of surgical research* 2014, **189**(2):232-237.

69. De Cruz S, Ross D: **Lung transplantation in patients with scleroderma**. *Curr Opin Rheumatol* 2013, **25**(6):714-718.

70. Richeldi L, du Bois RM, Raghu G, Azuma A, Brown KK, Costabel U, Cottin V, Flaherty KR, Hansell DM, Inoue Y *et al*: **Efficacy and safety of nintedanib in idiopathic pulmonary fibrosis**. *The New England journal of medicine* 2014, **370**(22):2071-2082.

71. Covvey JR, Mancl EE: **Recent Evidence for Pharmacological Treatment of Idiopathic Pulmonary Fibrosis**. *The Annals of pharmacotherapy* 2014, **48**(12):1611-1619.

72. Galie N, Hoeper MM, Humbert M, Torbicki A, Vachiery JL, Barbera JA, Beghetti M, Corris P, Gaine S, Gibbs JS *et al*: **Guidelines for the diagnosis and treatment of pulmonary hypertension: the Task Force for the Diagnosis and Treatment of Pulmonary Hypertension of the European Society of Cardiology (ESC) and the European Respiratory Society (ERS), endorsed by the International Society of Heart and Lung Transplantation (ISHLT)**. *European heart journal* 2009, **30**(20):2493-2537.

73. Peacock A: **Pulmonary hypertension**. *European respiratory review : an official journal of the European Respiratory Society* 2013, **22**(127):20-25.

74. Pope JE, Lee P, Baron M, Dunne J, Smith D, Docherty PS, Bookman A, Abu-Hakima M: **Prevalence of elevated pulmonary arterial pressures measured by echocardiography in a multicenter study of patients with systemic sclerosis**. *The Journal of rheumatology* 2005, **32**(7):1273-1278.

75. Hinz B, Phan SH, Thannickal VJ, Galli A, Bochaton-Piallat ML, Gabbiani G: **The Myofibroblast: One Function, Multiple Origins**. *The American Journal of Pathology* 2007, **170**(6):1807-1816.

76. McAnulty RJ, Campa JS, Cambrey AD, Laurent GJ: **The effect of transforming growth factor beta on rates of procollagen synthesis and degradation in vitro**. *Biochimica et biophysica acta* 1991, **1091**(2):231-235.

77. Young-Min SA, Beeton C, Laughton R, Plumpton T, Bartram S, Murphy G, Black C, Cawston TE: **Serum TIMP-1, TIMP-2, and MMP-1 in patients with systemic sclerosis, primary Raynaud's phenomenon, and in normal controls**. *Annals of the rheumatic diseases* 2001, **60**(9):846-851.

78. Leask A: **Getting out of a sticky situation: targeting the myofibroblast in scleroderma**. *The open rheumatology journal* 2012, **6**:163-169.

79. Tomasek JJ, Gabbiani G, Hinz B, Chaponnier C, Brown RA: **Myofibroblasts and mechano-regulation of connective tissue remodelling**. *Nature reviews Molecular cell biology* 2002, **3**(5):349-363.

80. Shi-Wen X, Thompson K, Khan K, Liu S, Murphy-Marshman H, Baron M, Denton CP, Leask A, Abraham DJ: **Focal adhesion kinase and reactive oxygen species contribute to the persistent fibrotic phenotype of lesional scleroderma fibroblasts**. *Rheumatology* 2012.

81. Darby I, Skalli O, Gabbiani G: **Alpha-smooth muscle actin is transiently expressed by myofibroblasts during experimental wound healing**. *Laboratory investigation; a journal of technical methods and pathology* 1990, **63**(1):21-29.

82. Desmouliere A, Darby IA, Gabbiani G: **Normal and pathologic soft tissue remodeling: role of the myofibroblast, with special emphasis on liver and kidney fibrosis**. *Laboratory investigation; a journal of technical methods and pathology* 2003, **83**(12):1689-1707.

83. Gabbiani G: **The myofibroblast in wound healing and fibrocontractive diseases**. *The Journal of pathology* 2003, **200**(4):500-503.

84. Chen Y, Shi-Wen X, van Beek J, Kennedy L, McLeod M, Renzoni EA, Bou-Gharios G, Wilcox-Adelman S, Goetinck PF, Eastwood M *et al*: **Matrix contraction by dermal fibroblasts requires transforming growth factor-beta/activin-linked kinase 5, heparan sulfate-containing proteoglycans, and**

MEK/ERK: insights into pathological scarring in chronic fibrotic disease. *Am J Pathol* 2005, **167**(6):1699-1711.

85. Whitfield ML, Finlay DR, Murray JI, Troyanskaya OG, Chi JT, Pergamenschikov A, McCalmont TH, Brown PO, Botstein D, Connolly MK: **Systemic and cell type-specific gene expression patterns in scleroderma skin**. *Proceedings of the National Academy of Sciences of the United States of America* 2003, **100**(21):12319-12324.

86. Sargent JL, Milano A, Bhattacharyya S, Varga J, Connolly MK, Chang HY, Whitfield ML: **A TGFbeta-responsive gene signature is associated with a subset of diffuse scleroderma with increased disease severity**. *J Invest Dermatol* 2010, **130**(3):694-705.

87. Greenblatt MB, Sargent JL, Farina G, Tsang K, Lafyatis R, Glimcher LH, Whitfield ML, Aliprantis AO: **Interspecies comparison of human and murine scleroderma reveals IL-13 and CCL2 as disease subset-specific targets**. *Am J Pathol* 2012, **180**(3):1080-1094.

88. Hsu E, Shi H, Jordan RM, Lyons-Weiler J, Pilewski JM, Feghali-Bostwick CA: **Lung tissues in patients with systemic sclerosis have gene expression patterns unique to pulmonary fibrosis and pulmonary hypertension**. *Arthritis and rheumatism* 2011, **63**(3):783-794.

89. Lindahl GE, Stock CJ, Shi-Wen X, Leoni P, Sestini P, Howat SL, Bou-Gharios G, Nicholson AG, Denton CP, Grutters JC *et al*: **Microarray profiling reveals suppressed interferon stimulated gene program in fibroblasts from scleroderma-associated interstitial lung disease**. *Respiratory research* 2013, **14**:80.

90. Manetti M, Guiducci S, Romano E, Rosa I, Ceccarelli C, Mello T, Milia AF, Conforti ML, Ibba-Manneschi L, Matucci-Cerinic M: **Differential expression of junctional adhesion molecules in different stages of systemic sclerosis**. *Arthritis and rheumatism* 2013, **65**(1):247-257.

91. Parsonage G, Filer AD, Haworth O, Nash GB, Rainger GE, Salmon M, Buckley CD: **A stromal address code defined by fibroblasts**. *Trends in immunology* 2005, **26**(3):150-156.

92. Chang HY, Chi JT, Dudoit S, Bondre C, van de Rijn M, Botstein D, Brown PO: **Diversity, topographic differentiation, and positional memory in human fibroblasts**. *Proceedings of the National Academy of Sciences of the United States of America* 2002, **99**(20):12877-12882.

93. Altorok N, Tsou PS, Coit P, Khanna D, Sawalha AH: **Genome-wide DNA methylation analysis in dermal fibroblasts from patients with diffuse and**

limited systemic sclerosis reveals common and subset-specific DNA methylation aberrancies. *Annals of the rheumatic diseases* 2014.

94. Hinz B: **Formation and function of the myofibroblast during tissue repair**. *J Invest Dermatol* 2007, **127**(3):526-537.

95. Hashimoto N, Phan SH, Imaizumi K, Matsuo M, Nakashima H, Kawabe T, Shimokata K, Hasegawa Y: **Endothelial-mesenchymal transition in bleomycin-induced pulmonary fibrosis**. *American journal of respiratory cell and molecular biology* 2010, **43**(2):161-172.

96. Arciniegas E, Neves CY, Carrillo LM, Zambrano EA, Ramirez R: **Endothelial-mesenchymal transition occurs during embryonic pulmonary artery development**. *Endothelium : journal of endothelial cell research* 2005, **12**(4):193-200.

97. Willis BC, Borok Z: **TGF-beta-induced EMT: mechanisms and implications for fibrotic lung disease**. *American journal of physiology Lung cellular and molecular physiology* 2007, **293**(3):L525-534.

98. Frid MG, Kale VA, Stenmark KR: **Mature vascular endothelium can give rise to smooth muscle cells via endothelial-mesenchymal transdifferentiation: in vitro analysis**. *Circulation research* 2002, **90**(11):1189-1196.

99. Kalluri R: **EMT: when epithelial cells decide to become mesenchymal-like cells**. *The Journal of clinical investigation* 2009, **119**(6):1417-1419.

100. Phillips RJ, Burdick MD, Hong K, Lutz MA, Murray LA, Xue YY, Belperio JA, Keane MP, Strieter RM: **Circulating fibrocytes traffic to the lungs in response to CXCL12 and mediate fibrosis**. *The Journal of clinical investigation* 2004, **114**(3):438-446.

101. Hoyles RK, Derrett-Smith EC, Khan K, Shiwen X, Howat SL, Wells AU, Abraham DJ, Denton CP: **An essential role for resident fibroblasts in experimental lung fibrosis is defined by lineage-specific deletion of high-affinity type II transforming growth factor beta receptor**. *American journal of respiratory and critical care medicine* 2011, **183**(2):249-261.

102. Budd DC, Holmes AM: **Targeting TGFbeta superfamily ligand accessory proteins as novel therapeutics for chronic lung disorders**. *Pharmacology & therapeutics* 2012, **135**(3):279-291.

103. Rajkumar VS, Howell K, Csiszar K, Denton CP, Black CM, Abraham DJ: **Shared expression of phenotypic markers in systemic sclerosis indicates a convergence of pericytes and fibroblasts to a myofibroblast lineage in fibrosis**. *Arthritis research & therapy* 2005, **7**(5):R1113-1123.

104. Acharya R, Tan PH, Subramaniam T, Tamura T, Chua KC, Goh SC, Lim CM, Goh SY, Chung KR, Law C: **Automated identification of diabetic type 2 subjects with and without neuropathy using wavelet transform on pedobarograph**. *Journal of medical systems* 2008, **32**(1):21-29.

105. Chesney J, Bucala R: **Peripheral blood fibrocytes: novel fibroblast-like cells that present antigen and mediate tissue repair**. *Biochemical Society transactions* 1997, **25**(2):520-524.

106. Yeager ME, Nguyen CM, Belchenko DD, Colvin KL, Takatsuki S, Ivy DD, Stenmark KR: **Circulating fibrocytes are increased in children and young adults with pulmonary hypertension**. *The European respiratory journal : official journal of the European Society for Clinical Respiratory Physiology* 2012, **39**(1):104-111.

107. Katebi M, Fernandez P, Chan ES, Cronstein BN: **Adenosine A2A receptor blockade or deletion diminishes fibrocyte accumulation in the skin in a murine model of scleroderma, bleomycin-induced fibrosis**. *Inflammation* 2008, **31**(5):299-303.

108. Field JJ, Burdick MD, DeBaun MR, Strieter BA, Liu L, Mehrad B, Rose CE, Jr., Linden J, Strieter RM: **The role of fibrocytes in sickle cell lung disease**. *PloS one* 2012, **7**(3):e33702.

109. Tourkina E, Bonner M, Oates J, Hofbauer A, Richard M, Znoyko S, Visconti RP, Zhang J, Hatfield CM, Silver RM *et al*: **Altered monocyte and fibrocyte phenotype and function in scleroderma interstitial lung disease: reversal by caveolin-1 scaffolding domain peptide**. *Fibrogenesis & tissue repair* 2011, **4**(1):15.

110. Lee CG, Homer RJ, Cohn L, Link H, Jung S, Craft JE, Graham BS, Johnson TR, Elias JA: **Transgenic overexpression of interleukin (IL)-10 in the lung causes mucus metaplasia, tissue inflammation, and airway remodeling via IL-13-dependent and -independent pathways**. *The Journal of biological chemistry* 2002, **277**(38):35466-35474.

111. Andersson-Sjoland A, de Alba CG, Nihlberg K, Becerril C, Ramirez R, Pardo A, Westergren-Thorsson G, Selman M: **Fibrocytes are a potential source of lung fibroblasts in idiopathic pulmonary fibrosis**. *The international journal of biochemistry & cell biology* 2008, **40**(10):2129-2140.

112. Bucala R, Spiegel LA, Chesney J, Hogan M, Cerami A: **Circulating fibrocytes define a new leukocyte subpopulation that mediates tissue repair**. *Molecular medicine* 1994, **1**(1):71-81.

113. Chan ES, Fernandez P, Merchant AA, Montesinos MC, Trzaska S, Desai A, Tung CF, Khoa DN, Pillinger MH, Reiss AB *et al*: **Adenosine A2A receptors in diffuse dermal fibrosis: pathogenic role in human dermal fibroblasts and in a murine model of scleroderma**. *Arthritis and rheumatism* 2006, **54**(8):2632-2642.

114. Fisher EA, Miano JM: **Don't judge books by their covers: vascular smooth muscle cells in arterial pathologies**. *Circulation* 2014, **129**(15):1545-1547.

115. Kallmeier RC, Somasundaram C, Babij P: **A novel smooth muscle-specific enhancer regulates transcription of the smooth muscle myosin heavy chain gene in vascular smooth muscle cells**. *The Journal of biological chemistry* 1995, **270**(52):30949-30957.

116. Maurer B, Reich N, Juengel A, Kriegsmann J, Gay RE, Schett G, Michel BA, Gay S, Distler JH, Distler O: **Fra-2 transgenic mice as a novel model of pulmonary hypertension associated with systemic sclerosis**. *Annals of the rheumatic diseases* 2012, **71**(8):1382-1387.

117. Hemnes AR, Zaiman A, Champion HC: **PDE5A inhibition attenuates bleomycin-induced pulmonary fibrosis and pulmonary hypertension through inhibition of ROS generation and RhoA/Rho kinase activation**. *American journal of physiology Lung cellular and molecular physiology* 2008, **294**(1):L24-33.

118. Loeys BL, Chen J, Neptune ER, Judge DP, Podowski M, Holm T, Meyers J, Leitch CC, Katsanis N, Sharifi N *et al*: **A syndrome of altered cardiovascular, craniofacial, neurocognitive and skeletal development caused by mutations in TGFBR1 or TGFBR2**. *Nature genetics* 2005, **37**(3):275-281.

119. Derrett-Smith EC, Dooley A, Gilbane A, Trinder S, Khan K, Baliga R, Holmes A, Hobbs A, Abraham D, Denton CP: **Endothelial injury in a TGFbeta dependent mouse model of scleroderma induces pulmonary arterial hypertension**. *Arthritis and rheumatism* 2013.

120. Eferl R, Hasselblatt P, Rath M, Popper H, Zenz R, Komnenovic V, Idarraga MH, Kenner L, Wagner EF: **Development of pulmonary fibrosis through a pathway involving the transcription factor Fra-2/AP-1**. *Proceedings of the National Academy of Sciences of the United States of America* 2008, **105**(30):10525-10530.

121. Venalis P, Distler O, Lundberg IE, Schett G, Distler JH: **Heart involvement in patients with systemic sclerosis is mimicked by Fra-2 transgenic mice**. *Annals of the rheumatic diseases* 2012, **71**(Suppl 1):A46.

122. Razani B, Lisanti MP: **Caveolin-deficient mice: insights into caveolar function human disease**. *The Journal of clinical investigation* 2001, **108**(11):1553-1561.

123. Razani B, Engelman JA, Wang XB, Schubert W, Zhang XL, Marks CB, Macaluso F, Russell RG, Li M, Pestell RG *et al*: **Caveolin-1 null mice are viable but show evidence of hyperproliferative and vascular abnormalities**. *The Journal of biological chemistry* 2001, **276**(41):38121-38138.

124. Saito E, Fujimoto M, Hasegawa M, Komura K, Hamaguchi Y, Kaburagi Y, Nagaoka T, Takehara K, Tedder TF, Sato S: **CD19-dependent B lymphocyte signaling thresholds influence skin fibrosis and autoimmunity in the tight-skin mouse**. *The Journal of clinical investigation* 2002, **109**(11):1453-1462.

125. Tan FK, Wang N, Kuwana M, Chakraborty R, Bona CA, Milewicz DM, Arnett FC: **Association of fibrillin 1 single-nucleotide polymorphism haplotypes with systemic sclerosis in Choctaw and Japanese populations**. *Arthritis and rheumatism* 2001, **44**(4):893-901.

126. Baxter RM, Crowell TP, McCrann ME, Frew EM, Gardner H: **Analysis of the tight skin (Tsk1/+) mouse as a model for testing antifibrotic agents**. *Laboratory investigation; a journal of technical methods and pathology* 2005, **85**(10):1199-1209.

127. Manne J, Markova M, Siracusa LD, Jimenez SA: **Collagen content in skin and internal organs of the tight skin mouse: an animal model of scleroderma**. *Biochemistry research international* 2013, **2013**:436053.

128. Gentiletti J, McCloskey LJ, Artlett CM, Peters J, Jimenez SA, Christner PJ: **Demonstration of autoimmunity in the tight skin-2 mouse: a model for scleroderma**. *Journal of immunology* 2005, **175**(4):2418-2426.

129. Bei Y, Hua-Huy T, Duong-Quy S, Nguyen VH, Chen W, Nicco C, Batteux F, Dinh-Xuan AT: **Long-term treatment with fasudil improves bleomycin-induced pulmonary fibrosis and pulmonary hypertension via inhibition of Smad2/3 phosphorylation**. *Pulmonary pharmacology & therapeutics* 2013, **26**(6):635-643.

130. Yoshizaki A, Yanaba K, Yoshizaki A, Iwata Y, Komura K, Ogawa F, Takenaka M, Shimizu K, Asano Y, Hasegawa M *et al*: **Treatment with rapamycin prevents fibrosis in tight-skin and bleomycin-induced mouse models of systemic sclerosis**. *Arthritis and rheumatism* 2010, **62**(8):2476-2487.

131. Yamamoto T, Takagawa S, Katayama I, Yamazaki K, Hamazaki Y, Shinkai H, Nishioka K: **Animal Model of Sclerotic Skin. I: Local Injections of Bleomycin Induce Sclerotic Skin Mimicking Scleroderma**. 1999, **112**(4):456-462.

132. Mutlu GM, Budinger GR, Wu M, Lam AP, Zirk A, Rivera S, Urich D, Chiarella SE, Go LH, Ghosh AK *et al*: **Proteasomal inhibition after injury prevents fibrosis by modulating TGF-beta(1) signalling**. *Thorax* 2012, **67**(2):139-146.

133. Peng R, Sridhar S, Tyagi G, Phillips JE, Garrido R, Harris P, Burns L, Renteria L, Woods J, Chen L *et al*: **Bleomycin induces molecular changes directly relevant to idiopathic pulmonary fibrosis: a model for "active" disease**. *PloS one* 2013, **8**(4):e59348.

134. Sonnylal S, Denton CP, Zheng B, Keene DR, He R, Adams HP, Vanpelt CS, Geng YJ, Deng JM, Behringer RR *et al*: **Postnatal induction of transforming growth factor beta signaling in fibroblasts of mice recapitulates clinical, histologic, and biochemical features of scleroderma**. *Arthritis and rheumatism* 2007, **56**(1):334-344.

135. Sonnylal S, Shi-Wen X, Leoni P, Naff K, Van Pelt CS, Nakamura H, Leask A, Abraham D, Bou-Gharios G, de Crombrugghe B: **Selective expression of connective tissue growth factor in fibroblasts in vivo promotes systemic tissue fibrosis**. *Arthritis and rheumatism* 2010, **62**(5):1523-1532.

136. Drab M, Verkade P, Elger M, Kasper M, Lohn M, Lauterbach B, Menne J, Lindschau C, Mende F, Luft FC *et al*: **Loss of caveolae, vascular dysfunction, and pulmonary defects in caveolin-1 gene-disrupted mice**. *Science* 2001, **293**(5539):2449-2452.

137. Samuel CS, Zhao C, Yang Q, Wang H, Tian H, Tregear GW, Amento EP: **The relaxin gene knockout mouse: a model of progressive scleroderma**. *J Invest Dermatol* 2005, **125**(4):692-699.

138. Wei J, Melichian D, Komura K, Hinchcliff M, Lam AP, Lafyatis R, Gottardi CJ, MacDougald OA, Varga J: **Canonical Wnt signaling induces skin fibrosis and subcutaneous lipoatrophy: a novel mouse model for scleroderma?** *Arthritis and rheumatism* 2011, **63**(6):1707-1717.

139. Kavian N, Servettaz A, Mongaret C, Wang A, Nicco C, Chereau C, Grange P, Vuiblet V, Birembaut P, Diebold MD *et al*: **Targeting ADAM-17/notch signaling abrogates the development of systemic sclerosis in a murine model**. *Arthritis and rheumatism* 2010, **62**(11):3477-3487.

140. Taraseviciene-Stewart L, Kasahara Y, Alger L, Hirth P, Mc Mahon G, Waltenberger J, Voelkel NF, Tuder RM: **Inhibition of the VEGF receptor 2 combined with chronic hypoxia causes cell death-dependent pulmonary endothelial cell proliferation and severe pulmonary hypertension**. *FASEB journal : official publication of the Federation of American Societies for Experimental Biology* 2001, **15**(2):427-438.

141. Ciuclan L, Bonneau O, Hussey M, Duggan N, Holmes AM, Good R, Stringer R, Jones P, Morrell NW, Jarai G *et al*: **A novel murine model of severe pulmonary arterial hypertension**. *American journal of respiratory and critical care medicine* 2011, **184**(10):1171-1182.

142. Adatia I, Haworth SG, Wegner M, Barst RJ, Ivy D, Stenmark KR, Karkowsky A, Rosenzweig E, Aguilar C: **Clinical trials in neonates and children: Report of the pulmonary hypertension academic research consortium pediatric advisory committee**. *Pulmonary circulation* 2013, **3**(1):252-266.

143. Stenmark KR, Fagan KA, Frid MG: **Hypoxia-induced pulmonary vascular remodeling: cellular and molecular mechanisms**. *Circulation research* 2006, **99**(7):675-691.

144. Stenmark KR, Meyrick B, Galie N, Mooi WJ, McMurtry IF: **Animal models of pulmonary arterial hypertension: the hope for etiological discovery and pharmacological cure**. *American journal of physiology Lung cellular and molecular physiology* 2009, **297**(6):L1013-1032.

145. Bubb KJ, Trinder SL, Baliga RS, Patel J, Clapp LH, MacAllister RJ, Hobbs AJ: **Inhibition of Phosphodiesterase 2 Augments cGMP and cAMP Signaling to Ameliorate Pulmonary Hypertension**. *Circulation* 2014.

146. Long L, Crosby A, Yang X, Southwood M, Upton PD, Kim DK, Morrell NW: **Altered bone morphogenetic protein and transforming growth factor-beta signaling in rat models of pulmonary hypertension: potential for activin receptor-like kinase-5 inhibition in prevention and progression of disease**. *Circulation* 2009, **119**(4):566-576.

147. Panzhinskiy E, Zawada WM, Stenmark KR, Das M: **Hypoxia induces unique proliferative response in adventitial fibroblasts by activating PDGFbeta receptor-JNK1 signalling**. *Cardiovascular research* 2012, **95**(3):356-365.

148. Reusser M, Hunter KS, Lammers SR, Stenmark KR: **Validation of a pressure diameter method for determining modulus and strain of collagen engagement for long branches of bovine pulmonary arteries**. *Journal of biomechanical engineering* 2012, **134**(5):054501.

149. Scott D, Tan Y, Shandas R, Stenmark KR, Tan W: **High pulsatility flow stimulates smooth muscle cell hypertrophy and contractile protein expression**. *American journal of physiology Lung cellular and molecular physiology* 2013, **304**(1):L70-81.

150. Stenmark KR, Davie N, Frid M, Gerasimovskaya E, Das M: **Role of the adventitia in pulmonary vascular remodeling**. *Physiology* 2006, **21**:134-145.

151. Zhang S, Fantozzi I, Tigno DD, Yi ES, Platoshyn O, Thistlethwaite PA, Kriett JM, Yung G, Rubin LJ, Yuan JX: **Bone morphogenetic proteins induce apoptosis in human pulmonary vascular smooth muscle cells**. *American journal of physiology Lung cellular and molecular physiology* 2003, **285**(3):L740-754.

152. Richter A, Yeager ME, Zaiman A, Cool CD, Voelkel NF, Tuder RM: **Impaired transforming growth factor-beta signaling in idiopathic pulmonary arterial hypertension**. *American journal of respiratory and critical care medicine* 2004, **170**(12):1340-1348.

153. Burke DL, Frid MG, Kunrath CL, Karoor V, Anwar A, Wagner BD, Strassheim D, Stenmark KR: **Sustained hypoxia promotes the development of a pulmonary artery-specific chronic inflammatory microenvironment**. *American journal of physiology Lung cellular and molecular physiology* 2009, **297**(2):L238-250.

154. Tian L, Lammers SR, Kao PH, Reusser M, Stenmark KR, Hunter KS, Qi HJ, Shandas R: **Linked opening angle and histological and mechanical aspects of the proximal pulmonary arteries of healthy and pulmonary hypertensive rats and calves**. *American journal of physiology Heart and circulatory physiology* 2011, **301**(5):H1810-1818.

155. Ciuclan L, Sheppard K, Dong L, Sutton D, Duggan N, Hussey M, Simmons J, Morrell NW, Jarai G, Edwards M *et al*: **Treatment with anti-gremlin 1 antibody ameliorates chronic hypoxia/SU5416-induced pulmonary arterial hypertension in mice**. *Am J Pathol* 2013, **183**(5):1461-1473.

156. Moreno-Vinasco L, Gomberg-Maitland M, Maitland ML, Desai AA, Singleton PA, Sammani S, Sam L, Liu Y, Husain AN, Lang RM *et al*: **Genomic assessment of a multikinase inhibitor, sorafenib, in a rodent model of pulmonary hypertension**. *Physiological genomics* 2008, **33**(2):278-291.

157. Jasmin JF, Lucas M, Cernacek P, Dupuis J: **Effectiveness of a nonselective ET(A/B) and a selective ET(A) antagonist in rats with monocrotaline-induced pulmonary hypertension**. *Circulation* 2001, **103**(2):314-318.

158. Kay JM, Harris P, Heath D: **Pulmonary hypertension produced in rats by ingestion of Crotalaria spectabilis seeds**. *Thorax* 1967, **22**(2):176-179.

159. Gomez-Arroyo JG, Farkas L, Alhussaini AA, Farkas D, Kraskauskas D, Voelkel NF, Bogaard HJ: **The monocrotaline model of pulmonary hypertension in perspective**. *American journal of physiology Lung cellular and molecular physiology* 2012, **302**(4):L363-369.

160. Schultze AE, Roth RA: **Chronic pulmonary hypertension--the monocrotaline model and involvement of the hemostatic system**. *Journal of toxicology and environmental health Part B, Critical reviews* 1998, **1**(4):271-346.

161. Abe K, Shimokawa H, Morikawa K, Uwatoku T, Oi K, Matsumoto Y, Hattori T, Nakashima Y, Kaibuchi K, Sueishi K *et al*: **Long-Term Treatment With a Rho-Kinase Inhibitor Improves Monocrotaline-Induced Fatal Pulmonary Hypertension in Rats**. *Circulation Research* 2004, **94**(3):385-393.

162. Hamid R, Cogan JD, Hedges LK, Austin E, Phillips JA, Newman JH, Loyd JE: **Penetrance of pulmonary arterial hypertension is modulated by the expression of normal BMPR2 allele**. *Human mutation* 2009, **30**(4):649-654.

163. Newman JH, Phillips JA, 3rd, Loyd JE: **Narrative review: the enigma of pulmonary arterial hypertension: new insights from genetic studies**. *Annals of internal medicine* 2008, **148**(4):278-283.

164. Beppu H, Ichinose F, Kawai N, Jones RC, Yu PB, Zapol WM, Miyazono K, Li E, Bloch KD: **BMPR-II heterozygous mice have mild pulmonary hypertension and an impaired pulmonary vascular remodeling response to prolonged hypoxia**. *American journal of physiology Lung cellular and molecular physiology* 2004, **287**(6):L1241-1247.

165. Burton VJ, Holmes AM, Ciuclan LI, Robinson A, Roger JS, Jarai G, Pearce AC, Budd DC: **Attenuation of leukocyte recruitment via CXCR1/2 inhibition stops the progression of PAH in mice with genetic ablation of endothelial BMPR-II**. *Blood* 2011, **118**(17):4750-4758.

166. Munz B, Tretter YP, Hertel M, Engelhardt F, Alzheimer C, Werner S: **The roles of activins in repair processes of the skin and the brain**. *Molecular and cellular endocrinology* 2001, **180**(1-2):169-177.

167. Mather JP, Moore A, Li RH: **Activins, inhibins, and follistatins: further thoughts on a growing family of regulators**. *Proceedings of the Society for Experimental Biology and Medicine Society for Experimental Biology and Medicine* 1997, **215**(3):209-222.

168. Kingsley DM: **What do BMPs do in mammals? Clues from the mouse short-ear mutation**. *Trends in genetics : TIG* 1994, **10**(1):16-21.

169. Massague J: **TGF-beta signaling in development and disease**. *FEBS letters* 2012, **586**(14):1833.

170. Massague J: **Integration of Smad and MAPK pathways: a link and a linker revisited**. *Genes & development* 2003, **17**(24):2993-2997.

171. Daniel C, Wiede J, Krutzsch HC, Ribeiro SM, Roberts DD, Murphy-Ullrich JE, Hugo C: **Thrombospondin-1 is a major activator of TGF-beta in fibrotic renal disease in the rat in vivo**. *Kidney international* 2004, **65**(2):459-468.

172. Shi-wen X, Stanton LA, Kennedy L, Pala D, Chen Y, Howat SL, Renzoni EA, Carter DE, Bou-Gharios G, Stratton RJ *et al*: **CCN2 is necessary for adhesive responses to transforming growth factor-beta1 in embryonic fibroblasts**. *The Journal of biological chemistry* 2006, **281**(16):10715-10726.

173. Ogo T, Chowdhury HM, Yang J, Long L, Li X, Torres Cleuren YN, Morrell NW, Schermuly RT, Trembath RC, Nasim MT: **Inhibition of overactive transforming growth factor-beta signaling by prostacyclin analogs in pulmonary arterial hypertension**. *American journal of respiratory cell and molecular biology* 2013, **48**(6):733-741.

174. Mori Y, Chen SJ, Varga J: **Expression and regulation of intracellular SMAD signaling in scleroderma skin fibroblasts**. *Arthritis and rheumatism* 2003, **48**(7):1964-1978.

175. Wang Y, Kahaleh B: **Epigenetic repression of bone morphogenetic protein receptor II expression in scleroderma**. *Journal of cellular and molecular medicine* 2013.

176. Mata-Greenwood E, Meyrick B, Steinhorn RH, Fineman JR, Black SM: **Alterations in TGF-beta1 expression in lambs with increased pulmonary blood flow and pulmonary hypertension**. *American journal of physiology Lung cellular and molecular physiology* 2003, **285**(1):L209-221.

177. Morrell NW, Yang X, Upton PD, Jourdan KB, Morgan N, Sheares KK, Trembath RC: **Altered growth responses of pulmonary artery smooth muscle cells from patients with primary pulmonary hypertension to transforming growth factor-beta(1) and bone morphogenetic proteins**. *Circulation* 2001, **104**(7):790-795.

178. Moustakas A, Heldin CH: **Non-Smad TGF-beta signals**. *Journal of cell science* 2005, **118**(Pt 16):3573-3584.

179. Gabrielli A, Svegliati S, Moroncini G, Luchetti M, Tonnini C, Avvedimento EV: **Stimulatory autoantibodies to the PDGF receptor: a link to fibrosis in scleroderma and a pathway for novel therapeutic targets**. *Autoimmunity reviews* 2007, **7**(2):121-126.

180. Tang X, Peng R, Phillips JE, Deguzman J, Ren Y, Apparsundaram S, Luo Q, Bauer CM, Fuentes ME, Demartino JA *et al*: **Assessment of Brd4 Inhibition in Idiopathic Pulmonary Fibrosis Lung Fibroblasts and in Vivo Models of Lung Fibrosis**. *Am J Pathol* 2013, **183**(2):470-479.

181. Das M, Burns N, Wilson SJ, Zawada WM, Stenmark KR: **Hypoxia exposure induces the emergence of fibroblasts lacking replication repressor signals of PKCzeta in the pulmonary artery adventitia**. *Cardiovascular research* 2008, **78**(3):440-448.

182. Stenmark KR, Yeager ME, El Kasmi KC, Nozik-Grayck E, Gerasimovskaya EV, Li M, Riddle SR, Frid MG: **The adventitia: essential regulator of vascular wall structure and function**. *Annual review of physiology* 2013, **75**:23-47.

183. Cogan JD, Pauciulo MW, Batchman AP, Prince MA, Robbins IM, Hedges LK, Stanton KC, Wheeler LA, Phillips JA, 3rd, Loyd JE *et al*: **High frequency of BMPR2 exonic deletions/duplications in familial pulmonary arterial hypertension**. *American journal of respiratory and critical care medicine* 2006, **174**(5):590-598.

184. Aldred MA, Vijayakrishnan J, James V, Soubrier F, Gomez-Sanchez MA, Martensson G, Galie N, Manes A, Corris P, Simonneau G *et al*: **BMPR2 gene rearrangements account for a significant proportion of mutations in familial and idiopathic pulmonary arterial hypertension**. *Human mutation* 2006, **27**(2):212-213.

185. Schermuly RT, Dony E, Ghofrani HA, Pullamsetti S, Savai R, Roth M, Sydykov A, Lai YJ, Weissmann N, Seeger W *et al*: **Reversal of experimental pulmonary hypertension by PDGF inhibition**. *The Journal of clinical investigation* 2005, **115**(10):2811-2821.

186. Perros F, Montani D, Dorfmuller P, Durand-Gasselin I, Tcherakian C, Le Pavec J, Mazmanian M, Fadel E, Mussot S, Mercier O *et al*: **Platelet-derived growth factor expression and function in idiopathic pulmonary arterial hypertension**. *American journal of respiratory and critical care medicine* 2008, **178**(1):81-88.

187. Welsh DJ, Scott PH, Peacock AJ: **p38 MAP kinase isoform activity and cell cycle regulators in the proliferative response of pulmonary and systemic artery fibroblasts to acute hypoxia**. *Pulmonary pharmacology & therapeutics* 2006, **19**(2):128-138.

188. Mortimer HJ, Peacock AJ, Kirk A, Welsh DJ: **p38 MAP kinase: essential role in hypoxia-mediated human pulmonary artery fibroblast proliferation**. *Pulmonary pharmacology & therapeutics* 2007, **20**(6):718-725.

189. Tang X, Peng R, Ren Y, Apparsundaram S, Deguzman J, Bauer CM, Hoffman AF, Hamilton S, Liang Z, Zeng H *et al*: **BET Bromodomain Proteins Mediate Downstream Signaling Events following Growth Factor Stimulation in Human Lung Fibroblasts and Are Involved in Bleomycin-Induced Pulmonary Fibrosis**. *Molecular pharmacology* 2013, **83**(1):283-293.

190. Murakami K, Mathew R, Huang J, Farahani R, Peng H, Olson SC, Etlinger JD: **Smurf1 ubiquitin ligase causes downregulation of BMP receptors and is induced in monocrotaline and hypoxia models of pulmonary arterial hypertension**. *Experimental biology and medicine* 2010, **235**(7):805-813.

191. Alan B, Nalbantgil S: **[Genetic, cellular and molecular mechanisms of pulmonary arterial hypertension]**. *Anadolu kardiyoloji dergisi : AKD = the Anatolian journal of cardiology* 2010, **10 Suppl 1**:9-13.

192. Sztrymf B, Coulet F, Girerd B, Yaici A, Jais X, Sitbon O, Montani D, Souza R, Simonneau G, Soubrier F *et al*: **Clinical outcomes of pulmonary arterial hypertension in carriers of BMPR2 mutation**. *American journal of respiratory and critical care medicine* 2008, **177**(12):1377-1383.

193. Ramos MF, Lame MW, Segall HJ, Wilson DW: **Smad signaling in the rat model of monocrotaline pulmonary hypertension**. *Toxicol Pathol* 2008, **36**(2):311-320.

194. Thomas M, Docx C, Holmes AM, Beach S, Duggan N, England K, Leblanc C, Lebret C, Schindler F, Raza F *et al*: **Activin-like kinase 5 (ALK5) mediates abnormal proliferation of vascular smooth muscle cells from patients with familial pulmonary arterial hypertension and is involved in the progression of experimental pulmonary arterial hypertension induced by monocrotaline**. *Am J Pathol* 2009, **174**(2):380-389.

195. AVOUAC J, AIRÒ P, MEUNE C, BERETTA L, DIEUDE P, CARAMASCHI P, TIEV K, CAPPELLI S, DIOT E, VACCA A *et al*: **Prevalence of Pulmonary Hypertension in Systemic Sclerosis in European Caucasians and Metaanalysis of 5 Studies**. *The Journal of rheumatology* 2010, **37**(11):2290-2298.

196. Fisher MR, Mathai SC, Champion HC, Girgis RE, Housten-Harris T, Hummers L, Krishnan JA, Wigley F, Hassoun PM: **Clinical differences between idiopathic and scleroderma-related pulmonary hypertension**. *Arthritis and rheumatism* 2006, **54**(9):3043-3050.

197. Mathai SC, Hummers LK, Champion HC, Wigley FM, Zaiman A, Hassoun PM, Girgis RE: **Survival in pulmonary hypertension associated with the scleroderma spectrum of diseases: impact of interstitial lung disease**. *Arthritis and rheumatism* 2009, **60**(2):569-577.

198. Morse J, Barst R, Horn E, Cuervo N, Deng Z, Knowles J: **Pulmonary hypertension in scleroderma spectrum of disease: lack of bone morphogenetic protein receptor 2 mutations**. *The Journal of rheumatology* 2002, **29**(11):2379-2381.

199. Weiss CH, Budinger GR, Mutlu GM, Jain M: **Proteasomal regulation of pulmonary fibrosis**. *Proceedings of the American Thoracic Society* 2010, **7**(1):77-83.

200. Ciechanover A, Hod Y, Hershko A: **A heat-stable polypeptide component of an ATP-dependent proteolytic system from reticulocytes. 1978**. *Biochemical and biophysical research communications* 2012, **425**(3):565-570.

201. Groll M, Huber R, Moroder L: **The persisting challenge of selective and specific proteasome inhibition**. *Journal of peptide science : an official publication of the European Peptide Society* 2009, **15**(2):58-66.

202. Imamura T, Oshima Y, Hikita A: **Regulation of TGF-beta family signalling by ubiquitination and deubiquitination**. *Journal of biochemistry* 2013, **154**(6):481-489.

203. Herhaus L, Sapkota GP: **The emerging roles of deubiquitylating enzymes (DUBs) in the TGFbeta and BMP pathways**. *Cellular signalling* 2014, **26**(10):2186-2192.

204. Durrington HJ, Upton PD, Hoer S, Boname J, Dunmore BJ, Yang J, Crilley TK, Butler LM, Blackbourn DJ, Nash GB *et al*: **Identification of a lysosomal pathway regulating degradation of the bone morphogenetic protein receptor type II**. *The Journal of biological chemistry* 2010, **285**(48):37641-37649.

205. Long L, Yang X, Southwood M, Lu J, Marciniak SJ, Dunmore BJ, Morrell NW: **Chloroquine prevents progression of experimental pulmonary hypertension via inhibition of autophagy and lysosomal bone morphogenetic protein type II receptor degradation**. *Circulation research* 2013, **112**(8):1159-1170.

206. Dou QP, Zonder JA: **Overview and Perspective of Proteasome Inhibitor-Based Anti-Cancer Therapies: Bortezomib and Second Generation Proteasome Inhibitors Versus Future Generation Inhibitors of Ubiquitin-Proteasome System**. *Current cancer drug targets* 2014.

207. Anan A, Baskin-Bey ES, Isomoto H, Mott JL, Bronk SF, Albrecht JH, Gores GJ: **Proteasome inhibition attenuates hepatic injury in the bile duct-ligated mouse**. *American journal of physiology Gastrointestinal and liver physiology* 2006, **291**(4):G709-716.

208. Wagner-Ballon O, Pisani DF, Gastinne T, Tulliez M, Chaligne R, Lacout C, Aurade F, Villeval JL, Gonin P, Vainchenker W *et al*: **Proteasome inhibitor bortezomib impairs both myelofibrosis and osteosclerosis induced by high thrombopoietin levels in mice**. *Blood* 2007, **110**(1):345-353.

209. Meiners S, Hocher B, Weller A, Laule M, Stangl V, Guenther C, Godes M, Mrozikiewicz A, Baumann G, Stangl K: **Downregulation of matrix metalloproteinases and collagens and suppression of cardiac fibrosis by inhibition of the proteasome**. *Hypertension* 2004, **44**(4):471-477.

210. Tashiro K, Tamada S, Kuwabara N, Komiya T, Takekida K, Asai T, Iwao H, Sugimura K, Matsumura Y, Takaoka M *et al*: **Attenuation of renal fibrosis by proteasome inhibition in rat obstructive nephropathy: possible role of nuclear factor kappaB**. *International journal of molecular medicine* 2003, **12**(4):587-592.

211. Fineschi S, Bongiovanni M, Donati Y, Djaafar S, Naso F, Goffin L, Argiroffo CB, Pache JC, Dayer JM, Ferrari-Lacraz S *et al*: **In vivo investigations on anti-fibrotic potential of proteasome inhibition in lung and skin fibrosis**. *American journal of respiratory cell and molecular biology* 2008, **39**(4):458-465.

212. Valerio CJ, Schreiber BE, Handler CE, Denton CP, Coghlan JG: **Borderline mean pulmonary artery pressure in patients with systemic sclerosis:**

transpulmonary gradient predicts risk of developing pulmonary hypertension. *Arthritis and rheumatism* 2013, **65**(4):1074-1084.

213. Chan MC, Nguyen PH, Davis BN, Ohoka N, Hayashi H, Du K, Lagna G, Hata A: **A novel regulatory mechanism of the bone morphogenetic protein (BMP) signaling pathway involving the carboxyl-terminal tail domain of BMP type II receptor**. *Molecular and cellular biology* 2007, **27**(16):5776-5789.

214. Hummers LK, Hall A, Wigley FM, Simons M: **Abnormalities in the regulators of angiogenesis in patients with scleroderma**. *The Journal of rheumatology* 2009, **36**(3):576-582.

215. Kang H, Davis-Dusenbery BN, Nguyen PH, Lal A, Lieberman J, Van Aelst L, Lagna G, Hata A: **Bone morphogenetic protein 4 promotes vascular smooth muscle contractility by activating microRNA-21 (miR-21), which down-regulates expression of family of dedicator of cytokinesis (DOCK) proteins**. *The Journal of biological chemistry* 2012, **287**(6):3976-3986.

216. Yang S, Banerjee S, Freitas A, Cui H, Xie N, Abraham E, Liu G: **miR-21 regulates chronic hypoxia-induced pulmonary vascular remodeling**. *American journal of physiology Lung cellular and molecular physiology* 2012, **302**(6):L521-529.

217. Dong C, Zhu S, Wang T, Yoon W, Goldschmidt-Clermont PJ: **Upregulation of PAI-1 is mediated through TGF-beta/Smad pathway in transplant arteriopathy**. *The Journal of heart and lung transplantation : the official publication of the International Society for Heart Transplantation* 2002, **21**(9):999-1008.

218. Soon E, Holmes AM, Treacy CM, Doughty NJ, Southgate L, Machado RD, Trembath RC, Jennings S, Barker L, Nicklin P *et al*: **Elevated Levels of Inflammatory Cytokines Predict Survival in Idiopathic and Familial Pulmonary Arterial Hypertension**. *Circulation* 2010, **122**(9):920-927.

219. Lagna G, Nguyen PH, Ni W, Hata A: **BMP-dependent activation of caspase-9 and caspase-8 mediates apoptosis in pulmonary artery smooth muscle cells**. *American journal of physiology Lung cellular and molecular physiology* 2006, **291**(5):L1059-1067.

220. Yu PB, Deng DY, Beppu H, Hong CC, Lai C, Hoyng SA, Kawai N, Bloch KD: **Bone morphogenetic protein (BMP) type II receptor is required for BMP-mediated growth arrest and differentiation in pulmonary artery smooth muscle cells**. *The Journal of biological chemistry* 2008, **283**(7):3877-3888.

221. Xie S, Sukkar MB, Issa R, Oltmanns U, Nicholson AG, Chung KF: **Regulation of TGF-beta 1-induced connective tissue growth factor expression in**

airway smooth muscle cells. *American journal of physiology Lung cellular and molecular physiology* 2005, **288**(1):L68-76.

222. Hirschi KK, Rohovsky SA, D'Amore PA: **PDGF, TGF-beta, and heterotypic cell-cell interactions mediate endothelial cell-induced recruitment of 10T1/2 cells and their differentiation to a smooth muscle fate**. *The Journal of cell biology* 1998, **141**(3):805-814.

223. Humbert M, Montani D, Perros F, Dorfmuller P, Adnot S, Eddahibi S: **Endothelial cell dysfunction and cross talk between endothelium and smooth muscle cells in pulmonary arterial hypertension**. *Vascular pharmacology* 2008, **49**(4-6):113-118.

224. Budhiraja R, Tuder RM, Hassoun PM: **Endothelial dysfunction in pulmonary hypertension**. *Circulation* 2004, **109**(2):159-165.

225. Loscalzo J: **Endothelial dysfunction in pulmonary hypertension**. *The New England journal of medicine* 1992, **327**(2):117-119.

226. Mack CP, Owens GK: **Regulation of Smooth Muscle α-Actin Expression In Vivo Is Dependent on CArG Elements Within the 5′ and First Intron Promoter Regions**. *Circulation research* 1999, **84**(7):852-861.

227. van der Loop FT, Schaart G, Timmer ED, Ramaekers FC, van Eys GJ: **Smoothelin, a novel cytoskeletal protein specific for smooth muscle cells**. *The Journal of cell biology* 1996, **134**(2):401-411.

228. Cahill E, Costello CM, Rowan SC, Harkin S, Howell K, Leonard MO, Southwood M, Cummins EP, Fitzpatrick SF, Taylor CT *et al*: **Gremlin plays a key role in the pathogenesis of pulmonary hypertension**. *Circulation* 2012, **125**(7):920-930.

229. Dorfmuller P, Humbert M, Capron F, Muller KM: **Pathology and aspects of pathogenesis in pulmonary arterial hypertension**. *Sarcoidosis, vasculitis, and diffuse lung diseases : official journal of WASOG / World Association of Sarcoidosis and Other Granulomatous Disorders* 2003, **20**(1):9-19.

230. Humbert M, Monti G, Brenot F, Sitbon O, Portier A, Grangeot-Keros L, Duroux P, Galanaud P, Simonneau G, Emilie D: **Increased interleukin-1 and interleukin-6 serum concentrations in severe primary pulmonary hypertension**. *American journal of respiratory and critical care medicine* 1995, **151**(5):1628-1631.

231. Bhargava A, Kumar A, Yuan N, Gewitz MH, Mathew R: **Monocrotaline induces interleukin-6 mRNA expression in rat lungs**. *Heart disease* 1999, **1**(3):126-132.

232. Miyata M, Sakuma F, Yoshimura A, Ishikawa H, Nishimaki T, Kasukawa R: **Pulmonary hypertension in rats. 2. Role of interleukin-6**. *International archives of allergy and immunology* 1995, **108**(3):287-291.

233. Murakami M, Nishimoto N: **The value of blocking IL-6 outside of rheumatoid arthritis: current perspective**. *Curr Opin Rheumatol* 2011, **23**(3):273-277.

234. Furuya Y, Satoh T, Kuwana M: **Interleukin-6 as a potential therapeutic target for pulmonary arterial hypertension**. *International journal of rheumatology* 2010, **2010**:720305.

235. Denton CP, Shi-Wen X, Sutton A, Abraham DJ, Black CM, Pearson JD: **Scleroderma fibroblasts promote migration of mononuclear leucocytes across endothelial cell monolayers**. *Clinical and experimental immunology* 1998, **114**(2):293-300.

236. Wood JG, Johnson JS, Mattioli LF, Gonzalez NC: **Systemic hypoxia increases leukocyte emigration and vascular permeability in conscious rats**. *J Appl Physiol (1985)* 2000, **89**(4):1561-1568.

237. Gourh P, Arnett FC, Assassi S, Tan FK, Huang M, Diekman L, Mayes MD, Reveille JD, Agarwal SK: **Plasma cytokine profiles in systemic sclerosis: associations with autoantibody subsets and clinical manifestations**. *Arthritis research & therapy* 2009, **11**(5):R147.

238. Desai TR, Leeper NJ, Hynes KL, Gewertz BL: **Interleukin-6 causes endothelial barrier dysfunction via the protein kinase C pathway**. *The Journal of surgical research* 2002, **104**(2):118-123.

239. Biffl WL, Moore EE, Moore FA, Carl VS, Franciose RJ, Banerjee A: **Interleukin-8 increases endothelial permeability independent of neutrophils**. *The Journal of trauma* 1995, **39**(1):98-102; discussion 102-103.

240. Watson C, Whittaker S, Smith N, Vora AJ, Dumonde DC, Brown KA: **IL-6 acts on endothelial cells to preferentially increase their adherence for lymphocytes**. *Clinical and experimental immunology* 1996, **105**(1):112-119.

241. Arndt H, Bolanowski MA, Granger DN: **Role of interleukin 8 on leucocyte-endothelial cell adhesion in intestinal inflammation**. *Gut* 1996, **38**(6):911-915.

242. Petreaca ML, Yao M, Liu Y, Defea K, Martins-Green M: **Transactivation of vascular endothelial growth factor receptor-2 by interleukin-8 (IL-8/CXCL8) is required for IL-8/CXCL8-induced endothelial permeability**. *Molecular biology of the cell* 2007, **18**(12):5014-5023.

243. Yu H, Huang X, Ma Y, Gao M, Wang O, Gao T, Shen Y, Liu X: **Interleukin-8 regulates endothelial permeability by down-regulation of tight**

junction but not dependent on integrins induced focal adhesions. *International journal of biological sciences* 2013, **9**(9):966-979.

244. Battegay EJ, Rupp J, Iruela-Arispe L, Sage EH, Pech M: **PDGF-BB modulates endothelial proliferation and angiogenesis in vitro via PDGF beta-receptors**. *The Journal of cell biology* 1994, **125**(4):917-928.

245. Thommen R, Humar R, Misevic G, Pepper MS, Hahn AW, John M, Battegay EJ: **PDGF-BB increases endothelial migration on cord movements during angiogenesis in vitro**. *Journal of cellular biochemistry* 1997, **64**(3):403-413.

246. Sato Y, Rifkin DB: **Inhibition of endothelial cell movement by pericytes and smooth muscle cells: activation of a latent transforming growth factor-beta 1-like molecule by plasmin during co-culture**. *The Journal of cell biology* 1989, **109**(1):309-315.

247. Goldberg AD, Allis CD, Bernstein E: **Epigenetics: a landscape takes shape**. *Cell* 2007, **128**(4):635-638.

248. Bird A: **Perceptions of epigenetics**. *Nature* 2007, **447**(7143):396-398.

249. Egger G, Liang G, Aparicio A, Jones PA: **Epigenetics in human disease and prospects for epigenetic therapy**. *Nature* 2004, **429**(6990):457-463.

250. Lachner M, Jenuwein T: **The many faces of histone lysine methylation**. *Current opinion in cell biology* 2002, **14**(3):286-298.

251. Feinberg AP, Vogelstein B: **Hypomethylation of ras oncogenes in primary human cancers**. *Biochemical and biophysical research communications* 1983, **111**(1):47-54.

252. Feinberg AP, Vogelstein B: **Hypomethylation distinguishes genes of some human cancers from their normal counterparts**. *Nature* 1983, **301**(5895):89-92.

253. Sakai T, Toguchida J, Ohtani N, Yandell DW, Rapaport JM, Dryja TP: **Allele-specific hypermethylation of the retinoblastoma tumor-suppressor gene**. *American journal of human genetics* 1991, **48**(5):880-888.

254. Herman JG, Latif F, Weng Y, Lerman MI, Zbar B, Liu S, Samid D, Duan DS, Gnarra JR, Linehan WM *et al*: **Silencing of the VHL tumor-suppressor gene by DNA methylation in renal carcinoma**. *Proceedings of the National Academy of Sciences of the United States of America* 1994, **91**(21):9700-9704.

255. Herman JG, Merlo A, Mao L, Lapidus RG, Issa JP, Davidson NE, Sidransky D, Baylin SB: **Inactivation of the CDKN2/p16/MTS1 gene is frequently associated with aberrant DNA methylation in all common human cancers**. *Cancer research* 1995, **55**(20):4525-4530.

256. Saito Y, Liang G, Egger G, Friedman JM, Chuang JC, Coetzee GA, Jones PA: **Specific activation of microRNA-127 with downregulation of the proto-oncogene BCL6 by chromatin-modifying drugs in human cancer cells**. *Cancer cell* 2006, **9**(6):435-443.

257. Esteller M: **Epigenetics in cancer**. *The New England journal of medicine* 2008, **358**(11):1148-1159.

258. Fraga MF, Herranz M, Espada J, Ballestar E, Paz MF, Ropero S, Erkek E, Bozdogan O, Peinado H, Niveleau A *et al*: **A mouse skin multistage carcinogenesis model reflects the aberrant DNA methylation patterns of human tumors**. *Cancer research* 2004, **64**(16):5527-5534.

259. Herman JG, Baylin SB: **Gene silencing in cancer in association with promoter hypermethylation**. *The New England journal of medicine* 2003, **349**(21):2042-2054.

260. Ueda K, Yoshimi A, Kagoya Y, Nishikawa S, Marquez VE, Nakagawa M, Kurokawa M: **Inhibition of histone methyltransferase EZH2 depletes leukemia stem cell of mixed lineage leukemia fusion leukemia through upregulation of p16**. *Cancer science* 2014, **105**(5):512-519.

261. Filippakopoulos P, Qi J, Picaud S, Shen Y, Smith WB, Fedorov O, Morse EM, Keates T, Hickman TT, Felletar I *et al*: **Selective inhibition of BET bromodomains**. *Nature* 2010, **468**(7327):1067-1073.

262. Asangani IA, Chinnaiyan AM: **BETting on a new prostate cancer treatment**. *Cell cycle* 2014, **13**(13):2015-2016.

263. Asangani IA, Dommeti VL, Wang X, Malik R, Cieslik M, Yang R, Escara-Wilke J, Wilder-Romans K, Dhanireddy S, Engelke C *et al*: **Therapeutic targeting of BET bromodomain proteins in castration-resistant prostate cancer**. *Nature* 2014, **510**(7504):278-282.

264. Saah AJ, Hoover DR, He Y, Kingsley LA, Phair JP: **Factors influencing survival after AIDS: report from the Multicenter AIDS Cohort Study (MACS)**. *Journal of acquired immune deficiency syndromes* 1994, **7**(3):287-295.

265. Shi-Wen X, Chen Y, Denton CP, Eastwood M, Renzoni EA, Bou-Gharios G, Pearson JD, Dashwood M, du Bois RM, Black CM *et al*: **Endothelin-1 promotes myofibroblast induction through the ETA receptor via a rac/phosphoinositide 3-kinase/Akt-dependent pathway and is essential for the enhanced contractile phenotype of fibrotic fibroblasts**. *Molecular biology of the cell* 2004, **15**(6):2707-2719.

266. Shi-Wen X, Denton CP, Dashwood MR, Holmes AM, Bou-Gharios G, Pearson JD, Black CM, Abraham DJ: **Fibroblast matrix gene expression and**

connective tissue remodeling: role of endothelin-1. *J Invest Dermatol* 2001, **116**(3):417-425.

267. Shi-Wen X, Denton CP, McWhirter A, Bou-Gharios G, Abraham DJ, du Bois RM, Black CM: **Scleroderma lung fibroblasts exhibit elevated and dysregulated type I collagen biosynthesis**. *Arthritis and rheumatism* 1997, **40**(7):1237-1244.

268. Shi-wen X, Kennedy L, Renzoni EA, Bou-Gharios G, du Bois RM, Black CM, Denton CP, Abraham DJ, Leask A: **Endothelin is a downstream mediator of profibrotic responses to transforming growth factor beta in human lung fibroblasts**. *Arthritis and rheumatism* 2007, **56**(12):4189-4194.

269. Shi-Wen X, Renzoni EA, Kennedy L, Howat S, Chen Y, Pearson JD, Bou-Gharios G, Dashwood MR, du Bois RM, Black CM *et al*: **Endogenous endothelin-1 signaling contributes to type I collagen and CCN2 overexpression in fibrotic fibroblasts**. *Matrix biology : journal of the International Society for Matrix Biology* 2007, **26**(8):625-632.

270. **Epigenetic Therapy Beneficial in Blood Cancers**. *Cancer Discovery* 2014, **4**(6):OF7.

271. Scotton CJ, Chambers RC: **Molecular targets in pulmonary fibrosis: the myofibroblast in focus**. *Chest* 2007, **132**(4):1311-1321.

272. Xu SW, Howat SL, Renzoni EA, Holmes A, Pearson JD, Dashwood MR, Bou-Gharios G, Denton CP, du Bois RM, Black CM *et al*: **Endothelin-1 induces expression of matrix-associated genes in lung fibroblasts through MEK/ERK**. *The Journal of biological chemistry* 2004, **279**(22):23098-23103.

273. Maekawa T, Jinnin M, Ohtsuki M, Ihn H: **Serum levels of interleukin-1alpha in patients with systemic sclerosis**. *The Journal of dermatology* 2013, **40**(2):98-101.

274. Khan YM, Kirkham P, Barnes PJ, Adcock IM: **Brd4 is essential for IL-1beta-induced inflammation in human airway epithelial cells**. *PloS one* 2014, **9**(4):e95051.

275. Shi-wen X, Parapuram SK, Pala D, Chen Y, Carter DE, Eastwood M, Denton CP, Abraham DJ, Leask A: **Requirement of transforming growth factor beta-activated kinase 1 for transforming growth factor beta-induced alpha-smooth muscle actin expression and extracellular matrix contraction in fibroblasts**. *Arthritis and rheumatism* 2009, **60**(1):234-241.

276. Shi-Wen X, Rodriguez-Pascual F, Lamas S, Holmes A, Howat S, Pearson JD, Dashwood MR, du Bois RM, Denton CP, Black CM *et al*: **Constitutive ALK5-independent c-Jun N-terminal kinase activation contributes to endothelin-1**

overexpression in pulmonary fibrosis: evidence of an autocrine endothelin loop operating through the endothelin A and B receptors. *Molecular and cellular biology* 2006, **26**(14):5518-5527.

277. Li M, Riddle SR, Frid MG, El Kasmi KC, McKinsey TA, Sokol RJ, Strassheim D, Meyrick B, Yeager ME, Flockton AR *et al*: **Emergence of fibroblasts with a proinflammatory epigenetically altered phenotype in severe hypoxic pulmonary hypertension**. *Journal of immunology* 2011, **187**(5):2711-2722.

278. Leask A, Holmes A, Abraham DJ: **Connective tissue growth factor: a new and important player in the pathogenesis of fibrosis**. *Current rheumatology reports* 2002, **4**(2):136-142.

279. Bogatkevich GS, Ludwicka-Bradley A, Singleton CB, Bethard JR, Silver RM: **Proteomic analysis of CTGF-activated lung fibroblasts: identification of IQGAP1 as a key player in lung fibroblast migration**. *American journal of physiology Lung cellular and molecular physiology* 2008, **295**(4):L603-611.

280. Steinman RA, Robinson AR, Feghali-Bostwick CA: **Antifibrotic effects of roscovitine in normal and scleroderma fibroblasts**. *PloS one* 2012, **7**(11):e48560.

281. Corrado A, Neve A, Costantino E, Palladino GP, Foschino Barbaro MP, Cantatore FP: **Effect of endothelin inhibition on lung fibroblasts on patients with systemic sclerosis**. *Minerva medica* 2013, **104**(5):505-517.

282. Christmann RB, Sampaio-Barros P, Stifano G, Borges CL, de Carvalho CR, Kairalla R, Parra ER, Spira A, Simms R, Capellozzi VL *et al*: **Association of Interferon- and transforming growth factor beta-regulated genes and macrophage activation with systemic sclerosis-related progressive lung fibrosis**. *Arthritis & rheumatology* 2014, **66**(3):714-725.

283. Bogatkevich GS, Ludwicka-Bradley A, Highland KB, Hant F, Nietert PJ, Singleton CB, Silver RM: **Down-regulation of collagen and connective tissue growth factor expression with hepatocyte growth factor in lung fibroblasts from white scleroderma patients via two signaling pathways**. *Arthritis and rheumatism* 2007, **56**(10):3468-3477.

284. Vancheri C: **Idiopathic pulmonary fibrosis: an altered fibroblast proliferation linked to cancer biology**. *Proceedings of the American Thoracic Society* 2012, **9**(3):153-157.

285. Ott CJ, Kopp N, Bird L, Paranal RM, Qi J, Bowman T, Rodig SJ, Kung AL, Bradner JE, Weinstock DM: **BET bromodomain inhibition targets both c-Myc and IL7R in high-risk acute lymphoblastic leukemia**. *Blood* 2012, **120**(14):2843-2852.

286. Kantor TV, Friberg D, Medsger TA, Jr., Buckingham RB, Whiteside TL: **Cytokine production and serum levels in systemic sclerosis**. *Clinical immunology and immunopathology* 1992, **65**(3):278-285.

287. Hassoun PM: **Inflammation in pulmonary arterial hypertension: is it time to quell the fire?** *The European respiratory journal : official journal of the European Society for Clinical Respiratory Physiology* 2014, **43**(3):685-688.

288. Rabinovitch M, Guignabert C, Humbert M, Nicolls MR: **Inflammation and immunity in the pathogenesis of pulmonary arterial hypertension**. *Circulation research* 2014, **115**(1):165-175.

289. Dorfmuller P, Perros F, Balabanian K, Humbert M: **Inflammation in pulmonary arterial hypertension**. *The European respiratory journal : official journal of the European Society for Clinical Respiratory Physiology* 2003, **22**(2):358-363.

290. Cool CD, Kennedy D, Voelkel NF, Tuder RM: **Pathogenesis and evolution of plexiform lesions in pulmonary hypertension associated with scleroderma and human immunodeficiency virus infection**. *Human pathology* 1997, **28**(4):434-442.

291. Tuder RM, Groves B, Badesch DB, Voelkel NF: **Exuberant endothelial cell growth and elements of inflammation are present in plexiform lesions of pulmonary hypertension**. *Am J Pathol* 1994, **144**(2):275-285.

292. Elhai M, Meunier M, Matucci-Cerinic M, Maurer B, Riemekasten G, Leturcq T, Pellerito R, Von Muhlen CA, Vacca A, Airo P *et al*: **Outcomes of patients with systemic sclerosis-associated polyarthritis and myopathy treated with tocilizumab or abatacept: a EUSTAR observational study**. *Annals of the rheumatic diseases* 2013, **72**(7):1217-1220.

293. Kadavath S, Zapantis E, Zolty R, Efthimiou P: **A novel therapeutic approach in pulmonary arterial hypertension as a complication of adult-onset Still's disease: targeting IL-6**. *International journal of rheumatic diseases* 2014, **17**(3):336-340.

294. Savai R, Pullamsetti SS, Kolbe J, Bieniek E, Voswinckel R, Fink L, Scheed A, Ritter C, Dahal BK, Vater A *et al*: **Immune and inflammatory cell involvement in the pathology of idiopathic pulmonary arterial hypertension**. *American journal of respiratory and critical care medicine* 2012, **186**(9):897-908.

295. Majka S, Hagen M, Blackwell T, Harral J, Johnson JA, Gendron R, Paradis H, Crona D, Loyd JE, Nozik-Grayck E *et al*: **Physiologic and molecular consequences of endothelial Bmpr2 mutation**. *Respiratory research* 2011, **12**:84.

296. Rosenzweig EB, Morse JH, Knowles JA, Chada KK, Khan AM, Roberts KE, McElroy JJ, Juskiw NK, Mallory NC, Rich S *et al*: **Clinical implications of determining BMPR2 mutation status in a large cohort of children and adults with pulmonary arterial hypertension**. *The Journal of heart and lung transplantation : the official publication of the International Society for Heart Transplantation* 2008, **27**(6):668-674.

297. Tada Y, Majka S, Carr M, Harral J, Crona D, Kuriyama T, West J: **Molecular effects of loss of BMPR2 signaling in smooth muscle in a transgenic mouse model of PAH**. *American journal of physiology Lung cellular and molecular physiology* 2007, **292**(6):L1556-1563.

298. West J, Harral J, Lane K, Deng Y, Ickes B, Crona D, Albu S, Stewart D, Fagan K: **Mice expressing BMPR2R899X transgene in smooth muscle develop pulmonary vascular lesions**. *American journal of physiology Lung cellular and molecular physiology* 2008, **295**(5):L744-755.

299. Tang K, Ma J, Zhang S, Chu JM, Zhang KJ, Wang FZ, Chen X: **Radiofrequency catheter ablation at the left coronary cusp in treatment of repetitive monomorphic tachycardia of the left ventricular outflow tract**. *Chinese medical journal* 2004, **117**(2):168-171.

300. Lu J, Shimpo H, Shimamoto A, Chong AJ, Hampton CR, Spring DJ, Yada M, Takao M, Onoda K, Yada I *et al*: **Specific inhibition of p38 mitogen-activated protein kinase with FR167653 attenuates vascular proliferation in monocrotaline-induced pulmonary hypertension in rats**. *The Journal of thoracic and cardiovascular surgery* 2004, **128**(6):850-859.

301. Tew MB, Arnett FC, Reveille JD, Tan FK: **Mutations of bone morphogenetic protein receptor type II are not found in patients with pulmonary hypertension and underlying connective tissue diseases**. *Arthritis and rheumatism* 2002, **46**(10):2829-2830.

302. Derrett-Smith EC, Denton CP, Sonnylal S: **Animal models of scleroderma: lessons from transgenic and knockout mice**. *Current Opinion in Rheumatology* 2009, **21**(6).

303. Burton VJ, Ciuclan LI, Holmes AM, Rodman DM, Walker C, Budd DC: **Bone morphogenetic protein receptor II regulates pulmonary artery endothelial cell barrier function**. *Blood* 2011, **117**(1):333-341.

304. Song Y, Jones JE, Beppu H, Keaney JF, Jr., Loscalzo J, Zhang YY: **Increased susceptibility to pulmonary hypertension in heterozygous BMPR2-mutant mice**. *Circulation* 2005, **112**(4):553-562.

305. Hagen M, Fagan K, Steudel W, Carr M, Lane K, Rodman DM, West J: **Interaction of interleukin-6 and the BMP pathway in pulmonary smooth**

muscle. *American journal of physiology Lung cellular and molecular physiology* 2007, **292**(6):L1473-1479.

306. Hong KH, Lee YJ, Lee E, Park SO, Han C, Beppu H, Li E, Raizada MK, Bloch KD, Oh SP: **Genetic ablation of the BMPR2 gene in pulmonary endothelium is sufficient to predispose to pulmonary arterial hypertension**. *Circulation* 2008, **118**(7):722-730.

307. Keller B, Yang T, Chen Y, Munivez E, Bertin T, Zabel B, Lee B: **Interaction of TGFbeta and BMP signaling pathways during chondrogenesis**. *PloS one* 2011, **6**(1):e16421.

308. Al-Salihi MA, Herhaus L, Sapkota GP: **Regulation of the transforming growth factor beta pathway by reversible ubiquitylation**. *Open biology* 2012, **2**(5):120082.

309. Foletta VC, Lim MA, Soosairajah J, Kelly AP, Stanley EG, Shannon M, He W, Das S, Massague J, Bernard O: **Direct signaling by the BMP type II receptor via the cytoskeletal regulator LIMK1**. *The Journal of cell biology* 2003, **162**(6):1089-1098.